Dissertation

submitted to the

Combined Faculties for the Natural Sciences and for Mathematics

of the Ruperto-Carola University of Heidelberg, Germany

for the degree of

Doctor of Natural Sciences

presented by

Diplom-Biologin Doris Quinkert

born in Heidelberg, Germany

Oral-examination:

Quantitative analysis of the Hepatitis C Virus replication complex and identification of associated cellular factors

Referees: Prof. Dr. Ralf Bartenschlager

Prof. Dr. Irmgard Sinning

Table of contents

Acknowledgements

First of all, I would like to thank Dr. Volker Lohmann for giving me the opportunity to work on these interesting projects in his group. I am greatly indebted to Volker for his excellent and intense supervision, great support and scientific enthusiasm throughout my PhD time.

I want to express my gratitude to Prof. Dr. Ralf Bartenschlager for giving me the chance to work within his department. His continuous support and helpful advice facilitated the completion of my PhD thesis.

I would like to thank Prof. Dr. Irmgard Sinning for agreeing to evaluate my thesis. I also thank Dr. Hans-Michael Müller and Prof. Dr. Lutz Gissmann for agreeing to be on the defense committee. I would like to thank Dr. Jacomine Krijnse-Locker and Dr. Stephan Urban for their outstanding help in the thesis advisory committee.

I am also grateful to Prof. Dr. Volker Gerke for supplying us with plenty of antibodies, especially the anti-ANXA2 antibody, and continuous discussion of my work.

I thank Rahel Klein for her generous assistance with cell culture, cloning and FACS experiments, and Uli Herian for providing me with cells whenever I needed them. A special thank you goes to Julia Bitzegeio, Giorgos Koutsoudakis, and Ina Allespach who introduced me into FACS analyses. A big thank you goes to Marco Binder, Olga Bochkarova, Leah Eustachi and Iris Scheirich for discussing absolutely every aspect in life (science). Many thanks go of course to all other current and previous members of the department making it possible to work in a very great atmosphere.

Ich danke auch allen meinen Freunden, ganz besonders Gitta Erdmann und Sonja Textor, die mir beim montäglichen Kalorien- und Frustabbau geholfen haben, den Kopf von der Arbeit freizubekommen.

Meine tiefste Dankbarkeit gilt meinen Eltern für ihre ununterbrochene Unterstützung während meines Studiums und meiner Promotion sowie in allen sonstigen Lebenslagen.

Jan, ich danke Dir aus tiefstem Herzen für Deine Liebe, Deine Motivation, Dein Verständnis und dafür, dass Du immer an meiner Seite stehst.

Summary

Hepatitis C virus (HCV) has a positive-strand RNA genome and is grouped into the family of *Flaviviridae*. Similar to other positive-stranded RNA viruses, HCV RNA replication takes place in the cytoplasm. The sites of viral replication are designated "membranous web" and represented by an accumulation of vesicular structures, which are induced by the viral non-structural proteins and probably originate from membranes of the Endoplasmic Reticulum. The aim of this work was to purify and characterize these viral replication complexes (RCs) *in vitro* and to identify potential host factors of viral replication.

First a purification strategy for enzymatically active viral replication complexes was developed to determine associated cellular proteins by proteomics. Thereby, several potential host factors of viral replication were identified and the most reproducible, Annexin II (ANXA2) was further characterized.

In immunofluorescence analyses, ANXA2 strongly colocalized to the sites of viral replication in all applicable cell lines supporting HCV replication, in HCV-transfected as well as in infected cells. In contrast, we found no obvious colocalization of HCV proteins with Annexin I, IV or V or with p11 (also denoted S100A10), a common cellular ligand of Annexin II. Specificity of the ANXA2-HCV interaction was further indicated by the lack of colocalization with replication sites of other positive-strand RNA viruses, namely Dengue virus and Semliki-Forest-Virus. By individual expression of the viral non-structural (NS) proteins we found that NS5A colocalized with Annexin II, indicating that NS5A might be involved in the recruitment of ANXA2. SiRNA-mediated silencing clearly reduced Annexin II levels but failed to block HCV replication. However, FACS analyses revealed a strong correlation of intracellular HCV and ANXA2 levels even in presence of ANXA2 siRNA, suggesting that Annexin II expression was induced by HCV, thereby counteracting siRNA-mediated knockdown. Still, ANXA2 silencing moderately reduced the number of HCV positive cells. Interestingly, the presence of replicating HCV sequences in HepG2 cells, harboring very little endogenous ANXA2, clearly induced Annexin II expression to detectable levels perfectly colocalizing with the viral NS proteins. However, the role and function of ANXA2 in the HCV life cycle has yet to be defined.

In a second line of investigations, a detailed stoichiometric analysis of HCV RCs was performed. Thus, the ratio of non-structural proteins to RNA that is required for HCV RNA replication could be determined. Almost the entire negative- and positive-strand RNA but <5% of the non-structural proteins present in HCV-harboring cells were protected against nuclease and protease treatments. Nevertheless, this protease-resistant portion of NS proteins accounted for the full *in vitro* replicase activity. Therefore, only a minor fraction of the HCV non-structural proteins was actively involved in RNA synthesis. However, due to the high amounts present in replicon cells, this still represented a huge excess compared to the viral RNA. Based on the comparison of nuclease-resistant viral RNA to protease-resistant viral proteins, an active HCV replication complex probably consists of one negative-strand RNA, two to ten positive-strand RNAs, and several hundred non-structural protein copies. These might be required as structural components of the vesicular compartments that are the site of HCV replication.

Zusammenfassung

Das Hepatitis C Virus (HCV) besitzt ein Plusstrang-RNA-Genom und gehört zur Familie der *Flaviviridae*. Die HCV RNA-Replikation findet, ähnlich wie bei anderen Plusstrang-RNA-Viren, im Zytoplasma statt. Die Stätten der viralen Replikation werden als „membranous web" bezeichnet und repräsentieren eine Anhäufung vesikulärer Strukturen, die durch die viralen Nichtstruktur-Proteine induziert werden und wahrscheinlich den Membranen des Endoplasmatischen Retikulums entstammen. Das Ziel dieser Arbeit war sowohl die Reinigung und Charakterisierung dieser viralen Replikations-Komplexe (RC) *in vitro* als auch die Identifikation möglicher Wirtsfaktoren der viralen Replikation.

Als Erstes wurde eine Reinigungsstrategie für enzymatisch aktive virale Replikations-Komplexe entwickelt, um assoziierte zelluläre Proteine durch Proteom-Analysen zu ermitteln. Einige potentielle Wirtsfaktoren der viralen Replikation konnten dadurch identifiziert werden, und der am häufigsten reproduzierbare, Annexin II (ANXA2), wurde eingehend charakterisiert. Immunfluoreszenz-Studien zeigten, dass in allen geeigneten, HCV-Replikation unterstützenden Zelllinien, in HCV-transfizierten sowie infizierten Zellen, ANXA2 deutlich mit den Stätten der viralen Replikation kolokalisiert. Im Gegensatz dazu fanden wir weder eine ersichtliche Kolokalisation von HCV-Proteinen mit Annexin I, IV, oder V, noch mit p11 (auch S100A10 genannt), einem häufigen zellulären Liganden von Annexin II. Die Spezifität der ANXA2-HCV Interaktion wurde noch betont durch die fehlende Kolokalisation mit Replikations-Stätten anderer Positiv-Strang-RNA-Viren wie Dengue Virus und Semliki-Forest-Virus. Durch die individuelle Expression viraler Nicht-Struktur- (NS-) Proteine fanden wir heraus, dass NS5A mit Annexin II kolokalisiert, was darauf hinweist, dass NS5A möglicherweise in die Rekrutierung von ANXA2 involviert ist. SiRNA-vermitteltes silencing reduzierte die Annexin II-Menge deutlich, führte jedoch nicht zur Hemmung der HCV Replikation. FACS-Analysen zeigten hingegen eine starke Korrelation von intrazellulären HCV- und ANXA2-Mengen, auch in Anwesenheit von ANXA2-siRNA. Daher ist anzunehmen, dass NS5A die ANXA2-Expression induziert, wodurch dem siRNA-vermittelten knockdown entgegengewirkt wird. Dennoch reduzierte ANXA2-Silencing moderat die Anzahl HCV-positiver Zellen. Interessanterweise verursachte die Anwesenheit replizierender HCV-Sequenzen in HepG2-Zellen, die äußerst wenig endogenes ANXA2 besitzen, eine ANXA2-Expression von deutlich nachweisbaren Mengen, welche mit den viralen NS-Proteinen perfekt kolokalisierten. Die Rolle und die Funktion von ANXA2 im HCV-Lebenszyklus müssen allerdings noch definiert werden.

Als Zweites wurde eine detaillierte stöchiometrische Analyse der HCV-Replikations-Komplexe durchgeführt. Auf diese Weise konnte das für die HCV-RNA-Replikation erforderliche Verhältnis von NS-Proteinen zu RNA ermittelt werden. Fast die gesamte Negativ- und Positiv-Strang-RNA, jedoch <5% aller Nicht-Struktur-Proteine, die in HCV-replizierenden Zellen vorhanden sind, waren gegen Nuklease- und Protease-Behandlungen geschützt. Dennoch war dieser Protease-resistente Anteil der NS-Proteine für die gesamte *in vitro* Replikase-Aktivität verantwortlich. Folglich war nur eine kleinere Fraktion der HCV Nicht-Struktur-Proteine aktiv an der RNA-Synthese beteiligt. Allerdings machte dies aufgrund der in Replikon-Zellen vorhandenen großen Mengen verglichen mit viraler RNA immer noch einen enormen Überschuss aus. Basierend auf dem Vergleich Nuklease-resistenter viraler RNA zu Protease-resistenten viralen Proteinen enthält ein aktiver HCV Replikations-Komplex wahrscheinlich eine Negativ-Strang-RNA, zwei bis zehn Positiv-Strang-RNA-Moleküle und einige hundert Kopien der Nicht-Struktur-Proteine. Diese werden möglicherweise als strukturelle Komponenten der vesikulären Kompartimente benötigt, welche die Stätten der HCV Replikation repräsentieren.

1. Introduction

1.1 Hepatitis C virus overview

The Hepatitis C Virus (HCV) is a major cause of chronic liver disease, including cirrhosis and liver cancer. Before the identification of the causative agent in 1989, the viral Hepatitis C infection had been referred to as parenterally transmitted "non A, non B hepatitis"[41,59]. Today, almost 20 years after the identification of the virus, the World Health Organization (WHO) estimates that about 180 million persons, 3% of the world's population, are chronically infected with HCV and 3 to 4 million persons are newly infected each year. The global prevalence of HCV is shown in Fig. 1. The discovery and the characterization of HCV led to the understanding of its primary role in causing hepatitis after blood transfusion and its tendency to induce persistent infection.

Based on WHO Wkly Epidemiol Rec 2002;77:41-48.
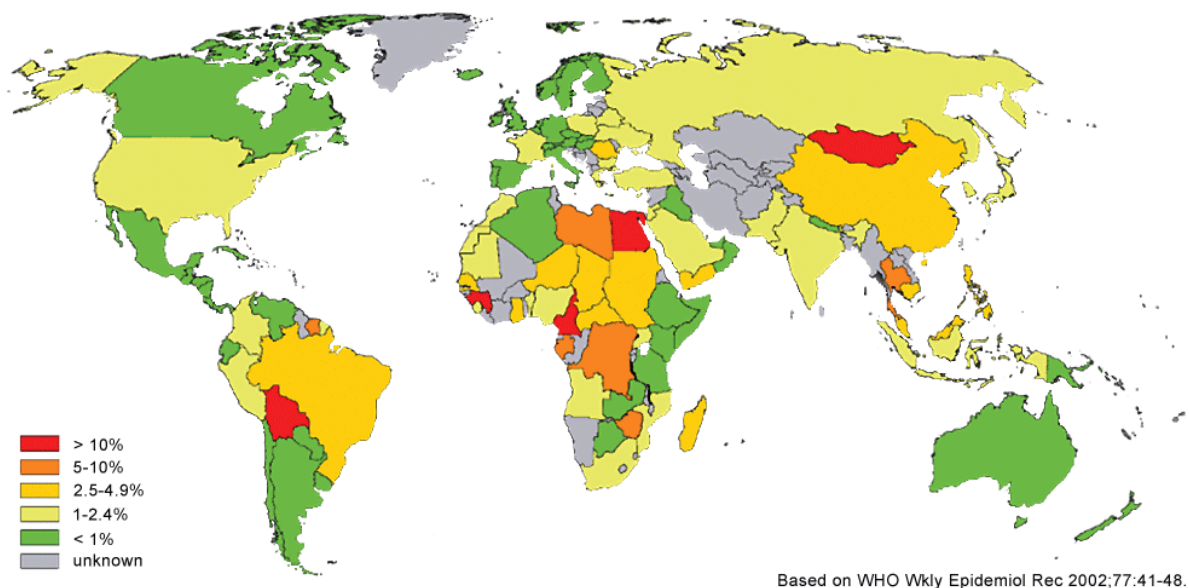
Fig. 1: Prevalence of HCV infection throughout the world.

HCV is transmitted by parenteral or permuscosal exposure to infected blood or body fluids[165]. Transmission through organ transplantations and blood transfusions not screened for HCV infection, through the reuse of inadequately sterilized needles, syringes or other medical equipment, or through needle-sharing among drug-users, is well documented[233]. Sexual and perinatal transmission may also occur, although less frequently.

1.2 Course of disease and therapy

Primary infection with HCV is predominantly asymptomatic, and in the majority of cases leads to persistent infection[64]. Individuals with chronic infection develop progressive hepatic fibrosis leading to an increased risk of cirrhosis, liver failure and hepatocellular carcinoma (HCC) with proceeding endurance of infection[191]. 15-30% of infected individuals succeed in eliminating the virus but in most cases (70-85%) persistent viremia and chronic hepatitis develop[165]. Hepatocellular carcinoma evolves in 1-4% of the cases per year. The stages of the progression after HCV infection are shown in Fig. 2. High virus titers are observed during the first few weeks of HCV infection, but inflammatory processes leading to liver injury are delayed, usually occurring after 2–3 months[93]. Chronically infected patients have viral loads that typically range from 10^3–10^7 genomes per ml of serum[135]. Mathematical modeling of viral dynamics during treatment with interferon-α (IFN-α) indicates that HCV virions turn over rapidly (with a half-life of about 3 h), and up to about 10^{12} viruses are produced per day in an infected person[161]. This is about 100-fold greater than the rate reported for HIV.
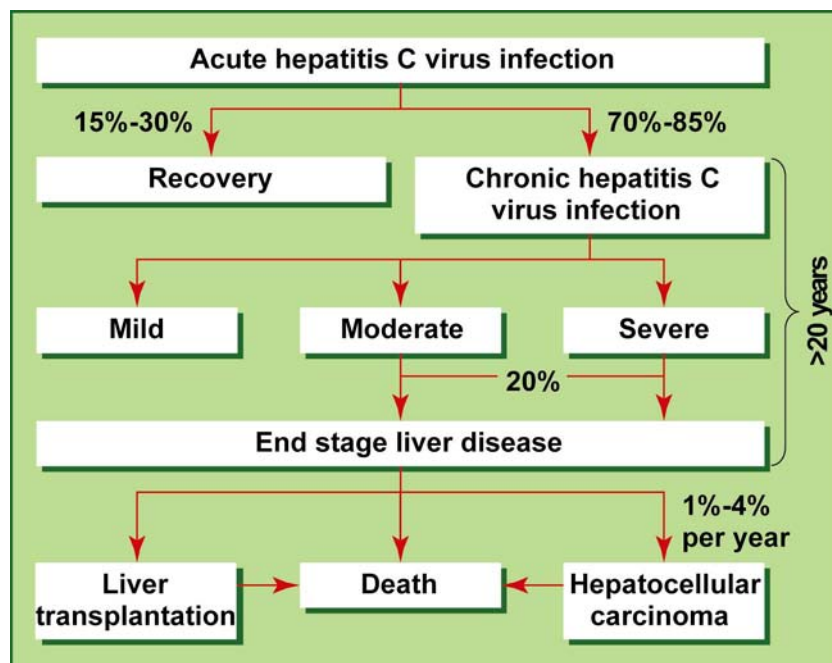
Fig. 2: Progression steps of HCV infection. Hepatitis C virus persists in most patients with acute hepatitis C virus infection, and some develop progressive hepatic injury and subsequent complications of end stage liver disease. *Adapted from Patel et. al., BMJ, 2006*[165].

Although the liver seems to be the major site of HCV replication, evidence exists for extrahepatic reservoirs including peripheral blood lymphocytes, epithelial cells in the

gut[44] and the central nervous system[62]. In infected tissues, HCV is proven by detection of either HCV-specific antibodies by ELISA or the viral genome by RT-PCR. Direct detection of virus antigens is difficult due to their low levels in infected cells *in vivo*. Nevertheless, gene-profiling studies of HCV-infected livers indicate that this organ is the major region of viral replication and host antiviral defenses[22,23,203,209]. The current standard of care for treating previously untreated patients with chronic HCV infection is combination of polyethylene glycol (PEG-) conjugated IFN-α and ribavirin[165]. The interferons are a group of naturally occurring cytokines that exhibit a variety of immunomodulatory, antiproliferative, and antiviral effects. Ribavirin is a purine nucleoside that has antiviral effects against hepatitis C virus only when combined with IFN-α. Combinated PEG-IFN-α and ribavirin therapy can achieve a sustained virological response in 54%-56% of patients, including 42%-46% of patients with genotype 1 infection and about 80% of those with genotype 2 or 3 infection. Therefore, the development of new antiviral strategies against HCV is imperative. The development of efficient cell culture systems for HCV[140,219] has led to the identification of several novel therapeutic targets and the subsequent development of hepatitis C virus specific antiviral compounds.

1.3 Molecular organization of HCV

1.3.1 Genetic diversity

HCV is an enveloped positive-strand RNA virus belonging to the genus *Hepacivirus* in the family *Flaviviridae*. Based on sequence analyses, HCV genomes can be classified into six major genetic groups. On average, these genotypes differ in 30-33% of their nucleotide sites[198]. Each HCV genotype comprises a series of more closely related subtypes which show a nucleotide sequence heterogeneity of circa 20-25% and are designated with subtype labels such as 1a and 1b. Furthermore, since the RNA synthesis is error-prone, HCV exists as a mixture of variants, the so-called "quasispecies", within an infected individual.

 The most common variants found in Western countries are genotype 1 and genotype 2. During the past 50 to 70 years, these variants have become widely distributed as a result of transmission through blood transfusion and various other medical procedures, and by needle sharing between injection drug users. They now represent the vast majority of infections in Western countries, for which the most

information has been collected on disease progression and response to IFN-α-based treatment. Nevertheless, the widespread distribution of genotypes 1-6 in human populations indicates that each is equally successful in maintaining infections[197].

1.3.2 Genome organization and function of viral proteins

The Hepatitis C virus particle is about 50-60 nm in diameter. HCV possesses an RNA genome of positive polarity that is approximately 9.6 kb in length. The genome encodes a large polyprotein of roughly 3000 amino acids (aa) that is flanked at the N- and C-terminus by highly structured nontranslated regions (NTRs) (Fig. 3). The 5'-NTR is about 341 nucleotides (nts) in length and contains an internal ribosome entry site (IRES) mediating the cap-independent expression of the polyprotein[213,223]. This process is additionally regulated by an RNA pseudoknot structure upstream of the initiation codon AUG critical for translation initiation[222]. It has been shown that the first 125 nucleotides are essential for RNA replication, but that the entire 5'-NTR is required for maximal replication efficiency[69,112]. It is generally believed that the function of the 5'-NTR in RNA replication, namely initiation of positive-strand synthesis, is exerted by the complementary sequence, corresponding to the 3'-end of the negative-strand, which adopts a secondary structure that is different from the mirror image of the 5'-NTR[189,199]. The 3'-NTR of the positive-strand RNA has a tripartite structure: (i) a variable region, that is in part dispensable for replication *in vivo* [232] and *in vitro* but seems to be important for efficient RNA replication[67,234]; (ii) a polyU/UC tract of variable length, which is essential *in vivo* and *in vitro* and which requires a minimal length of 26 to 50 nucleotides[67,234]; (iii) the very 3'-end of the HCV genome designated X-tail. It comprises an almost invariant 98 nucleotides sequence[115,206] containing 3 highly conserved stem-loop structures (SL I-III)[28], which are all critical for RNA replication *in vitro* and *in vivo*[67,232,234]. Further important cis-acting RNA elements are located in the coding region of NS5B[237], one of which undergoes a kissing loop interaction with SL II in the X-region being essential for RNA replication[68]. In addition, both NTRs contain genotype-specific signals that are critical for efficient initiation of RNA synthesis[24].
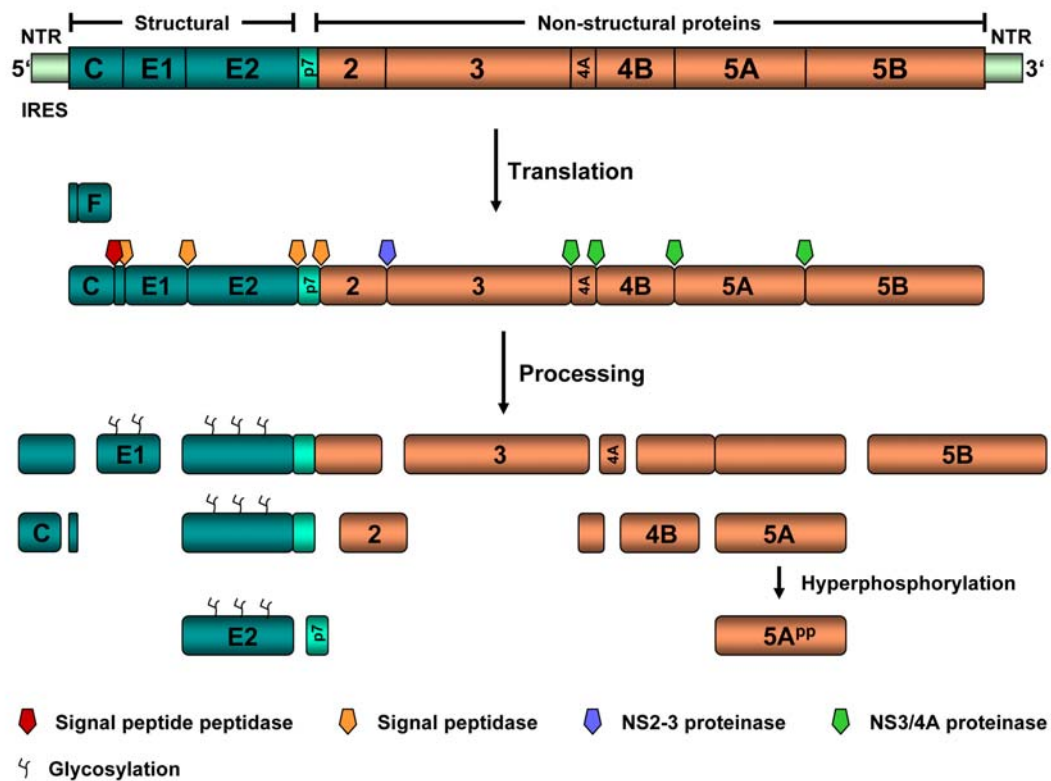
Fig. 3. Genomic organization of HCV and processing pathways of the polyprotein. A schematic representation of the HCV genome with the 5'- and 3'-NTRs is shown in the top, the translation products are given below. Proteinases involved in the processing of the polyprotein are indicated by arrows that are specified at the bottom of the picture. The major cleavage pathways leading to distinct processing intermediates, most notably E2-p7-NS2 and NS4B-5A, are indicated. The hyperphosphorylation of NS5A probably occurs after full proteolytic cleavage. Glycosylation of E1 and E2 is indicated by branched lines. The F protein generated by ribosomal frameshifting is depicted above the polyprotein. *Adapted from Bartenschlager et. al., Adv. Virus Res., 2004.*[15].

The polyprotein is co- and posttranslationally processed by cellular and viral proteinases into at least ten different polypeptides: the structural proteins core, E1, and E2, forming the virus particle, the p7 protein functioning as an ion channel[78,167], as well as the non-structural (NS) proteins NS2, NS3, NS4A, NS4B, NS5A, and NS5B which are involved in HCV RNA replication. Besides, the expression of a novel HCV protein has been reported[31,220,230]. Translation of this additional viral gene product begins at the same AUG start codon as core, but then ribosomes shift into an alternative reading frame. The resulting protein has a molecular weight of 17 kDa and is called the frameshift (F) or alternative reading frame (ARF) protein[217,230]. The role of the F protein in the HCV life cycle – if it has any at all – is currently unknown.

The individual functional products of the polyprotein are liberated by various cleavage events (Fig. 3). The core to NS2 region is processed by the cellular enzymes signal peptidase and signal peptide peptidase, the carboxyterminus of NS2 is released from

NS3 by the NS2-3 proteinase, and all other cleavages are mediated by the main viral proteinase complex build by NS3 and NS4A.

Core, a 21 kDa protein, functions primarily in the assembly of the viral capsid shell[151] and interacts with the envelope protein E1[137,147].

The glycosylated envelope proteins E1 (30-35 kDa) and E2 (70-72 kDa)[77,180] probably are responsible for the attachment to the cell by binding to cell surface receptors, e.g. CD81, SR-BI (scavenger receptor class B type I), and LDL (low density lipoprotein) receptor[3,174,185].

The integral membrane protein p7 is a small hydrophobic protein (63 aa) of unknown function that is located between the structural and non-structural regions of the polyprotein[130,192]. It was suggested that p7 belongs to the viroporin ion channel family since it can mediate membrane ion permeability[78,167]. Recently, it was shown that p7 is essential for the production of infectious virions[104,202].

NS2 is a hydrophobic 23 kDa membrane protein[184] which functions as a cysteine protease[142,163]. Together with the N-terminal third of NS3, this protein forms the NS2-3 proteinase which is responsible for self-cleavage between NS2 and NS3[76,90,184]. The precise biological function of NS2 still has to be clarified. Although NS2 itself is not required for RNA replication[140], its cleavage from NS3 is essential[116,226]. Recent work suggests that NS2 plays a role in infectious virus production[104,171,235].

NS3, a primarily cytosolic 70 kDa protein[91], is a multifunctional molecule. Besides being part of the NS2-3 proteinase responsible for autocatalytic cleavage at the NS2-NS3 site[14], NS3 contains a serine proteinase domain in the N-terminal 180 amino acids of the protein[84,114,201,207], and a NTPase/helicase in the C-terminal portion[108,204]. Although the N-terminal serine proteinase domain of NS3 shows enzymatic activity on its own, NS4A, a 54-residue viral protein containing an N-terminal membrane anchor, is a proteinase cofactor required for efficient proteolytic processing downstream of NS3[14,58,131,208]. The NS3 helicase is classified into the superfamily 2 helicases[124]. The helicase/NTPase is essential for viral replication[116], however, its precise role has yet to be defined. NS4B, a 27 kDa hydrophobic protein, associates with membranes of the ER presumably via an internal signal sequence[98,110]. It reorganizes intracellular membranes into distinct membranous structures that represent the site of viral replication in Huh-7 cells[51,74,156]. Thus, NS4B has been proposed to play a structural role in RNA replication by serving as the scaffold for

replication complex assembly[170,177]. Moreover, several replication-enhancing adaptive mutations map to NS4B[81,138].

NS5A is a predominantly hydrophilic, RNA-binding[97] phosphoprotein containing an N-terminal amphipathic α-helix that mediates association with the ER membrane[33,169]. Two phosphoproteins, the basally phosphorylated p56 and the hyperphosphorylated p58 (56 kDa and 58 kDa, respectively) are detectable due to differential phosphorylation[106]. Hyperphosphorylation depends on the presence of other viral non-structural proteins (NS3, NS4A, and NS4B)[9,106,113,159] and is performed by casein kinase I[178,179]. p58 has a shorter half life than p56[173], suggesting that both NS5A forms have distinct roles in the viral replication cycle which are so far unknown. It seems that NS5A is involved in genomic RNA replication[140], since the central region of NS5A is a hot spot for cell culture adaptive mutations in the replicon system (see below and references[13,25,120]) and the protein itself is a pivotal regulator of replication[25,139].

The NS5B protein is the RNA-dependent RNA polymerase (RdRp) of HCV, the key enzyme of viral RNA replication. It has a molecular weight of 68 kDa and belongs to a relatively small class of membrane proteins termed tail-anchored proteins[101,188]. Characteristic features of these proteins include (i) posttranslational membrane targeting via a hydrophobic C-terminal insertion sequence (which in the case of NS5B was mapped to the C-terminal 21 amino acid residues), (ii) integral membrane association, and (iii) a cytosolic orientation of the functional protein domain (reviewed in[29,225]). NS5B can initiate RNA synthesis *de novo* or primer-dependent; presumably, *de novo* initiation occurs also *in vivo*[145,162,241]. The viral NTRs contain specific signals important for the efficient initiation of positive- and negative-strand RNA synthesis which are recognized (but not exclusively) by the HCV polymerase[24].

1.4 Model systems to study HCV replication in cell culture

1.4.1 Tissue culture models

Subgenomic replicons

Despite the numerous attempts that have been undertaken, the propagation of HCV in cell culture turned out to be surprisingly difficult. Most experiments were based on the cultivation of primary cells isolated from tissues of persistently infected patients or the infection of primary cell cultures or cell lines with HCV (reviewed in[16]). However,

the reproducibility in these systems was poor, and the low level of HCV replication demanded the use of highly sensitive RT-PCR-based detection methods which were additionally subject to inherent technical problems[80,127,205].

A breakthrough came in 1999 when Lohmann et al. reported the first functional "subgenomic replicons"[140] (Fig. 4). This system is based on the self-replication of selectable subgenomic HCV RNAs, the so-called replicons (Fig. 4A). These RNAs were derived from a cloned consensus genome of genotype 1b by deleting the region coding for core to p7 or core to NS2 and inserting a selectable marker instead (neomycin phosphotransferase (neo), conferring resistance against the antibiotic G418). A second IRES element from a picornavirus (EMCV, encephalomyocarditis virus) was introduced to allow translation of the HCV non-structural proteins. Upon transfection of the human hepatoma cell line Huh-7, a low number of neomycin (G418)-resistant colonies was obtained that carried high amounts of autonomously replicating HCV RNAs[140]. These cells provided a suitable tool for the investigation of HCV replication. When replicon cells are passaged under continuous selection pressure, these RNAs show stable replication and translation levels for many years[173] (Fig. 4, B and C). With the identification of cell culture-adaptive mutations that enormously enhanced HCV RNA replication in Huh-7 cells, it was also possible to develop various replication assays with modified replicons[25,81,120,139] harboring – for example – genes coding for luciferase or auto-fluorescent proteins (Fig.4A).

Another important outcome from work with HCV replicons was the identification of highly permissive cell clones[15]. Individual cells within a given Huh-7 cell pool vary dramatically in their ability to support high levels of HCV RNA replication[138]; cells that can support high levels of RNA replication are enriched during selection (with G418 in the case of neo replicons). Upon removal of HCV replicons from such established cell clones, for example by treatment with IFN-α or an HCV-selective drug, a "cured" cell clone is obtained, which, upon reintroduction of the replicon, in many cases supports HCV RNA replication to a much higher level as compared to that of the parental (naïve) cells. Two highly permissive cell clones designated Huh7.5 and Huh7-Lunet have been generated in this way[27,68].

In addition to subgenomic replicons, selectable full-length HCV genomes carrying cell culture-adaptive mutations were constructed that stably or transiently replicate efficiently in Huh-7 cells[26,27,99,172]. Despite the high levels of RNA amplification and

expression of all viral proteins, virus particle production was not obtained in these systems[34].
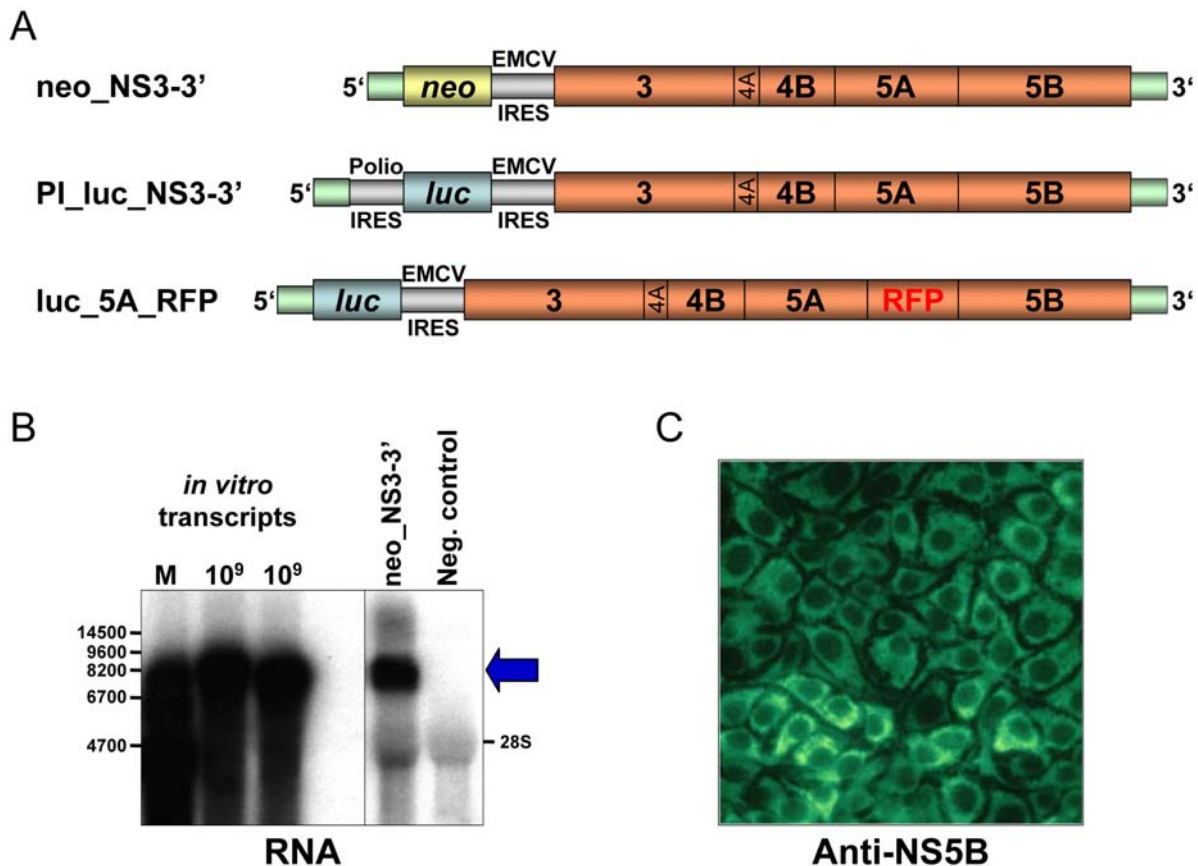
Fig. 4. Huh-7 cells harboring subgenomic replicon possess high levels of viral RNA and HCV NS proteins. (A) Structures of a selectable subgenomic replicon (top) and two different subgenomic reporter replicons (middle and bottom). All replicons contain the 5' HCV-IRES, the EMCV-IRES, directly followed by the HCV sequences from NS3 up to the authentic 3' end. The selectable replicon possesses additionally the neomycin phosphotransferase (neo) gene (top), the reporter replicons the firefly luciferase (luc) gene and the red fluorescent protein (RFP) gene fused to NS5A, respectively. In the bicistronic PI_luc_NS3-3' construct the expression of the luciferase is driven by the Poliovirus-IRES. (B) Detection of HCV RNA in Huh-7 replicon cells. Total RNA was isolated from the cells and analyzed by denaturing agarose gel electrophoresis. Replicon RNA was detected by Northern blot with a radiolabeled RNA probe complementary to the neo gene and the HCV-IRES. In vitro transcripts (10[9]) corresponding to a NS2-3' and a NS3-3' replicon were analyzed in parallel (left and right lane, respectively). The blue arrow points to HCV RNAs. Lane M, positions of RNA size markers (in nucleotides); the position of the 28S ribosomal RNA is indicated on the right. The RNA marker fragments contained HCV sequences and therefore hybridized with the RNA probe. (C) Subcellular localization of HCV NS5B in Huh-7 replicon cells was determined by immunofluorescence. NS5B was detected by a polyclonal antibody raised against NS5B. *Northern blot (B) adapted from Lohmann et al., Science, 1999*[140].

Cell culture-produced Hepatitis C Virus (HCVcc)

Studies on HCV entry were previously investigated by HCV pseudoparticles (HCVpp). These were based on retroviruses containing the HCV glycoproteins in their envelope[17,95].

In 2005, three independent groups[133,219,240] reported the production of authentic HCV particles in cell culture. All these reports were based on a genotype 2a isolate designated JFH1, that was obtained from a patient in Japan with fulminant hepatitis[107]. After RNA transfection of Huh-7 cells with full-length RNA from the JFH1 genome, viral particles infectious for naïve cells as well as for chimpanzees are released from the cells, although the titers initially were rather low[219]. Different groups reported that this hurdle could be overcome by the construction of infectious intragenotypic and intergenotypic HCV chimeras whose transfection resulted in efficient virus production[133,171]. Moreover, Lindenbach et al. demonstrated that the recombinant viruses generated in Huh7.5 cells are infectious in chimpanzees and in a mouse model, and that viruses recovered from these animals remain infectious in cultured cells[134]. These results convincingly demonstrate that HCV grown in cell culture is authentic. Lately, the production of infectious genotype 1a HCV in cultured human hepatoma cells was shown[236], demonstrating that other isolates apart from JFH1 can produce infectious viruses *in vitro*, however far less efficient.

To facilitate studies of HCV infection, different genotype 2a-based reporter viruses had been generated. Koutsoudakis and colleagues constructed JFH1-based bicistronic luciferase reporter virus genomes[119], and Schaller and coworkers inserted genes encoding fluorescent proteins (GFP) in frame into the 3'-terminal NS5A coding region resulting in fluorochrome gene-tagged viral genomes[187].

1.5 HCV life cycle

The current understanding of the HCV replication cycle is still hypothetical in parts, since the fully permissive cell culture systems allowing efficient propagation became available only recently. However, some details began to emerge due to the availability of the other *in vitro* systems discussed above. Of most importance have been replicons that recapitulate the intracellular steps of RNA replication. HCV pseudoparticles were instrumental for analyzing the early events in the infection process before the production of infectious HCV particles in cell culture became possible. The overall outline of the HCV replication cycle is depicted in Fig. 5. HCV particles interact with specific surface receptor(s), e.g. CD81, SR-BI and Claudin 1[57,174,185], and are internalized. Fusion of the viral and the cellular membranes, presumably triggered by the low pH of the endocytic compartment[95,119,212] leads to

uncoating and subsequent release of the positive-stranded RNA ((+)ssRNA) genome into the cytoplasm of a newly infected cell. This RNA first functions as messenger RNA (mRNA) for the viral protein synthesis at the rough ER. Then, the non-structural proteins form together with the viral RNA the replication complex which resides in vesicular membrane structures, the so-called membranous web (described later in detail). An EM picture of the membranous web is shown in Fig. 5. The replication complexes are responsible for the amplification of the HCV genome. Probably, the (+)ssRNA is transcribed into a negative-stranded RNA that presumably remains base-paired with its template. The resulting double-stranded RNA, the so-called replicative form (RF), is then most likely copied multiple times semi-conservatively and asymmetrically into a single positive-stranded RNA via this replicative intermediate (RI) generating a five- to tenfold molar excess over negative-stranded RNA. This hypothetical model of viral RNA replication is depicted in Fig. 5. The progeny HCV RNA genomes may be used for translation, synthesis of new RFs, or packaging into new virus particles. Newly synthesized virions probably form by budding into the ER and leave the cell through the secretory pathway.
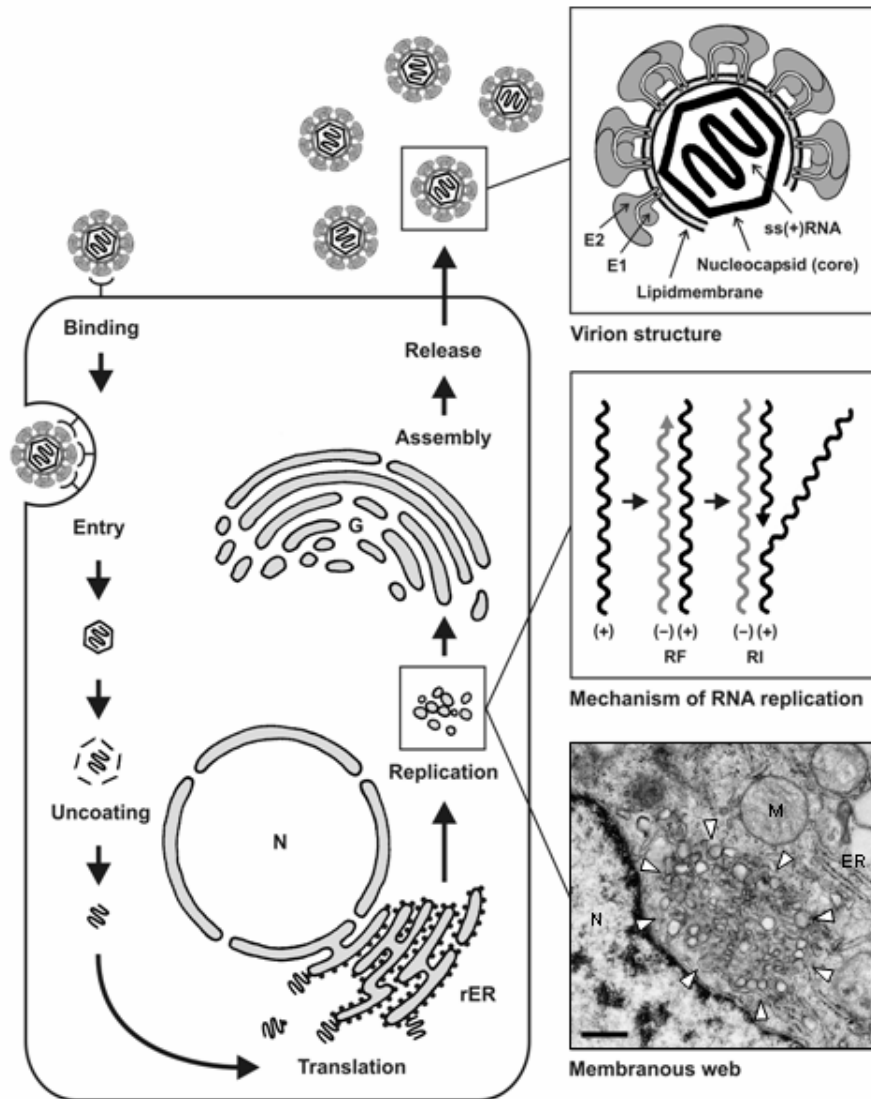
Fig. 5: Schematic diagram of HCV replication cycle. HCV binds to specific receptor(s) on the surface of the cells to gain entry. After entry into the cell and uncoating, the HCV genome serves three main roles: translation, replication and packaging into nascent virions. NS4B (perhaps in conjunction with other viral or cellular factors) induces the formation of membranous vesicles (referred to as the membranous web; electron micrograph lower right), which are supposed to serve as scaffolds for the viral replication complex. Newly produced virus particles leave the host cell by the constitutive secretory pathway. The upper right panel of the figure shows a schematic representation of an HCV particle. The envelope proteins E1 and E2 are drawn according to the proposed structure and orientation of the TBEV envelope proteins M and E, respectively. The middle panel shows a model for the synthesis of negative-strand (-) and positive-strand (+) progeny RNA via a double stranded replicative form (RF) and a replicative intermediate (RI). The bottom panel shows an electron micrograph of a membranous web (arrow heads) in a Huh-7 cell containing subgenomic HCV replicons. Bar, 500 nm. N, nucleus; ER, endoplasmic reticulum; M, mitochondria. *The electron micrograph is adapted from Gosert et al. 2003, J Virol 2003*[74]. *The diagram of HCV replication cycle is adapted from Bartenschlager et al., Adv. Virus Res., 2004*[15].

1.6 The HCV RNA Replication Complex

The RNA replication mechanism of all positive-stranded RNA viruses shows a common peculiarity. Infection of cells leads to a rearrangement of intracellular membranes[21,75,123,168,186,190,227] which is a precondition for the formation of viral

replication complexes (RCs). These membrane-associated complexes comprise the viral proteins, replicating RNA and most likely cellular host proteins that interact with their viral partners. This strategy may offer multiple advantages including (i) compartmentalization and local concentration of viral products, (ii) physical support and organization of the RNA replication complex, (iii) tethering of the viral RNA during unwinding[146], (iv) provision of lipid constituents important for replication[4,229], and (v) protection of the viral RNA from double-stranded RNA-mediated host defenses or RNA interference.

After the establishment of the replicon system (see 1.4.1) it became clear that the proteins NS3-to-NS5B are necessary and sufficient for RNA replication in Huh-7 cells harboring autonomously replicating subgenomic HCV RNAs[140]. All NS proteins are associated with ER-membranes by one or several transmembrane domains or an amphipathic α-helix, as depicted in Fig. 6. The only exception is NS3 whose membrane-connection is mediated by its cofactor NS4A.
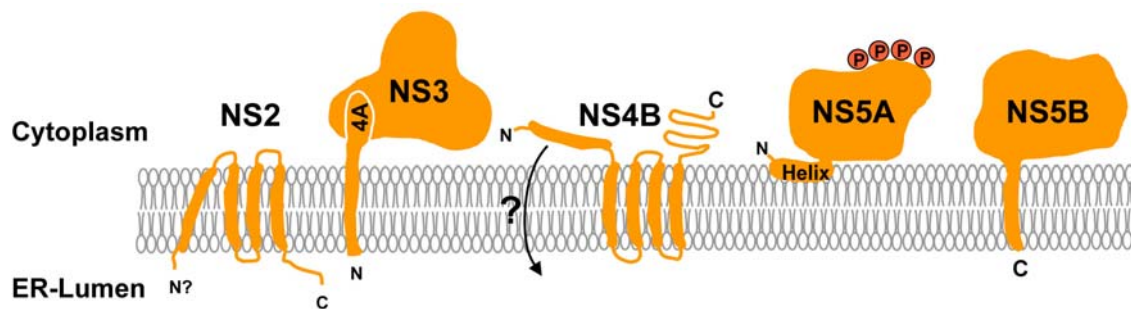
Fig. 6. Membrane topology of HCV non-structural proteins after polyprotein cleavage. The location of the N terminus and C terminus of the proteins relative to the ER lumen is given. The phosphorylation of NS5A and the amphipathic helix are indicated. Note that in the case if NS2, some molecules may also carry their N terminus on the cytosolic side. Further note that the N-terminal transmembrane domain of NS4B may have a dual topology[144]. *Adapted from Bartenschlager et. al., Adv. Virus Res., 2004*[15].

Several groups demonstrated that the membrane-interactions of the NS proteins NS4B, NS5A, and NS5B are critical for viral RNA replication[53,54,155,169]. Likewise, their interaction with each other has been extensively studied and seems to be essential for replication, too[48,100,132,176,195,196]. Together with the viral RNA, the NS proteins NS3 to NS5B form the so-called replication complex in which the replication of HCV RNA occurs.

In subgenomic replicon cells as well as in liver cells of HCV-infected chimpanzees, a specific membrane alteration was identified[51,74]. It was shown that NS4B induced this tight structure, designated membranous web, consisting of vesicles in a membranous

matrix[51]. These membranous vesicular structures were closely associated with the rough ER and contained the HCV non-structural proteins necessary for viral replication as well as viral RNA[74] Gosert and coworkers showed that the NS proteins colocalized with newly synthesized RNA (Fig. 7A). Therefore, it was assumed that the membranous web represents the HCV replication complex (RC), the site of viral RNA replication. A hypothetical model of the RC as well as an EM picture of the membranous web is shown in Fig. 7.
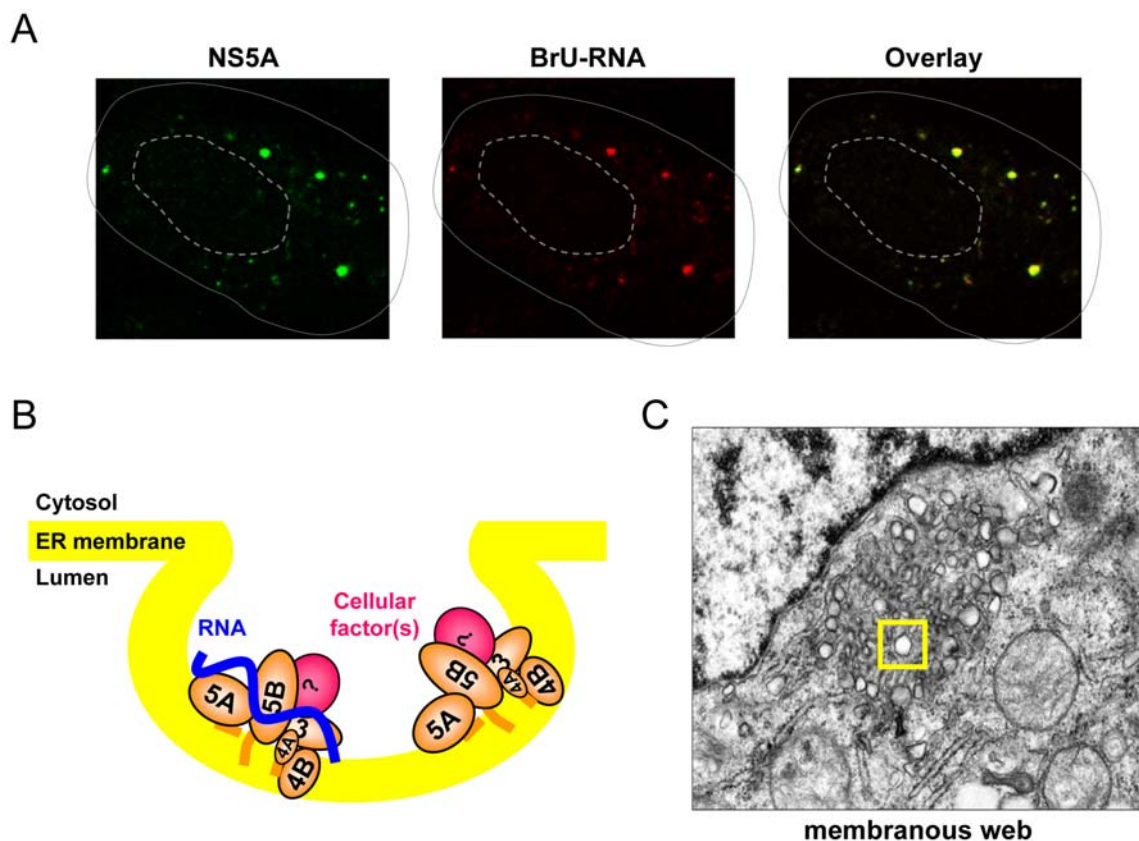
Fig. 7. (A) Colocalization of nascent HCV RNA and NS5A in Huh-7 cells harboring a subgenomic replicon. 9-13 replicon cells were metabolically labeled with 5-bromouridine 5'-triphosphate in the presence of Actinomycin D. NS5A was detected of with a polyclonal antiserum specific for NS5A and newly synthesized, bromo-uridine-labeled viral RNA with a monoclonal antibody directed against bromo-deoxyuridine. (B) Hypothetical model of the HCV replication complex. HCV NS proteins are indicated by orange ellipses, potential cellular factors by pink ellipses, and viral RNA by a blue wavy line. Individual NS proteins and RNA are not drawn to scale. (C) Electron micrograph of the membranous web, membrane alterations in Huh-7 cells containing subgenomic HCV replicons. The web is composed of small vesicles embedded in a membrane matrix and closely associated to the rough ER. These vesicular structures (one highlighted by a yellow rectangle) harbor the HCV replication complexes containing viral NS proteins and RNA and represent the site of viral RNA replication. *The immunofluorescence as well as the electron micrograph (A and C) are both adapted from Gosert et al., J Virol, 2003[74].*

One way of analyzing the properties of RCs has been the biochemical preparation of intracellular membrane fractions of HCV-containing cells by hypotonic lysis and differential centrifugation. These so-called crude replication complexes (CRCs)

contain the NS proteins and the viral RNA and exhibit distinct properties *in vitro*: upon addition of radiolabeled nucleotides, these membrane fractions are capable of RNA synthesis *in vitro*, without need of an exogenous RNA template[5]. CRCs were resistant to the detergents NP-40 and Triton X-100 at 4°C indicating that the RCs are associated with cholesterol-rich lipid rafts[5,71,193]. Positive- and negative-strand HCV RNA detected in RCs was resistant to nuclease, as well as the NS proteins were protected against proteases[5,52,153]. This resistance of RCs to enzymatic treatments was most probably mediated by membranes[153].

1.7 Known cellular cofactors of HCV replication

Viruses are obligatory intracellular parasites always exploiting host cell resources: besides using general cellular mechanisms like translation, energy supply, secretion, etc., many viruses recruit specific host cell factors for particular purposes. These host cell factors may serve as targets of antiviral therapeutics and are therefore extensively studied. A number of cellular proteins important for HCV RNA replication has already been identified by proteomic approaches, for example Y2H assays. One class of those host factors are RNA-binding proteins. Besides the ribosomal proteins, other host cell factors are also involved in the viral translation process, e.g. the La antigen and the polypyrimidine tract-binding protein (PTB). It was shown that PTB interacts with HCV NS3 and NS5B[49], whereas NS5A cooperates with the RNA-binding protein La[94]. The important role of La in the HCV replication was proven by siRNA silencing[49].

Other cellular proteins acting as cofactors of viral replication include the F-box and leucine rich protein 2 (FBL2), amphiphysin II, Vap-A, Vap-B, and cyclophilin B (CyPB).

Amphiphysin II is a multifunctional adaptor protein that is thought to act in clathrin-mediated endocytosis. The interaction of amphiphysin II with HCV NS5A was first reported in 2003[238]; furthermore, it was shown that this interplay results in a reduction of NS5A phosphorylation[149].

Cyclophilin B (CyPB) is a cyclosporine A (CsA)-binding chaperone with a peptidyl prolylisomerase (PPI) activity. It is a member of the immunophilin family of soluble cytosolic receptors and is mainly localized within endoplasmic reticulum vesicles. Cyclophilin B is secreted in response to inflammatory stimuli and interferes in

complex with CsA the T-cell activation signaling cascade. Watashi and coworkers demonstrated that CyPB functions as a positive regulator of the NS5B polymerase by directly stimulating its RNA binding activity[224]. When CyPB is targeted by CsA, the HCV genome replication is drastically suppressed.

The widely expressed F-box and Leucine rich protein 2 (FBL2) is likely involved in an ubiquitination reaction, but its substrates are not known. In its geranylgeranylated form, FBL2 interacts with HCV NS5A building a complex that is crucial for HCV RNA replication[221]. So far, the function of the interaction between NS5A and FBL2 is not known, since ubiquitination of NS5A has not been demonstrated.

Interestingly, NS5A and NS5B also interact with the human vesicle-associated-membrane-protein associated protein A(hVAP-A)[214]. hVAP-A belongs to the class of tSNARE (target-membrane soluble N-ethylmaleimide-sensitive fusion protein attachment protein receptor) proteins which are involved in intracellular vesicle transport and has been implicated in directing the non-structural proteins to cholesterol-rich, detergent-resistant membranes (rafts) on which HCV replication is thought to occur[71]. Furthermore, it was shown that an interruption of the interaction of NS5B with hVAP-A leads to a decrease in viral replication[239]. Recently, an interaction between VAP-B, NS5A and NS5B has also been described[83]. Both proteins, VAP-B in addition to VAP-A, seem to play an important role in the replication of the HCV genome.

In spite of all these already identified cellular factors involved in HCV replication, the mechanism of the viral progeny RNA synthesis still remains largely unknown. In many cases, an interaction of cellular with HCV proteins is evident and even an effect onto viral replication is demonstrated but the function of many of these interplays has to be revealed. The continuous detection of new cellular interaction partners of HCV replication leads to the assumption that the viral replication mechanism has not yet presented all its secrets. Therefore, a comprehensive picture of the structure and biogenesis of the HCV RC including its host factors is still missing.

1.8 Aim of thesis

At the beginning of this PhD thesis, the detailed composition of viral and cellular components of the replication complex was unknown.

The first aim was the characterization of enzymatically active replication complexes *in vitro* as well as the development of an appropriate purification protocol for these membrane-bound complexes. Using this protocol, I intended to identify so far unknown cellular candidate proteins associated with the replication complex and therefore probably involved in HCV replication by proteomic approaches.

Subsequently, candidate proteins found by mass spectrometry would be evaluated. Their association with viral components of the replication complex had to be analyzed intracellularly and biochemically. Furthermore, their effect onto HCV replication would be investigated.

During the second part of the PhD thesis, a quantitative analysis of the HCV replication complex was aimed. Starting from a quantitative analysis of viral RNA and protein content in HCV harboring cells, a detailed stoichiometric analysis of the HCV replication complex should be carried out. The aim was to determine the ratio of viral positive- and negative-strand RNA to proteins in replicon cells and CRCs and to analyze which portions are actively involved in viral RNA synthesis. This should provide deeper insight into the structure and composition of HCV replication complexes.

2. Materials and Methods

2.1 Materials

2.1.1 Cells

<u>Bacteria:</u>

♦ **DH5α**: F'/endA1 hsdR17($r_K^-$$m_K^+$) supE44 thi-1 recA1 gyrA (Nal^r) relA1 Δ(lacZYA-argF)U169 deoR (Φ80dlacΔ(lacZ)M15)

<u>Mammalian Cell Lines:</u>

♦ **11-1**: human hepatoma cell line with persistent HCV subgenomic replicon (NS2-3')[140]

♦ **5-15**: human hepatoma cell line with persistent HCV subgenomic replicon (NS3-3')[140]

♦ **9-13**: human hepatoma cell line with persistent HCV subgenomic replicon (NS3-3')[140]

♦ **HEK293T**: human embryonic kidney cells expressing the SV40 large T-antigen

♦ **Hep56D**: murine liver derived cell line

♦ **HepG2**: human hepatoma cell line

♦ **HuH6**: human hepatoblastoma cell line[228]

♦ **Huh-7.5**: Huh-7 cells which originally carried a selectable HCV replicon and were cured by treatment with an HCV-specific inhibitor. They are characterized by high permissiveness for HCV RNA replication[27].

♦ **Huh-7**: human hepatoma cell line[158]

♦ **Huh7-Lunet**: Huh-7 cells which originally carried a selectable luciferase HCV replicon and were cured by treatment with an HCV-specific inhibitor. They are characterized by high permissiveness for HCV RNA replication[68].

♦ **Iucubineo ET**: human hepatoma cell line with persistent HCV subgenomic replicon (Iucubineo NS3-3')[65]

♦ **Lunet-T7**: Huh7-Lunet cells constitutively producing T7 RNA polymerase from a retrovirally transduced expression cassette (T.P. and R.B., unpublished observations).

♦ **sh ANXA2 Huh7.5**: Huh-7.5 cells stably expressing a shRNA directed against ANXA2 (this work)

♦ **sh ANXA2 lunet**: Huh-7 lunet cells stably expressing a shRNA directed against ANXA2 (this work)

♦ **sh p53 Huh7.5**: Huh-7.5 cells stably expressing a shRNA directed against p53 (this work)

♦ **sh p53 lunet**: Huh-7 lunet cells stably expressing a shRNA directed against p53 (this work)

2.1.2 Media

Bacteria:

♦ **LB-Medium**: 10 g trypton, 5 g yeast extract, 5 g NaCl per 1 l medium; ampicillin was added at a concentration of 50-100 µg/ml. For hardening 1.5% agar-agar was added to the liquid medium.

Yeast cells:

♦ **YPD**: 20 g/l Difco peptone, 10 g/l yeast extract, 2% glucose, pH 6.5 with HCl. For plates 18 g/l agar was added.

♦ **SD -Leu/-Trp agar plates**: 6.7 g/l Difco yeast nitrogen base without amino acids, yeast synthetic dropout medium supplement without leucine and tryptophane (Sigma, Y-0750), pH 6.5 with NaOH; 20 g/l agar

Mammalian cell lines:

♦ **DMEM complete**: Dulbecco's modified minimal essential medium (Gibco-BRL, #41965-039; Life Technologies, Karlsruhe, Germany) supplemented with 2 mM L-glutamine, nonessential amino acids, 100 U/ml of penicillin, 100 µg/ml of streptomycin (all Gibco), and 10% fetal calf serum (FCS, Seromed, inactivated at 56°C for 30 min).
For selections, antibiotics were added in the following concentrations: 100 µg/ml G418 (Invitrogen), 10 µg/ml zeocin (Invitrogen), and 10 µg/ml blasticidin (Invitrogen).

♦ **DMEM without methionine and cysteine**: DMEM supplied with 2% dialyzed fetal calf serum; 10 mM Hepes; 2 mM L-glutamine

♦ **OptiMEM**: defined medium formulation with reduced serum (Gibco #31985)

♦ **Cryo medium**: for long term storage, cells were frozen in liquid nitrogen in 90% FCS, 10% DMSO

2.1.3 Antibodies and antisera

Primary Antibodies:

antibody	comments	Method							Company/
		WB	Dil.	IP	Dil.	IFA	Dil.	FACS	Dil.	Ordering number
α-Annexin II (ANXA2); HH7; mouse				+	10 µl/IP	+	1:100	+	1:100	Prof. Gerke; Uni Münster
α-LAMP1 (H4A3); mouse	late endosome marker					+	1:200			EMBL
α-BrdU; mouse						-	1:50			Roche; Clone BMC 9318; #1170376
α-Rab5B; rabbit										Santa Cruz SC-598
α-Annexin IV (ANXA4); K411; rabbit						+	1:50			Prof. Gerke; Uni Münster
α-p11; mouse						+	1:100			Prof. Gerke; Uni Münster

α-dsRNA; J2; mouse						-	1:50			
α-Annexin II (ANXA2); H-50; rabbit		+/-	1:500	-	6 µl/IP	+/-	1:200			Santa Cruz; SC-9061
α-Annexin I (ANXA1); mouse						+	1:100			BD #610066
α-Annexin V (ANXA5); mouse						+	1:100			Sigma A8604
α-Vap-A; rabbit		+	1:1000							
α-EEA1; rabbit	early endosome marker					+	1:300 to 1:500			Acris antibodies SP5141P
α-Annexin II (ANXA2); mouse		+	1:5000	-	10 µl/IP	+/-	1:100			BD #610068
α-Calnexin	ER marker	+	1:2000			+	1:100			Stressgen, SPA-865
α-E2; rabbit	Only used as negative control				6 µl/IP					
α-Core (C7-50); mouse		+	1:2600							
α-NS3 (new batch, NS3B 04/10/01); rabbit	Recognizes genotypes 1b and 2a	+	1:1000	+	6 µl/IP					
α-NS3 (old batch, NS3B #8); rabbit	Recognizes genotypes 1b and 2a	+	1:2500			+	1:1000			
α-NS3 (protease, 136.14.2); mouse		+	1:500							
α-NS4B (7/99; #86); rabbit	Recognizes genotypes 1b and 2a	+	1:2500	+	6 µl/IP	+	1:200			
α-NS5A (11/01); rabbit	Recognizes genotype 1b			+	6 µl/IP	+	1:100			
α-NS5A (9E10/A3); rabbit	Recognizes genotypes 1b and 2a					+	1:250			
α-NS5B (pool 2, `93); rabbit	Recognizes genotypes 1b			+	6 µl/IP	+	1:100			
α-NS5B Con (12B7.54.1); mouse	Conformational epitope									
α-NS5B Con (3B1.5.3); mouse	Linear epitope	+	1:1000							

C7-50, 5B3.5.1, and 12B7.54.1 antibodies kindly provided by D. Moradpour[154,157]; 9E10 Ab kindly provided by T. Tellinghuisen[133]; HH7, K411 and anti-p11 kindly provided by V. Gerke.

Secondary antibodies:

♦ α-mouse IgG, HRP conjugate (Sigma-Aldrich): 1:10,000 for Western Blot

♦ α-rabbit IgG, HRP conjugate (Sigma-Aldrich): 1:25,000 for Western Blot

♦ α-mouse IgG , Alexa 488 conjugate (Molecular Probes, Leiden, Netherlands): 1:1,000 for IF

♦ α-mouse IgG , Alexa 546 conjugate (Molecular Probes, Leiden, Netherlands): 1:1,000 for IF

♦ α-rabbit IgG , Alexa 488 conjugate (Molecular Probes, Leiden, Netherlands): 1:1,000 for IF

♦ α-rabbit IgG , Alexa 546 conjugate (Molecular Probes, Leiden, Netherlands): 1:1,000 for IF

♦ α-mouse IgG , PE conjugate (eBioscience, San Diego, USA): 1:200 for FACS analysis

♦ α-mouse IgG , APC conjugate (Dianova, Hamburg, Germany): 1:200 for FACS analysis

♦ α-mouse IgG , FITC conjugate (Sigma-Aldrich): 1:200 for FACS analysis

2.1.4 Vectors

♦ **pACT2-ANXA2**: NcoI-BamHI fragment from pACT2 replaced with NcoI-BamHI fragment from pTM-ANXA2 endo.

♦ **pBABE-HI-SV40-EGZ-ΔU3 shANXA2ivt**: pBABE-HI-SV40-EGZ-ΔU3-based retroviral vector[121] encoding ANXA2-specific shRNA.

♦ **pBABE-HI-SV40-EGZ-ΔU3 shANXA2mwg**: pBABE-HI-SV40-EGZ-ΔU3-based retroviral vector[121] encoding ANXA2-specific shRNA.

♦ **pBABE-HI-SV40-EGZ-ΔU3 shlacZ**: pBABE-HI-SV40-EGZ-ΔU3-based retroviral vector[121] encoding lacZ-specific shRNA.

♦ **pCMV XM:** construct encodes a chimeric protein (XM) comprising the 18 N-terminal aa of Annexin II fused to the complete p11 molecule. XM acts as transdominant mutant of the $(ANXA2-p11)_2$ heterotetramer[85]. Construct was kindly provided by V. Gerke.

♦ **pCMV-ΔR8.91**: HIV-Gag-Pol expression construct[244].

♦ **pCZ VSV-G**: CMV promoter-dependent expression construct for the expression of the G protein of the Vesicular Stomatitis Virus[105].

♦ **pECFP-N1-ANXA2-CFP**: ANXA2-CFP fusion protein expression construct[242]; CFP was fused to the C-terminus of ANXA2. Construct was kindly provided by V. Gerke.

♦ **pFK$_i$341PI-luc-EI-NS3-3'/ET**: PI_luc_ET, construct encodes bicistronic subgenomic Con1 replicon in which luciferase expression is driven by a poliovirus IRES (PI).

♦ **pFK$_i$341PI-luc-EI-NS3-3'/JFH**: PI_luc_JFH, construct encodes bicistronic subgenomic JFH1 replicon in which luciferase expression is driven by a poliovirus IRES (PI).

♦ **pFK$_i$389lucEIJFH1/J6/C-846/δg**: Jc1, bicistronic luciferase construct that encodes chimeric HCV polyprotein which consist of codons 1-846 derived from J6/CF combined with codons 847 to 3033 of JFH1.

♦ **pFK$_i$389lucEIJFH1wt/δg/ΔE1E2**: luciferase construct that encodes HCV full-length polyprotein of JFH1 but lacks the envelope proteins.

♦ **pFK$_i$389neoNS3-3'/δg/JFH/NS5A-RFP**: neo-5A-RFP, construct encodes subgenomic JFH1 replicon in which GFP is fused to NS5A.

- **pFK_i389neoNS3-3'δg/JFH/NS5A-cherry_aa383**: XbaI-PmeI fragment from pFKi389neoNS3-3'δg/JFH/NS5A-RFP_aa383 replaced with XbaI-PmeI fragment from PCR with S cherry Xba and A cherry Pme on CI cherry.

- **pGex6P ANXA2**: BamHI-SpeI fragment from pGex6P Vap-A replaced with BamHI-HindIII fragment from PCR with S ANXA2 Bam and A ANXA2 stop Spe on pTM-ANXA2 endo and HindIII-SpeI fragment from pTM-ANXA2 endo.

- **pHIT60**: CMV promoter-dependent expression construct for the expression of gag and pol protein of the Murine Leukemia Virus[200].

- **pTM NS3-5B JFH/5A-RFP**: NsiI-BsrGI fragment from pTM NS3-5B/JFH replaced with NsiI-BsrGI fragment from pFKi389neoNS3-3'/δg/JFH/NS5A-RFP.

- **pTM-ANXA2 endo**: NcoI-SpeI fragment from pTM NS4B replaced with NcoI-SpeI fragment from PCR with S ANXA2 Nco and A ANXA2 stop Spe on reverse transcribed endogenous ANXA2 sequence.

- **pTM-ANXA2-eGFP**: NcoI-AgeI fragment from pTM DV4A GFP replaced with NcoI-AgeI fragment from PCR with S ANXA2 Nco and A ANXA2 inframe Age on pEGFP-N1-A2-CFP.

- **pWPI-BLR**: KpnI-XbaI fragment from pWPI MCS replaced with KpnI-XhoI fragment from pTM BLR and with XhoI-XbaI fragment from pWPI MCS.

- **pWPI-BLR-ANXA2**: AscI-SpeI fragment from pWPI-BLR replaced with AscI-SpeI fragment from PCR with S ANXA2 Asc and A ANXA2 stop Spe on pTM ANXA2 endo.

- **pWPI-GUN-ANXA2**: AscI-SpeI fragment from pWPI-GUN replaced with AscI-SpeI fragment from PCR with S ANXA2 Asc and A ANXA2 stop Spe on pTM ANXA2 endo.

2.1.5 Oligonucleotides

Name	Sequence (5` → 3`)
A ShANXA2ivt	agcttttccaaaaaaccttatgacatgttggaaatctcttgaatttccaacatgtcataagggggg
S ShANXA2ivt	gatccccccttatgacatgttggaaattcaagagatttccaacatgtcataaggtttttggaaa
A ShANXA2mwg	agcttttccaaaaattaacagagtctacaaggatctcttgaatccttgtagactctgttaagggg
S ShANXA2mwg	gatccccttaacagagtctacaaggattcaagagatccttgtagactctgttaattttttggaaa
S ANXA2 Nco	ataccatggccatgtctactgttcacgaaatcctg
A ANXA2 stop Spe	tatactagtcagtcatctccaccacacag
A ANXA2 inframe Age	tatactagtcagtcatctccaccacacag
S mRFP Age	ataaccggtatggcctcctccgaggacgtcatc
A mRFP Spe	tatactagtttaggcgccggtggagtggcgg
S Anxa2 360 seq	gctgggaaccgacgaggactctc
S Anxa2 739 seq	gaggttaaaggagacctggaaaatg
S Anxa2 Asc	ataggcgcgccatgtctactgttcacgaaatcc
S Nhe Anxa2	gtacgctagcgccatgtctactgttcacg
S ANXA2 Bam	ctgggatccatgtctactgttcacgaaatc
S cherry Xba	aattctagagtgagcaagggcgaggagg
A cherry Pme	cacgtttaaaccccttgtacagctcgtccatgc

2.1.6 siRNAs

Name	Sequence (5` → 3`)
HCV-321	aggucucguagaccgugcatt
sip53	gacuccagugguaaucuactt
lacZ	agcuggcuggagugcgauctt
ANXA2mwg	uuaacagagucuacaaggatt
ANXA2ivt	ccuuaugacauguuggaaatt
DV 3'UTR	agaagucaggccauuacaatt

2.1.7 Buffers and Solutions

2D equilibration solution: 6 M urea; 50 mM Tris (pH 8.8); 2% SDS; 30% glycerol

2D protein solubilization buffer: 5 M urea; 2 M thiourea; 2% CHAPS; 2% SB3-10; 2 mM tributylphosphine; 0.5% IPG buffer; 1x protease inhibitor mix; 75 U/ml benzonase; trace bromophenolblue

30% Acryl amide stock solution: acryl amide and bisacrylamide were mixed in a concentration 29:1; solution was filtered and degassed before use

Bradford reagent: 100 mg Coomassie Brilliant Blue G250 solved in 50 ml 95% ethanol; add 100 ml 85% phosphoric acid; ad 1 l with H_2O; filter; store at 4°C

Coomassie destaining solution: 5% methanol; 5% acetic acid

Coomassie staining solution: 0.6 g/l Coomassie brilliant blue R250 (Serva) dissolved in 50% methanol/10% acetic acid, filtered

Core ELISA 1x washing buffer: mix 150ml 20x washing buffer concentrate with 3l deionized H_2O and add 1 bottle of urea (180 g) additive and mix carefully

Core ELISA cell lysis buffer: 1% Triton X-100 in PBS; before use add proteinase inhibitors 1 mM PMSF; 0.001 U/ml aprotinin and 4 µg/ml leupeptin

Core ELISA Conjugate solution: for 10x 10-well strips mix 170 µl conjugate concentrate with 16.83 µl conjugate diluent at least 30 min before usage

Cytomix: 120 mM KCl; 0.15 mM $CaCl_2$; 10 mM potassium phosphate buffer (pH 7.6); 25 mM Hepes (pH 7.6); 2 mM EGTA; 5 mM $MgCl_2$; pH of the solution was adjusted to pH 7.6 with KOH; before use, ATP (pH 7.6) and glutathione were freshly added to a final concentration of 2 mM and 5 mM, respectively.

DNA loading buffer: 1 mg/ml bromophenolblue blue; 2 mg/ml xylene cyanol; 1mM EDTA; 50% sucrose

FACS assay buffer: 1x PBS; 0.1% BSA (w/v); 0.005% sodium azide (w/v)

GITC solution: 4 M Guanidine thiocyanate; 25 mM sodium citrate; 0.5% sarcosyl. 0.1 M β-mercapto-ethanol (70 µl per 10 ml) was added before use, solution was then usable for one month.

Glyoxal loading buffer: 0.25 mg/ml bromophenolblue blue; 0.25 mg/ml xylene cyanol; 10 mM $NaPO_4$ (pH 7.0); 50% (v/v) glycerol

HBS (2x): 50 mM Hepes pH 7.05; 10 mM KCl; 12 mM Dextrose*H_2O; 280 mM NaCl; 1.5 mM Na_2HPO_4; pH adjusted with HCl; sterile filtration; store at -20°C.

Ligase buffer (10x): 400 mM Tris-HCl; 100 mM $MgCl_2$; 100 mM DTT, 5 mM ATP

Luciferase assay buffer: 25 mM glycyl glycine; 15 mM potassium phosphate-buffer (pH 7.8); 15 mM $MgSO_4$; 4 mM EGTA; before use, addition of 1 mM DTT and 2mM ATP

Luciferase lysis buffer: 1% Triton X-100; 25 mM glycyl glycine; 15 mM $MgSO_4$; 4 mM EGTA; storage at 4 °C; before use, addition of 1 mM DTT

Luciferase substrate solution: 1:5 dilution of 1 mM luciferin solution with 25 mM glycyl glycine solution

Methylene blue: 0.03% methylene blue; 0.3 M NaAc; pH 5.2

Mops buffer (10x): 0.4 M Mops, 0.1 M NaAc; 0.01 M EDTA; pH 7 with NaOH

$NaPO_4$ pH 7.0 (1 M): mix 423 ml 1M NaH_2PO_4 with 577 ml 1M Na_2HPO_4

Northern blot hybridization solution: 5x SSC; 5x Denhardt-Solution; 50% (w/v) formamide; 1% (w/v) SDS; after addition of 100 µg/ml salmon sperm DNA, solution was used for prehybridization

Northern blot wash I: 2x SSC; 0.1% SDS

Northern blot wash II: 0.2x SSC; 0.1% SDS

NPB buffer: 50 mM Tris/HCl (pH 7.5); 150 mM NaCl; 1% DOC; 1% NP-40; 0.1% SDS; store at 4°C. Before use add 1 mM PMSF and 1 mU Aprotinin per ml

OPD substrate solution: for 10x 10-well strips dissolve 4 OPD tablets in 24 ml substrate buffer

PBS (10x): 80 mM Na_2HPO_4; 20 mM NaH_2PO_4; 1.4 M NaCl

PCR buffer (10x): 100 mM Tris/HCl (pH 8.3); 500 mM KCl; 15 mM $MgCl_2$; 0.01% gelatin

PEG/LiAc: 40% PEG 4000; 10 mM Tris-HCl; 1 mM EDTA; 100 mM LiAc; pH 7.5

Protein sample buffer new (2x): 150 mM Tris/HCl (pH 6.8); 1.2% SDS; 30% (v/v) glycerol; 15% (v/v) β-mercapto-ethanol; 1.8 mg bromophenolblue blue

Protein sample buffer old (2x): 200 mM Tris/HCl (pH 8.8); 5 mM EDTA; 0.1% bromophenolblue; 10% (w/v) sucrose; before use add 3% SDS and 2% β-ME

Protein sample buffer old (6x): 600 mM Tris/HCl (pH 8.8); 15 mM EDTA; 0.3% bromophenolblue; 30% (w/v) sucrose; before use add 9% SDS and 6% β-ME

RC assay buffer (10x): 200 mM Tris/Cl pH 7.5; 100 mM $MgCl_2$; 50 mM KCl

RC lysis buffer: 10 mM Tris/Cl pH 7.5; 10 mM KCl; 1.5 mM $MgCl_2$; 0.5 mM PMSF; 2 µg/ml Aprotinin

RC resuspension buffer: 10 mM Tris/Cl pH 8.0; 10 mM NaCl; 15% glycerol

RNA loading buffer for formaldehyde gels: 50% (v/v) glycerol; 0.25 mg/ml bromophenolblue blue; 0.25 mg/ml xylene cyanol; 1 mM EDTA (pH 8.0)

SDS-PAGE resolving gel buffer: 1.5 M Tris/HCl pH 8.8; 0.4% (w/v) SDS

SDS-PAGE stacking gel buffer: 1M Tris/HCl pH 6.8; 0.8% (w/v) SDS

SSC (20x): 3 M NaCl; 0.3 M sodium citrate

TAE (50x): 242 g Tris; 100 ml 0.5 M Na_2EDTA (pH 8.0) and 57.1 ml glacial acetic acid. The volume was adjusted to 1 liter.

TE/LiAc: 10 mM Tris-HCl; 1 mM EDTA; 100 mM LiAc; pH 7.5

TE: 10 mM Tris/Cl (pH 8.0), 1 mM EDTA

TGS (10x): 250 mM Tris; 1.92 M glycine; 1% SDS

Thermo-Pol-Puffer (10x): 100 mM Tris/Cl (pH 8.3); 500 mM KCl; 15 mM $MgCl_2$; 0.01% gelatine

Transcription buffer RRL (5x): 400 mM Hepes (pH 7.5); 60 mM MgCl$_2$; 10 mM spermidine; 200 mM DTT

Western blot blocking buffer: 1x PBS; 0.5% (w/v) Tween 20; 2-5% milk powder

Western blot semi-dry buffer: 48 mM Tris; 39 mM glycine; 0.00375% SDS; 20% methanol

Western blot stripping solution (PVDF): 0.2 M NaOH

Western blot tank blot buffer: 20 mM Tris; 150 mM glycine; 20% methanol; store at 4°C

Western blot wash buffer: 1x PBS; 0.5% (w/v) Tween 20

Z buffer/X-gal: per 100 ml Z buffer add 270 µl β-ME and 1.67 ml [20mg/ml; in N,N-dimethyl-formamide] X-gal

Z buffer: 60 mM Na$_2$HPO$_4$; 40 mM NaH$_2$PO$_4$; 10 mM KCl; 1 mM MgSO$_4$; pH 7.0; sterile filtrated

2.2 Preparation, analysis, and manipulation of nucleic acids

2.2.1 Plasmid DNA isolation

Small scale preparations of low copy plasmid DNA were performed with the NucleoSpin® Plasmid kit from Macherey-Nagel (Düren, Germany) according to the manufacturer's protocol.

Small scale preparations of high copy plasmid DNA were performed with the NucleoSpin® Plasmid Quick Pure kit from Macherey-Nagel (Düren, Germany) according to the manufacturer's protocol.

Medium scale preparations of plasmid DNA were performed with the NucleoSpin® Plasmid kit from Macherey-Nagel (Düren, Germany). Bacteria from 80-100 ml of overnight culture were pelleted by 10 min centrifugation at 6,000 x rpm (4°C; rotor F15, FIBERLite®, Piramoon Technologies, in a Sorvall RC 5C plus centrifuge) and resuspended in 5 ml buffer A1. Then, cells were lysed by addition of 5 ml buffer A2 and incubated for 5 min at RT. After addition of 6 ml buffer A3 and further 5 min incubation at RT, solution was clarified by centrifugation for 20-30 min at 12,000 x rpm (4°C; rotor F15). The supernatant was filtered through gauze and loaded onto four NucleoSpin® Plasmid columns. These were then washed twice with AW buffer (500 µl, 50°C) and once with 700 µl buffer A4. After drying the columns, DNA was eluted twice by applying 50 µl 10 mM Tris pH 8.0 (70°C).

Large scale preparation of plasmid DNA was performed by using QIAGEN® Plasmid Maxi kit from QIAGEN (Hilden, Germany) according to the manufacturer's protocol.

2.2.2 Agarose gel electrophoresis

DNA molecules can be separated according to their size by agarose gel electrophoresis. Therefore DNA was mixed with $^{1}/_{10}$ vol 10x bromophenolblue blue loading dye and loaded onto an agarose gel. A molecular weight marker from MBI Fermentas (Lambda-DNA/Eco130I/MluI or pUC19 DNA/MspI; St. Leon-Rot, Germany) was used for comparison to determine the size of the DNA fragments. In general 1-2% agarose gels were prepared for separation of DNA fragments. 1x TAE was used as running buffer; running-conditions were 5-10V/cm. For a better separation of very small fragments, agarose concentration was increased up to 2.5%. In the case of very large fragments, it was decreased to 0.8% agarose. For visualization of the DNA, ethidium bromide was added to the gel in a final

concentration of 1 µg/ml. Gels were documented by a video supported system after radiation with UV-light (312 nm).

2.2.3 DNA extraction from agarose gels

Extraction and purification of DNA from agarose gels was performed by using the NucleoSpin® Extract II kit from Macherey-Nagel, (Düren, Germany) according to the manufacturer's protocol.

2.2.4 Phosphorylation and dephosphorylation of DNA

Linearized plasmid vectors were dephosphorylated by calf intestine phosphatase (CIP; NEB) to avoid religation. 2 U CIP per µg vector were used in the appropriate buffer, subsequently to restriction digest, for 30-60 min at 37°C. The dephosphorylated DNA was purified by a preparative agarose gel.
For the phosphorylation of synthetic oligonucleotides, the polynucleotide kinase (PNK, Amersham) was used. 150 pmol of the oligonucleotide was mixed with 1 µl 10x ligase buffer (400 mM Tris-HCl; 100 mM MgCl$_2$; 100 mM DTT, 5 mM ATP) and 2 µl [10 U/µl] PNK in a total volume of 50 µl and incubated for 1 h at 37°C. For the annealing of complementary oligonucleotides, 25 µl of each phosphorylated oligonucleotide were mixed and incubated for 5 min at 98°C. During cooling down to RT, the annealing of the single strands to a double strand fragment occurred, which subsequently could be cloned into an appropriate vector.

2.2.5 Ligation of DNA-fragments

For standard ligation 0.1 pmol of digested vector DNA and 0.3 pmol of insert were used. For achieving reaction conditions 1 µl 10x ligase buffer (MBI-Fermentas, St. Leon-Rot), 1U T4-DNA ligase (MBI-Fermentas) and water were added to a final volume of 10 µl. After incubation at RT for 2 h (or ON at 16°C) the ligation mix was added directly to competent bacteria for transformation. To avoid a high number of background colonies caused by religation of the vector, the vector DNA was incubated subsequent to the restriction digest for 30 min at 37°C in 1x reaction buffer with 2 U calf intestinal alkaline phosphatase (CIP; NEB, Frankfurt/Main, Germany) per µg linearized vector DNA, in order to dephosphorylate the 5' ends. After preparative gel electrophoresis, DNA was extracted, purified, and used for ligation.

2.2.6 Transformation of E. coli

Competent bacteria DH5α were generated by the CaCl$_2$-method. For transformation 100 µl bacteria suspension were incubated with plasmid DNA or ligation reactions for 30 min on ice. After heat shock of the cells at 42°C for 2 min, a 5 min incubation on ice followed. Cells were mixed with 1 ml of LB-medium and incubated for 20-40 min at 37°C (rocking thermo bloc). After centrifugation for 2 min at 6,000 rpm, supernatants were removed and cells resuspended in 200 µl of LB medium. After plating the cells on an antibiotic-containing LB-agar plate, colonies were grown over night at 37°C.

2.2.7 Analysis of DNA with restriction enzymes

Restriction digests of DNA were performed with enzymes from the manufacturers NEB (Frankfurt/M) and Böhringer (Mannheim). Depending on the amount of DNA, restrictions were performed in a total volume of 15 to 200 µl (≤ 0.1 µg/µl, standard: 15 µl analytic digestions, preparative digestions 100 µl). Usually, reactions were performed in 1x reaction buffer for 2 h at the recommended temperature. The amount of enzyme added to the reactions was dependent on the DNA concentration and on the unit definition given by the manufacturers. One unit of endonuclease activity is defined as the amount of enzyme that is needed to completely digest 1 µg substrate DNA (often DNA of the λ-bacteriophage) within one hour. 1 µg λ-DNA corresponds to 1/32 pmol of λ-DNA molecules. Therefore, complete digestion of 1 pmol λ-DNA within one hour is achieved when 32 units of an enzyme cutting the DNA once are added.

2.2.8 Purification and precipitation of DNA

Purification of DNA after digestion was performed by phenol/chloroform extraction. In general, the DNA was mixed with 1/10 volume of 3M NaAc pH 6.0 and extracted twice with 1 volume TE-saturated phenol and once with 1 volume chloroform (3 min, 13,000 rpm). The upper phase harboring the DNA was constantly transferred into a new tube. Finally, the DNA was precipitated by addition of 2.5 volumina ethanol. The sample was then incubated for 30 min at –20°C and centrifuged for at least 25 min at 13,000 rpm. The precipitated DNA was washed once with 70% ethanol and dissolved in an appropriate volume of water. As an alternative method the 'QIAEX II Gel extraction Kit' of Qiagen (Hilden) was used according to the manufacturer's protocol to purify and concentrate DNA in a small volume of buffer.

2.2.9 Polymerase Chain Reaction (PCR)

PCR is a method to selectively multiply a defined DNA sequence from a complex template DNA. The flanking sequences of the target DNA are used to generate a sense and an anti-sense oligonucleotide primer (usually 18-30 bp). The opposed primers are designed in a way that they surround the target sequence. The primers are used as the starting point by the polymerase for amplification. Chain elongation in 5´- to 3´-direction is yielded by addition of dNTPs. The steps of PCR amplification are as follows:

o   Heat denaturation of the double-stranded template DNA at 95°C

o   Primer annealing to the complementary sequences of the single stranded target (42-59°C)

o   Extension by the action of DNA polymerase at 68°C or 72°C (synthesis efficiency around 1 kb/min)

After primer extension the mixture is heated again to separate the strands. Cooling down the mixture allows the primers to hybridize with the complementary regions of newly synthesized DNA. Each cycle literally doubles the content of the original target DNA. In general, 20-30 cycles are run yielding a 10^6- to 10^9-fold increase of the target DNA.

The reaction mixture was prepared on ice. Each reaction contained 250 µM dNTPs (each dNTP), 1x buffer, 1 pmol/µl primer, H_2O, 100 ng-1µg template DNA (for cloning PCR) and 1 µl of polymerase (FideliTaq™) which was added in a final step. The total reaction volume usually was 50 µl. Annealing temperature and also elongation time depended on the primer composition and the length of the amplified sequence, respectively. All nucleotide sequences of PCR products were confirmed by sequencing.

Standard program for PCR:

95°C	90 s	
95°C	30 s	
42°C	45 s	3x
68°C	90 s	
95°C	30 s	
50°C	50 s	15x
68°C	90 s	
68°C	300 s	
10°C	∞	

2.2.10   Site directed mutagenesis

To introduce mutations in a nucleotide sequence, an overlap PCR[92] was performed. For each mutagenesis, two mutagenesis primers were required, one in sense, the other one in anti-sense direction. Both were complementary to each other and harbored the desired mutation. Furthermore, two primers flanking the region that will be mutated upstream and downstream were necessary. Two separated PCRs were performed. One PCR contained the upstream binding sense primer and the anti-sense mutagenesis primer, the second one the sense mutagenesis primer and the anti-sense primer binding downstream. The PCR products overlapped in the mutagenesis region, i.e. the mutagenesis primer binding sites. PCR products were purified by agarose gel electrophoresis and used for a third PCR containing the sense and anti-sense primer flanking the mutagenesis region upstream and downstream. The PCR product possessed now the mutation at the desired site and was cloned into the appropriate vector.

2.2.11   DNA sequencing analysis

Nucleotide sequences of the final constructs were confirmed by automated nucleotide sequencing using an ABI 310 sequencer (Applied Biosystems). Big dye version 1.1 (Applied Biosystems) was used for cycle sequencing according to the instruction of the manufacturer with slight modifications. 200-500 ng of plasmid DNA was mixed with 2 µl big dye mix (containing buffer, deoxy- and fluorochrome-labeled di-deoxy-nucleotides and polymerase), 1 µl sequencing primer (5 pmol/µl), 1 µl 5x buffer and water to a final volume of 10 µl. The following program was used for cycle sequencing:

95°C	10 s
55°C	15 s
60°C	240 s
10°C	∞

(30x applies to the first three rows)

To remove unincorporated dye-labeled di-deoxy nucleotides the reaction was scaled up to 100 µl containing 0.2% SDS and boiled for 5 min at 98°C. Afterwards DNA solution was mixed with 10 µl 3M NaAc and DNA fragments were precipitated with 2.5 volumina ethanol by centrifugation for 20 min at maximum speed, RT. Finally, the DNA pellet was washed once with fresh 80% ethanol, air-dried and dissolved in 20 µl formamide. Analysis of the resulting sequences was done by using vector NTI (Invitrogen).

2.2.12   Transfection of cells with plasmid DNA

DNA was transfected by Effectene (Qiagen) or Lipofectamine 2000 (Invitrogen) according to the manufacturer's protocol.

2.2.13   Quantification of DNA and RNA with absorption spectroscopy

The concentration of nucleic acid-containing solutions was determined by using spectrophotometry. A_{260} measurements are quantitative for nucleic acid preparations in microgram quantities, but absorbency readings at 260 nm cannot discriminate between DNA and RNA. The ratio of absorbance at 260 and 280nm can be used as an indicator of nucleic acid purity. Proteins for example, have peak absorption at 280 nm that will reduce the A_{260}/A_{280} ratio. Absorption at 320 nm is an indicator for particulates in the solution or dirty cuvettes. Contaminations by aromatic moieties such as phenol absorb at 230 nm. Before measurement, samples were diluted 1:50 to 1:100 with 10 mM Tris pH 8. The concentration of the sample was calculated by using the Lambert-Beersche law $C_{DNA}[µg/ml]=$ OD_{260} x ε x dilution factor. (ε_{DNA}: 40; ε_{RNA}: 50)

2.2.14   *In vitro* transcription

For the generation of defined 5'-ends either plasmids were linearized with the appropriate restriction endonucleases to prepare "run off" transcripts, or constructs were used carrying the genomic ribozyme of hepatitis δ (δg) just downstream of the 5'-end of the RNA. DNA was extracted with phenol and chloroform, precipitated with ethanol, and dissolved in RNase-free water. *In vitro* transcription reaction mixtures contained 80 mM HEPES (pH 7.5), 12 mM $MgCl_2$, 2 mM spermidine, 40 mM dithiothreitol (DTT), 3.125 mM of each nucleoside triphosphate, 1 U of RNasin (Promega)/µl, 0.05 µg of plasmid DNA/µl, and 0.8 U of T7 RNA polymerase (Promega)/µl. After 2 h at 37°C, an additional 0.4 U of T7 RNA polymerase/µl was added, and the reaction was incubated for another 2 h. Transcription was terminated by the addition of 1.2 U of RNase-free DNase (Promega) per µg of plasmid DNA and a 30 min incubation at 37°C. After extraction with acidic phenol and chloroform, RNA was precipitated with

isopropanol and dissolved in RNase-free water. The concentration was determined by measurement of the optical density at 260 nm, and the RNA integrity was checked by denaturing agarose gel electrophoresis.

To generate α-^{32}P-radiolabelled riboprobes for Northern hybridization, 0.5 µg linearized, phenol/chloroform extracted DNA was added to 4 µl 5x transcription buffer RRL, 2 µl 100 mM DTT, 40 U RNasin, 2 µl 5 mM non-radioactive NTP mix (ATP, GTP, UTP), 2 µl 100 µM non-radioactive CTP, 5 µl 50 µCi α-^{32}P-CTP and 1 µl T3- or T7-RNA polymerase in a total volume of 20 µl. The mixture was incubated for 1 h at 37°C. Afterwards DNA, was degraded by addition of 1 µl DNase and the probe was cleared from non-incorporated nucleotides by using a Sephadex G25 column (Amersham). The probe was eluted from the column with 1 ml H_2O according to the manufacturer's protocol.

2.2.15   RNA transfection by electroporation

Single cell suspensions of naïve Huh7-Lunet cells were prepared by trypsinization of monolayers, and subsequent resuspension with DMEM complete. Cells were washed with PBS, counted, and resuspended at 10^7 cells per ml in Cytomix containing 2 mM ATP and 5 mM glutathione. Unless otherwise stated, 10 µg of *in vitro* transcribed RNA was mixed with 400 µl of the cell suspension by pipetting, electroporated, and immediately transferred to 12-20 ml of complete DMEM. Electroporation conditions were 960 µF and 270 V by using a Gene Pulser system (Bio-Rad, Munich, Germany) and a cuvette with a gap width of 0.4 cm (Bio-Rad). Transfected cells were harvested at different time points and analyzed by Northern blot, luciferase assay or FACS.

For selection of cell lines with persistent replicons, 1 µg in vitro transcript of a selectionable replicon was transfected and the cells seeded after electroporation in 20 ml complete DMEM on a 15 cm dish. 24 h after electroporation medium was replaced by DMEM complete containing the appropriate antibiotic and changed weekly until resistant colonies appeared. These colonies were either picked or unified and passaged until enough cells were present for cell stocks.

2.2.16   RNA formaldehyde gel electrophoresis

To obtain 100 ml of a 1% gel, 1 g agarose was dissolved in 72 ml of water by boiling and then cooled down to 60°C. Before gel polymerization, 10 ml 10x MOPS buffer and 18 ml 12.3 M formaldehyde were added. For preparation of the samples, 3 µl of *in vitro* transcript were mixed with 2.5 µl 10x MOPS buffer; 4.5 µl 12.3 M formaldehyde and 12.5 µl formamide in a total volume of 25 µl and incubated for 15 min at 55°C. Then the mixture was incubated for 5-10 min at RT and 1.5 µl ethidium bromide solution (10 mg/ml) was added. After further 5 min incubation time, 10 µl RNA loading dye was added and the sample was loaded onto the gel. Electrophoresis was performed in 1x MOPS-buffer at 5 V/cm.

2.2.17   Total RNA isolation from eukaryotic cells

Total RNA from mammalian cells was prepared by a single-step isolation method as previously described[40]. Briefly, 1×10^7 cells were lysed with 750 µl of GITC solution. Pipetting the solution up and down sheared the genomic DNA. Then $^1/_{10}$ volume 2 M NaAc (pH 4) and 1 volume acidic phenol were added to the mixture. After addition of $^1/_5$ volume chloroform, the mixture was vortexed and incubated on ice for 15 min. The phases of the milky solution were separated again by 10 min centrifugation at 13,000 rpm, 4°C, and the RNA containing upper phase was transferred into a new tube. During this step, the interphase should not be swirled up, since it contains the degraded DNA. Now the RNA was precipitated by addition of 1 volume isopropanol. After 30 min incubation at minus 20°C, the RNA was pelleted by centrifugation for 15 min at maximum speed, 4°C. Finally the pellet was washed once with 70% ethanol and dissolved in an appropriate volume of water (25 µl for 6 cm dish). The RNA was stored at -70°C, whereas 2 µl of it were used for quantification.

For quantitative RT-PCR, total RNA from eukaryotic cells was prepared by using the NucleoSpin RNA II kit from Macherey-Nagel (Düren, Germany) according to the manufacturer's protocol.

2.2.18   RNA glyoxal gel electrophoresis

Denaturing glyoxal agarose gel electrophoresis was performed for Northern blot analysis or *in vitro* replicase activity assays. 1% agarose was solved in H_2O, then $NaPO_4$ pH 7.0 to final concentration of 10 mM was added. During sample preparation, up to 10 µg RNA in a volume of 10 µl were mixed with 4.1 µl 100 mM $NaPO_4$ pH 7.0, 6 µl 6 M deionized glyoxal, and 20.5 µl DMSO (no premix!), incubated at 50°C for 1 h, briefly cooled on ice, and mixed with 10.9 µl glyoxal loading buffer. 25 µl of the sample were loaded onto the gel. Electrophoresis was performed in 10 mM $NaPO_4$ pH 7.0 at 4V/cm gel. To keep the pH constant, the buffer was mixed by magnetic stir bars from 5-10 min after begin of the electrophoresis until its end.

2.2.19   Northern blot analysis

To determine the quantity of HCV RNA within total cellular RNA, Northern hybridization was performed using α-^{32}P CTP labeled complementary riboprobes. Total RNA was prepared by a single-step isolation method as described previously (paragraph 2.2.13). Up to 10 µg of total RNA in 10 µl H_2O were mixed 4.1 µl 100 mM $NaPO_4$ ph 7, 6 µl 6M glyoxal, and 20.5 µl DMSO, and denatured for 1 h at 50°C. Samples were mixed with 10.9 µl glyoxal RNA loading dye and separated by denaturing agarose gel electrophoresis. RNA was transferred to positively charged nylon membranes (Hybond-N+; Amersham Biosciences, Freiburg, Germany) with 50 mM NaOH (0.2 bar low pressure for 1 h, vacuum transfer machine from Keutz, Gießen) and cross-linked by UV-irradiation. For prehybridization of the membrane, it was incubated for 15 min at 58°C in hybridization solution containing salmon sperm DNA. Positive-strand HCV RNA was detected by hybridization with α-^{32}P-labeled negative-sense riboprobe complementary to nt 5979 to 6699 of the HCV JFH1 isolate (pBSK$^-$ C1 5979-6699 x KpnI $\rightarrow$ T3) in hybridization solution at 58°C ON. Negative-strand HCV RNA was detected by

hybridization with α-^{32}P-labeled positive-sense riboprobe complementary to nt 5979 to 6699 of the HCV JFH1 isolate (pBSK⁻ C1 5979-6699 x EcoRI → T7). Hybridization with a β-Actin-specific riboprobe was used to monitor equal sample loading in each lane of the gel (pBSK β-Actin x HindIII → T7). Membranes were washed twice with 2x SSC/0.1% SDS for 15 min at 58°C, and then washed twice with 0.2x SSC/0.1% SDS for 15 min at 58°C (additional third wash at 80°C for 15 min possible to reduce background), briefly dried and signals were detected by autoradiography.

As quantity standards for the positive-strand RNA served defined numbers (10^9, 10^8, and 10^7 RNA molecules per 25 µl) of *in vitro* transcripts of pFKi389neoNS3-3'/ET (x AseI x ScaI → T7) and for the negative-strand RNA served *in vitro* transcripts of pFKi389neoNS3-3'/5.1 (x AscI → T3).

2.2.20   HCV RNA quantification by RT-PCR

For quantitative analysis of HCV RNA from HCV-harboring cells RT-PCR, RNA was prepared by using "NucleoSpin® RNA II" columns (Macherey-Nagel, Düren, Germany), and eluted in a volume of 40 µl RNase-free water. Concentration of the RNA was determined spectrometrically and adjusted to 0.1 µg/µl. Five microliter of the respective sample was used for quantitative RT-PCR analysis employing an ABI PRISM 7000 Sequence Detector (Applied Biosystems, Darmstadt, Germany). Amplifications were conducted at least in duplicate with the One Step RT-PCR Kit (Qiagen, Hilden, Germany) using the following primers and 3′-phosphate-blocked, 6-carboxyfluorescine (6-FAM)- and tetrachloro-6-carboxyfluorescine (TAMRA)-labeled probes (TIB Molbiol, Berlin, Germany): HCV-Con1 Taqman probe, 5′-6FAM-TCC TGG AGG CTG CAC GAC ACT CAT-TAMRA-3′; HCV-Con1-S66, 5′-ACG CAG AAA GCG TCT AGC CAT-3′; and HCV-Con1-A165, 5′-TAC TCA CCG GTT CCG CAG A-3′; HCV-JFH1 Taqman probe, 5′-6FAM-AAA GGA CCC AGT CTT CCC GGC AA-TAMRA-3′; HCV-JFH1-S147, 5′-TCT GCG GAA CCG GTG AGT A-3′; HCV-JFH1-A221, 5′-GGG CAT AGA GTG GGT TTA TCC A-3′. GAPDH S 5'-GAA GGT GAA GGT CGG AGT C-3'; GAPDH A 5'-GAA GAT GGT GAT GGG ATT TC-3'. Reactions were carried out in three stages exactly as already described[172].

For SYBR green based qRT-PCR, the QuantiTect SYBR green kit from Qiagen was used and gene specific primer pairs were designed and ordered from MWG. The reaction mix was set up to the manufacturer's recommendation but scaled down to 15 µl (1.5 µl total RNA). Reactions and detections were performed using an ABI PRISM 7000 Sequence Detector (Applied Biosystems). The passive dye ROX had to be disregarded due to the small volume. ANXA2 SYBR green primer: ANXA2 SYBR S 5'-GCCATCAAGACCAAAGGTGT-3'; ANXA2 SYBR A 5'-TCAGTGCTGATGCAAGTTCC-3'. GAPDH primers see above.

Each gene was typically measured in triplicates in each RNA sample. For data evaluation, in most cases, automatic detection of baseline and threshold values was used. Resulting C_t values for a target gene were subtracted from the C_t value of the GAPDH gene in the same sample RNA to yield the ΔC_t value. To compare expression levels of a given gene between several RNA samples (cell lines), the average difference between their ΔC_t values was calculated, $\Delta\Delta C_t$, and, for the sake of easier interpretation, delogarithmized using a base of 2, assuming an idealized PCR reaction (doubling the product level in every cycle). Error bars in diagrams represent the limits of the standard deviation as

calculated on basis of the ΔC_t values and only subsequently delogarithmized. They can therefore be looked at as conservative estimates of the standard error.

2.3 Expression, purification, and analysis of proteins

2.3.1 Isolation of HCV replication complexes

Replicon cells showing an 80-90% confluency were washed once with PBS, scraped in PBS (2 ml per 15 cm dish) and pelleted at 800 g (4°C, 10 min). Cells were resuspended to a density of 2.5 x 10^7 cells/ml in hypotonic buffer (10 mM Tris/Cl pH 7.5; 10 mM KCl; 1.5 mM $MgCl_2$; 0.5 mM PMSF; 2 µg/ml Aprotinin) and lysed by 75 strokes with a dounce homogenizer. Nuclei and unbroken cells were removed by centrifugation at 1,000 x g for 10 min at 4°C. The intracellular membranes in the resulting supernatant (S1) were then sedimented on 300 µl of 60% (w/w) sucrose in 10 mM Tris-HCl (pH 7.5), 10 mM KCl, 1.5 mM $MgCl_2$ in an ultracentrifuge at 71,000 x g for 1h at 4°C. The resulting supernatant (S2) was carefully removed, the membrane fraction containing the CRCs was resuspended in the sucrose cushion to obtain ca. 500 µl CRC fraction from $2x10^8$ cells. Total protein concentrations of standard CRC preparations are in the range of 5 mg /ml CRC. Alternatively, S1 obtained from $2x10^8$ cells was directly pelleted for 1 h at 71,000 x g, resuspended in 200 µl 10 mM Tris-HCl, pH 8.0, 10 mM NaCl, 15% glycerol to obtain the CRC fraction and stored in aliquots at -70°C.

2.3.2 Sucrose density gradient centrifugation

Resuspended CRCs that were sedimented on a sucrose cushion were loaded under a continuous 15-60% (w/w) sucrose gradient (sucrose in 10 mM Tris-HCl (pH 7.5), 10 mM KCl, 1.5 mM $MgCl_2$) and spun in an ultracentrifuge at 71,000 x g for 16 h at 4°C. The gradient was aliquoted in 1 ml fractions whose density was determined by their index of refraction using a refractometer. Glycerol was added to an end concentration of 15%, before the fractions were stored at -70°C.

2.3.3 Bradford assay for protein quantification

Using this method, protein amounts ranging from 1-10 µg can reliably be quantified. 5 µl of a sample were filled up to 100 µl with an appropriate buffer, mixed with 1 ml Bradford reagent, and incubated at RT for 2 min. 100 µl buffer was used as blank value and incubated in the same way. To generate a standard curve, BSA was used in serial dilutions (1-20 µg). Absorption was measured at 595 nm and was correlated with the protein amount via the standard curve. Measurement was performed using duplicates.

2.3.4 SDS polyacrylamide gel electrophoresis (SDS-PAGE)

Proteins can be separated by their molecular weight under denaturing conditions in a sodium dodecyl sulfate polyacrylamide gel. Therefore, gels were made using an acryl amide concentration of between 8 and 12% for the resolving gel. The acryl amide/bisacrylamide amide solution was a 30% stock solution, containing a 29:1 composition of acryl amide: bisacrylamide amide. The polymerization reaction was started after addition of 1/1,000 volume TEMED and 1/1,000 volume saturated ammonium persulphate to the separating gel and it was poured immediately into gel casts. 5 ml of isopropanol was applied to remove air bubbles, and the gel was left to set for around 30 minutes. The stacking gel contained 5% acryl amide stock solution. Protein samples were denatured in protein sample buffer for 5 min at 95°C before loading onto the gel. Electrophoresis was performed in 1x TGS buffer at a steady current of 45 mA. To estimate the molecular weight of the sample proteins, a protein standard designated "Prestained Protein Marker" (NEB, Schwalbach) was used for comparison. This standard was composed of a mixture of proteins with defined molecular weight. After electrophoresis, proteins were transferred onto a PVDF or nitrocellulose membrane for western blot analysis (described below in paragraph 2.3.5) or were stained with Coomassie blue solution for 20 min at 60°C. Thereby proteins were fixed within the gel. For destaining, gels were incubated for 20 min at 60°C in a 5% methanol/5% acetic acid solution. For analysis of immunoprecipitated or radiolabeled proteins, the separating gel was dried and signals were detected by autoradiography.

2.3.5 Western blot

Proteins were separated by SDS-PAGE and after electrophoresis transferred to a polyvinylidene difluoride membrane (PVDF) (PolyScreen; NEN Life Science Products, Zaventem, Belgium) or nitrocellulose (Protran®, Whatman Schleicher & Schuell) using a semidry blotter (Bio-Rad, Munich, Germany). Blotting conditions were $1mA/cm^2$ for $\geq$ 1 h. Membranes were incubated at least 1 h in blocking buffer (PBS containing 0.5% Tween 20 and 5% milk powder [w/v]) to saturate unspecific binding sites, and a primary antibody was added thereafter at a given dilution for 1 h (for dilutions of antibodies see Table in paragraph 2.1.3). After being washed three times with 0.5% Tween 20 in PBS, the membrane was incubated with a secondary antibody conjugated with horse radish peroxidase (Sigma-Aldrich) in blocking buffer for 1 h and washed three times as described above. Bound antibodies were detected by chemiluminescence using luminol and a specific enhancer (SuperSignal West Dura Extended Duration Substrate; KMF Laborchemie, St. Augustin, Germany) or the ECL[+]-system (Amersham) according to the manufacturer's protocol. Chemiluminescence was detected by exposure to X-ray films.

2.3.6 Proteinase K, S7 nuclease and Triton X-100 treatment of CRCs

To test the protease and nuclease resistance of the CRCs, different amounts of [20 mg/ml] proteinase K (Sigma; 0.8 or 8 mg/ml final concentrations) and/or S7 nuclease (0.2 or 2 U/µl final concentrations; together with 1 mM $CaCl_2$) and/or 1% (v/v) Triton X-100 were directly added to 50 µl of freshly prepared CRCs and incubated for 60 min at 25°C. After the incubation, proteinase K and S7 nuclease

were inactivated by the addition of 1 µl 100 mM PMSF and 1 µl 200 mM EGTA, respectively. 4 µl CRCs were directly analyzed by *in vitro* replicase assays, 2 µl were mixed with protein sample buffer and analyzed by SDS-PAGE and immunoblot. 10 µl CRCs were used for total RNA-preparation. Total RNA was dissolved in 10 µl water and 5 µl were subjected to Northern blot analysis.

Fivefold concentrated fractions of proteinase K treated CRCs were generated by TCA precipitation.

2.3.7 TCA precipitation

The sucrose and glycerol concentration of CRC fractions were diluted at least twofold by addition of RC lysis buffer. This fraction was then mixed with 1 volume 100% TCA (trichloroacetic acid) and $^1/_5$ volume 20% SDS (end concentration 2%). After incubation for 1 h on ice, protein precipitates were pelleted for 20 min at 10,000 g (4°C). The supernatant was removed qualitatively. Pellets were solved in an appropriate volume of protein sample buffer by shaking for 10 min at RT. After solving, samples were denatured at 95°C for 5 min and then analyzed by SDS-PAGE.

2.3.8 2-dimensional gel electrophoresis

Sample preparation

CRCs were prepared from 2×10^8 cells (replicon 9-13 or cured cells as negative control) by sedimentation of the intracellular membranes onto a sucrose cushion. This fraction was then treated with Proteinase K (final: 8 mg/ml) for 60 min at 25°C. After the incubation, proteinase K was inactivated by the addition of 1 µl 100 mM PMSF per 50 µl CRC fraction. This fraction was then subjected to sucrose gradient centrifugation and subsequently aliquoted into 1 ml fractions. The fractions were analyzed for density and protein amounts (by Bradford) as well as for *in vitro* replicase activity. The fraction containing most *in vitro* replicase activity and proteins was combined with its neighboring fractions and diluted with RC lysis buffer to reduce the sucrose concentration. The therein comprised intracellular membranes were pelleted by ultracentrifugation at 284,300 g for 60 min. The pellet was lysed in 500 µl 2D protein solubilization buffer (for 4 ml: 608 mg thiourea; 80 mg CHAPS; 80 mg SB3-10; 2.32 ml 8.5 M urea solution (deionized); 40 µl 100x protease inhibitor mix (2D compatible, Sigma); 100 µl tributylphosphine (2D compatible, Sigma); 40 µl IPG buffer pH 3-11NL (Amersham); 300 U benzonase; ad 4 ml H_2O (caution: very small volume needed!)) by vortexing and incubated for 60 min at RT with regular vortexing. Then iodoacetamide was added to final concentration of 15 mM (15 µl of a freshly prepared 500 mM solution) and incubated for additional 90 min. Insoluble material was pelleted during 30 min at 100,000 g in a bench top ultracentrifuge (Beckman TL-100) and the cleared supernatant was collected.

Isoelectric focusing

IPG strips (Amersham 3-11NL) were loaded passively during rehydration. 1000 µg protein sample in 350 µl 2D protein solubilization buffer were loaded in a strip holder, the IPG strip was placed on top, gel-side down, and overlaid with 2D mineral oil. After 10 h of rehydration, moist wedges of Whatman paper were placed between the ends of the strip and the electrodes to ensure conductivity. Then,

isoelectric focusing was performed in an IPGphor II unit (Amersham) using the following voltage scheme: 0 h 300 V – 3 h gradient to 3,500 V – 3 h 3,500 V – 12 h 5,000 V.

Strip equilibration

After isoelectric focusing, strips were either drained and frozen at -80°C or processed directly. Equilibration was done in two steps. In the first step 10 ml of 2D equilibration buffer were used per strip, supplemented with 2% DTT for reduction of thiol groups. The strip was incubated for 10 min, gently shaking in this solution. The first equilibration solution was discarded and the strip drained and then placed for 10 min into 10 ml of fresh 2D equilibration solution, supplemented with 2.5% iodoacetamide for alkylation of the reduced thiol groups, preventing unspecific disulfide-bridge formation. Afterwards, the strip was drained and ready for loading on the second dimension gel.

2nd dimension electrophoresis

Second dimension electrophoresis was standard SDS-PAGE. A 30x20 cm gel was prepared (typically 10% polyacrylamide) without SDS; gels were 1 mm thick; no stacking gel (and no comb) was needed. The strip was carefully placed on the top surface of the polymerized gel plastic backing facing the glass plate. The strip was then overlaid with 0.5% high purity agarose in TGS to fix its position. 15 µl of prestained protein marker (NEB) were applied to a 0.5x1 cm piece of Whatman paper, which was then stuck into the agarose overlay next to one end of the IPG strip. The gel was run in standard TGS buffer at 45 mA per gel for 5-6 h until dye front reached the end of the gel. Gels were the fixed, silver stained and sealed in clear plastic foil. Protein spots of interest were investigated by mass spectrometry analysis in the Core Facility for Mass Spectrometry and Proteomics at the ZMBH, Heidelberg.

2.3.9 Silver staining of proteins after SDS-PAGE

Gels were fixed ON (or at least 1 h) in fixation solution 1 (50% methanol, 12% acetic acid). Then, they were fixed once for 30 min in fixation solution 2 (10% ethanol, 5% acetic acid) and twice for 15 min in fixation solution 3 (10% ethanol). Subsequently, gels were impregnated for 2 min in 0.0185% formaldehyde and 0.018% sodium thiosulfate and washed three times in H_2O for 60 s. The gels were then stained with 0.2% silver nitrate and 0.0185% formaldehyde for 12 min. After washing twice with H_2O for 30 s, the stain was developed in developer solution (3% sodium carbonate; 0.0185% formaldehyde; 0.000258% sodium thiosulfate) until staining intensity was as desired. Developing was stopped by addition of acetic acid directly to the developing solution (3%) and cooling on ice. The gel was then washed in 3% acetic acid and put in 3% acetic acid for longer term storage.

2.3.10   HCV replicase activity assay

HCV *in vitro* replicase activity was determined in a reaction mixture containing 20 mM Tris-HCl (pH 7.5), 10 mM MgCl$_2$, 5 mM DTT, 5 mM KCl, 40 µg/ml Actinomycin D, 20 µCi α-[^{32}P]CTP, 10 µM CTP, 1 mM each of ATP and UTP, 5 mM GTP, 2.5 mM phosphoenol pyruvate, 1 U pyruvate kinase (Sigma,

Taufkirchen, Germany), 1 U of RNasin, and 4 µl sample fraction in a total volume of 10 µl at 35°C for 60 min. A radioactively labeled *in vitro* transcript corresponding to the length of a replicon RNA was used to determine the size of the reaction products. This length standard was generated by radiolabeled run-off transcripts of pFKi389neoNS3-3'/ET (x AseI x ScaI). In a total volume of 20 µl, 0.5 µg linearized template DNA were incubated with 4µl 5x transcription buffer RRL buffer (400 mM Hepes (pH 7.5); 60 mM $MgCl_2$; 10 mM spermidine; 200 mM DTT), 0.5 µl RNasin, 2.5 µl 25mM NTPs, 0.5 µl [α-^{32}P]-CTP, and 1 µl T7 RNA polymerase, for 1 h at 35°C. After adjusting the volume of the samples with RC lysis buffer to 100 µl, reaction products were purified by phenol/chloroform extraction (1:1 mix, 1 vol) and isopropanol precipitation (0.7 vol) and analyzed by denaturing glyoxal agarose gel electrophoresis followed by autoradiography.

2.3.11   Metabolic ^{35}S-labeling of proteins

Lunet-T7 cells were seeded in 6-well plates and transiently transfected with T7 promoter dependent expression constructs encoding the Con1-derived NS proteins NS3-5B proteins or an individual NS protein, or the empty vector (pTM1) by Lipofectamine™ 2000 (Invitrogen) according to the manufacturer's protocol. 4 h after transfection, cells were washed with DMEM without methionine and cysteine (DMEM; 2% dialyzed fetal calf serum; 10 mM Hepes; 2 mM L-glutamine) and then incubated in this medium for 60 min at 37°C (starving phase). Subsequently, medium was exchanged for DMEM without methionine and cysteine containing 100 µCi ^{35}S per ml. Cells were incubated for 4-6 h at 37°C, then cells were washed with PBS and lysed for the subsequent immunoprecipitation by NPB buffer or 0.5% TX-100 in PBS.

2.3.12   Immunoprecipitation

50 µl per IP of a 1:1 slurry of protein A (for polyclonal antibodies) or protein G (for monoclonal antibodies) Sepharose™ beads (Amersham Biosciences, Munich, Germany) were washed thrice in lysis buffer (NPB or 0.5% TX-100 in PBS) for equilibration (6,000 *g*, 4°C). Then they were incubated ≥2 h at 4°C with the antibodies on a rotating wheel in lysis buffer (per IP: 6 µl polyclonal; 10 µl monoclonal) and afterwards washed three times. Equal amounts of cell lysates were incubated at 4°C for ≥2 h with equal amounts of protein A or G beads coupled with the antibodies. Subsequently, beads were washed three times with lysis buffer and bound proteins were resolved by 10% SDS-PAGE. Finally, in case of metabolic ^{35}S-labeling, gels were dried and subjected to autoradiography or, in case of replicon cells, proteins were transferred to a PVDF membrane and detected by immunoblot assay.

For stabilization of weak or transient protein interactions, cells were treated with the crosslinker DSP (Pierce). DSP was dissolved immediately before crosslinking in DMSO (20 mM). Cells were washed twice with PBS, and then DSP was added to a final concentration of 2 mM (in PBS) and incubated for 30 min at RT. To stop the reaction , stop solution (1 M Tris pH 7.5) was added to final concentration of 20 mM and incubated for 15 min at RT. Cells were washed once with PBS and lysed in NPB.

2.3.13   Transient silencing by siRNA

Cells were transfected with siRNA by Lipofectamine™ 2000 (Invitrogen) or HiPerFect (QIAGEN). siRNA transfections of cell culture dishes up to 10 cm dishes by Lipofectamine™ 2000 were performed according to the manufacturer's protocol but using 2.5 fold more siRNA and 1.5 fold more Lipofectamine reagent than recommended.

15 cm dishes were transfected with siRNA by HiPerFect as following:

4.8 µl [100 pmol/µl] siRNA were diluted in 2.4 ml DMEM without FCS (final 25 nM siRNA). Then 96 µl of HiPerFect reagent were added, mixed, and incubated for 5-10 min at RT. This solution was then added dropwise to the cells which were incubated for up to 3 d at 37°C.

2.3.14   Immunofluorescence analysis (IF)

In general, cells were seeded on cover slips in 24-well plates to be confluent at the time point of fixation. For infection, naïve cells were seeded on cover slips in 24-well plates at a density of 2×10^4 per well 24 h prior to infection, followed by inoculation with 250 µl of filtered cultured supernatant for 4 h. Transiently transfected cells were seeded on cover slips directly after electroporation (250 or 500 µl of cell suspension). For fixation, cells were washed three times with PBS and fixed in 4% paraformaldehyde solution for about 10 min at RT. Thereafter, cells were again washed three times with PBS and then stored for 2-3 days at 4°C or directly used for further preparation. For permeabilization, cells were incubated for 5 min with 0.5% Triton X-100 in PBS and washed 3 times with PBS prior to incubation with the first antibody. The primary antibody was diluted to the desired concentration with a 1x PBS buffer containing 3% BSA, to prevent unspecific binding of the antibody. After 45 min incubation at RT the cells were washed 3 times with PBS and incubated with the second antibody. This antibody was conjugated with fluorescent dyes (Alexa 488, Alexa 546) again diluted in 3% BSA in PBS. After 30 min incubation in the dark, the cells were washed once with PBS and counterstaining of the nucleus was performed using DAPI (4', 6'-diamidino-2-phenylindole; Molecular Probes, Karlsruhe, Germany). To this end, the cells were incubated for 1 min with a 1:4,000 diluted DAPI solution and immediately washed 3 times for 10 min with PBS. Finally, the cells were washed once with water and mounted on glass slides with Fluoromount G.

2.3.15   Flow cytometry analysis

For analyses of ANXA2 and HCV expression in silenced cells, cells were silenced twice by siRNAs. First silencing was performed using HiPerFect (Qiagen), second silencing was performed by co-electroporation of siRNA (1000 pmol per electroporation) and HCV sg replicon RNA (10 µg; luc-JFH/5A-eGFP). Cell monolayers were treated with PBS/0.2% EDTA to prepare single cell suspensions which were washed with PBS (700 rpm, 5 min) and passed through a cell strainer. Cells were fixed in 4% PFA (10 min, RT), stored at 4°C or directly used for antibody staining.

Staining of fixed cells

Fixed cells were washed with PBS (4,000 rpm, 4 min, 4°C; in eppendorf table top centrifuge) and incubated with the first antibody (α-ANXA2, Gerke) diluted in PBS/0.5% saponin (500,000 cells per 100 µl) on ice for 1 h. Permeabilization of the cells occurred during this incubation step. Cells were washed once with PBS and then incubated with the secondary fluorescence-coupled antibody (allophycocyanin, APC) diluted in PBS/0.5% saponin (500,000 cells per 100 µl) on ice for 1 h in the dark. Cells were washed twice with PBS, were resuspended in 200-500 µl PBS and analyzed immediately using a FACScan or FACSCalibur apparatus (BD Biosciences) and Cell Quest Pro software (Becton Dickinson).

2.3.16 Luciferase assay

For assaying the luciferase activity, cells were washed once with PBS, lysed directly on the plate in ice cold lysis buffer (500 µl/6-well; 350 µl/12-well) and frozen. Upon thawing, lysates were resuspended by pipetting and 100 µl were mixed with 360 µl of assay buffer and, after the addition of 200 µl of a 200 µM luciferin solution, measured in a luminometer (Lumat LB9507; Berthold, Freiburg, Germany) for 20 s. All luciferase assays were done in duplicate measurements.

2.3.17 Competence induction and transformation of yeast cells

Y2H assays were performed according to the MATCHMAKER Two-Hybrid System 2 protocol (CLONTECH Laboratories).

Briefly, a 50 ml YPD culture was inoculated with several colonies (2-3 mm in diameter) of the yeast strain Y187 and incubated at 30°C for 16-18 h. 250 ml fresh YPD medium were added to produce an OD_{600} of 0.2-0.3 and incubated at 30°C for 3 h. Cells were pelleted at 1,000 g (5min, RT) and then washed with 25-50 ml H_2O (vortex). After pelleting the cells again (1,000 g, 5min, RT), the cell pellet was resuspended in 1.5 ml freshly prepared, sterile 1x TE/LiAc (10 mM Tris-HCl; 1 mM EDTA; 100 mM LiAc; pH 7.5). These competent cells were now ready for transformation.

0.2 µg of the DNA BD vector construct and 0.2 µg of the DNA AD vector construct were mixed with 0.1 mg of herring testes carrier DNA and freshly denatured at 98°C for 20 min. Afterwards, this was mixed with 0.1 ml of competent yeast cells. Then 0.6 ml sterile PEG/LiAc solution (40% PEG 4000; 10 mM Tris-HCl; 1 mM EDTA; 100 mM LiAc; pH 7.5) were added, vortexed and incubated for 30 min at 30°C with shaking. DMSO was added to 10% and mixed gently by inversion. After heat shock (15 min at 42°C), cells were chilled on ice and subsequently pelleted (5 s, 13,000 rpm). The cell pellet was resuspended in 0.5 ml H_2O. 100 µl of the cell suspension were plated on a SD -Leu/-Trp agar plate and incubated at 30°C until colonies appeared.

2.3.18 Y2H β-galactosidase filter assay

This was a colony lift filter assay for qualitative blue/white screening from the MATCHMAKER Two-Hybrid System 2 protocol (CLONTECH Laboratories). Fresh colonies (1-3 mm in diameter) should be

used. For each plate of transformants, a sterile Whatman #5 filter was presoaked in Z buffer/X-gal solution. A clean, dry filter was placed over the surface of the colony plate, carefully lifted and completely submerged (colonies facing up) in liquid nitrogen for 10 s. Filters thawed for 10 min at RT (permeabilization of cells) and were placed (colonies facing up) on a presoaked filter. They were incubated at 30°C (≤ 8 h) and checked for the appearance of blue colonies indicating an interaction of prey and bait.

2.3.19   Quantitative detection of HCV core protein

HCV core protein was quantified using the Trak C Core (Ortho Clinical Diagnostics, Neckargemünd, Germany) enzyme-linked immunosorbent assay (ELISA) according to the instructions of the manufacturer. When intracellular core expression was analyzed, cells were lysed in ice-cold PBS supplemented with 1% Triton X-100, 1 mM PMSF, and 0.1 µg/ml aprotinin. Lysates were cleared at 20,000 g for 10 min and measured at a dilution of 1:10 (or higher) in PBS. Cell culture medium was filtered through 0.45 µm pore-size filters and either directly used for ELISA or diluted with DMEM complete medium prior to measurement.

2.4 Working with viruses

2.4.1 Lentiviral transduction of cells

Calcium phosphate transfection of DNA was performed to introduce lentiviral vector plasmid DNA (pWPI) along with two packaging constructs into HEK293T cells in order to produce viral particles. We used the CalPhos mammalian transfection kit from Becton-Dickinson. 1.2×10^6 cells were seeded into a 6 cm cell culture dish one day prior to transfection. On the next day, medium on the cells was changed for 4 ml of fresh complete DMEM. At least 1 h later, for transfection, 6.42 µg lentiviral vector (pWPI), 6.42 µg gag-pol plasmid (pHIT60 for shRNA cell lines, pCMVΔR8.91 for HepG2 cells overexpressing ANXA2) and 2.14 µg VSV envelope glycoprotein plasmid (pCZ VSV-G for shRNA cell lines, pMD.G for HepG2 cells overexpressing ANXA2) were mixed and diluted to a final volume of 438 µl in H_2O. Then, 62 µl 2M $CaCl_2$ and 500 µl of 2x HBS buffer were added and mixed well by pipetting up and down. The mixture was immediately added dropwise to the cells and the plate was gently swirled to evenly distribute the transfection mix throughout the plate. After 3-4 h. a fine precipitate formed which could be easily confirmed under the microscope. After 6-16 h, the medium was changed to fresh complete DMEM. On the day after transfection, the target cells (lunet, Huh7.5, and HepG2 cells, respectively) were seeded at 4×10^4 cells per well into a 12-well plate. 24 h later (48 h post transfection), the lentiviral particle containing supernatant from the 293T cells was harvested and replaced by another 4 ml of fresh complete DMEM. The supernatant was filtered through a 0.45 µm syringe mounted filter twice to remove cells. From the target cells, the medium was aspired and 500 µl of the infectious supernatant were added to them per cell. 6-8 h later, the supernatant on the target cells was replaced with fresh infectious supernatant. On the next day, the medium from the 293T cells was harvested a second time (cells were discarded), again filtered twice through a 0.45 µm filter and pooled with the

infectious supernatant from the previous day (if remainders were left). Target cells were a third time supplied with new 500 ml of infectious supernatant for 4-6 hours and were then supplied with complete DMEM containing the appropriate selection antibiotic, zeocin, G418 or blasticidin. Target cells were incubated for another 72 hours or until they reached confluence and were then expanded to a 25 cm^2 cell culture flask.

2.4.2 Preparation of Hepatitis C virus stocks

Huh7-Lunet cells were electroporated with virus constructs as described above. Culture fluid of transfected cells was harvested and cleared by passing through 0.45 mM pore size filters. In case of Luc-JFH1 and Luc-Con1 medium was harvested 72 to 96 h after transfection, whereas maximal yield for Luc-Jc1 was obtained at 48 h. Jc1 wild type and Con1/wt virus containing supernatant was harvested as early as 24 h post electroporation. Virus preparations were used directly, or stored at 4 °C or -80 °C. (Each cycle of freeze and thaw resulted in 2-fold reduction of infectivity!). As the virus is stable at 4 °C for at least several days, for short term storage virus preparations were kept at this temperature.

2.4.3 HCV infection of cells

For standard infection assays, cells were seeded at a density of 4 x 10^4 per well of a 12-well plate 24 h prior to inoculation with 500 µl of virus preparation. Maximum infectivity can be achieved when cells are inoculated for 4 h at 37°C. Depending on the experimental setup, cells were harvested or fixed at the appropriate time point.

3. Results

It is known that the HCV replication complex harbors the non-structural proteins NS3 to NS5B which are necessary and sufficient for viral RNA amplification as well as the viral RNA. However, different cellular host proteins seem to play an important role in the HCV RNA replication, too. Since most of the NS proteins possess membrane anchors or transmembrane domains, the HCV replication complex is tightly associated with intracellular membranes, probably derived from the ER. The first aim of the present work was the development of purification strategies in order to isolate enzymatically active HCV replication complexes thus allowing the identification of cellular host factors involved in HCV replication.

3.1 Development of purification strategies for active viral replication complexes from HCV subgenomic replicon cells

The source for the isolation and characterization of HCV replication complexes were Huh-7 cell clones persistently harboring subgenomic HCV replicons. These cells keep constant HCV RNA and protein levels over years, even in the absence of selective pressure[173].

3.1.1 Establishment of a replicase activity assay for purified HCV replication complexes

Since the HCV replication complex (RC) is associated with intracellular membranes[74], we decided to enrich and concentrate the replication complexes by differential centrifugation. Similar procedures for the preparation of RCs have already been described for HCV and related viruses[8,52,86,125,210]. The method is shown schematically in Fig. 8A. In order to isolate RCs, replicon cells of cell clone 9-13[140] were lysed in a hypotonic buffer and homogenized (total lysate, TL). The nuclei were pelleted (nuclei pellet; NP) and the cytoplasmic supernatant (S1) was again centrifuged. Thereafter, I received a second, largely membrane-free supernatant (S2) and a membrane-containing pellet in which the so-called crude replication complexes (CRCs) could be found in high concentrations. To test for *in vitro* replicase activity, the cell lysates were incubated with radiolabeled nucleotides in the presence of Actinomycin D and in the absence of exogenous template RNA. Reaction products were further analyzed by denaturing agarose gel electrophoresis (Fig. 8C). The

dominant product of *in vitro* replication was a single band which corresponded in size to the full-length replicon RNA (ca. 8 kb, arrowhead). HCV replicase activity was already detectable in the total hypotonic lysate of replicon cells but was enriched in CRCs that were obtained by pelleting the membranous material contained in supernatant 1. The resulting supernatant 2 contained only marginal replicase activity. Contrary to the corresponding fractions of naïve Huh-7 cells, fractions of the RC preparation of replicon cells should contain the viral NS proteins and probably associated cellular proteins. We wanted to analyze whether this can already be detected in a SDS-PAGE by variations in the protein band patterns, especially in the CRC fraction. However, differences in the complex protein band pattern between corresponding fractions of naïve Huh-7 and replicon cells were not observed (Fig. 8D).

The distribution of the non-structural proteins in different fractions of the CRC preparation was investigated by immunoblot analyses and is shown in Fig. 8B. Similar proportions of NS3, NS4B, NS5A, and NS5B were retrieved in S1 and concentrated in parallel to the replicase activity in the CRC fraction, in S2 only minor amounts were detected.

A variable amount of NS proteins and replicase activity always stayed associated with the nuclear pellet. This could not be recovered even by vigorous douncing, probably due to the accumulation of replication complexes in the perinuclear region[74] and due to the mild extraction conditions omitting any detergents.
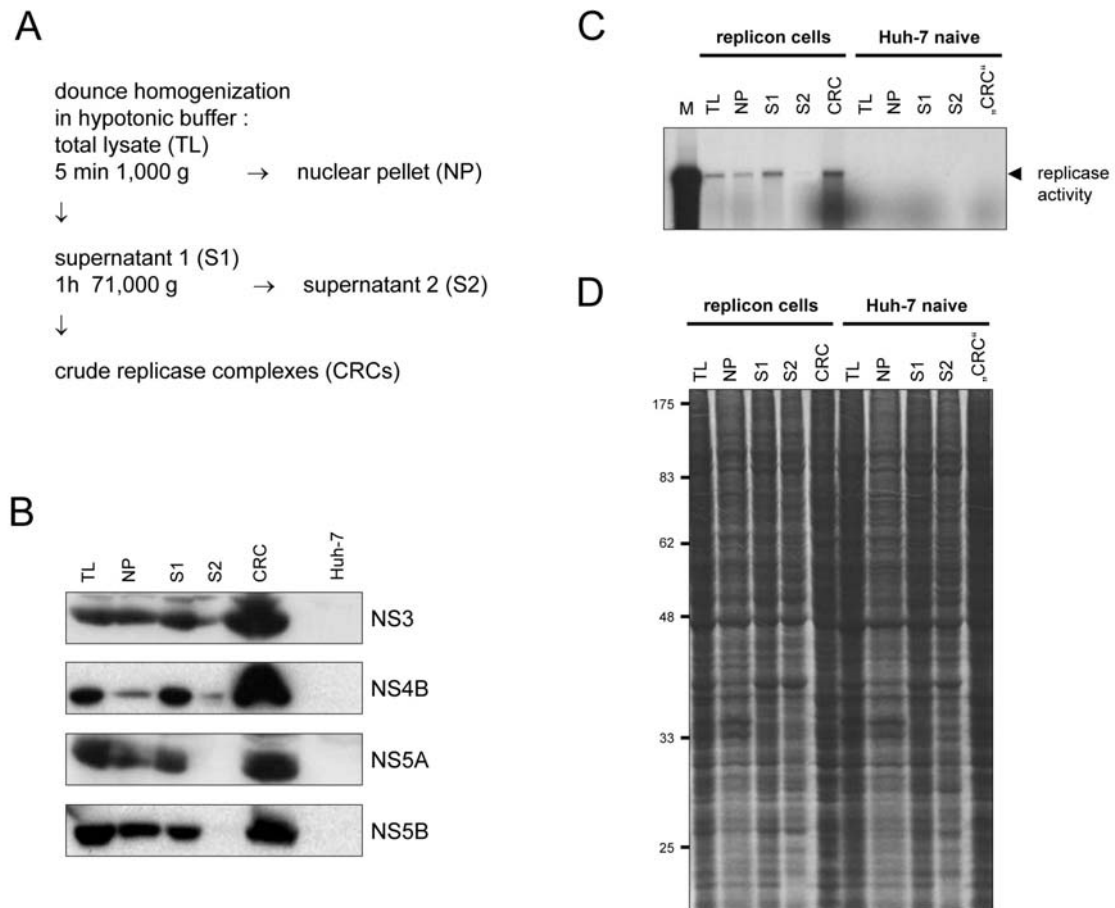
Fig. 8. Preparation and characterization of CRCs from HCV replicon cells. (A) Schematic diagram of the CRC preparation protocol. (B) Detection of NS3, NS4B, NS5A and NS5B in different fractions of the CRC preparation. The volume of the NP fraction was adjusted to the volume of S1 and 10 µl of each fraction were analyzed by immunoblot using a polyclonal antiserum raised against HCV NS3 (top panel), NS4B (upper middle panel) or NS5A (lower middle panel) or monoclonal antibodies specific for NS5B[154] (lower panel) and compared to 10 µl of "CRC" fraction from naive Huh-7 cells (Huh-7). (C) Analysis of *in vitro* replicase activity in total lysates (TL) and different subcellular fractions of replicon cells (left half) and naïve Huh-7 cells (right half). *In vitro* replicase activity was determined in 4 µl of each fraction, reaction products were analyzed by denaturing glyoxal gel electrophoresis followed by autoradiography of the dried gel. A radioactively labeled *in vitro* transcript identical in size to the replicon was loaded as a marker (M). The major reaction product of the *in vitro* replicase assay is indicated by an arrowhead. (D) Distribution of proteins in the different fractions of the CRC preparation from replicon cells (left half) and naïve Huh-7 cells (right half). The volume of the NP fraction was adjusted to the volume of S1 and 10 µl of each fraction were analyzed by SDS-PAGE. Proteins were visualized by Coomassie stain.

3.1.2 CRC activity is different from polymerase activity

The replicase activity shown in Fig. 8C could be exclusively due to the RdRp activity of NS5B present in the cellular lysates. To exclude this, we were looking for criteria by which the activity of replication complexes could be differentiated from polymerase activity. Previous reports have shown that HCV replication complexes act selectively on endogenous templates *in vitro* and are blocked by an inhibitor of NS3 helicase[86], indicating that replicase activity can be distinguished from RNA synthesis exerted by

isolated NS5B polymerase. To search for additional differentiators, we wanted to analyze different compounds inhibiting RdRp activity *in vitro* for their impacts on *in vitro* replicase activity.

Using recombinant NS5B protein for screening, nucleotide and non-nucleoside inhibitors of HCV polymerase activity have been identified. Nucleotide analogs target the polymerase active site, are mostly competitive inhibitors relative to the natural nucleotide substrates, and can cause chain termination upon incorporation into the RNA molecules[36,152,194]. Non-nucleoside inhibitors of NS5B RNA synthesis activity have been independently identified by several laboratories and belong to a number of different structural classes[18,37,38,46,150]. Furthermore, Moradpour and coworkers generated a monoclonal antibody (α-NS5B 12B7) that efficiently inhibits the HCV RdRp *in vitro* by binding to a conformational epitope in NS5B[154].

We tested whether this monoclonal antibody, as well as the chain-terminating nucleotide analog 3'-deoxy-CTP and the non-nucleoside NS5B polymerase inhibitor Japan Tobacco DB-III-17-02 also had an impact on *in vitro* replicase activity.

The inhibitory effects of the monoclonal antibody α-NS5B 12B7 were compared to those of the NS5B-specific monoclonal antibody α-NS5B 3B1 which did not interfere with polymerase activity *in vitro*[154]. As shown in Fig. 9A, neither the control antibody α-NS5B 3B1 (right half). nor the α-NS5B 12B7 antibody (left half), generally inhibiting the polymerase activity *in vitro*, interfered with the activity of HCV replication complexes in any used concentration, even not when used in an up to 30-fold molar excess.

Likewise, the non-nucleoside NS5B polymerase inhibitor Japan Tobacco DB-III-17-02 was tested in different concentrations in an *in vitro* replicase activity assay (Fig. 9B). Though, this non-nucleoside inhibitor did also not show any impact on the replicase activity.

Solely 3'-deoxy-CTP, the chain-terminating nucleotide analog, interfered with the activity of the viral replication complex (Fig. 9C). This inhibition occurred in a concentration-dependent manner.

These results further confirmed that *in vitro* replicase activity exhibited features distinct from isolated HCV polymerase, since it was not inhibited by a monoclonal antibody or a non-nucleoside inhibitor generally interfering with RdRp activity *in vitro*. Moreover, these data indicated that CRCs most likely depicted a representative fraction of HCV replication complexes in replicon cell clones and were therefore the

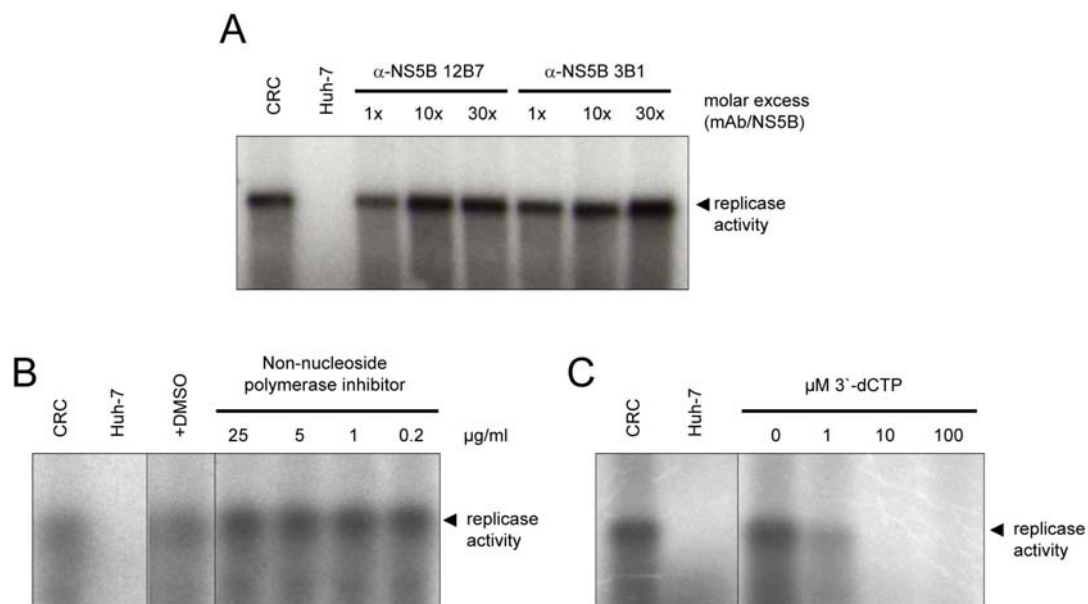appropriate tool to develop a purification strategy for the identification of associated host factors.

Fig. 9. Different effects of various inhibitors on *in vitro* replicase activity. (A) Effect of NS5B specific monoclonal antibodies on *in vitro* replicase activity. 2 µl of a standard CRC preparation containing 40 ng NS5B were preincubated 5 min on ice with 0.1, 1 or 3 µg of purified monoclonal antibodies as indicated in the top, resulting in a 1x, 10x or 30x molar excess, or incubated in the absence of antibodies (CRC) and analyzed for *in vitro* replicase activity. The same amount of "CRC" fraction from naive Huh-7 cells was used as a negative control (Huh-7). (B) Effect of the non-nucleoside polymerase inhibitor Japan Tobacco DB-III-17-02 on *in vitro* replicase activity. 3 µl of a standard CRC preparation were preincubated 30 min on ice with different amounts of the non-nucleoside polymerase inhibitor or its solvent DMSO (concentration in assay 1.25%), resulting in an total concentration of 0.2, 1, 5 or 25 µg/ml as indicated in the top or incubated in the absence of inhibitor (CRC) and analyzed for *in vitro* replicase activity. The same amount of "CRC" fraction from naive Huh-7 cells was used as a negative control (Huh-7). (C) Effect of 3'-dCTP on *in vitro* replicase activity. 3 µl of a standard CRC preparation were preincubated 30 min on ice with different concentrations of 3'-dCTP or its solvent H_2O, resulting in an total concentration of 1, 10, or 100 µM as indicated in the top or incubated in the absence of inhibitor (CRC) and analyzed for *in vitro* replicase activity. The same amount of "CRC" fraction from naive Huh-7 cells was used as a negative control (Huh-7). For further details refer to the text.

3.1.3 Purification of HCV replication complexes by sucrose floatation gradient centrifugation

As shown in Fig. 8D, preparation of CRCs by pelleting heavy-membrane fractions from hypotonic cell lysates resulted in a fraction comprised of numerous cellular proteins in addition to the viral and cellular components of the HCV replication complex. Therefore, it was necessary for the characterization of these complexes to eliminate as many as possible of the cellular proteins not involved in HCV replication.
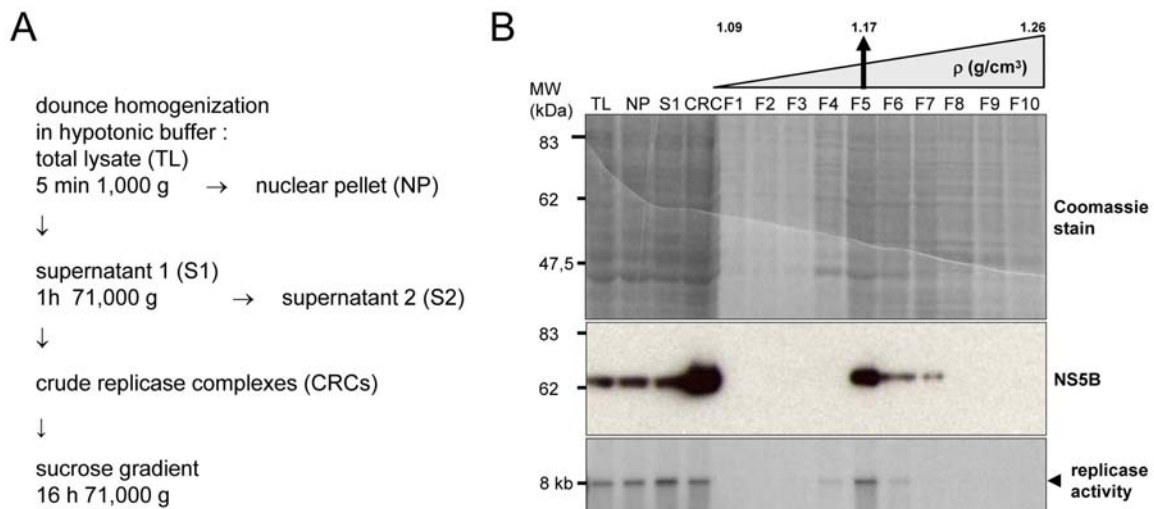
Fig. 10. Purification of HCV replication complexes by membrane floatation in a sucrose gradient. (A) Schematic diagram of the CRC purification protocol. (B) Analysis of total lysate, subcellular fractions and gradient fractions (F1 to F10) of the CRC purification by a sucrose floatation gradient. The CRC fraction was loaded under a continuous 15-60% (w/w) sucrose gradient and spun about 16 h at 71,000 g in an ultracentrifuge at 4°C. The gradient was subsequently fractionated in 1 ml aliquots. 10 µl of each fraction were analyzed by SDS-PAGE; the proteins were stained by Coomassie brilliant blue (upper panel) and NS5B was detected by immunoblot using a monoclonal antibody specific for NS5B (middle panel). *In vitro* replicase activity was determined in 4 µl of each fraction; the major reaction product of the *in vitro* replicase assay is indicated by an arrowhead (lower panel).

On that account, I tried to purify the viral replication complexes contained in the CRC fraction by a sucrose floatation gradient. CRCs were prepared as described before and loaded under a continuous sucrose gradient (15-60% (w/w) sucrose). The method is shown schematically in Fig. 10A. Following an overnight ultracentrifugation, the gradient was fractionated and the different fractions were analyzed by density and protein concentration determination (Bradford assay), Coomassie protein stain, immunoblot analysis against NS5B, and replicase activity assay. As demonstrated in Fig. 10B (middle panel), the major amount of the viral polymerase was retrieved in fraction F5 at a density of 1.17 g/ml. Minor amounts of NS5B were detected in the fractions F6 and F7, whereas in all other gradient fractions NS5B was not detectable. Corresponding to the immunoblot results, fraction F5 also comprised the maximum replicase activity (Fig. 10B, lower panel). In the neighboring fractions F4 and F6, only traces of replicase activity were detected; the remaining gradient fractions showed no evidence for viral RNA synthesis.

The fraction F5 contained about 30% of the total protein amount but almost the entire replicase activity as well as the bulk of NS5B polymerase. Therefore, a noticeable purification of the replication complexes was achieved by this floatation gradient centrifugation. However, this peak fraction F5 still displayed a very complex protein

pattern not much different from the other fractions (Fig. 10B, upper panel, compare lanes F1-F10), indicating that further purification steps were necessary for proteomic analyses of the HCV RCs.

3.1.4 Purification of HCV replication complexes by detergent treatment

A partial purification of the replication complexes was obtained by sucrose gradient centrifugation. Since almost all HCV non-structural proteins are tightly associated with intracellular membranes, many cellular membrane proteins are unavoidably also purified by this method. Furthermore, I forfeit approximately one half of the replication complexes linked with the nuclear pellet as this bond was not broken by the used lysis conditions. I tried to increase the yield and the purification by application of detergents. It has previously been shown that the HCV replication seems to proceed at detergent-resistant membranes, the so-called lipid rafts[5,193]. Proteins located at detergent-sensitive membranes lose their membrane-association upon detergent treatment which leads to a change in their buoyant density. Therefore, they can be separated from the membrane-bound RCs by a density gradient centrifugation. Based on the observation mentioned above, I treated a CRC fraction with 1% Triton X-100 (TX-100) at 4°C and performed a sucrose floatation gradient centrifugation. The different fractions were analyzed by density and protein concentration determination, silver staining of the proteins, immunoblot analysis to detect NS5B, and replicase activity assay (Fig. 11). In contrast to the previous sucrose floatation gradient shown in Fig. 10B, NS5B was detected in all gradient fractions apart from fractions F1 and F13 (Fig. 11A, bottom panel). Two different peak gradient fractions for the polymerase were found, F4 and F8, at a density of 1.11 g/ml and 1.19 g/ml, respectively. Fraction F8 also contained the highest protein concentration (Fig. 11A, top panel). I assumed that gradient fractions F3 to F5 may represent the detergent-resistant membranes and analyzed all gradient fractions in an *in vitro* replicase assay. As shown in Fig. 11B, replicase activity was not clearly detectable in any of the gradient fractions. Only in the assays corresponding to fractions 7 and 8 a smear was visible which might have been an indication for RNA synthesis.

However, different laboratories previously reported that the HCV RCs were associated with lipid rafts or detergent-resistant membranes[5,71,193]. Potentially, RCs stayed intact when treated with TX-100 at 4°C but replicase activity was destroyed due to the heating-up to the replicase assay incubation temperature of 35°C. This

probably left the lipid rafts not intact any longer in the presence of the remaining TX-100.
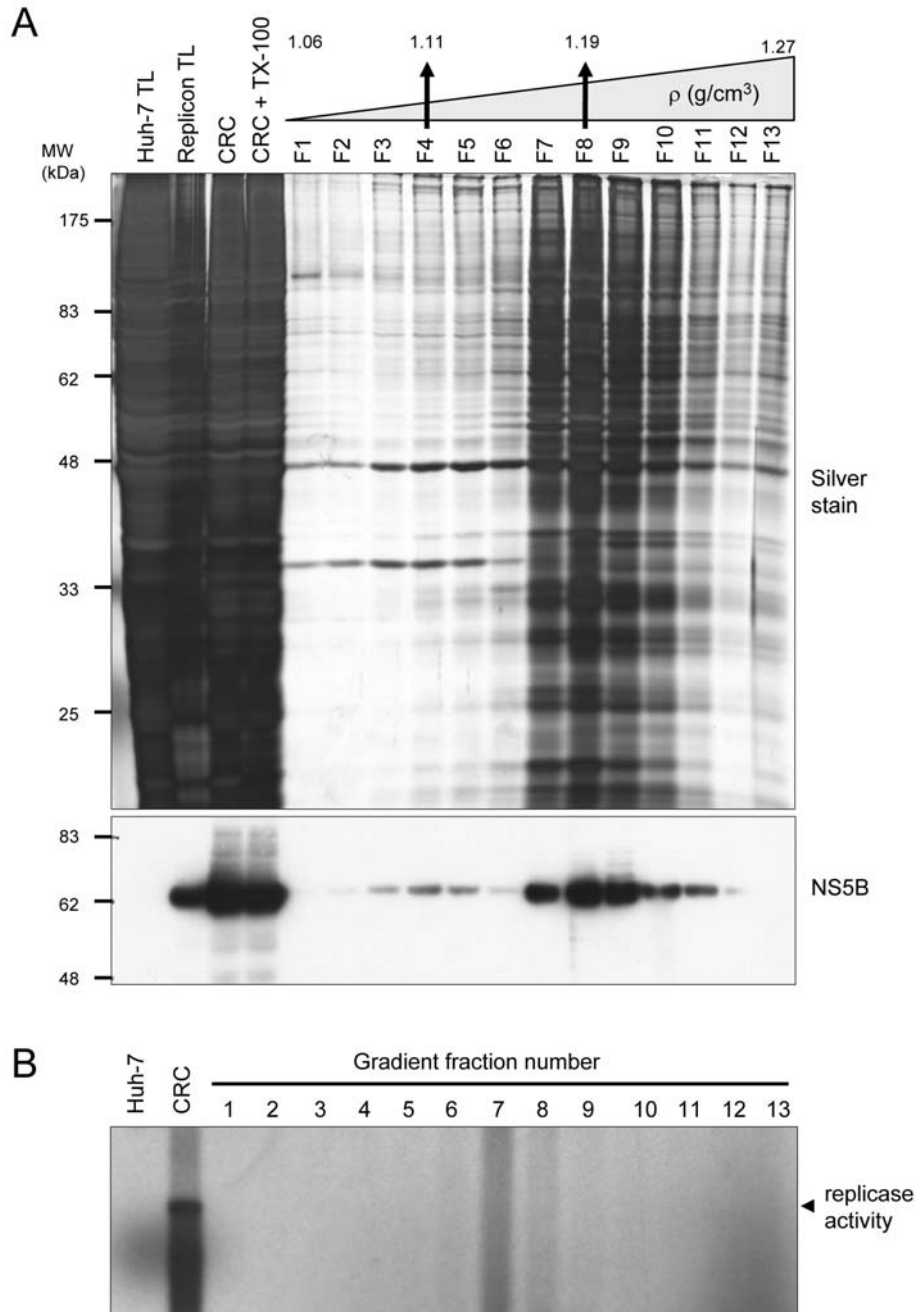

Fig. 11. Purification of CRCs by treatment with Triton X-100 at 4°C. A CRC fraction was incubated with 1% Triton X-100 (TX-100) 1h at 4°C. This fraction was then loaded under a sucrose floatation gradient and spun about 16 h at 71,000 g at 4°C. The gradient was fractionated in 1 ml aliquots. (A) 10 µl of the CRC fraction with or without TX-100 incubation as well as 20 µl of each gradient fraction (F1-F13) were analyzed by SDS-PAGE; both the proteins were visualized by silver staining (top panel) and NS5B was detected by immunoblot using a monoclonal antibody specific for NS5B (bottom panel). 10 µl of total lysates (TL) of naïve Huh-7 cells and replicon cells served as negative and positive control, respectively. (B) *In vitro* replicase activity was determined in 4 µl of each gradient fraction; the CRC fraction of replicon cells was used as a positive control, the corresponding fraction of naïve Huh-7 cells as negative control. The major reaction product of the *in vitro* replicase assay is indicated by an arrowhead.

The membrane association seemed be crucial for the activity of the HCV replication complex, therefore I controlled which detergents did not affect replicase activity *in vitro* (Fig. 12) and could be used for further purification studies. CRC fractions were incubated in the presence of different detergents on ice and subsequently subjected to an *in vitro* replicase assay.
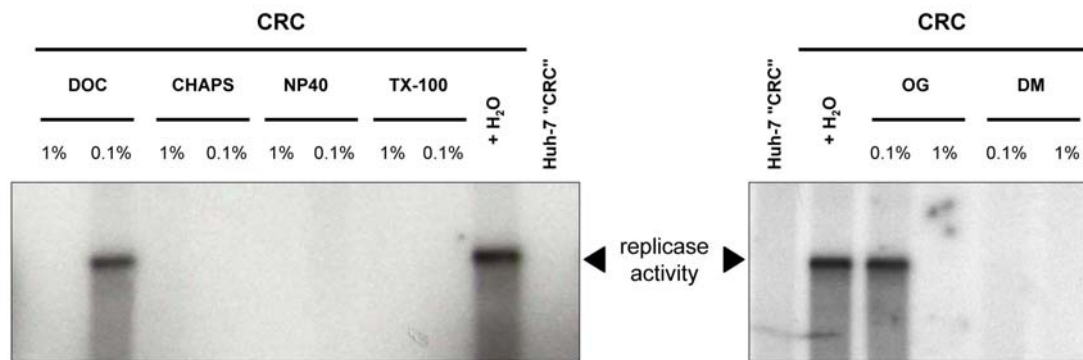

Fig. 12. Effect of various detergents on HCV replication complex activity. Equal volumina of CRC fraction were incubated 5 min on ice in reaction buffer together with 0.1% or 1% of the detergents desoxycholic acid (DOC), CHAPS, NP40, Triton X-100 (TX-100), octyl glucoside (OG), and dodecyl maltoside (DM), respectively. Subsequently, the replicase activity assay was started by addition of nucleotides and incubated 1 h at 35°C. A CRC fraction preincubated with H_2O instead of detergent served as positive control, an analog membrane fraction of naïve Huh-7 cells as negative control. An *in vitro* transcript with a length of 8 kb was used as size control.

The results exhibited clearly that the replication complexes were only still active at a concentration of 0.1% of the detergents desoxycholic acid (DOC) or octyl glucoside (OG). A ten fold higher concentration of DOC or OG inhibited the replication in the *in vitro* assay. The other detergents (CHAPS, NP40, TX-100, and dodecyl maltoside) already blocked the activity of the replication complexes completely at a concentration of 0.1%. However, a concentration of 0.1% of DOC or OG lies below the critical micellar concentration (CMC), i.e. the proteins were not entirely solubilized from the membrane and thus the cellular proteins not involved in HCV replication could not be disposed by this detergent treatment. The replicase activity inhibition on the one hand and the insufficient solubilization of cellular proteins on the other hand rendered the application of detergents for the purification of HCV replication complexes not practicable.

Although the isolation of detergent-resistant membranes might be a plausible way to purify RCs[193], we decided to search for alternative strategies because in our hands replicase activity could not be determined in these fractions. Miyanari and colleagues showed that *in vitro* replicase activity in digitonin-permeabilized cells was resistant to

protease treatment[153]. To evaluate whether this treatment was also applicable as a purification strategy for HCV replication complexes, CRCs were treated with high concentrations of proteinase K (PrK), the reaction was stopped by adding PMSF, and aliquots of the pretreated CRCs were analyzed for *in vitro* replicase activity, immunoblot against NS5B, and protein silver stain following SDS-PAGE. As shown in Fig. 13A, *in vitro* replicase activity was not affected by pretreatment with proteinase K (upper panel, lanes 5 and 6). In contrast to the fully maintained replicase activity, NS5B protein was not detectable in the PrK treated fractions (Fig. 13A, lower panel, lanes 5 and 6) until the sample was TCA-precipitated and fivefold concentrated (lane 7). Consistent with this result, cellular proteins were massively degraded to nearly undetectable amounts even with the lower protease concentrations (Fig. 13B, lanes 8-11), whereas detergent treatment as expected had no significant effect (lanes 6 and 7).
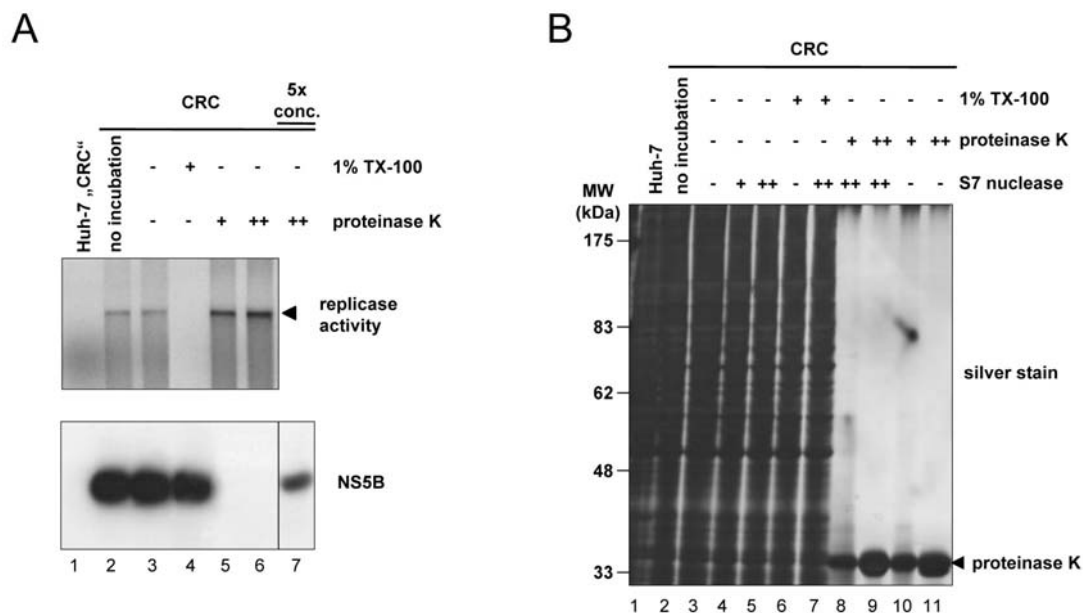

Fig. 13. Proteinase K does not affect the *in vitro* replicase activity of HCV replication complexes. Equal amounts of CRCs prepared from replicon cell clone 9-13 were incubated for 60 min at 25°C in the presence or absence of 1% Triton X-100 and/or 0.8 (+) or 8 (++) mg/ml proteinase K, respectively as indicated above each lane. The reaction of proteinase K was stopped by addition of 1.4 mM PMSF. (A) Effect of proteinase K on *in vitro* replicase activity and on HCV NS5B. *In vitro* replicase activity was determined in 4 μl of each fraction, a "CRC" fraction of naïve Huh-7 cells was used as negative control (top panel). Total protein equivalent to 2 μl CRCs was subjected to SDS-10%PAGE. In case of the 5x concentrated sample, proteins were TCA-precipitated and the equivalent of 10 μl CRCs was loaded. Proteins were either subjected to immunoblot analysis using monoclonal antibodies specific for HCV NS5B (A, bottom panel) or visualized by silver staining (B) as indicated at the right. The concentrated fraction (A, lane 7) is shown from the identical exposition of the same blot.

The PrK treatment of CRCs led to the degradation of the bulk of cellular proteins as well as a large part of the viral NS proteins. However, the *in vitro* replicase activity

was fully maintained. Therefore, the application of PrK seemed to be a useful method to enrich and purify replication complexes and their associated cellular cofactors which potentially could be identified by following proteomic approaches.

3.2 Identification of Cellular Factors Associated with the Hepatitis C Virus Replication Complex

Based on the previous results, we developed a purification strategy by combining the PrK treatment with the sucrose density gradient centrifugation. This allowed us to enrich and purify enzymatically active HCV replication complexes and to investigate their associated cellular cofactors by two-dimensional (2D) SDS-PAGE. The purification strategy is shown schematically in Fig. 14. CRCs were isolated from replicon cells (cell clone 9-13) as described in chapter 3.1.1. Thereafter, the CRC fraction was treated with PrK and subsequently loaded under a sucrose floatation gradient after stopping the PrK activity by addition of PMSF. The gradient was fractionated, and the fractions containing the major part of replicase activity and NS5B polymerase were combined. The therein comprised membranes and accordingly RCs were pelleted by ultracentrifugation. After resuspension of the pellet in an appropriate lysis buffer, this fraction was investigated by 2D gel electrophoresis, and proteins were visualized by silver stain. A corresponding fraction prepared from naïve Huh-7 cells that were cured from an HCV replicon was analyzed in the same way and the resulting protein spot patterns of the different cell lines were compared. Protein spots that were present in the CRC fraction of HCV replicon cells but missing or expressed at lower levels in the control fraction of cured Huh-7 cells could represent either viral proteins or cellular factors probably involved in viral replication and were subjected to mass spectrometry analysis.

We first tested whether this combination of purification steps would preserve the activity of RCs. Therefore, equal amounts of CRCs prepared from replicon cells were incubated in the presence or absence of proteinase K. After stopping PrK activity by adding PMSF, the CRC fraction was subjected to a sucrose floatation gradient assay.
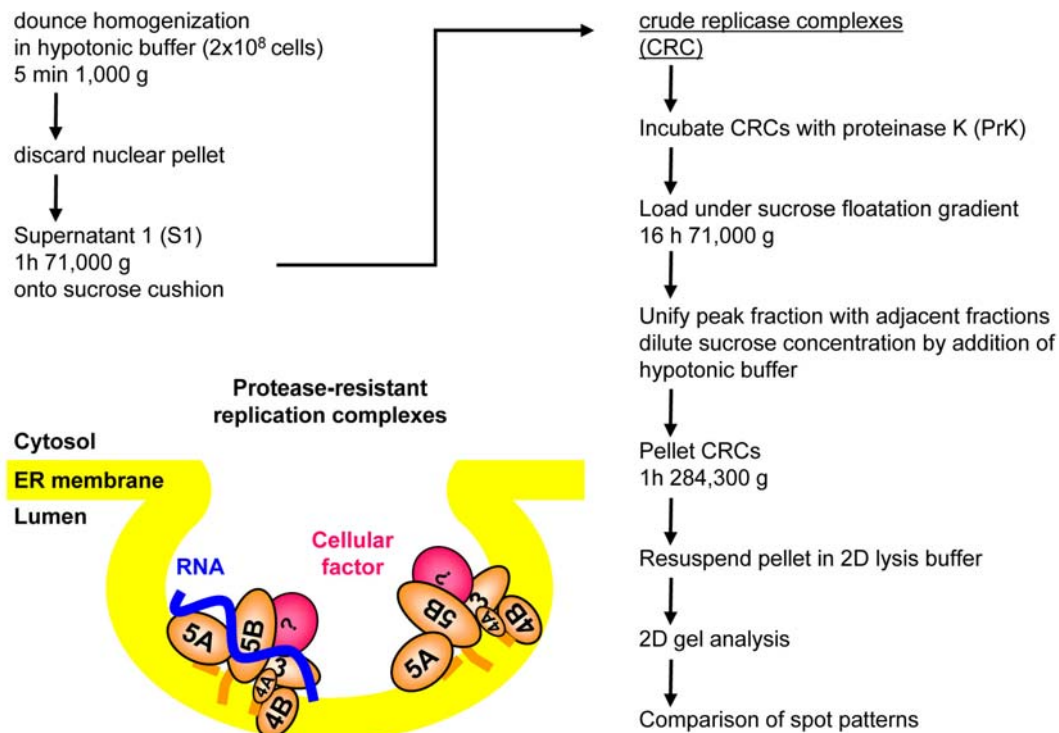
Fig. 14. Schematic diagram for the biochemical purification of HCV replication complexes by proteinase K to identify associated cellular factors and hypothetical model of HCV replication complexes. HCV NS proteins are indicated by orange ellipses; potential cellular factors by pink ellipses, and viral RNA by a blue wavy line. Individual NS proteins and RNA are not drawn to scale.

In order to identify the gradient fraction encompassing the bulk of replicase activity, the individual gradient fractions were analyzed by density and protein concentration determination, as well as by *in vitro* replicase activity assay. The highest protein concentration was found at a density of 1.14 g/ml, both in gradient fractions of non-treated CRCs and those treated with PrK. In both cases, the same fraction (#6) also featured the principal part of the replicase activity (Fig. 15A). This showed that the combination of the two different purification steps (PrK treatment and sucrose gradient centrifugation) had no negative effect on the activity of the RCs. Furthermore, these results clearly excluded a different behavior of PrK treated CRCs and non-treated CRCs in a sucrose floatation gradient.

Having defined the gradient fraction from PrK treated CRCs containing the majority of replicase activity and proteins, I pooled it with the two neighboring fractions and pelleted the therein enclosed intracellular membranes. This pellet was then resuspended in lysis buffer and subjected to a one-dimensional (1D) SDS-PAGE. Proteins were either visualized by Coomassie staining or analyzed by immunoblot using antibodies specific for the detection of NS3, NS5A, and NS5B, respectively (Fig. 15B). As control, I used a corresponding fraction prepared from cured Huh-7

cells. Despite the purification that was achieved, no significant differences in the protein band pattern between CRCs from replicon and cured Huh-7 cells were observed (Fig. 15B, top panel). This indicated that the protein composition of the CRC fraction was too complex to be investigated by 1D SDS-PAGE. For subsequent analyses, this fraction was subjected to 2D gel electrophoresis. As shown in Fig. 15B, the HCV NS proteins NS3, NS5A, and NS5B were still clearly detectable in this fraction by a 1D immunoblot.
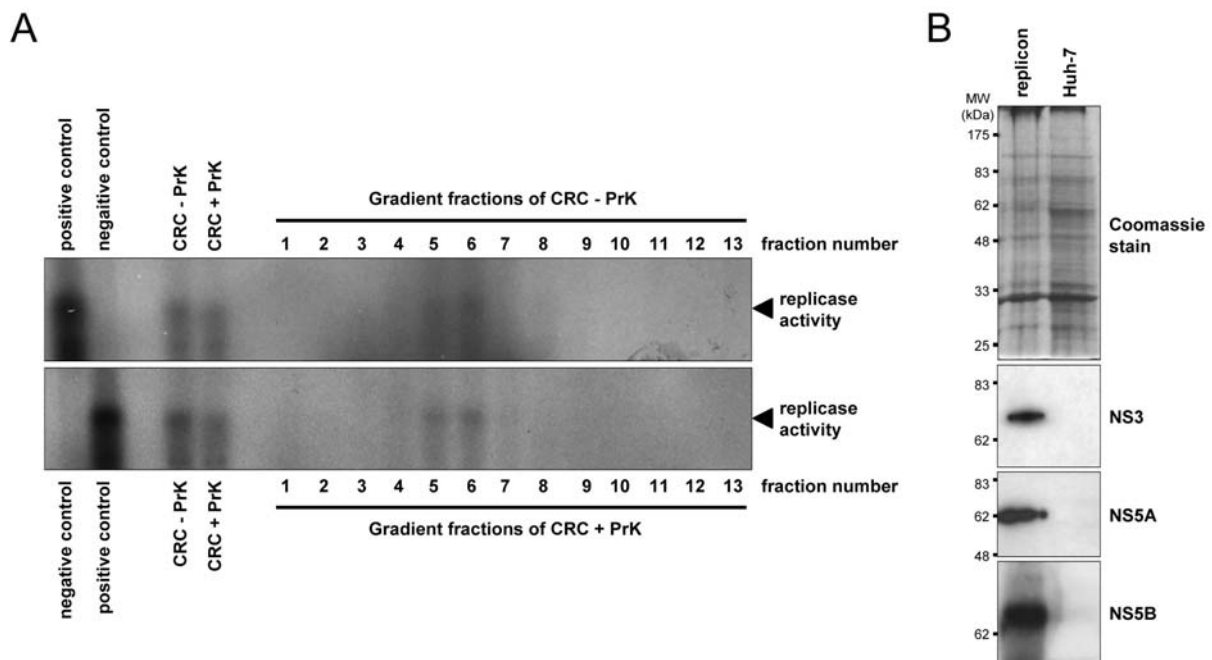

Fig. 15. Analysis of different fractions of the biochemical purification of HCV replication complexes by proteinase K (PrK). (A) Replicase activity of sucrose gradient fractions of CRCs treated or non-treated with PrK. 4 µl of each gradient fraction as well as PrK non-treated (- PrK) and treated (+ PrK) CRCs were analyzed for *in vitro* replicase activity. The upper panel represents the gradient fractions of PrK non-treated CRCs, the lower panel those of PrK treated CRCs. A non-incubated CRC fraction from replicon cells served as positive control, a corresponding fraction from naïve Huh-7 cells as negative control. (B) CRC fraction for 2D gel analysis subjected to 1-dimensional SDS-PAGE. Membranes contained in the peak gradient fractions were pelleted and lysed. Proteins included in this fraction were either visualized by Coomassie staining (top panel) or subjected to immunoblot analysis using either a polyclonal antiserum raised against HCV NS3 (middle upper panel) or monoclonal antibodies specific for HCV NS5A (middle lower panel) or monoclonal antibodies specific for HCV NS5B (lower panel). Huh-7 refers to a corresponding fraction prepared from cured Huh-7 cells.

Purification of HCV replication complexes by the protocol depicted in Fig. 14 seemed to be an appropriate method to investigate which cellular proteins are involved in viral replication, since HCV replicase activity was retained while most of the cellular proteins were removed by this procedure. As the purified CRC fraction still contained a complex mixture of proteins, we decided to analyze this fraction by 2D SDS-PAGE.

3.2.1 Comparative 2-dimensional gel analysis of CRCs from replicon cells and naïve cells

As shown in the previous chapter, purification of CRCs by PrK and sucrose density gradient did result in the elimination of most cellular proteins without affecting HCV replicase activity. However, the protein pattern was still to complex for 1D gel electrophoresis. Therefore, I analyzed the cellular proteins that stayed associated with the PrK treated CRCs by 2-dimensional SDS-PAGE. Resolution of the heterogenous protein mixture contained in the CRC fraction occurred in the first dimension by isoelectric focusing (IEF), e.g. segregation of proteins by their charge (pI; isoelectric point). In the second dimension, proteins were separated by their molecular weight in a standard SDS-PAGE.
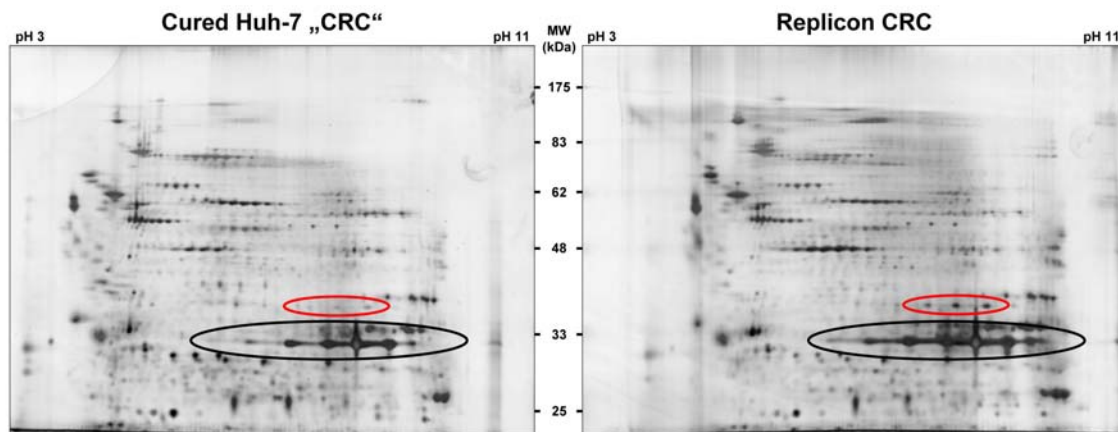
Fig. 16. Silver stained 2-dimensional SDS-PAGE of proteinase K treated CRC fraction prepared from cured Huh-7 cells and subgenomic replicon cells, respectively. Black ellipses indicate regions of spots corresponding to proteinase K; red ellipses regions of spots corresponding to Annexin II.

A typical outcome of such an analysis is shown in Fig. 16. Despite the substantial application of proteinase K, I still found a great variety of different proteins probably protected by membranous structures. The exceeding amount of proteinase K used for the purification of the replication complexes was reflected by massive protein spots at the corresponding size of 30 kDa (Fig. 16, black ellipses). The complex protein spot patterns were very similar between the investigated samples of replicon and cured cells and readily reproducible. However, distinct differences between the two gels also were detected. We were looking for additional protein spots in the HCV CRC gel that were absent or at least present in lower amounts in the control gel as exemplified by the spots encircled by red ellipses in Fig. 16. Those spots were then subjected to mass spectrometry analysis.

Unexpectedly, protein spots representing the HCV non-structural proteins were neither identified by mass spectroscopy nor verified in an immunoblot assay of 2D gels; however, in an immunoblot assay of a one-dimensional SDS-PAGE of PrK treated CRCs they were clearly detectable (Fig. 15B). The reason might be that membrane and hydrophobic proteins (like the viral NS proteins) are poorly represented in the second dimension, which is probably due to protein/gel interactions during IEF [2]. Some larger proteins might also have been lost and it has been suggested that this is due to size exclusion when the proteins are loaded onto the gel. In addition, it was possible that the NS protein amount was simply below the detection limit, since the majority of proteins had been digested by PrK (see also Fig. 13).

The analysis of the CRC fraction by 2-dimensional SDS-PAGE showed a protein spot pattern that was reproducible from gel to gel and comparable between the HCV CRC gel and the control gel, however some differences were detectable.

3.2.2 Identification of cellular proteins associated with HCV replication complexes by mass spectrometry

Protein spots present in the CRC fraction of replicon cells after PrK treatment but missing or present in lower amounts in the control fraction of cured Huh-7 cells were analyzed by matrix-assisted laser desorption/ionization (time of flight) mass spectrometry (MALDI-TOF MS) in order to identify cellular proteins associated with the viral RC. The results of two independent experiments are depicted in Fig. 17; several spots found by 2D gel analyses to show different expression levels (marked by circles) were subjected to mass spectroscopy.

We analyzed eight comparative 2D SDS-PAGEs and found three to nine differentially expressed protein spots in each gel. These were subsequently investigated by MALDI-TOF mass spectrometry; by virtue of too little protein content not every spot could be identified by this method.
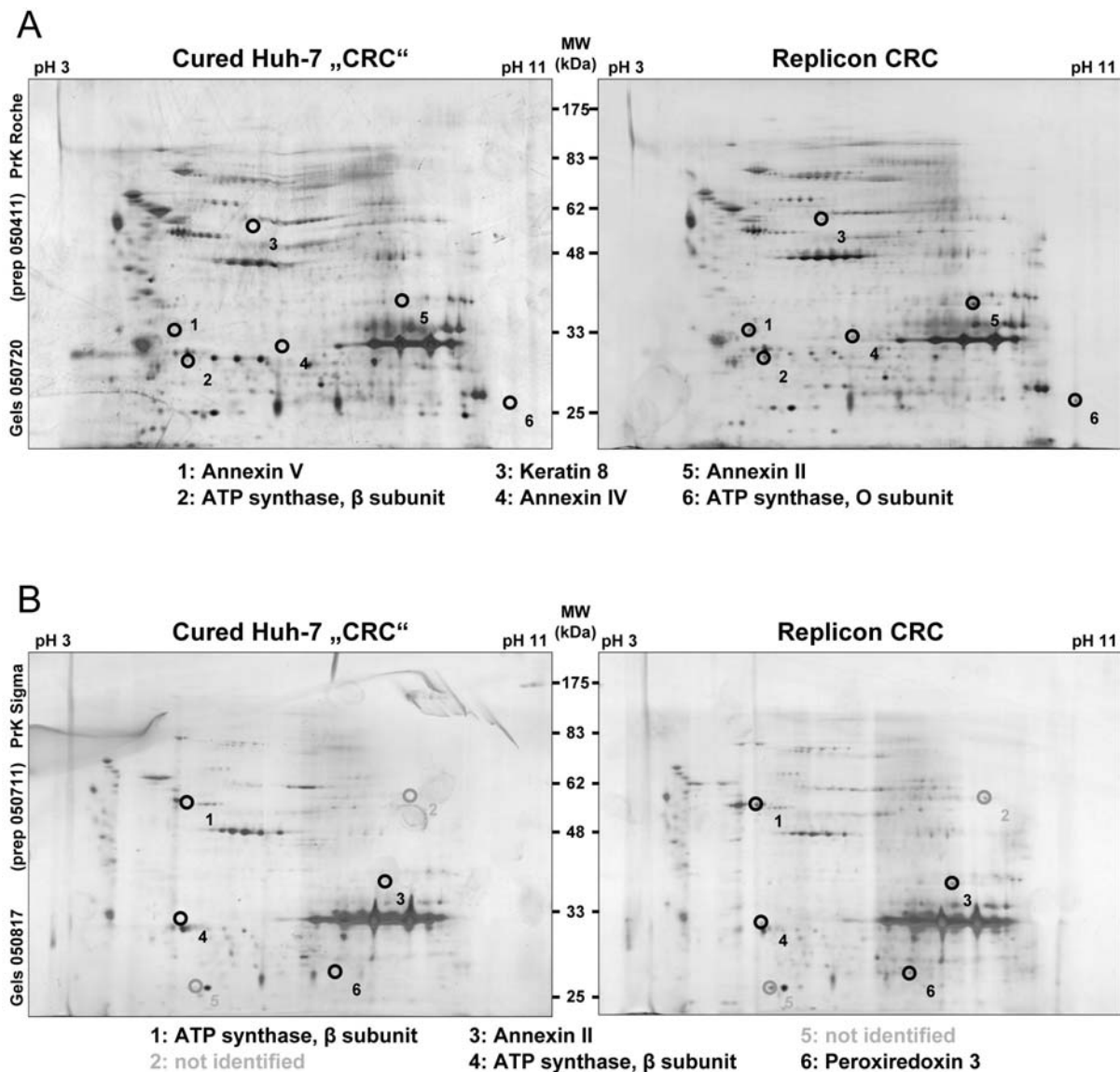
Fig. 17. Silver stained 2D SDS-PAGEs of proteinase K treated CRC fractions from replicon cells (right) and their corresponding control gels (left). (A and B) Analysis of different CRC preparations as indicated on the far left. Proteins spots missing or expressed at a lower level in the corresponding 2D SDS-PAGE of cured Huh-7 CRCs are highlighted by circles. Black circles and numbers indicate protein spots identified by mass spectrometry, grey circles and numbers represent non-identified protein spots. The protein identities are specified beneath each SDS-PAGE.

After having identified a particular protein by MALDI-TOF, the spots corresponding to this protein were also analyzed on all other gels and judged for differential representation. Table 1 summarizes which proteins were found by mass spectroscopy and in how many gels they were present in the CRC fraction of replicon cells but missing or present in lower amounts in the control fraction of cured Huh-7 cells. In seven of eight experiments, Annexin II (ANXA2) was present at higher levels in the investigated CRC fraction prepared from replicon cells compared to the corresponding fraction from cured Huh-7 cells. The β-subunit of the ATP synthase was detected in half of all analyses, but the locations of these identified protein spots

varied greatly in molecular weight in each experiment (demonstrated in Fig. 17B, spots #1 and #4). Therefore, this protein was not considered for further investigations. Peroxiredoxin 3, Annexin IV (ANXA4), and Annexin V (ANXA5) were found twice, other cellular proteins, e.g. Calnexin and BiP, were only identified once.

Table 1. Proteins identified by mass spectrometry and their frequency of differential representation in all comparative 2D gel analyses.

Identified protein	Differential spot intensities found x times in eight 2D-PAGEs
Annexin II (ANXA2)	7
Annexin IV (ANXA4)	2
Annexin V (ANXA5)	2
ATP synthase, β subunit	4 (at very varying positions!)
BiP	1
Calnexin	1
Peroxiredoxin 3	2
Ubiquinol-cytochrome-c reductase complex core protein I	1

In Fig. 18, the differences in the expression levels of two of these cellular candidate proteins, ANXA2 and Peroxiredoxin 3, respectively, are shown in several comparative 2D SDS-PAGEs. Both proteins were located at the expected molecular weights and isoelectric points. In the case of ANXA2, both protein spots were verified by mass spectrometry and were found differentially represented in seven cases (Fig. 18A). In contrast to this, Peroxiredoxin 3 was only twice present at higher levels in the replicon CRCs than in the control fraction from cured Huh-7 cells (Fig. 18B; 050811 and 050817). In all other experiments the expression levels of this protein were identical.
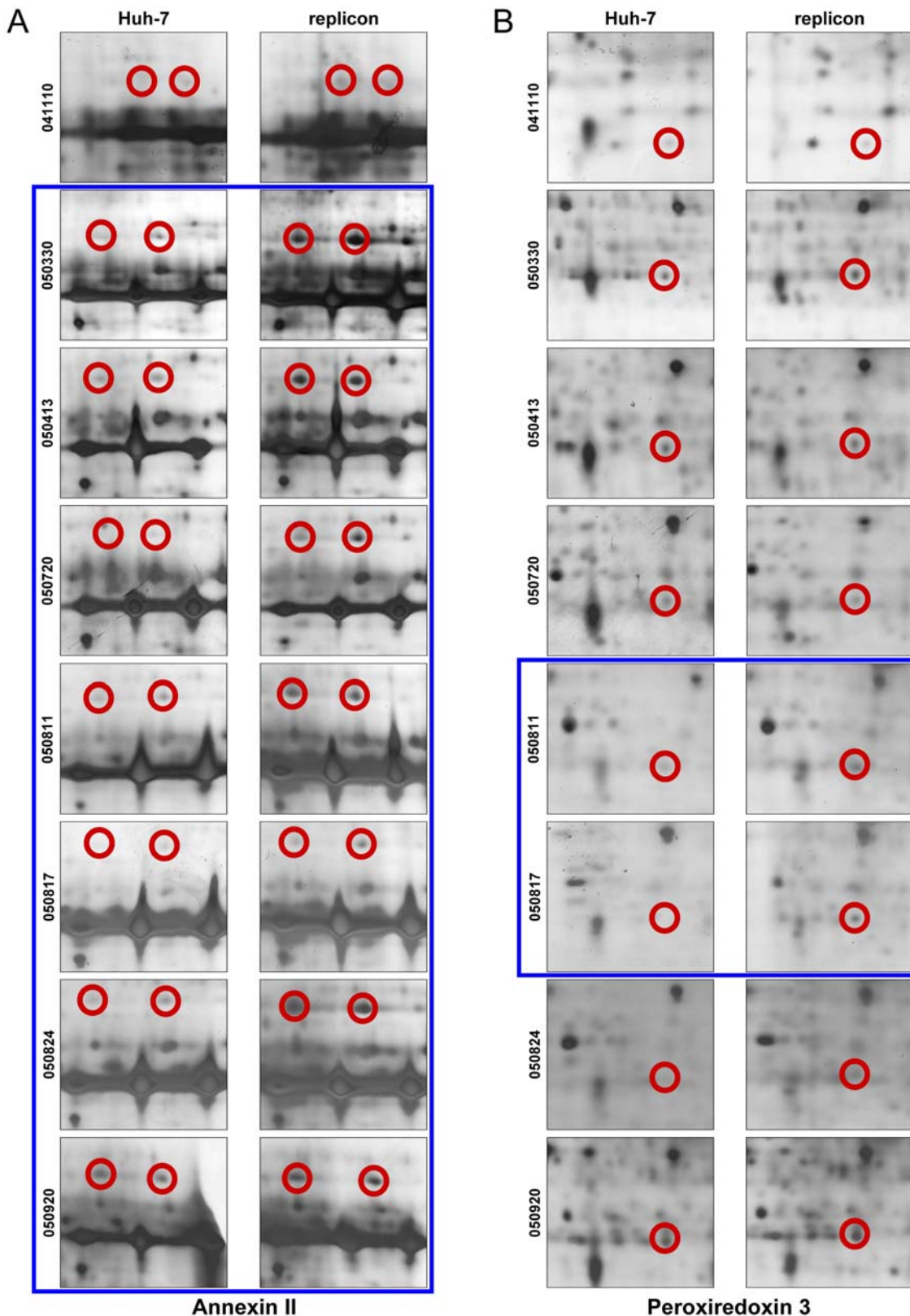
Fig. 18. Divers sections of comparative 2D gel analyses to contrast the differential representation of two disparate cellular candidate proteins found to be associated with the HCV replication complex. Red circles assign the positions of the protein spots. Annexin II was differentially represented in seven comparative 2D gel analyses (A; exception: 041110), Peroxiredoxin 3 twice (B; 050811 and 050817). Gel sections showing a differential representation are encircled by a blue line. For further details refer to the text.
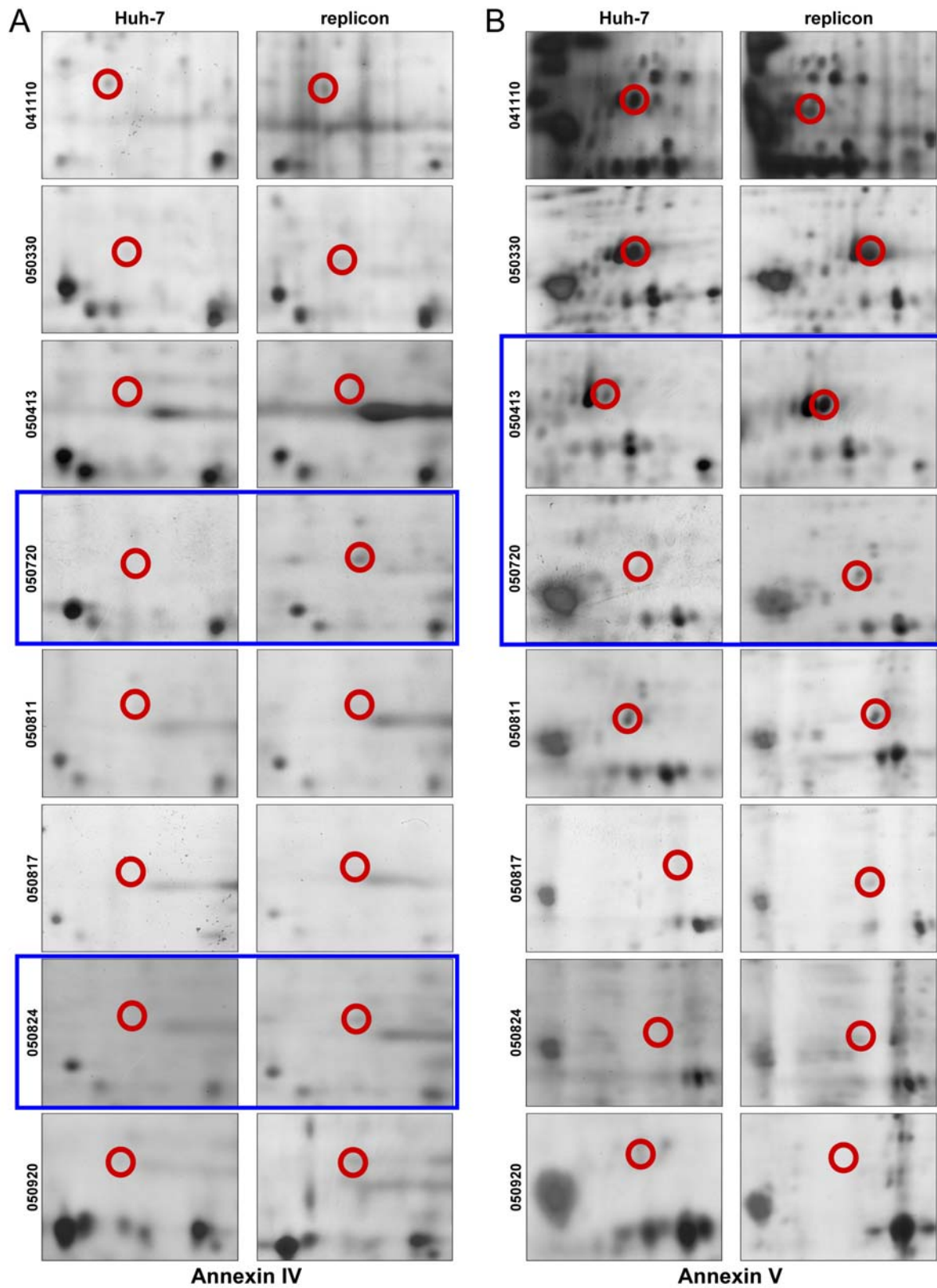
Fig. 19. Differential representation of two disparate cellular candidate proteins found to be associated with the HCV replication complex by 2D SDS-PAGEs. Red circles assign the positions of the protein spots. Annexin IV and Annexin V, respectively, were differentially represented in two comparative 2D gel analyses (050720/050824 and 050413/050720). Gel sections showing a differential representation are encircled by a blue line. For further details refer to the text.

Fig. 19 shows the differential representation of two other cellular candidate proteins, ANXA4 (A) and ANXA5 (B), respectively. Both were found twice to be present in the CRC fraction of replicon cells but missing or present in lower amounts in the control fraction and were identified by mass spectrometry. However, the spots for these proteins were not detectable in every gel (ANXA4: 050413, 050811, 050817; ANXA5: 050817, 050920), therefore, only the assumed spot positions were marked by circles in these cases. Especially the protein spots for ANXA4 showed a very low intensity due to little protein amounts. In most of the experiments, the expression levels of ANXA4 and ANXA5 did not show any variations or were not even traceable.

In summary, Annexin II (ANXA2) was the most promising candidate of the proteomic studies and was further analyzed for a potential role in the HCV life cycle.

3.3 Analysis of the role of Annexin II in HCV replication

The frequency of differential expression of ANXA2 found in the comparative 2D gel analyses of HCV replication complexes turned this cellular protein into a promising candidate as a potential cofactor of HCV replication. ANXA2 belongs to the great family of Annexins which are involved in many membrane-related events, such as the regulated organization of membrane domains and/or membrane-cytoskeleton linkages, certain endocytic and exocytic transport steps, and the regulation of ion fluxes across membranes[39,73]. Recently, Ryzhova and coworkers showed that ANXA2 is essential for the proper assembly of HIV in monocyte-derived macrophages[183]; furthermore, it is able to bind to mRNA and is involved in the organization of lipid rafts[12,218]. Therefore, we decided to investigate if this protein really played a role in the viral RNA replication.

The differential representation of ANXA2 in PrK-resistant CRCs and their corresponding control fraction in 2D gel analyses led to the question whether this was also detectable in a 1D immunoblot assay. Previous studies showed that the RC-associated cellular protein Vap-A is important for HCV replication[71,214,239], although its precise mode of action has yet not been classified. Therefore, its presence in the PrK treated CRC fraction was also investigated in this approach. The ER marker Calnexin served as additional control since the site of viral RNA replication, the membranous web, is derived from ER membranes. In a one-dimensional immunoblot assay, the levels of these distinct cellular proteins in the

CRC fraction prepared from HCV replicon cells were analyzed and compared to the protein levels in a corresponding fraction from cured Huh-7 cells (Fig. 20).
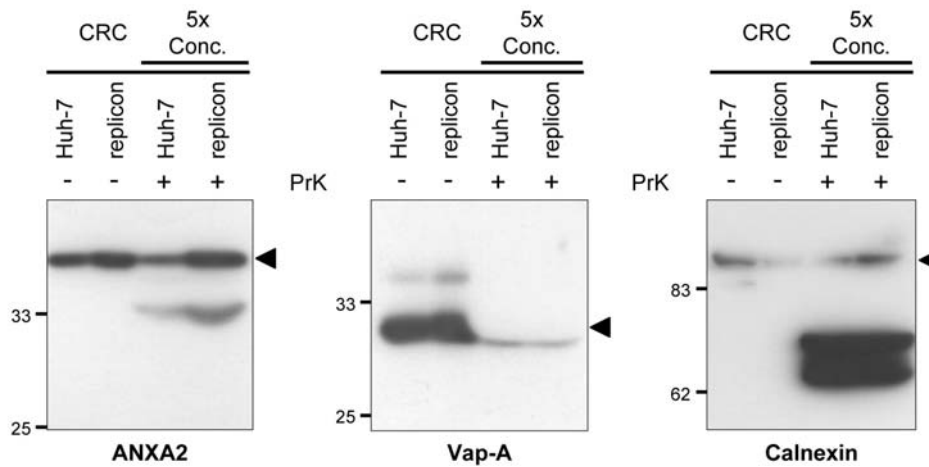

Fig. 20. Expression levels of different cellular proteins in PrK treated CRC fractions. Equal amounts of CRCs prepared from replicon cell clone 9-13 or cured Huh-7 cells were incubated for 60 min at 25°C in the presence (+) or absence (-) of 8 mg/ml proteinase K, respectively as indicated above each lane. The reaction of proteinase K was stopped by addition of 1.4 mM PMSF. Total protein equivalent to 2 µl CRCs was subjected to SDS-10%PAGE. In case of the 5x concentrated sample, proteins were TCA-precipitated and the equivalent of 10 µl CRCs was loaded. Proteins were subjected to immunoblot analysis using either monoclonal antibodies specific for ANXA2 (left panel), a polyclonal antiserum raised against the cellular protein Vap-A (middle panel), and a polyclonal antiserum raised against the N-terminus of Calnexin (right panel). The corresponding sizes of the different proteins are indicated by arrowheads to the right of each immunoblot.

The levels of Vap-A as well as the levels of the ER marker Calnexin - which has not yet been shown to be involved in HCV replication – showed no difference between CRCs from replicon and cured cells, independent whether the CRC fractions were treated with PrK or not. Calnexin is a type I transmembrane protein with a cytosolic C-terminus and a luminal aminoterminus. The Calnexin-specific antibody used in the immunoblot assay was directed against the N-terminus of this protein. The shift in the mobility of Calnexin observed after PrK treatment was due to the digestion of the cytosolic protein part resulting in a shortened polypeptide (see also[153]).

In contrast to Vap-A and Calnexin, the level of ANXA2 was enhanced in replicon CRCs compared to the control fraction. This phenotype was observed before as well as after PrK digest, the latter was confirming the results of the 2D gel analyses. The difference before PrK treatment indicated that either ANXA2 expression may be induced by the replicon or that the mRNA or the protein could be stabilized by HCV or that more ANXA2 is bound to membranes in the presence of HCV.

The results of this experiment clearly showed that ANXA2 was enriched in the CRC fraction and – compared to the control fraction – more ANXA2 protein was resistant to PrK.

3.3.1 Colocalization studies of Annexin II with viral proteins in different cell types

ANXA2 was found to be associated with purified CRCs from replicon cells by comparative 2D gel analyses. In contrast, the ER marker Calnexin and other cellular candidates (e.g. Vap-A) were not identified by this proteomic approach. As a first step to evaluate the role of ANXA2 in the HCV life cycle, we investigated whether ANXA2 colocalizes with HCV proteins in immunofluorescence analyses (IFA).

We started with two different subgenomic replicon cell clones (9-13 and 5-15[140]); both harboring genotype 1b replicons as used in the proteomic study. In naïve Huh-7 cells, ANXA2 showed a cytoplasmic distribution, whereas HCV NS3 was of course not detectable (Fig. 21A, lower panels). In the stable subgenomic replicon cells a rearrangement of ANXA2 took place, resulting in a punctuated staining perfectly colocalizing with the spot pattern of HCV NS3. This phenotype was more pronounced in 9-13 replicon cells (Fig. 21A, middle panels) than in cells harboring the 5-15 replicon (upper panels) in which the spot pattern of NS3 was less prominent, too. These spot patterns are generally believed to harbor the membranous web, the site of HCV RNA replication[74]. Therefore, the spot patterns of the viral NS proteins generally showed an explicit colocalization, which is exemplary shown with the colocalization of NS3 and NS5A (Fig. 21B), indicating that ANXA2 colocalized with all viral components of the HCV replication complex. Colocalization of ANXA2 with the HCV RNA could not be proven because the viral RNA was neither detected by a dsRNA-specific antibody nor by BrdU-labeling (data not shown). However, Gosert and colleagues showed that the sites of HCV NS proteins colocalized with the sites of newly synthesized RNA in the cytoplasm indicating that those spots represented the viral replication complexes[74].
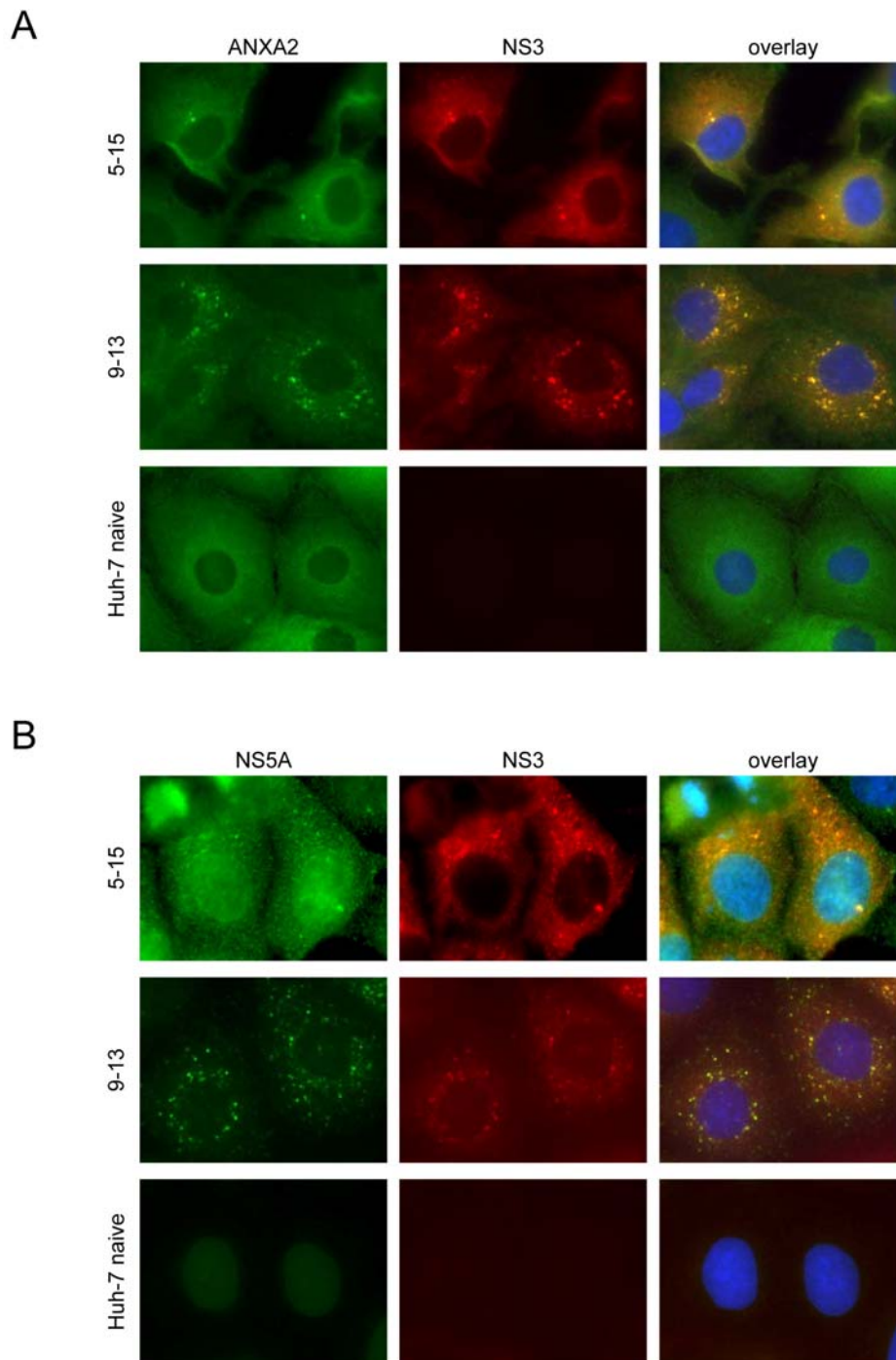
Fig. 21. Colocalization of ANXA2 and viral NS proteins in HCV subgenomic replicon cells. Paraformaldehyde-fixed (PFA-fixed) and permeabilized monolayers of replicon cells were subjected to IFA using either monoclonal antibodies specific for ANXA2 (A) or HCV NS5A (B), and a polyclonal antiserum raised against HCV NS3 (A and B). (A) Colocalization of ANXA2 with HCV NS3 in different subgenomic replicon cell clones. (B) Colocalization of HCV NS5A with HCV NS3 in different subgenomic replicon cell clones. Naïve Huh-7 cells served as negative control for the viral proteins.

Since ANXA2 colocalized with viral non-structural proteins in cells persistently replicating HCV RNA from genotype 1b, I analyzed whether this colocalization and the relocation of ANXA2 depended on a particular viral genotype. Huh-7 cells harboring HCV RNA from genotype 1b and genotype 2a, respectively, were

investigated and again the rearrangement of ANXA2 was found in both cells harboring the different viral genotypes (Fig. 22). In addition, in the cells containing HCV genotype 2a ANXA2 perfectly colocalized with HCV NS3, just as in cells comprising HCV genotype 1b, indicating that ANXA2 colocalization with HCV NS proteins might be common feature of HCV RCs.
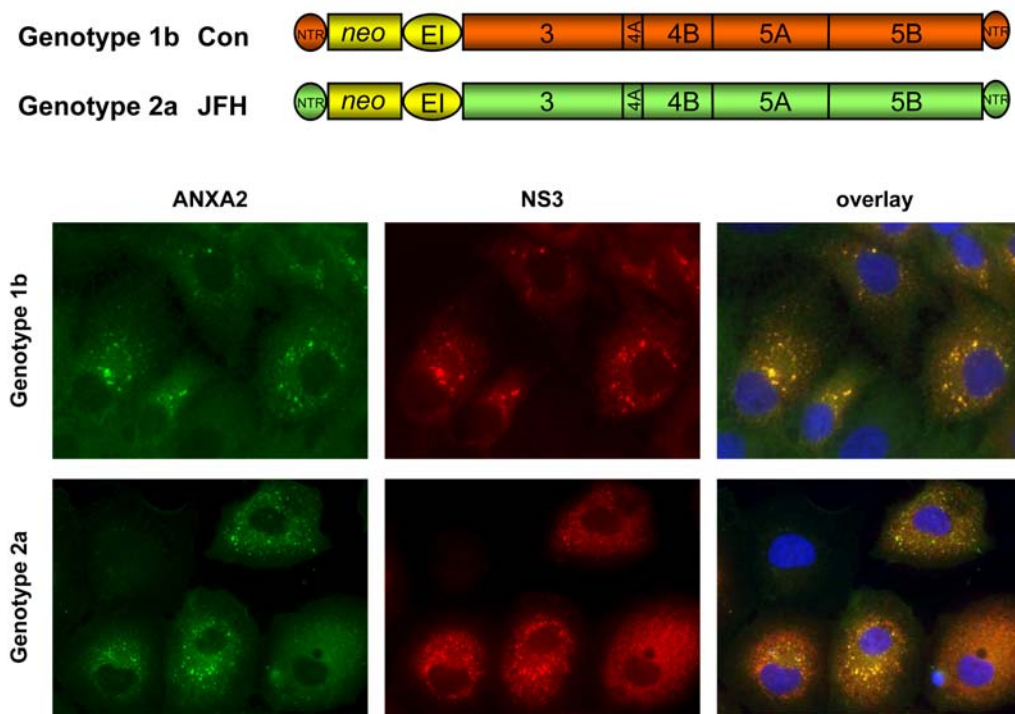
Fig. 22. Colocalization of ANXA2 and viral NS3 from different HCV genotypes. PFA-fixed and permeabilized monolayers of Huh-7 cells harboring subgenomic HCV replicon RNA of either genotype 1b (upper panels) or 2a (lower panels) were subjected to IFA using monoclonal antibodies specific for ANXA2 and a polyclonal antiserum raised against HCV NS3. The structures of the different subgenomic RNAs contained in the cells used in this experiment are depicted above the IF pictures.

In the previous colocalization studies of ANXA2 and viral NS proteins, I used cells replicating only subgenomic HCV RNAs. I was interested if the redistribution of ANXA2 would also occur in cells harboring HCV full-length RNA. To answer this question, naïve Huh7.5 cells - which are a Huh-7 subclone and most permissive for HCV infection[118] - were infected with Hepatitis C viruses expressing the complete viral genome of Jc1 (Fig. 23A). This chimeric full-length genome was constructed by fusing fragments from two different genotype 2a isolates, J6CF[231] and JFH1. The 5'-NTR and the part from the second transmembrane domain (TMD) of NS2 to the 3'-NTR originate from JFH1 and the region encoding core to the first TMD of NS2 from J6CF. This hybrid yielded infectious titers 100- to 1,000-fold higher than the parental JFH1 isolate[171].

48 hours post infection (p.i.), the cells were fixed in paraformaldehyde (PFA) and subjected to IFA. The normal cytosolic ANXA2 localization was seen in the non-infected cells (Fig. 23 B-D, right panels). In the infected cells however, the same alteration in the cytoplasmic ANXA2 distribution was observed as in cells containing subgenomic HCV replicons. Likewise, as illustrated in Fig. 23B-D left panels, the non-structural HCV proteins NS3, NS4B, and NS5A all showed a clear colocalization with ANXA2 in infected cells.

I wanted to exclude that the colocalization of ANXA2 and HCV NS proteins depends on the cell type of the different Huh-7 cells (naïve Huh-7, Huh7.5) I used for the previous colocalization studies. Therefore, other cell lines supporting HCV replication were examined.
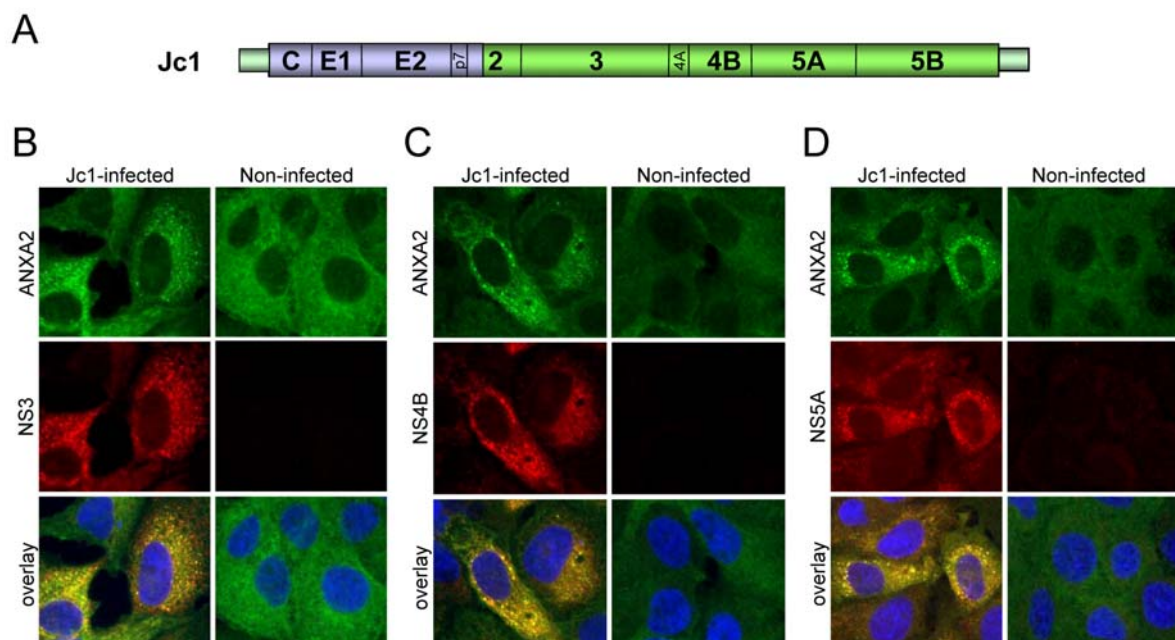
Fig. 23. Colocalization of ANXA2 and varying viral NS proteins in HCV infected cells. (A) Structure of the full-length RNA genome (Jc1) of the viruses used in this study. Shown in blue are the genes of the J6 isolate, in green are depicted the remaining genes and the NTRs of the JFH1 isolate. Both isolates belong to the HCV genotype 2a. (B-D) PFA-fixed and permeabilized monolayers of HCV-infected Huh-7.5 cells were subjected to IFA using monoclonal antibodies specific for ANXA2 and either a polyclonal antiserum raised against HCV NS3 (B), or a polyclonal antiserum raised against HCV NS4B (C), or a polyclonal antiserum raised against HCV NS5A (D). Mock-infected Huh-7.5 cells served as negative controls for the viral proteins.

Recently, it has been shown that genotypes 1b and 2a replicons also replicate persistently in the human hepatoblastoma cell line HuH6[228]. Similar to Huh-7 cells, efficient HCV replication in HuH6 cells depends on the presence of cell culture-adaptive mutations and the permissiveness of the host cell. However, three major differences exist: in HuH6 cells, viral replication is (i) independent from ongoing cell

proliferation, (ii) less sensitive to certain antiviral compounds, and (iii) highly resistant to IFN-gamma[228]. Furthermore, Hep56D JFH cells were available, a murine liver derived cell line supporting the consistent replication of a genotype 2a replicon (Marc Windisch, PhD thesis).

All these different cell lines were analyzed by IFA and it was tested whether the phenotype of ANXA2 redistribution to the HCV RCs could be retrieved in these cells. In naïve HuH6 and Hep56D cells, the regular cytoplasmic distribution of ANXA2 was observed (Fig. 24 and 25). In contrast, in HuH6 cells harboring subgenomic replicons from genotype 2a (HuH6 JFH, Fig. 24) or 1b (HuH6 Con, Fig. 25A), ANXA2 exhibited the typical HCV-associated rearrangement into dotted structures. Likewise, an evident colocalization of ANXA2 with the viral non-structural proteins NS3 (Fig. 24A), NS4B (Fig. 24B), and NS5A (Fig. 24C) was found in the HuH6 JFH cell line.

The same was true for murine Hep56D JFH cells (Fig. 25B), harboring a subgenomic genotype 2a replicon (JFH1).
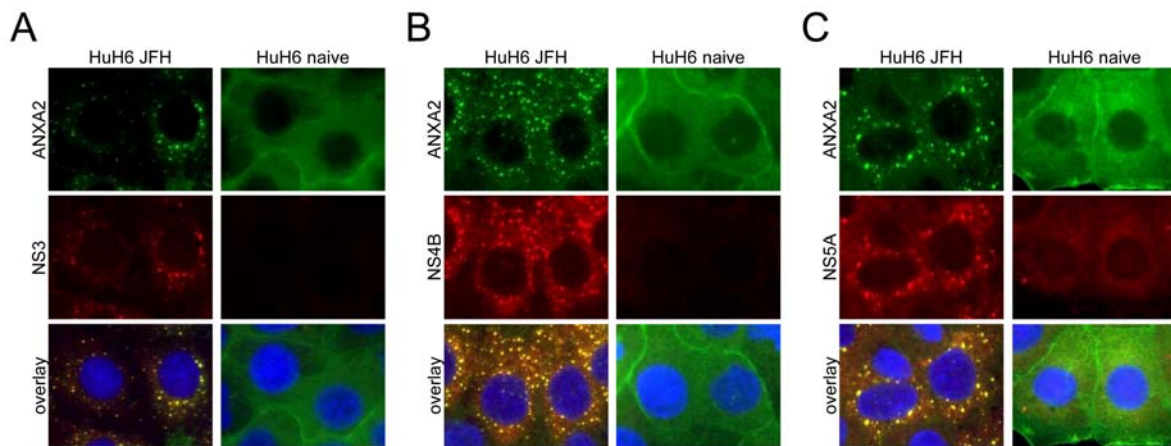
Fig. 24. Colocalization of ANXA2 with different viral NS proteins in HuH6 cells harboring a subgenomic replicon from genotype 2a (HuH6 JFH). PFA-fixed and permeabilized monolayers of HuH6 JFH cells were subjected to IFA using monoclonal antibodies specific for ANXA2 and either a polyclonal antiserum raised against HCV NS3 (A), or a polyclonal antiserum raised against HCV NS4B (B), or a polyclonal antiserum raised against HCV NS5A (C). Naïve HuH6 cells served as negative controls for the viral proteins.
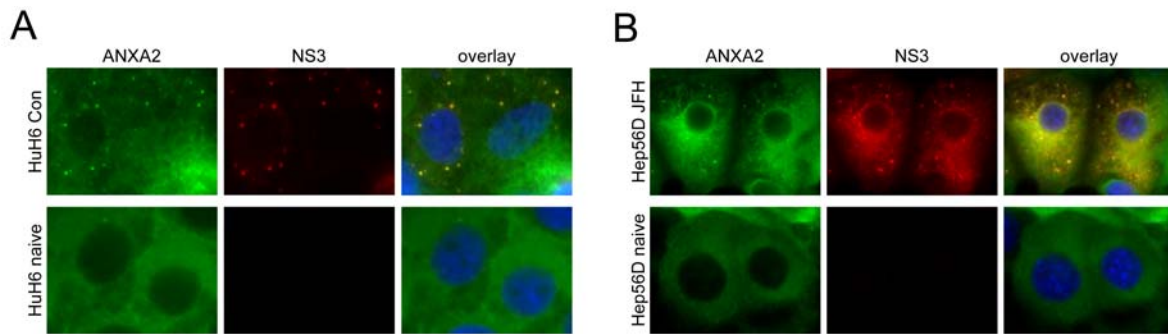
Fig. 25. Colocalization of ANXA2 and viral NS3 in HuH6 cells and murine Hep56D cells harboring subgenomic HCV replicons from genotype 1b (Con) and genotype 2a (JFH), respectively. Cells were fixed by PFA and permeabilized by TX-100, subsequently subjected to IFA using monoclonal antibodies specific for ANXA2 and a polyclonal antiserum raised against HCV NS3. (A) Colocalization of ANXA2 and HCV NS3 in HuH6 Con cells (upper panels). Naïve HuH6 cells served as negative control for the viral protein (lower panels). (B) Colocalization of ANXA2 and HCV NS3 in Hep56D JFH cells (upper panels). Naïve Hep56D cells served as negative control for HCV NS3 (lower panels).

3.3.2 No colocalization of HCV with other host proteins and of ANXA2 with other positive-stranded RNA viruses

So far, I had demonstrated that the change of the ANXA2 distribution upon HCV replication and its colocalization with viral NS proteins were found in different replication systems and cell types. The next step was to investigate whether other cellular proteins were colocalizing with the viral components of the HCV replication complex to address the specificity of the ANXA2-HCV colocalization. HCV replication takes place at the membranous web, vesicular membrane structures which are derived from the endoplasmic reticulum (ER) [50,51]. On account of this, I analyzed replicon cells for a potential colocalization of HCV NS proteins with an ER marker protein. I transiently transfected naïve Huh-7 cells with a selectable subgenomic genotype 2a replicon (neo_JFH) whose structure is depicted in Fig. 26A. As shown in the same figure, a specific colocalization of the ER marker protein Calnexin and the viral NS5A protein in HCV-transfected cells could not be observed. A change in the pattern of the typical ER stain of Calnexin due to HCV replication was not noticed either. This result indicated that HCV RCs did not specifically colocalize with the ER.

The major cellular interaction partner of ANXA2 is the protein p11[19,102]. Both proteins form a heterotetramer which brings two different membranes closely together[103] but does not trigger membrane fusion. Thus, we were interested if p11 would colocalize with HCV NS proteins.
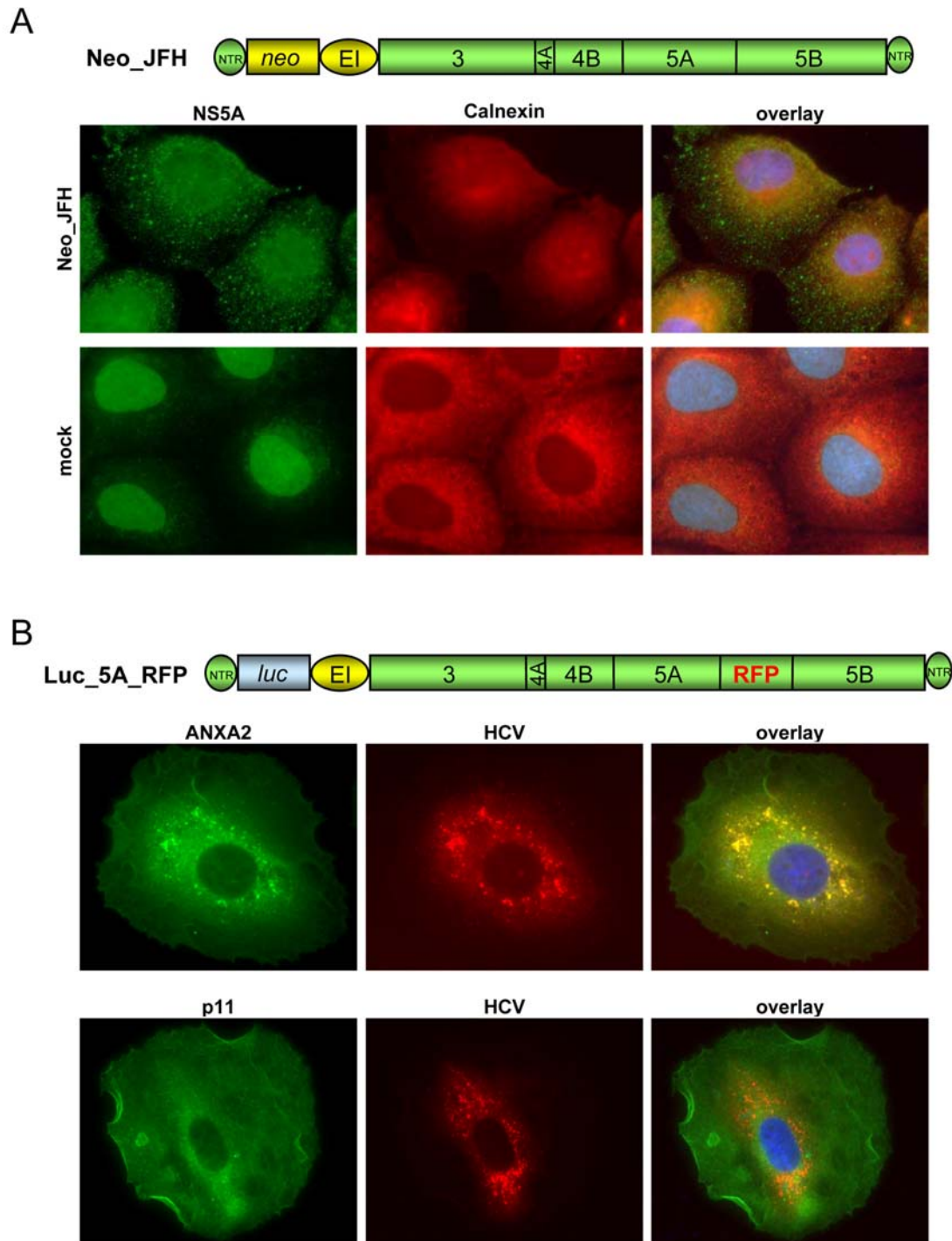
Fig. 26. Colocalization studies of HCV with different host cell proteins. After PFA fixation and permeabilization, Huh-7 cells transiently transfected with subgenomic HCV RNA (genotype 2a; Neo_JFH and Luc_5A_RFP, respectively) were subjected to IFA. (A) Colocalization study of HCV NS5A and Calnexin in Huh-7 cells transfected with subgenomic HCV RNA (Neo_JFH; upper panels) using monoclonal antibodies specific for HCV NS5A and a polyclonal antiserum raised against Calnexin. Mock-transfected Huh-7 cells served as negative control for HCV NS5A (lower panels). (B) Colocalization studies of RFP-coupled HCV NS5A with ANXA2 (upper panels) or p11 (lower panels) in transiently transfected Huh-7 cells, using monoclonal antibodies specific for the respective cellular protein. (A and B) The structure of the subgenomic RNAs used in these experiments are depicted above the corresponding IF pictures.

To answer this question, I transiently transfected naïve Huh-7 cells with a subgenomic genotype 2a replicon (luc_5A_RFP). This replicon encoded a luciferase

(luc) reporter gene and comprises the sequence coding for a red fluorescent protein (RFP) fused to the NS5A sequence. The structure of this luc_5A_RFP replicon is illustrated in Fig. 26B. The rearrangement of ANXA2 and its colocalization with the RFP which corresponded to the HCV signal was clearly detectable in the transfected cells (Fig. 26B, top panels). However, neither a change in the localization pattern of p11 between naïve and HCV-transfected cells (naïve cells not shown) was recognized nor a colocalization with HCV proteins (Fig. 26B, bottom panels). This indicated that the ANXA2 colocalization with HCV was independent of the interaction with p11.

ANXA2 belongs to the large family of Annexins which provide a link between Ca^{2+}-signalling and membrane functions exhibiting structural and functional homology[73]. Besides ANXA2, also ANXA4 and ANXA5 were identified as cellular candidate proteins to be associated with the HCV replication complex in the proteomic analyses (Table 1). Therefore, I wanted to know if other members of the Annexin family also were potentially involved in HCV replication and tested if they - like ANXA2 - colocalized with the HCV NS proteins building the replication complex. Naïve Huh-7 cells were transfected with a selectable subgenomic genotype 2a replicon RNA (neo_JFH). The fixed cells were analyzed by IFA for a colocalization of HCV NS proteins with Annexin I (ANXA1), Annexin IV (ANXA4), and Annexin V (ANXA5). As shown in Fig. 27A, ANXA1 was found in the nucleus, in the cytoplasm and at some cytosolic granule structures in naïve Huh-7 cells. A redistribution of ANXA1 upon HCV replication was not observed and neither was a colocalization with HCV proteins. ANXA4 showed a homogeneous cytoplasmic distribution in mock transfected cells. In HCV-harboring cells, a rearrangement of the ANXA4 localization to the sites of viral RCs was not detectable and consequently no distinct colocalization with HCV proteins (Fig. 27B). ANXA5 exhibited a diffuse cytosolic localization as well but also associated with some granules in the cytoplasm in naïve Huh-7 cells (Fig. 27C). This phenotype was not changed in HCV replicating cells, and – just as ANXA1 and ANXA4 – ANXA5 did not colocalize with HCV proteins. This demonstrated that the colocalization of ANXA2 with HCV RCs was not a common attribute of Annexin family members and emphasized its specificity.
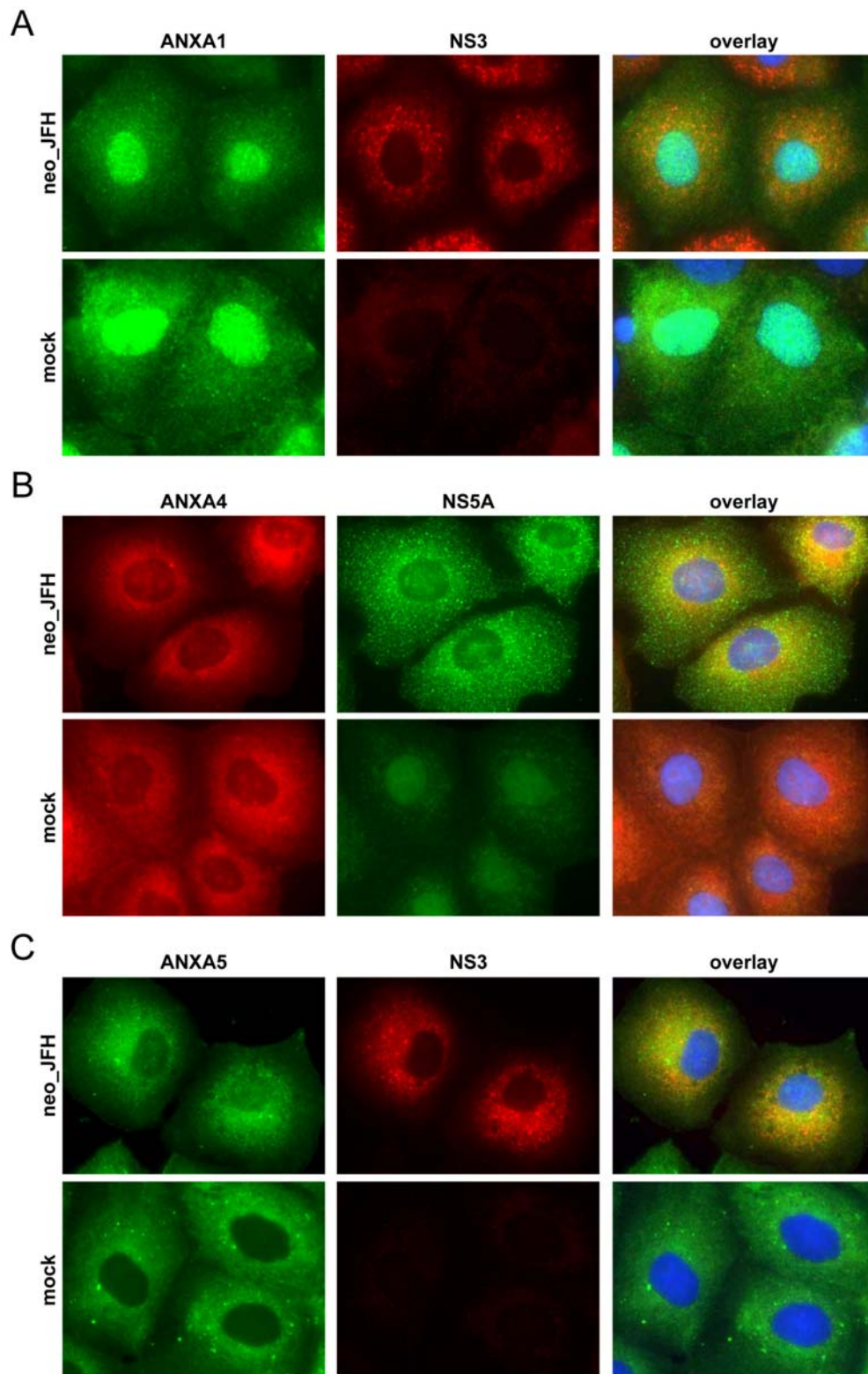
Fig. 27. No colocalization of other Annexins with HCV NS proteins. Huh-7 cells transiently transfected with a subgenomic genotype 2a HCV replicon (neo_JFH) were subjected to IFA. (A) Colocalization studies of ANXA1 and HCV NS3 using monoclonal antibodies specific for ANXA1 and a polyclonal antiserum raised against HCV NS3. (B) Colocalization studies of ANXA4 and HCV NS5A using monoclonal antibodies specific for HCV NS5A and a polyclonal antiserum raised against ANXA4. (C) Colocalization studies of ANXA5 and HCV NS3 using monoclonal antibodies specific for ANXA5 and a polyclonal antiserum raised against HCV NS3. Mock transfected naïve Huh-7 cells served as negative control for the HCV NS proteins.

After showing that the colocalization of ANXA2 with the sites of HCV RNA replication was not observed for other members of the Annexin family, we were interested if ANXA2 also colocalized with NS proteins of other positive-strand RNA viruses. To answer this question, naïve Huh-7 cells were infected with Dengue viruses (DV), fixed 24 hours post infection and analyzed by an immunofluorescence assay. Like HCV, DV is a member of the family *Flaviviridae*, but belongs to the genus *Flavivirus*. The DV replication complex was visualized by staining with antibodies raised against the DV non-structural proteins resulting in a punctuated pattern in the cytosol (Fig. 28A, left panel). ANXA2 showed a very homogeneous cytoplasmic distribution in uninfected cells (top left-hand corner of the panels in Fig. 28A). Its cellular localization was neither changed due to DV infection nor did it colocalize with DV NS proteins.

Another prominent member of the positive-strand RNA viruses is Semliki Forest virus (SFV) which is classified into the alphavirus family. To address a potential involvement of ANXA2 in SFV replication, a subgenomic replicon was transfected into naïve Huh-7 cells. 48 hours after transfection, cells were analyzed for colocalization of SFV NS3 with ANXA2. By staining with SFV NS3-specific antibodies the intracellular sites of viral RNA replication were determined. Similar to HCV and DV RCs, the SFV replication complexes appeared as cytosolic dot-like structures (Fig. 28B), although these structures have been shown to derive from late endosomes and lysosomes[123]. ANXA2 possessed its typical cytoplasmic distribution in non-transfected cells. In SFV-transfected cells, ANXA2 was mainly localized in the cytoplasm, although it was found in some granular structures, too. However, these granules did not colocalize with the dots representing the SFV RCs (Fig. 28B) indicating that this partial rearrangement of ANXA2 might not play a role in the SFV replication. These results confirmed that the redistribution of ANXA2 and its colocalization with viral NS proteins was specific for HCV and was not observed for other positive-stranded RNA viruses.
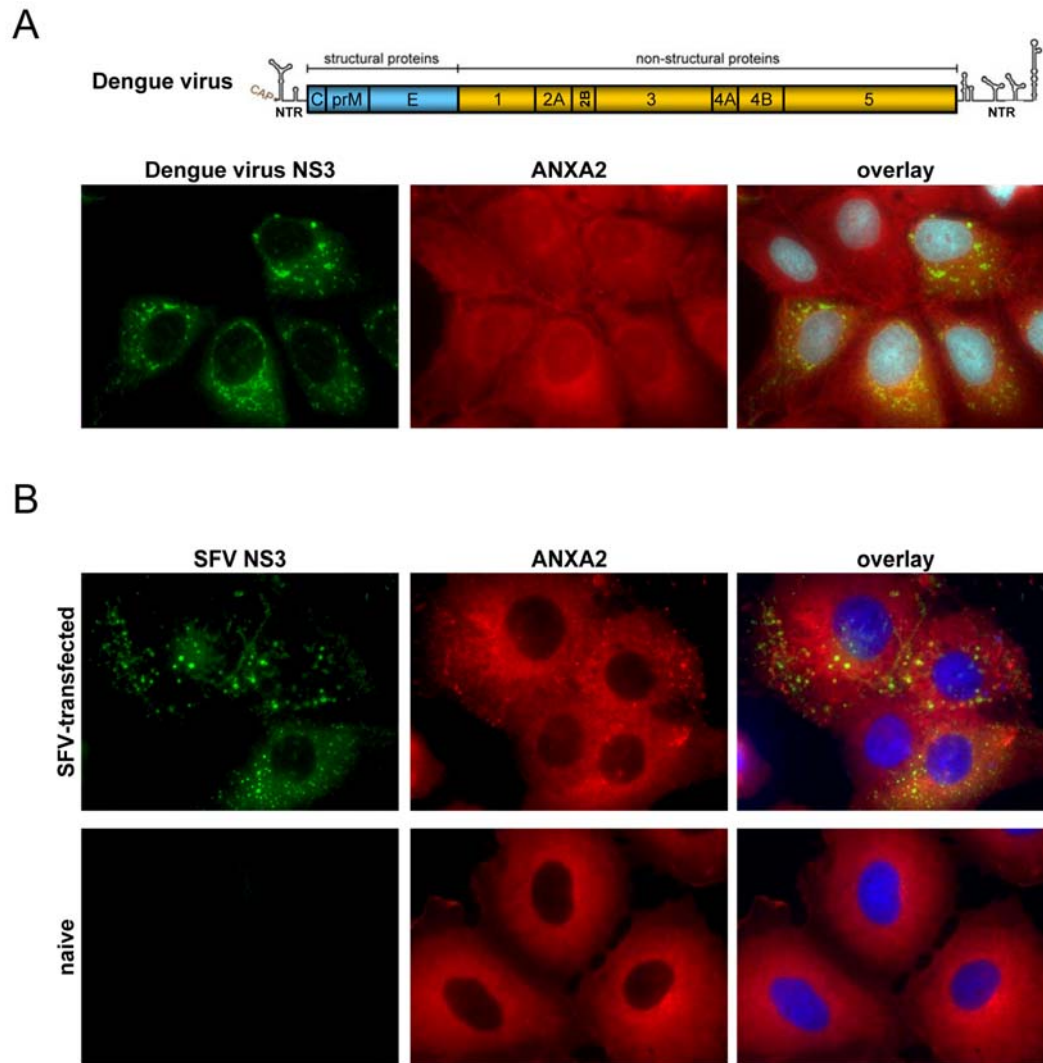
Fig. 28. No colocalization of ANXA2 with NS proteins of other positive-stranded RNA viruses. (A) Dengue virus infected Huh-7 cells were analyzed by immunofluorescence using monoclonal antibodies specific for ANXA2 and a polyclonal antiserum raised against Dengue virus NS3. The structure of the Dengue virus RNA is given above the IF panels. (B) Huh-7 cells transfected with Semliki Forest virus (SFV) RNA were analyzed by immunofluorescence using monoclonal antibodies specific for ANXA2 and a polyclonal antiserum raised against SFV NS3 (upper panels). Naïve Huh-7 cells served as negative control for SFV NS3 (lower panels).

Taken together, our studies showed that ANXA2 colocalized with HCV NS proteins and was redistributed to the sites of HCV RNA replication. This was independent from the experimental system, the HCV genotype, and the host cell type. I found no specific colocalization of HCV NS proteins with Calnexin and could rule out that p11, the major cellular interaction partner of ANXA2, interacted with the viral non-structural proteins since a colocalization of p11 with HCV NS proteins was not observed. In addition, the HCV NS proteins did not colocalize with any member of the Annexin family, but specifically with ANXA2. Further on, I demonstrated that ANXA2 was not colocalizing with the replication sites of other positive-stranded RNA viruses. The specific colocalization of HCV RCs with ANXA2 indicated that this protein might

play a vital role in viral replication. To answer this question, we evaluated the effects of ANXA2 overexpression and silencing onto HCV RNA replication.

3.3.3 Studies of the role of Annexin II in HCV replication in HepG2 cells

The previous colocalization studies indicated an interaction between the cellular protein ANXA2 and the viral protein components of the HCV replication complex. To gain further insights into the functional relevance of the ANXA2-HCV colocalization, we included the human hepatoma cell line HepG2 in our analysis. Puisieux and coworkers found that these cells comprised inherently no or only very low levels of ANXA2[175]. Interestingly, Date and colleagues established a HepG2 replicon cell line persistently replicating a subgenomic HCV genotype 2a replicon (JFH1)[43]. Due to their low endogenous ANXA2 levels, these cells appeared to be the appropriate tool to study overexpression as well as silencing of ANXA2 and its impact on HCV replication.

In a first step, naïve HepG2 cells and those harboring persistently a subgenomic HCV JFH1 replicon (HepG2_JFH1) were analyzed by IFA in order to investigate whether a colocalization of ANXA2 could also be found in these cells. Concordantly with the publication mentioned before, ANXA2 was not detected in naïve HepG2 cells (Fig. 29). In HepG2_JFH1 cells however, the ANXA2 protein was explicitly visible and was located in the cytoplasm in distinct dotted structures which perfectly colocalized with the pattern of the HCV non-structural proteins NS3, NS4B, and NS5A (Fig. 29 A-C). This indicated that the expression of ANXA2 was maybe induced or that the protein itself was potentially stabilized by HCV, thereby reaching protein amounts that were detectable by IFA. Since HepG2_JFH1 cells were derived from selected cell clones, those HepG2 cells might be selected because they harbored higher endogenous level of ANXA2 allowing HCV replication.

To evaluate whether an induction or a stabilization of ANXA2 occurred, HepG2 replicon and naïve cells were analyzed by immunoblot and quantitative RT-PCR for their ANXA2 protein and mRNA content, respectively. The difference of the ANXA2 protein level in these cells which was clearly visible in IFA could not be confirmed by immunoblot assay since ANXA2 was not detectable in the cell lysates (data not shown). The amount of ANXA2 mRNA between both different cell lines differed in one quantitative RT-PCR approach showing a higher level of ANXA2 mRNA in HepG2_JFH1 cells. However, this was not confirmed in a second experiment in

which both cell lines possessed similar mRNA amounts (data not shown). Therefore, it remains to be determined whether ANXA2 was induced or stabilized by HCV.
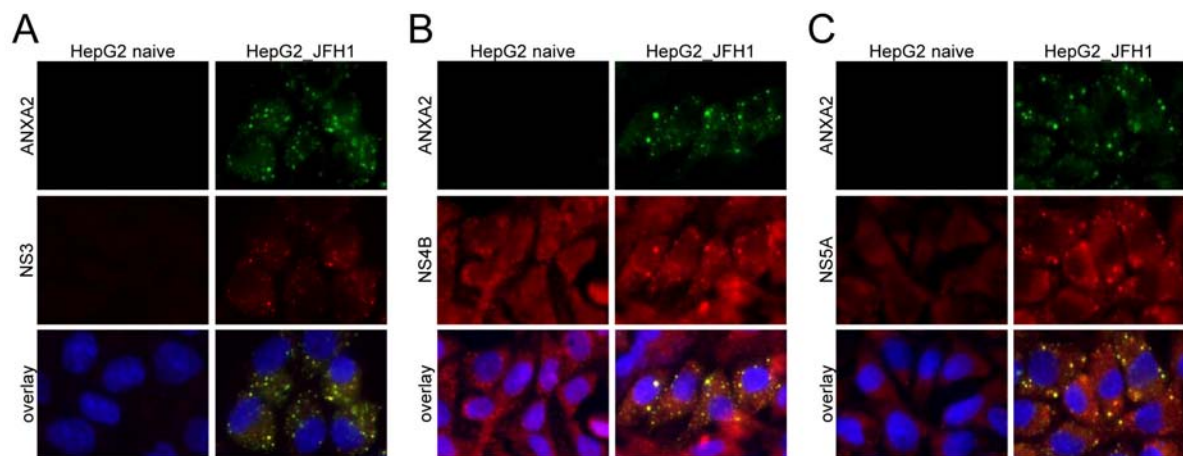
Fig. 29. ANXA2 expression and colocalization with HCV NS proteins in HepG2 cells harboring a subgenomic replicon from genotype 2a (HepG_JFH1). PFA-fixed and permeabilized monolayers of HepG2_JFH1 cells were subjected to IFA using monoclonal antibodies specific for ANXA2 and either a polyclonal antiserum raised against HCV NS3 (A), or a polyclonal antiserum raised against HCV NS4B (B), or a polyclonal antiserum raised against HCV NS5A (C). Naïve HepG2 cells served as negative controls for the viral proteins as well as for ANXA2.

The HCV replication level in HepG2 cells harboring subgenomic replicons was rather low, so I investigated whether an overexpression of ANXA2 in HepG2 cells would lead to an increase in HCV replication. To answer this question, cell lines constitutively expressing high amounts of ANXA2 were generated. Naïve HepG2 cells were stably transduced using lentiviral vectors encoding the ANXA2 gene and a selection marker gene (neomycin phosphotransferase in GUN constructs, blasticidin resistance gene in BLR constructs) and selected by the appropriate antibiotic. Control cell lines were produced by transduction with lentiviral vectors only coding for the respective selection marker. The expression levels of ANXA2 in these different HepG2 cell lines were analyzed by immunoblot (Fig. 30B). In both cell lines overexpressing ANXA2 (HepG2_GUN_ANXA2 and HepG2_BLR_ANXA2) this protein was readily traceable by immunoblot assay, whereas it was not detected in the control cell lines HepG2_GUN and HepG2_BLR. Having succeeded in generating HepG2 cell lines permanently overexpressing ANXA2, I analyzed if permissiveness for HCV replication was increased in these cell lines. Therefore, the cells were transiently transfected with *in vitro* transcripts of a viral subgenomic JFH replicon (Fig. 30A) and a non-replicating GND construct harboring an inactivating point mutation in the NS5B gene; both possessed a luciferase reporter gene. At different time points post transfection, cells were lysed and analyzed for luciferase activity

which was taken as a correlate of HCV replication[120,138]. In Fig. 30C, the replication levels are depicted as fold 4h values; this time point marks the luciferase expression from the input RNA and was arbitrarily set to 1. In all transfected cells - regardless if they were overexpressing ANXA2 or not - the replication levels at 24, 48 or 72 hours were very similar: they were below the 4 hour value, but about tenfold higher than the respective negative control; revealing that in fact only low levels of replication occurred in these cells. The increased amount of ANXA2 did not lead to an advantage for HCV replication in HepG2 cells, indicating that ANXA2 is not limiting HCV replication in HepG2 cells.
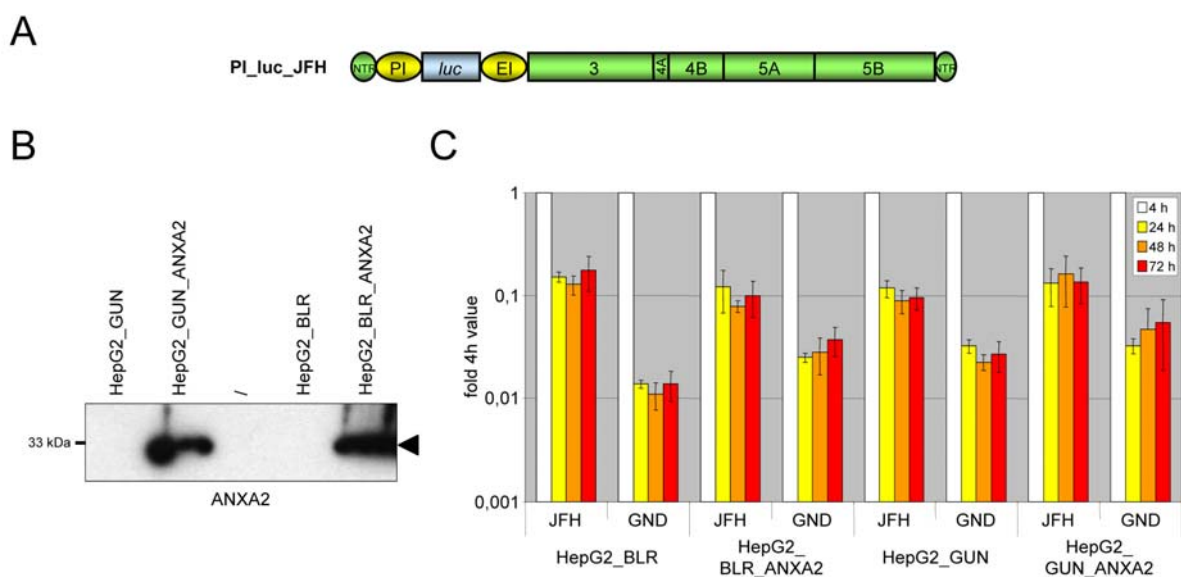
Fig. 30. ANXA2 overexpression in HepG2 cells and its effect on HCV replication. (A) Structure of the subgenomic RNA replicon used in this study. (B) Expression levels of ANXA2 in HepG2 cells stably transduced by recombinant lentiviruses. Equal cell amounts of different HepG2 cell lines were lysed and subjected to 10% SDS-PAGE. ANXA2 was detected in an immunoblot analysis using monoclonal antibodies specific for ANXA2. HepG2 cells durably transduced by lentiviruses expressing only the resistance gene (HepG2_GUN and HepG2_BLR) served as negative controls. (C) Time course of viral RNA replication levels in HepG2 cells stably overexpressing ANXA2. ANXA2 expressing HepG2 cells were transiently transfected with a subgenomic HCV RNA (JFH) harboring a luciferase reporter. Cells were harvested at the indicated time points and tested for luciferase activity. As controls, HepG2 cells permanently transduced by lentiviruses expressing only the resistance gene (HepG2_GUN and HepG2_BLR) were used. A non-replicating HCV replicon construct (GND) served as negative control for replication.

This was further confirmed by a colony formation assay. The same cell lines used for the time course experiment were transfected with a selectable HCV subgenomic replicon (JFH) or a replication-deficient control replicon (ΔGDD) (neo_JFH/blr_JFH and neo_ΔGDD/blr_ΔGDD). The transfected cells were then selected by the appropriate antibiotics. ANXA2 overexpressing cells showed only a minor increase in colony formation numbers compared to the control cells (data not shown). This

indicated again that ANXA2 – despite its low levels in HepG2 cells - was not limiting HCV replication in these cells. However, the low endogenous levels provided a good starting point to impact HCV replication by further reduction of ANXA2 using siRNA in HepG2 cells. If ANXA2 really was directly involved in HCV replication, one would expect that a reduction of the endogenous ANXA2 would also result in a decrease of viral replication. To answer this question, I transfected HepG2_JFH1 cells already containing rather minor amounts of ANXA2 protein with siRNA directed against ANXA2. Further, as controls, cells were transfected with either a siRNA specific for HCV (HCV321) or an unrelated control (p53). The ANXA2 mRNA amounts as well as the number of HCV RNA copies in these cells were determined by RT-PCR. ANXA2 mRNA levels of HepG2_JFH1 cells transfected repeatedly with different siRNAs were normalized to intracellular GAPDH mRNA levels and are shown in Fig. 31A. Compared to the HepG2_JFH1 cells transfected with siRNAs directed against p53 or HCV, the cells in which ANXA2 was silenced showed a slight decrease in ANXA2 mRNA levels (by a factor of two; note that higher delta CT values correspond to lower mRNA levels).
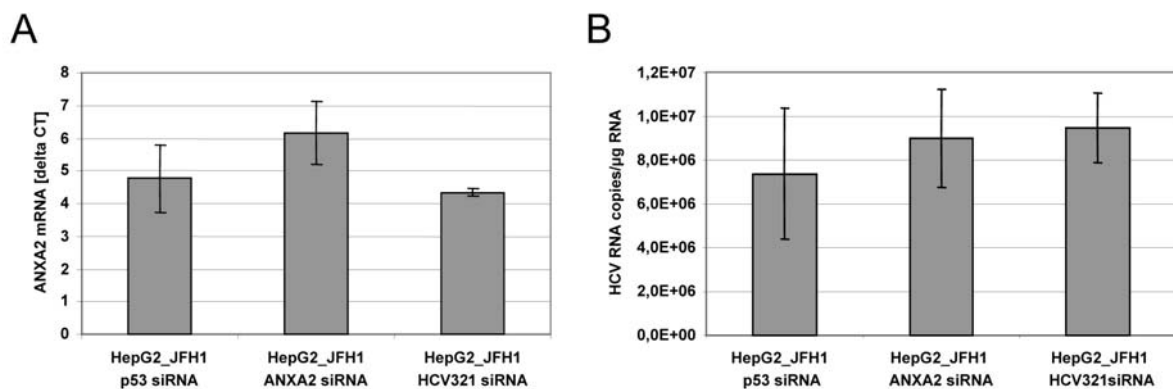
Fig. 31. ANXA2 silencing in HepG2_JFH1 cells. (A) ANXA2 mRNA levels in HepG2_JFH1 cells transfected with siRNAs effecting p53, ANXA2, and HCV RNA, respectively. The ANXA2 mRNA levels were analyzed by SYBR Green real-time PCR and were normalized to intracellular GAPDH mRNA levels. Note that higher bars represent lower mRNA levels. (B) HCV RNA levels in HepG2_JFH1 cells transfected with siRNAs effecting p53, ANXA2, and HCV RNA, respectively. The viral RNA was detected by real-time RT-PCR using HCV specific primers and probe and normalized for different loadings by GAPDH mRNA levels. It was quantified by means of a standard curve generated with known numbers of *in vitro* transcripts corresponding to a subgenomic replicon.

Since the silencing of ANXA2 seemed to work out at least to some extent, I analyzed the same samples for their content of HCV RNA (Fig. 31B). The number of viral RNA copies in HepG2_JFH1 cells transfected with siRNA directed against ANXA2 was in the same range to that of the control-silenced (p53 siRNA) cells. The siRNA specific for HCV (HCV321) which should serve as a positive control for silencing seemed not

to work in this experiment, since the HepG2_JFH1 cells transfected by this siRNA showed no reduction in their HCV RNA level compared to the other silenced cells. This indicated that the overall transfection efficiency was low. The fact that a decrease of HCV RNA copies was not observed in ANXA2-silenced HepG2_JFH1 cells was presumably due to the low silencing efficiency of about 50%.

We found that the ANXA2 level was increased in HepG2 cells harboring a HCV subgenomic replicon compared to naïve HepG2 cells which was clearly seen in IFA. However, overexpression or silencing of ANXA in HepG2 cells had no impact on the viral replication. Since the protein levels of ANXA2 expressed from the endogenous locus were below the detection limit of an immunoblot, it remained an open question whether ANXA2 was induced or stabilized in presence of HCV.

3.3.4 Silencing of Annexin II and its effect on HCV replication in Huh-7 cells

The most efficient cells to study HCV replication are Huh-7 cells. Therefore, we decided to analyze the impact of ANXA2 silencing onto transient HCV replication in these cells. However, their high endogenous levels of ANXA2 could complicate functional silencing.

In a first line of experiments, shRNA cell lines stably silencing ANXA2 were generated to reach a sufficient decrease in the steady state protein level. An shRNA directed against p53 mRNA was chosen as a control, since it was shown by Krönke and colleagues that silencing of p53 did not affect HCV replication[121] whereas several other control shRNAs had negative pleiotropic effects (data not shown). The differences in ANXA2 amounts between Huh-7 cells producing shRNAs directed against ANXA2 (sh ANXA2 lunet) and control cells generating p53-specific shRNAs (sh p53 lunet) were analyzed by immunofluorescence assay and are depicted in Fig. 32A. The cells had been sorted by FACS (fluorescence activated cell sorting) due to their GFP co-expression to have a cell population providing high amounts of shRNA. However, there was still a substantial number of cells visible containing high levels of ANXA2 in the sh ANXA2 cell line. Nevertheless, these shRNA cell lines were transiently transfected with *in vitro* transcripts of subgenomic replicons from different HCV genotypes (PI_luc_JFH, PI_luc_ET, and PI_Luc_GND as non-replicating control), lysed at varying time points and tested for luciferase activity. As

demonstrated in Fig. 32B, PI_luc_JFH and PI_luc_ET, respectively, showed no variances in their replication levels in the different shRNA cell lines. This could be due to the inefficient silencing of ANXA2 in the sh ANXA2 lunet cell line, and therefore the remaining ANXA2 level was sufficient for an efficient HCV replication.
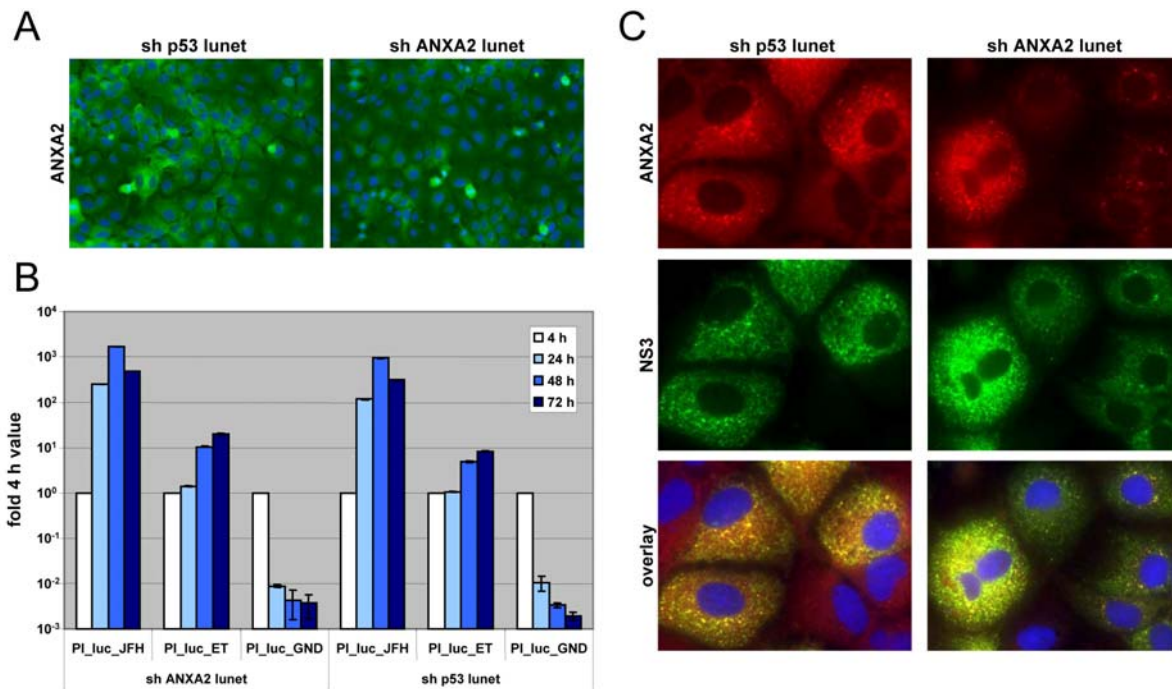
Fig. 32. Stable silencing of ANXA2 in shRNA cell lines and its effect on transient HCV replication. (A) ANXA2 levels in different shRNA cell lines. ShRNA cells were subjected to IFA using monoclonal antibodies directed against ANXA2. (B) Time course of viral RNA replication in different shRNA cell lines. ShRNA cells were transiently transfected with different subgenomic HCV luciferase replicons, harvested and lysed at the indicated time points, and analyzed for luciferase activity. A replication-deficient HCV replicon construct (GND) served as negative control. (C) Colocalization studies of ANXA2 with HCV NS3 in shRNA cells transiently transfected with a subgenomic HCV JFH1 replicon. Transfected cells were PFA-fixed, permeabilized and subjected to IFA using monoclonal antibodies specific for ANXA2 and a polyclonal antiserum raised against HCV NS3.

Immunofluorescence analyses of the HCV-transfected sh ANXA2 cells revealed a strict correlation of HCV and ANXA2 levels: cells containing plenty of ANXA2 seemed to support high levels of HCV replication, no ANXA2 was visible in HCV non-transfected cells, and lower levels of HCV NS proteins were observed in cells with low ANXA2 amounts (Fig. 32C). Although an impact of stable ANXA2 silencing onto HCV replication was not found, the findings of the colocalization studies pointed to a potential correlation of ANXA2 and HCV NS protein levels.

I also tested whether stable ANXA2 silencing in Huh7.5 cells had an influence on HCV infection. However, neither the viral replication nor the infectivity of the resulting supernatants was affected, even if the cells were additionally transfected by siRNA to boost the silencing efficiency (data not shown).

Stable silencing of ANXA2 in shRNA cell lines was not as efficient as expected. Therefore, we decided to silence ANXA2 transiently using specific siRNAs. Since ANXA2 was identified as putative cofactor of the HCV replication complex by comparative 2D gel analyses of subgenomic replicon cells, it was obvious to analyze the effect of decreased ANXA2 amounts in those cell lines. Though, transient silencing of ANXA2 in subgenomic replicon cell lines persistently replicating viral RNAs (lucubineo ET, 9-13, and 5-15 cells) had no impact on the HCV replication levels and the HCV RNA copy numbers, respectively (data not shown).

Likewise, I investigated whether transient ANXA2 silencing was affecting HCV infection. For this experiment, Huh7.5 cells were silenced twice with siRNA directed against ANXA2 or a control siRNA. The infection with virus harboring a full-length genotype 2a genome and a luciferase reporter gene (Jc1-luc) was performed between the two rounds of silencing. However, neither the replication of the virus nor the infectivity of the resulting supernatants was influenced by ANXA2 silencing (data not shown).

To answer the question, whether ANXA2 silencing influences transient HCV replication, naïve Huh-7 cells were transfected twice with siRNA directed against ANXA2 or an unspecific control. Simultaneously with the second siRNA transfection, *in vitro* transcripts of subgenomic HCV replicons from different genotypes were transfected by electroporation. The luciferase replicons used in this experiment are depicted in Fig. 33A. The replicon PI_luc_JFH contains NTRs and NS protein-coding sequences of genotype 2a, PI_luc_ET those of genotype 1b. The ANXA2 protein levels in the differently silenced and transfected Huh-7 cells were determined qualitatively by immunoblot (Fig. 33B). The amount of ANXA2 was considerably lower in ANXA2-silenced cells compared to the control-silenced cells indicating that the silencing was efficient. This was also irrespective from the transfected HCV RNA genotype or a mock transfection. In order to investigate whether the transient silencing of ANXA2 in Huh-7 cells had an impact on HCV replication, I lysed the cells at different time points after transfection and analyzed them for luciferase activity (Fig. 33C). The replication of the PI_luc_ET construct was similar in ANXA2-silenced cells and in control-silenced cells, i.e. exhibited no differences due to ANXA2 silencing. The PI_luc_JFH replicon also did not show any discrepancies in replication levels as a result of the reduction of ANXA2 compared to the control cells. Therefore,

silencing of ANXA2 by siRNA did not affect transient HCV replication rates irrespective from the viral genotype.

Fig. 33. Transient silencing of ANXA2 and its effect on transient HCV replication. (A) Structures of the luciferase reporter replicon constructs used in this study. (B) ANXA2 protein levels in naïve Huh-7 cells transiently transfected with subgenomic HCV replicons as well as with siRNA specific for ANXA2 or an unrelated control siRNA. Cells were lysed 48 h p. tr., subjected to SDS-PAGE and analyzed by immunoblot assay using monoclonal antibodies raised against ANXA2 and Actin, respectively. The signal of the latter was used as loading control. (C) Time course of HCV RNA replication in naïve Huh-7 cells transiently transfected with HCV luciferase replicons and siRNA anti-ANXA2 or control siRNA. Cells were harvested at different time points and tested for luciferase activity. (D) Colocalization studies of ANXA2 with HCV NS3 in Huh-7 cells transiently transfected with a subgenomic HCV JFH1 replicon and siRNA directed against ANXA2 or a control siRNA. Transfected cells were PFA-fixed, permeabilized and subjected to IFA using monoclonal antibodies specific for ANXA2 and a polyclonal antiserum raised against HCV NS3.

However, IFA of these cells still revealed a strict correlation of ANXA2 and HCV levels as indicated by colored arrowheads in the lower panels of Fig. 33D: (i) cells not

transfected by HCV showed hardly any signal for ANXA2 (yellow), (ii) cells containing high levels of HCV NS protein had still a large amount of ANXA2 (red), and (iii) in cells comprising low amounts of HCV and presenting only isolated spots for NS proteins, ANXA2 was found to colocalize with these spots but was barely recovered at other locations in the cytoplasm (blue). This result implied that low amounts of ANXA2 were associated with minor levels of HCV and was also observed upon stable silencing of ANXA2. As a putative cofactor of the HCV replication complex, ANXA2 was maybe protected and/or stabilized by HCV (at least partially) and therefore could still be found in HCV-transfected, ANXA2-silenced cells. In contrast, in the control-silenced cells only two distinct phenotypes were detected: HCV non-transfected cells showed the general cytoplasmic distribution of ANXA2, whereas in cells replicating HCV the typical rearrangement of ANXA2 was observed as well as its colocalization with viral proteins (Fig. 33D, upper panels).

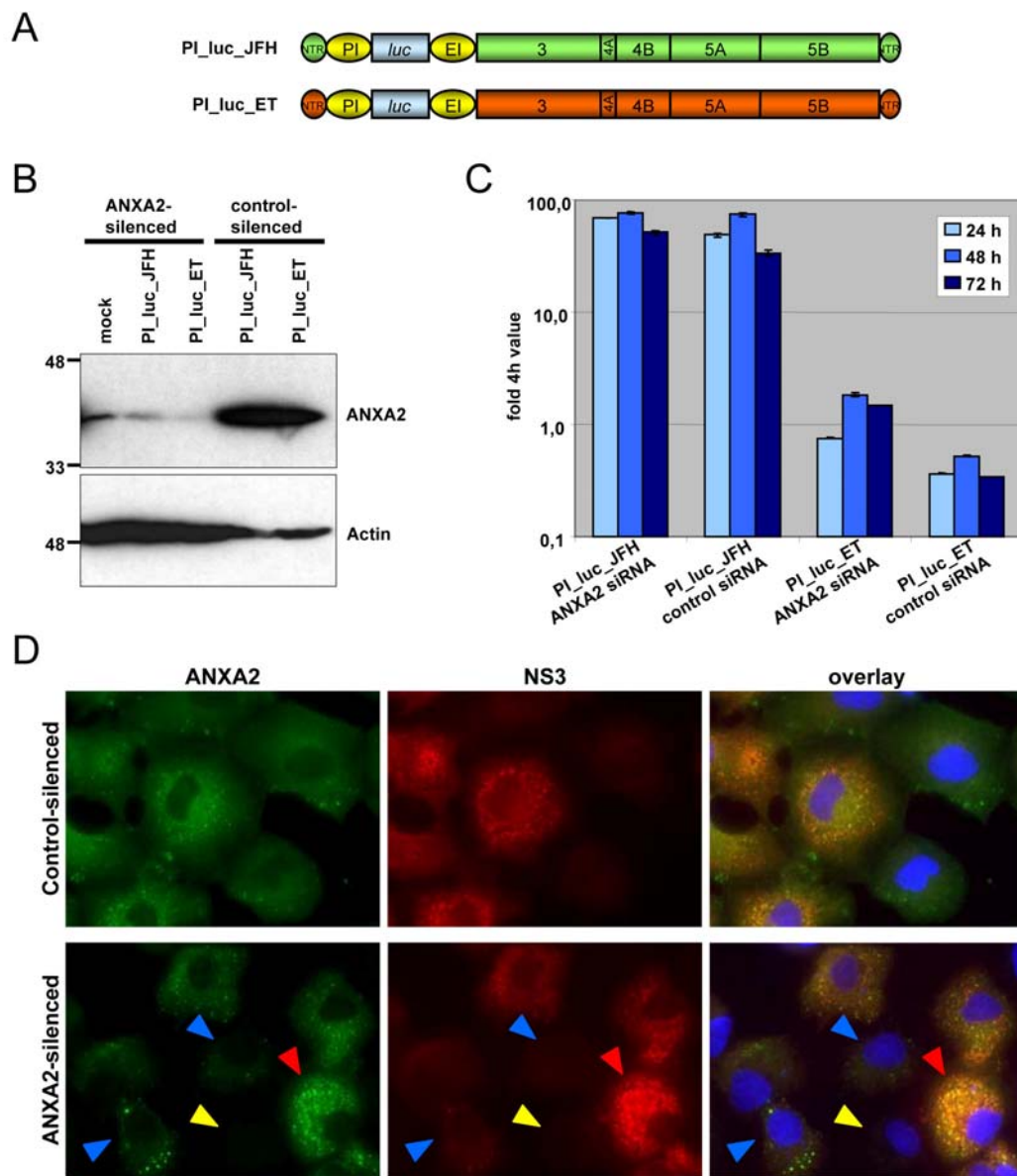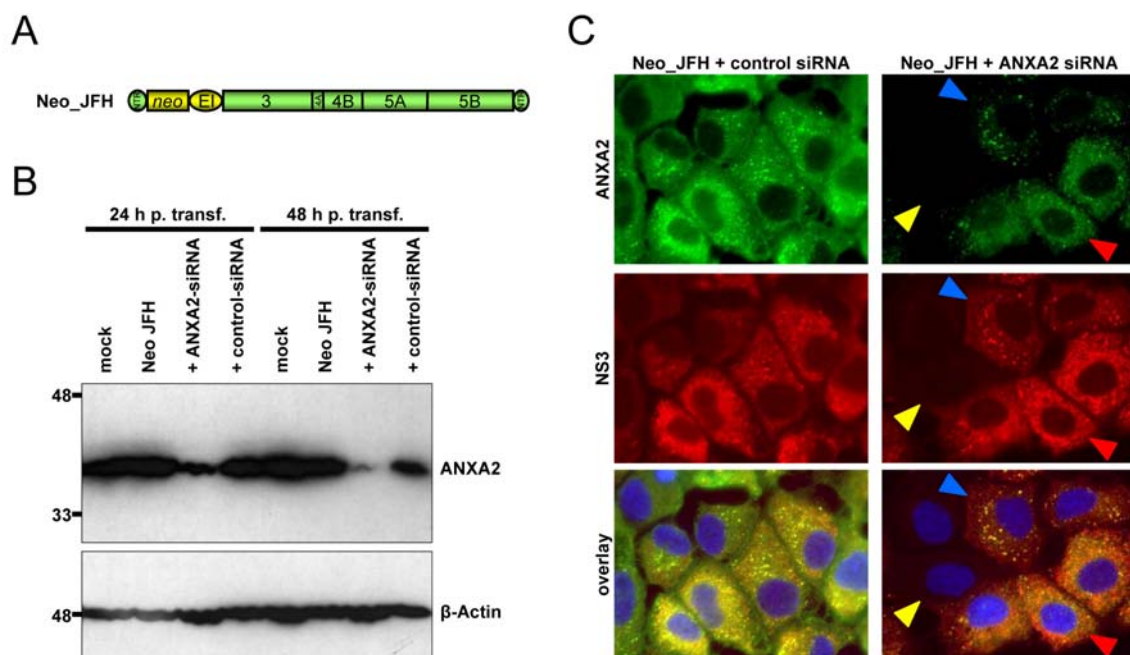**Fig. 34.** Transient silencing of ANXA2 and its effect on transient HCV replication. (A) Structure of the HCV replicon used in this study. (B) ANXA2 protein levels in naïve Huh-7 cells transiently transfected with a subgenomic HCV replicon as well as with siRNA specific for ANXA2 or an unrelated control siRNA. Cells were harvested and lysed at the indicated time points, subjected to SDS-PAGE and analyzed by immunoblot assay using monoclonal antibodies raised against either ANXA2 or Actin. The signal of the latter was used as loading control. (C) Colocalization studies of ANXA2 with HCV NS3 in Huh-7 cells transiently transfected with a subgenomic HCV JFH1 replicon and siRNA anti-ANXA2 or a control siRNA. Transfected cells were PFA-fixed (48 h p.tr.), permeabilized and subjected to IFA using monoclonal antibodies specific for ANXA2 and a polyclonal antiserum raised against HCV NS3.

A repetition of this experiment using a slightly different replicon construct illustrated the different stainings found in ANXA2-silenced cells yet even more obvious. In this

experimental setup, naïve Huh-7 cells were also transfected twice with siRNA specific for ANXA2 or a control siRNA. At the same time as the second silencing, these cells were transiently transfected with a selectable subgenomic RNA from genotype 2a harboring a neomycin phosphotransferase gene (Neo_JFH; Fig. 34A). Cells were harvested 24 and 48 hours after HCV transfection, and analyzed for ANXA2 protein levels by immunoblot assay. As shown in Fig. 34B, already 24 h post transfection a decrease in the ANXA2 amount was observed in ANXA2-silenced cells, and this reduction was even more obvious after 48 hours. The ANXA2 levels in the control cells stayed unchanged. The phenotypes of ANXA2 staining found in the preceding experiment and mentioned above were affirmed by immunofluorescence studies of ANXA2- and control-silenced cells both transfected with Neo_JFH RNA (Fig. 34C). Again, a strict correlation of ANXA2 and NS3 levels was observed in cells treated with siRNA directed against ANXA2.

Transient as well as stable ANXA2 silencing did not massively affect any aspect of the HCV life cycle, in particular the viral replication. However, although the ANXA2 silencing was done in different ways, we always found a clear correlation of ANXA2 and HCV NS protein levels in individual cells in all experimental settings.

To analyze this aspect more quantitatively, the same experiments were investigated by FACS. Therefore, naïve Huh-7 cells were transfected twice with siRNA specific for ANXA2 or - as control - the DV 3'UTR. Simultaneously with the second silencing, these cells were transiently transfected with a subgenomic RNA from genotype 2a harboring an emerald GFP (emGFP) inserted into the C-terminus of NS5A (luc_JFH/5A_emGFP). Therefore, the HCV replication could be directly correlated to the GFP expression, whereas the ANXA2 protein levels were determined by staining with a specific monoclonal antibody. Cells were fixed in PFA 48 hours after transfection, permeabilized, and stained intracellularly against ANXA2. GFP expression levels upon HCV replication and ANXA2 protein amounts were analyzed by FACS. To confirm a correlation between ANXA2 and HCV, cells being positive for HCV replication (GFP expression) should also be positive for ANXA2. Dot blot analyses of ANXA2- and control-silenced cells, both transfected with HCV, are shown in Fig. 35. To determine the cell pool negative for HCV as well as for ANXA2, mock silenced, mock transfected Huh-7 cells were investigated by FACS (Fig. 35A). These cells were only stained with a secondary fluorescence-coupled antibody to evaluate the background caused by this antibody as well as their autofluorescence.

Based on that, the dot blots were subdivided in four quadrant regions representing HCV- and ANXA2-negative cells (lower left), HCV-positive and ANXA2-negative cells (upper left), HCV- negative and ANXA2-positive cells (lower right), and HCV- and ANXA2-positive cells (upper right). After ANXA2 silencing in mock transfected cells, as expected, the portion of ANXA2-positive cells was diminished from 58.6% to 1%, compared to the control-silenced cells (Fig. 35B and C). This showed that the ANXA2 silencing was efficient. In HCV-transfected cells, the portion of HCV- and ANXA2-positive cells was reduced from 63% to 13.5% upon ANXA2 silencing (Fig. 35E and F). The increased number of HCV-transfected cells remaining positive for ANXA2 despite ANXA2 silencing (13.5%, Fig. 35F) compared to the ANXA2-positive cell population in mock transfected, ANXA2-silenced cells (1%, Fig. 35C) pointed to possible induction or stabilization of ANXA2 by HCV. The FACS analyses also indicated a general correlation between HCV replication and ANXA2 protein level, irrespective of the silencing. This was reproducible in several independent experiments, thus, it was investigated in greater detail.
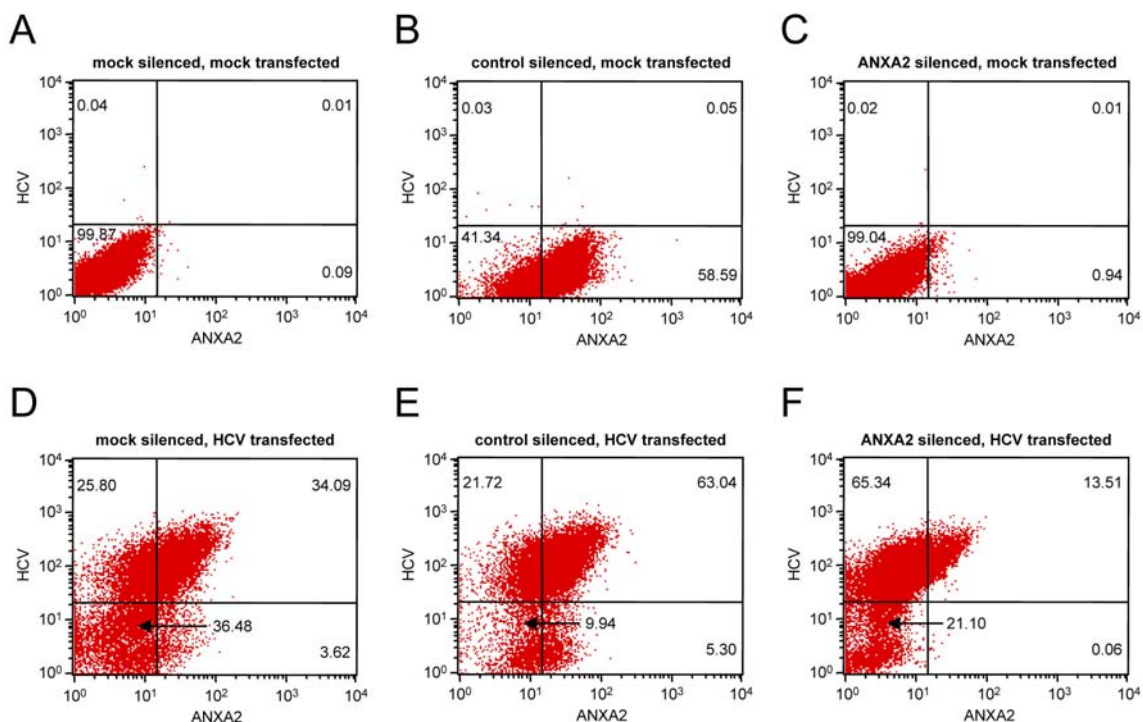
Fig. 35. FACS analyses of ANXA2-silenced Huh-7 cells transiently transfected with an GFP-harboring HCV subgenomic replicon. (A) Mock transfected, mock silenced Huh-7 cells. Cells were only stained with the secondary antibody and served as control to evaluate the cell pool being negative for HCV as well as for ANXA2 and determine the quadrant regions. (B) Control-silenced (DV 3'UTR), mock transfected Huh-7 cells. (C) ANXA2-silenced, mock transfected Huh-7 cells. (D) HCV-transfected, mock silenced Huh-7 cells. (E) Control-silenced (DV 3'UTR), HCV-transfected Huh-7 cells. (F) ANXA2-silenced, HCV-transfected Huh-7 cells. (B-F) Cells were stained against ANXA2. The fraction of cells (in %) detected in the respective quadrants are given.

Therefore, the dot blots were subdivided into smaller regions, this is shown exemplarily for control-silenced, HCV-transfected cells in Fig. 36. The horizontal line separates the HCV-negative (below) from the HCV-positive cells (above). The blot was further subdivided by the logarithmic scale of the abscissa into smaller regions. For each upper region (HCV-positive) the mean fluorescence intensities (MFIs) for ANXA2 as well as for HCV were determined and compared with each other in order to investigate a possible correlation.
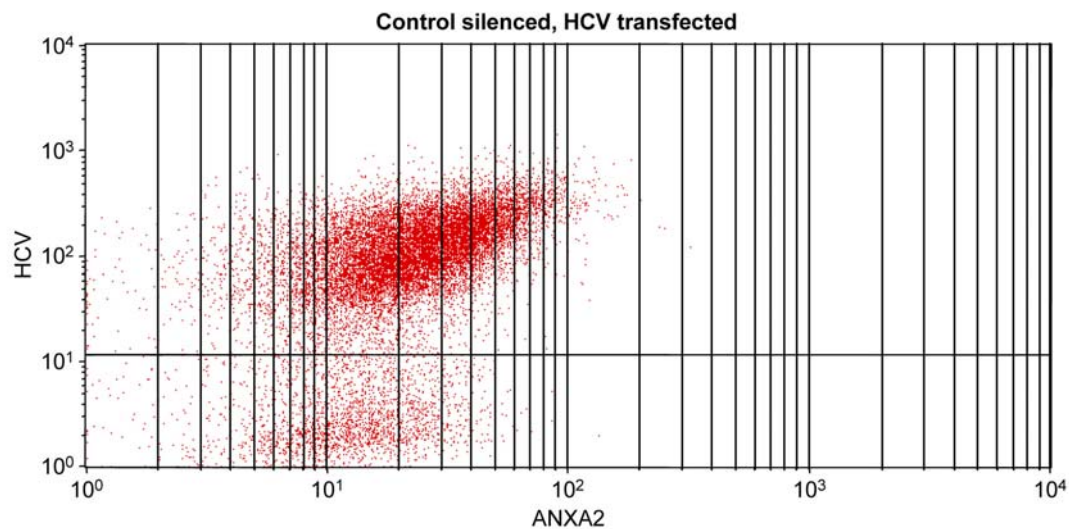
Fig. 36. Example of a FACS dot blot subdivision to determine the mean fluorescence intensities (MFIs) of HCV and ANXA2. Cells negative for HCV are located in the regions below the horizontal line, HCV-positive cells in the regions above. Only the MFIs of the upper regions were determined.

The MFI values were related to each other resulting in a graph which is exemplarily shown for a single experiment in Fig. 37. Increasing MFIs of ANXA2 were positively correlated with ascending MFIs for HCV, i.e. the more ANXA2 protein was contained in the cell the higher was the HCV replication level and vice versa. This phenotype was observed in all cells regardless of their siRNA treatment. This indicated that the level of HCV replication in a cell depended on its ANXA2 amount or that HCV induced higher ANXA2 levels.
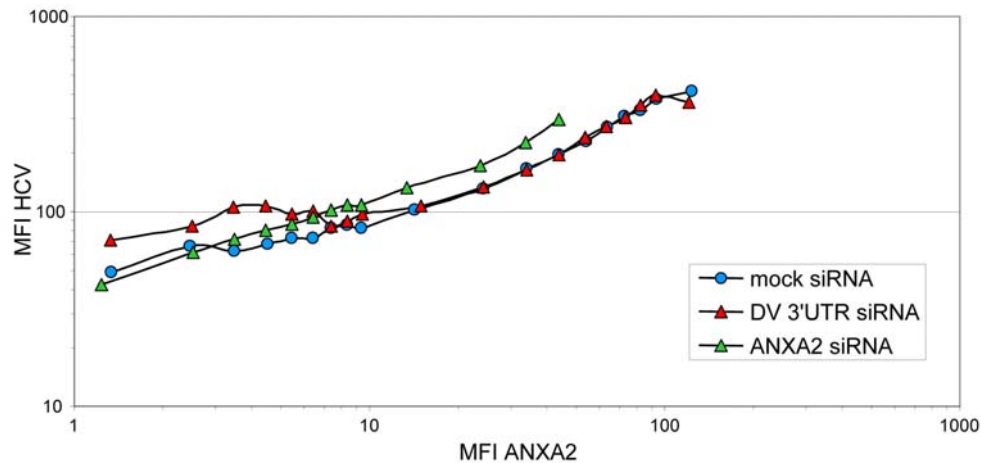
Fig. 37. Positive correlation of ANXA2 levels and HCV replication. Naïve Huh-7 cells were transfected twice with siRNAs directed against ANXA2 or the 3'UTR of DV, or with PBS (as mock control), respectively. Additional to the second siRNA transfection, the cells were simultaneously transfected with a subgenomic HCV replicon comprising emGFP fused to NS5A. 48 hours post transfection, cells were singularized and fixed in PFA. Subsequently they were permeabilized, stained intracellularly by using monoclonal antibodies directed against ANXA2 and analyzed by FACS. The abscissa shows the mean fluorescence intensities (MFI) of ANXA2, the ordinate shows the corresponding MFI of HCV (GFP). Blue filled circles represent mock silenced cells, red filled triangles control-silenced cells (DV 3'UTR), and green filled triangles ANXA2-silenced cells.
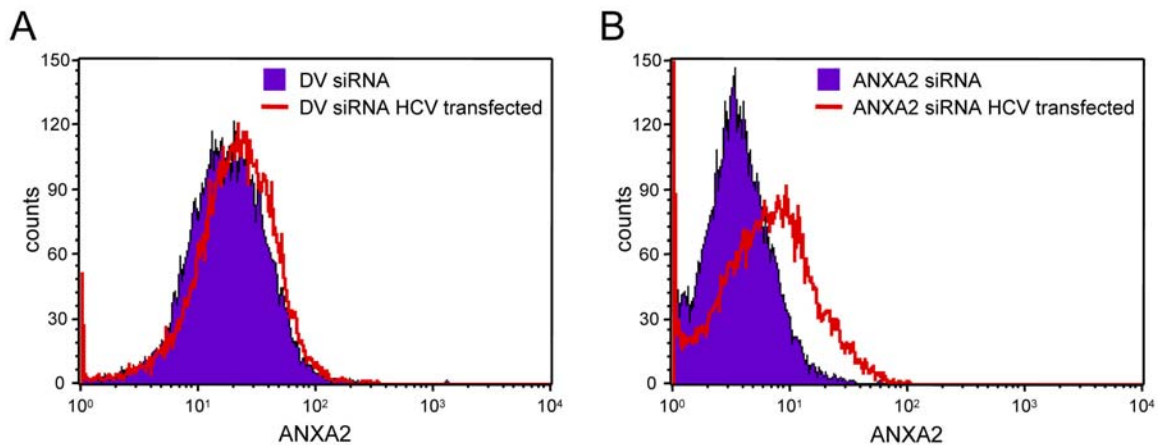
Fig. 38. Slightly increased ANXA2 levels upon HCV transfection. (A) ANXA2 levels in HCV-transfected and non-transfected Huh-7 cells both additionally transfected with siRNA directed against the 3'-UTR of DV (DV siRNA). (B) ANXA2 levels in HCV-transfected and non-transfected Huh-7 cells both additionally transfected with siRNA directed against ANXA2 (ANXA2 siRNA). In both diagrams, the abscissa shows the fluorescence intensity of ANXA2, the ordinate specifies the number of cells. The silenced, HCV non-transfected cells are given in blue; the silenced, HCV-transfected cells are indicated by a red line.

The latter aspect, increased ANXA2 levels in presence of HCV, was visible more clearly in a histogram, especially upon ANXA2 silencing (Fig. 38). The increased ANXA2 levels could be due to an induction of ANXA2 expression or a stabilization of the ANXA2 protein by HCV. To test the first alternative, the ANXA2 mRNA levels in different cell lines were analyzed by RT-PCR assay. If the ANXA2 expression was

induced by any HCV component, an increased ANXA2 mRNA level could be expected in cells persistently replicating viral RNA compared to the naïve cells. I compared different naïve cell lines with replicon cell lines originating from those naïve cells and - if present - also with corresponding cured replicon cell lines, e.g. 9-13 and cured 9-13 cells; naïve HuH6 cells, HuH6_JFH cells, and cured HuH6 cells, as well as further cell lines. Unfortunately, the results of two independent RT-PCR assays were not reproducible. Between the different experiments, the ANXA2 mRNA levels of the single cell lines showed big fluctuations and therefore did not permit reliable conclusions whether ANXA2 expression was induced by HCV replication (data not shown). On the other hand, as mentioned before, we observed a slight decrease in HCV replication when ANXA2 was silenced. This result was reproducible in several independent experiments and is depicted for two of them in Fig. 39. It was unambiguously visible that the number of cells harboring high levels of HCV was lower in ANXA2-silenced cells compared to control-silenced cells. This result clearly indicated that ANXA2 played a functional role in controlling HCV replication.
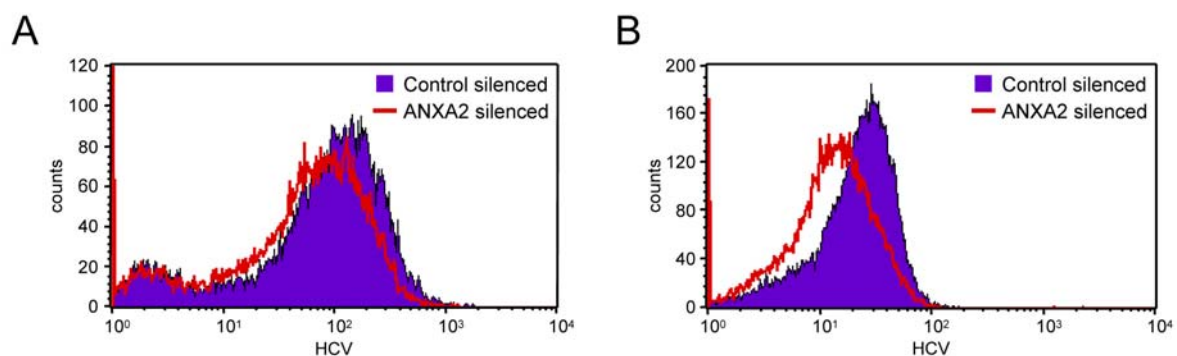
Fig. 39. Slightly reduced HCV levels upon ANXA2 silencing. HCV levels in ANXA2-silenced and control-silenced (DV 3'UTR) cells transiently transfected with HCV. (A) and (B) represent two independent experiments. In both diagrams, the abscissa shows the fluorescence intensity of HCV, the ordinate specifies the number of cells. The control-silenced cells are given in blue; the ANXA2-silenced cells are indicated by a red line.

In summary, the ANXA2 silencing experiments showed a positive correlation between the ANXA2 protein amount and the rate of HCV replication. However, a strong reduction or even inhibition of HCV replication was not achieved by either of the used silencing methods. This possibly implies that the silencing of ANXA2 was not efficient enough to have a major impact on viral replication or was counteracted by a positive induction via HCV.

3.3.5 Studies to identify the viral interaction partner of Annexin II

Since ANXA2 strictly colocalized with the sites of HCV replication in cell experimental systems and cell lines, it seemed likely that the cellular protein was retrieved by a viral NS protein. In order to identify the viral interaction partner of ANXA2, I first analyzed the subgenomic replicon cell line 5-15 by co-immunoprecipitation (co-IP) studies. Cured replicon cells were used as negative control. The cells were lysed in NPB and subjected to IP with different polyclonal antisera as indicated in Fig. 40. Antisera raised against NS proteins were used to co-precipitate ANXA2, the E2-specific antiserum served as unspecific binding control because the used subgenomic replicon did not code for structural proteins. The antiserum raised against ANXA2 was used as positive control for binding. The proteins precipitated in this way were separated by SDS-PAGE and subsequently subjected to immunoblot assay using an anti-ANXA2 antibody. ANXA2 was detected in the total lysates (pure) of the different cell lines (upper panel; lanes 1 and 8). However, ANXA2 was not precipitated by any of the antibodies directed against a HCV NS protein and not even by the ANXA2-specific antiserum. This indicated either a very weak interaction of ANXA2 with the viral protein(s) or technical problems in this experiment.
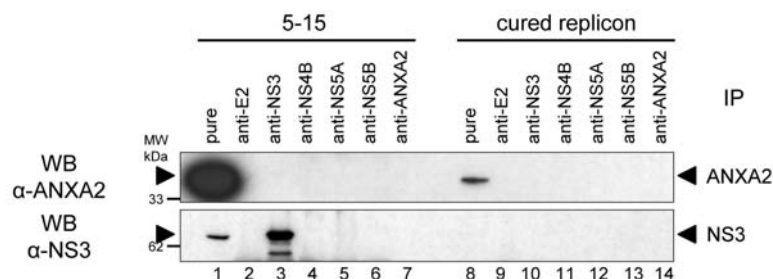
Fig. 40. Co-immunoprecipitation analysis of subgenomic replicon cells. Cells of the subgenomic replicon cell clone 5-15 were lysed in NPB and subjected to immunoprecipitation assay using protein A agarose-coupled polyclonal antibodies (rabbit) directed against the viral proteins E2, NS3, NS4B, NS5A, NS5B, and cellular ANXA2, respectively. Cured replicon cells served as control cells. Precipitated proteins were analyzed by SDS-PAGE followed by immunoblot assay using monoclonal antibodies either raised against ANXA2 (above) or specific for HCV NS3 (below). As positive controls, total cell lysates (pure) were analyzed in this immunoblot, too.

To control the efficiency of the IP, the western blot membrane was stripped and reprobed against NS3. As shown in the lower panel of Fig. 40, NS3 was recovered in the total lysate of 5-15 cells and precipitated by NS3-specific antibodies using the same cell lysate (lanes 1 and 3), indicating that the IP worked in general. Nevertheless, ANXA2 could not be revealed. However, other experiments showed

that the ANXA2-specific antibody used in this experiment did not work in immunoprecipitation (data not shown).

The viral interaction partner of ANXA2 could also not be identified by using the crosslinking reagent DSP prior to cell lysis and immunoprecipitation to stabilize weak or transient protein interactions (data not shown).

Co-precipitation studies of stable subgenomic replicon cell lines did not reveal which NS protein interacted with ANXA2. Therefore, the HCV proteins NS3-to-5B (genotype 1b, pTM NS3-5B_ET) were heterologously expressed in naïve Huh-7 cells harboring a T7 RNA polymerase (lunet-T7), and the newly synthesized proteins were metabolically labeled with ^{35}S. The advantage of this system was the higher expression level of the viral proteins which was caused by a T7 promoter-driven expression. The cells were lysed and subjected to an immunoprecipitation assay (Fig. 41). However, none of the IPs using antisera against HCV NS proteins showed a co-precipitation of ANXA2 (Fig. 41A and B, lanes 8 to 11). On the other hand, ANXA2-specific antibodies seemed to precipitate at least a low amount of NS3, but this result was not very convincing due to the low efficiency and the high background of the anti-ANXA2 antibody (compare lanes 6 and 12). A precipitation of other NS proteins with this antiserum was not detectable. In addition, co-precipitation of NS3 was also observed in the anti-NS4B and anti-NS5A reaction (compare lanes 3 and 9 as well as lanes 4 and 10). These co-precipitations are regularly observed due to the association of the non-structural proteins (V. Lohmann, personal communication). Due to this fact, the presence of NS3 in the anti-ANXA2 IP could therefore be caused by co-precipitation of another NS protein. Therefore, this experiment indicated an interaction of ANXA2 with HCV NS protein but did not unambiguously identify the distinct viral partner.
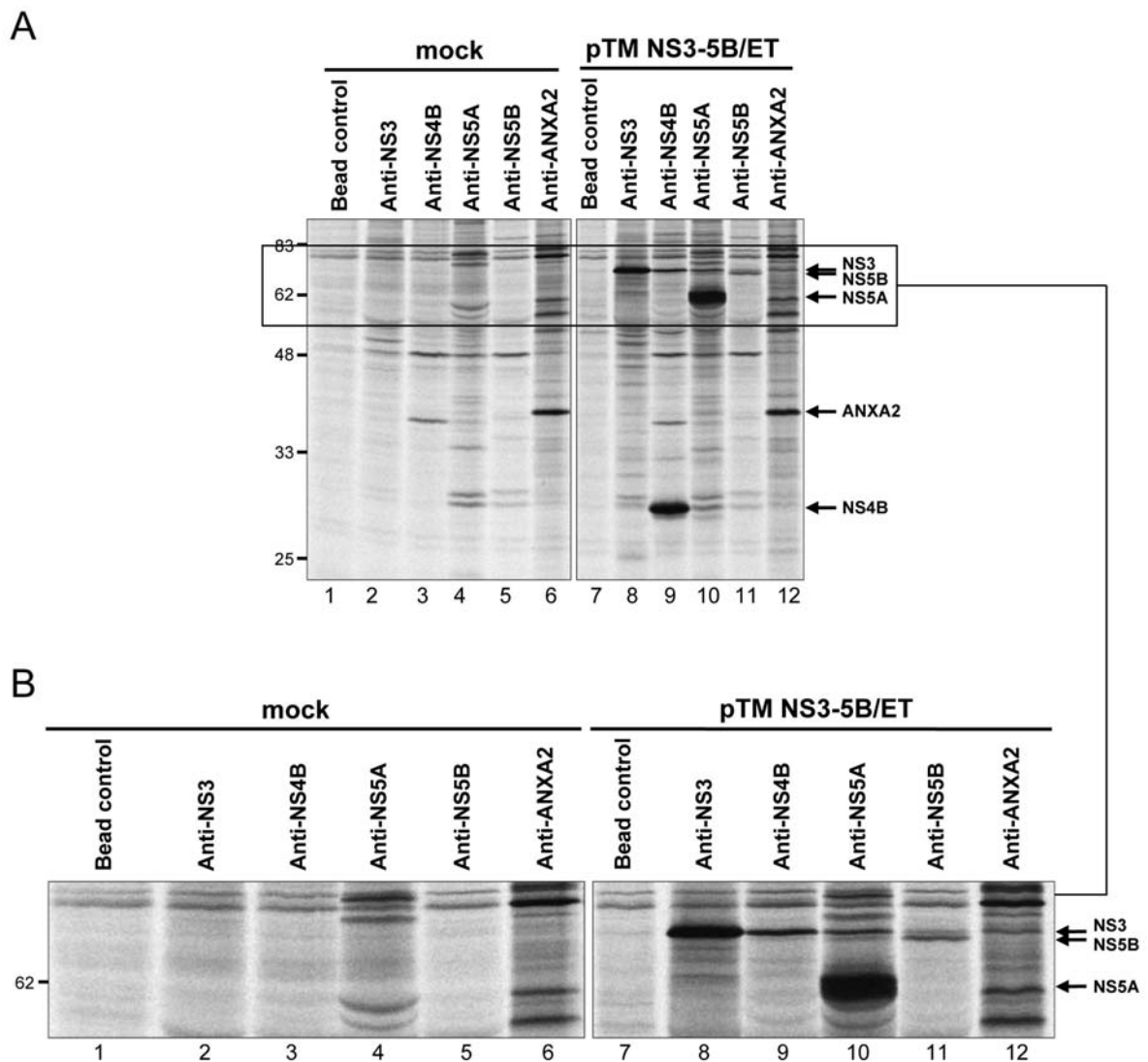
Fig. 41. Heterologous expression of HCV non-structural proteins. (A) Co-immunoprecipitation analysis of cells heterologously expressing HCV NS proteins. 4 h post transfection, lunet-T7 cells transfected with pTM NS3-5B/ET as well as mock transfected cells were subjected to a metabolic ^{35}S-labeling followed by an immunoprecipitation analysis using protein A agarose-coupled polyclonal antibodies (rabbit) directed against the viral proteins NS3, NS4B, NS5A, NS5B, and protein G sepharose-coupled monoclonal antibodies specific for ANXA2, respectively. Protein A agarose was used as control for unspecific binding (bead control). Precipitated proteins were separated in a SDS-PAGE and detected by autoradiography. Arrows on the right side (top down) indicate the molecular weights of NS3 (70 kDa), NS5B (68 kDa), NS5A (56/58 kDa), ANXA2 (36 kDa), and NS4B (27 kDa). (B) Enlargement of (A).

Therefore, I tried to identify the interaction partner of ANXA2 by co-precipitation studies using lunet-T7 cells transfected with DNA coding for single HCV non-structural proteins. The newly synthesized proteins were metabolically labeled with ^{35}S and subjected to immunoprecipitation assay using antisera specific for the HCV NS proteins or ANXA2. Precipitated proteins were separated by SDS-PAGE and detected by autoradiography. However, also in this experiment an interaction of ANXA2 with viral NS proteins was not observed. None of the antibodies directed against a viral NS protein was able to co-precipitate ANXA2 (Fig. 42; lanes 8, 14, 20,

28, and 35). Likewise, the ANXA2-specific antibody did not coprecipitate any HCV NS protein (Fig. 42; lanes 12, 18, 24, 30, and 36).
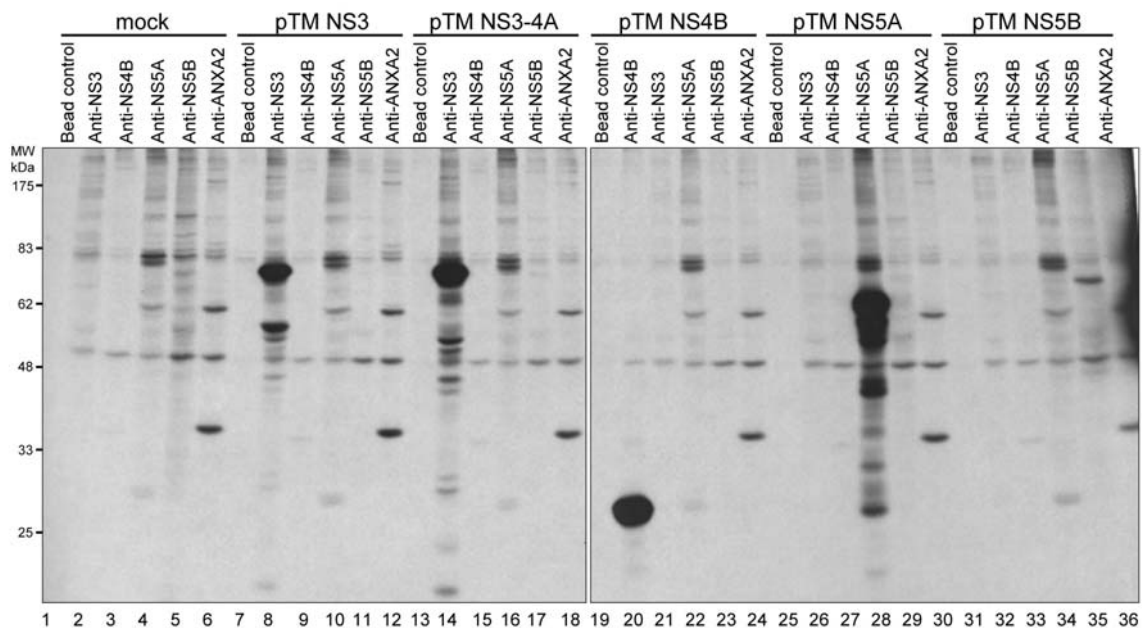
Fig. 42. Co-immunoprecipitation analysis of cells heterologously expressing individual HCV NS proteins. 4 h post transfection, lunet-T7 cells transfected with pTM constructs encoding different single NS proteins as well as mock transfected cells were subjected to a metabolic ^{35}S-labeling followed by an immunoprecipitation analysis using protein A agarose-coupled polyclonal antibodies (rabbit) directed against the proteins NS3, NS4B, NS5A, NS5B, and ANXA2, respectively. Protein A agarose was used as control for unspecific binding (bead control). Precipitated proteins were separated in a SDS-PAGE and detected by autoradiography.

Co-precipitation studies of cells harboring subgenomic replicons or heterologously expressing the viral NS proteins either individually or as polyprotein did not clearly reveal the viral interaction partner of ANXA2. Another widely-used approach to investigate the putative interaction between two different proteins is the yeast two-hybrid (Y2H) assay. Although this experimental system was more prone to artifacts than those utilized before, it represented a possible alternative for the identification of the viral NS protein interrelated with ANXA2. Therefore, NS3, NS3 helicase, NS5A (all genotype 1b), as well as truncated forms of the NS5B polymerase of genotype 1b and 2a (NS5BΔC21 Con and NS5BΔC21 JFH, respectively; deletion of the C-terminal 21 aa) served as bait, whereas ANXA2 was the prey in this Y2H assay. ANXA2 showed only a very weak interaction with NS5A and none with any other of the tested viral non-structural proteins (data not shown).

In the co-precipitation studies, it was shown that ANXA2-specific antibodies are able to precipitate a small portion of NS3. These interactions with NS3 as well as with

NS5A in Y2H assays still had to be verified by other experiments to confirm their reliability.

In HCV-harboring cells, an intracellular redistribution of ANXA2 as well as its colocalization with viral NS proteins was always detectable. We were interested whether this would also be visible in cells heterologously expressing the HCV proteins and in using this assay to address the viral protein retrieving ANXA2. Cells were transfected with DNA for the heterologous expression of the viral non-structural proteins and analyzed by IFA (Fig. 43). In mock transfected lunet-T7 cells, ANXA2 showed a homogeneous cytosolic distribution (Fig. 43A). However, upon transient exogenous expression of the NS proteins NS3-to-5B (pTM NS3-5B, Fig. 43B), a modification in the intracellular distribution of ANXA2 was clearly visible, just as in the immunofluorescence studies of HCV replicating cells before (see chapters 3.3.1 to 3.3.4). ANXA2 was found in dot-like structures and, furthermore, an explicit colocalization with HCV NS3 was also observed in this experimental setup (Fig. 43B). Therefore, this assay was suitable to analyze the redistribution of ANXA2 due to the expression of individual NS proteins. The analysis was complicated by the fact that the HCV NS proteins in general showed an ER-like arrangement when they were expressed individually except for the membranous web inducing NS4B which exhibits a clearly punctuated pattern (V. Lohmann, personal communication). Since it was possible that ANXA2 is reallocated upon interaction with an HCV non-structural protein, lunet-T7 cells expressing a single viral NS protein (genotype 1b) were investigated by IFA (Fig. 43C-G). ANXA2 did not specifically colocalize with individually expressed NS3, NS3-4A, NS4B, and NS5B, but retained a cytoplasmic distribution as in naïve lunet-T7 cells (compare Fig. 43A with Fig. 43 C-E, and G). However, as shown in Fig. 43F, ANXA2 clearly colocalized with heterologously expressed NS5A which was detected in a spotted pattern probably due to the overexpression. Apparently, ANXA2 was also induced by HCV NS5A, since in neighboring cells not expressing NS5A the signal for ANXA2 was significantly lower.

In cells exogenously expressing the NS proteins NS3-to-5B, ANXA2 was redistributed and colocalized with the NS proteins. IFAs of cells expressing the individual non-structural proteins revealed that NS5A was most likely the viral interaction partner of ANXA2 and responsible for the increased ANXA2 levels in HCV-harboring cells.
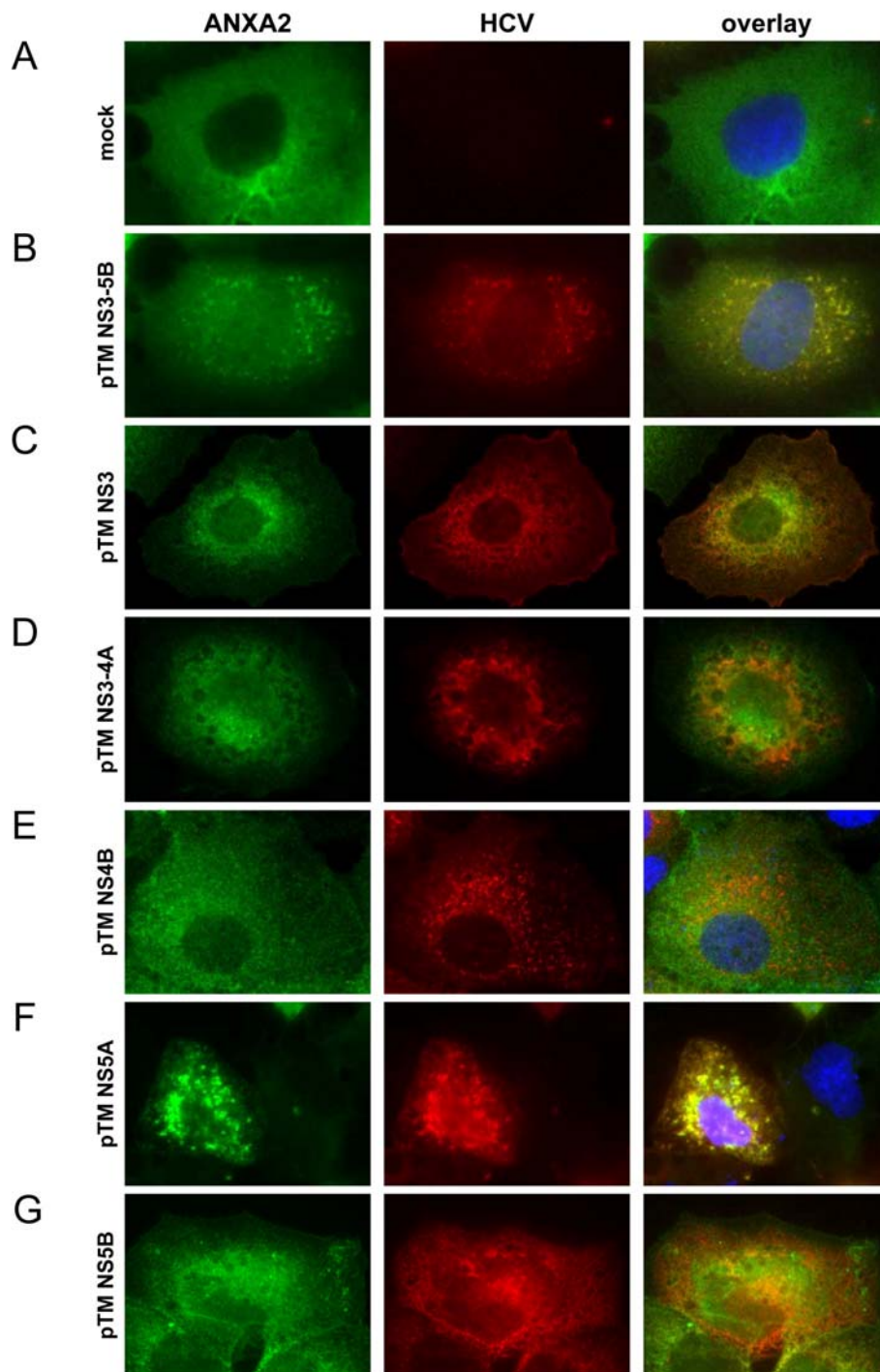
Fig. 43. Colocalization studies of ANXA2 and HCV NS proteins heterologously expressed in lunet-T7 cells. Cells transfected with DNAs coding for either NS3-to-5B (B) or different individual non-structural proteins (C-G) were fixed 8 hours post transfection and subjected to IFA using monoclonal antibodies specific for ANXA2 (A-G), and polyclonal antisera raised against NS3 (A-D), NS4B (E), NS5A (F), and NS5B (G), respectively. Mock transfected cells were used as a negative control (A). Indicated on the left are the constructs used for transfection.

In summary, 2D gel analyses of PrK-resistant CRCs of cells harboring subgenomic replicons (9-13; genotype 1b) showed that ANXA2 was a potential cellular cofactor of the viral replication complex. The subcellular distribution of ANXA2 was rearranged upon HCV replication as well as infection and was neither dependent on the HCV

genotype nor on a certain host cell line. It was rather specific for HCV, since redistribution of ANXA2 was not caused by other positive-strand RNA viruses. Overexpression and silencing of ANXA2 had so far no major impact on HCV replication, but it seemed that ANXA2 expression was induced upon HCV transfection, potentially interfering with efficient silencing. Furthermore, a positive correlation between ANXA2 levels and HCV replication was observed. The viral interaction partner probably was NS5A, however, the function of ANXA2 in the viral life cycle remains to be determined.

3.4 Quantitative analysis of the Hepatitis C Virus replication complex

As mentioned before, the non-structural proteins NS3 to 5B are necessary and sufficient for HCV RNA replication. They form a membrane-associated complex containing viral proteins and RNA as well as cellular cofactors. Biochemical analyses of CRCs prepared from lysates of replicon cells provided deeper insights into the organization and structure of the viral replication complex[5,8,52,86,125,153,193], however, a detailed stoichiometric analysis of the HCV replication complex has not been carried out yet.

Due to the polyprotein nature of the HCV genome, all viral proteins should be produced equimolarly, independent on their function. However, one could assume that the structural proteins which are involved in particle morphogenesis are required in higher amounts than the non-structural proteins. I determined if there is indeed an overproduction of non-structural proteins and which ratio of non-structural proteins to RNA is required for HCV RNA replication.

3.4.1 Quantification of the HCV RNA to protein ratio in Huh-7 cells

The first question addressed in my study was, how the number of HCV positive- and negative-strand RNA molecules correlates with the amount of different HCV proteins in cells with productive HCV RNA replication. Therefore I transfected a full-length HCV genome with cell culture adaptive mutations (Con1/ET, Fig. 44,[172]) into Huh7-Lunet cells, a cured replicon cell clone featuring increased permissiveness for HCV replication. Cells were seeded in aliquots after electroporation, harvested at different

time points, counted and analyzed for the amount of HCV RNA and proteins. Fig. 44B shows a typical northern blot analysis of such a transient replication assay by using known numbers of *in vitro* transcripts to determine the quantity of positive- and negative-strand RNA in cells transfected with Con1/ET. The obvious detectable negative-strand RNA signal displays that RNA replication had already started 24 h after transfection, reached its maximum at 48 h and 72 h after transfection and slightly decreased at 96 h, after the cells had reached confluence (Fig. 44B, top and middle panel).

HCV core and non-structural proteins 4B and 5B were quantified by western blot analysis of cell lysates in comparison with well-defined amounts of purified proteins from the same HCV isolate[141], and by using antibodies raised against these particular antigens (Fig. 44C). The number of core, NS4B and NS5B molecules in the transfected cells followed the same changes over time as the RNA. The results obtained for the quantitative evaluation are summarized in Table 2.

Earlier studies have shown that transfected RNA of replication-deficient genomes is degraded to trace amounts 24 h after transfection and completely absent after 48 h[34,172]. On account of this, the quantitative analysis was limited to the data obtained at 48-96 h, thereby preventing any impact of transfected input RNA. I found on average 40 copies of negative-strand RNA, a fivefold excess of positive-strand RNA and approximately one million copies of core, NS4B and NS5B per cell, indicating a vast excess of viral proteins to RNA molecules. Within the expected range of accuracy the ratio of the non-structural proteins NS4B and NS5B was very similar. The 3-6-fold higher relative levels of core might be due to premature termination of translation leading to an overrepresentation of the aminoterminal portions of the HCV polyprotein. Nevertheless, the data were consistent in showing a tremendous surplus of HCV proteins compared to RNA molecules.

Since we intended to ascertain the stoichiometry of RNA to protein in the HCV replication complex, I searched for the most appropriate biochemical equivalent. Every active replication complex must bear at least one negative-strand RNA molecule, therefore the maximal number of HCV replication complexes per cell can be estimated by the amount of negative-strand RNA copies. Based on this assumption, I found on average less than forty active replication complexes per cell, but each of it was attended by 20,000-40,000 copies of non-structural proteins.
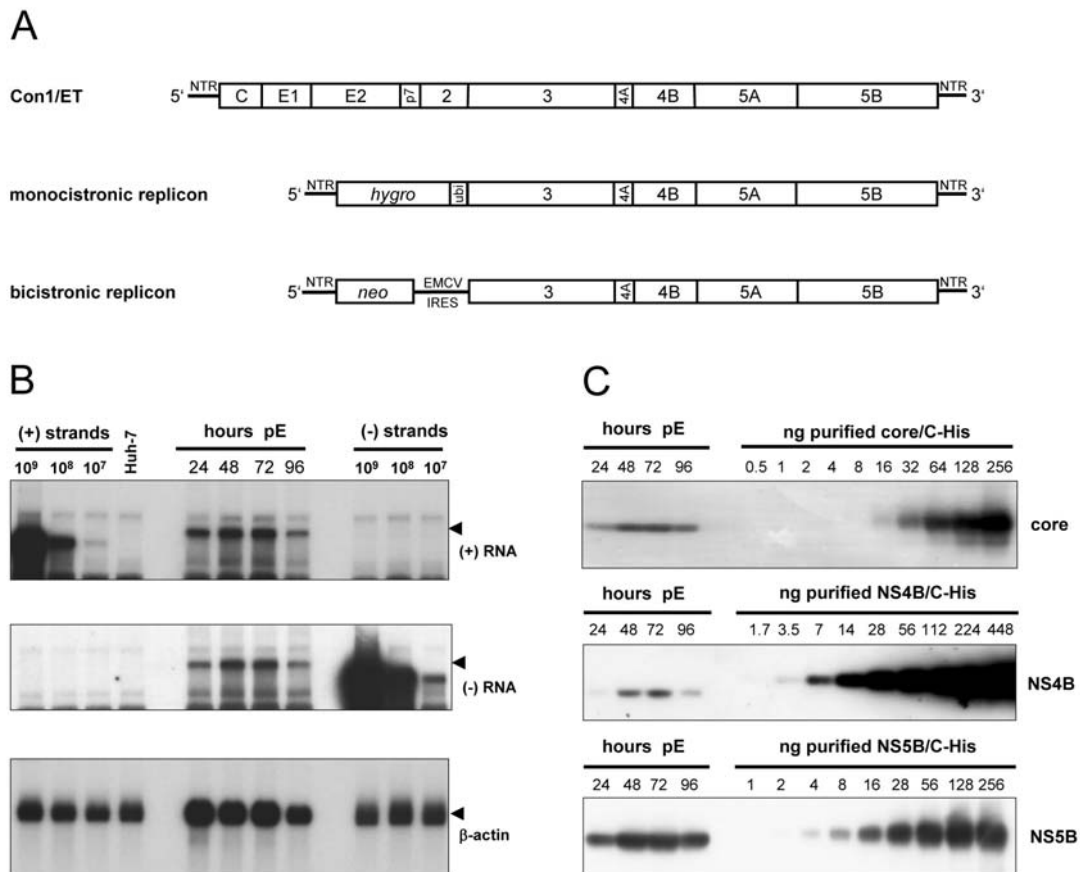
Fig. 44. Quantification of HCV RNA and non-structural proteins in Huh-7 cells transfected with a full-length genome. (A) Structure of the HCV RNAs used in this study. Con1/ET represents a full-length HCV genome harboring cell culture adaptive mutations in NS3 and NS4B [172]. The monocistronic replicon contains only a single open reading frame consisting of nt 342–389 of the core-coding region, the hygro gene (encoding the hygromycin phosphotransferase), the ubiquitin-encoding sequence (Ubi) and the HCV non-structural proteins NS3–NS5B [66] and was used to select Huh-7 cell clone 11-1, which was analyzed in this study (Table 2). The bicistronic replicon is composed of the first 377 nucleotides of the HCV genome fused to the neo gene (encoding the neomycin phosphotransferase). Translation of the HCV non-structural proteins NS3-5B is initiated by the EMCV-IRES. The bicistronic replicon was used to generate cell-clone 9-13 [140]. (B) Time course of HCV positive and negative-strand synthesis following transfection of Con1/ET RNA into Huh7-Lunet cells. Cells were harvested and counted at the time points indicated above the figure (hours pE, post electroporation) and total RNA was prepared. 5µg of total RNA corresponding to 2.5, 2.1, 2.1 and 2.3 x10^5 cells at 24 h, 48 h, 72 h and 96 h, respectively, was subjected to Northern hybridization using radiolabeled riboprobes specific for the detection of HCV positive-strand (top panel), negative-strand (middle panel) or β-Actin (lowest panel). Specific signals are indicated by arrowheads. Signals were quantified by phosphor imaging using known amounts of *in vitro* transcripts of positive or negative polarity corresponding to a subgenomic replicon and normalized for different loadings by the β-Actin signal. Total RNA from naïve Huh-7 cells was used as negative control (Huh-7). (C) Quantification of HCV core (upper panel) NS4B (middle panel) and NS5B (lowest panel) expression following transfection of Con1/ET RNA into Huh7-Lunet cells. An aliquot of the cells harvested for total RNA preparation at the time points given above each panel was lysed in protein sample buffer and subjected to immunoblot analysis using monoclonal antibodies (NS5B) or polyclonal antisera (core, NS4B) with the specificities given on the right. Samples were quantified by comparison of signal intensities derived from known amounts of the respective antigens as indicated above each panel. The amount of loaded proteins correspond to 1.2, 1.8, 1.6, 2.0 x 10^5 cells at 24 h, 48 h, 72 h and 96 h, respectively.

Although the analysis of a HCV full-length genome should reflect the properties of viral translation and replication most accurately, I wanted to confirm the data in a steady-state situation, which resembles a persistent infection. The most efficient and

convenient systems to study persistent HCV RNA replication are Huh-7 cell clones with subgenomic replicons, keeping constant HCV RNA and protein levels over years, even in the absence of selective pressure[173]. Therefore I analyzed two different types of replicon cells to evaluate the data obtained with the full-length genome (Fig. 44A): (i) a Huh-7 cell clone designated 11-1, harboring a monocistronic replicon resembling closely the translational properties of a full-length genome[66] and (ii) a Huh-7 cell clone designated 9-13[139,140] with a bicistronic replicon representing the most efficient and most often used system to investigate persistent HCV replication. I seeded cells bearing the respective replicons in aliquots and analyzed them in the same way as the full-length genome at different time points after seeding. Despite the different architecture of the replicons and the assay format (transient replication versus stable replicon cell clones), I obtained very similar results (table 2) with more than 10,000 NS4B or NS5B copies per negative-strand RNA molecule. This outcome indicated that the synthesis of a massive excess of NS proteins over RNA seems to be an elemental property of HCV translation and replication in Huh-7 cells. Since the half-lives of the NS proteins (11-16h[173]) were shown to be comparable to the half-life of RNA (about 11h[166]) in replicon cells and HCV RNA and proteins are kept on similar steady-state levels over years of continuous passaging, HCV RNA and protein synthesis should also be quite constant. Therefore, based on the data shown in table 2, each positive-strand RNA template is translated numerous times giving rise to one thousand to ten thousand polyprotein copies. Another important conclusion was that the stoichiometry of HCV protein to RNA in replicon cell clones closely resembles the one found with full-length genomes. Therefore, replicon cell clones were an appropriate tool for further analyses.

Table 2: Number of positive-strand RNA, negative-strand RNA, core, NS4B and NS5B molecules per Huh-7 cell.

HCV sequence	negative-strand	positive-strand	Core	NS4B	NS5B
Con1/ET (transient transfection*)	40 +/- 4	$2.0 +/- 0.3 \times 10^2$	$4.9 +/- 1.4 \times 10^6$	$7.7 +/- 1.8 \times 10^5$	$1.5 +/- 0.4 \times 10^6$
monocistronic replicon (cell clone 11-1)	81 +/- 11	$4.4 +/- 1.5 \times 10^2$	na	$8.9 +/- 3.2 \times 10^5$	$2.2 +/- 0.8 \times 10^6$
bicistronic replicon (cell clone 9-13)	94 +/- 31	$7.6 +/- 2.9 \times 10^2$	na	$8.0 +/- 0.4 \times 10^5$	$1.2 +/- 0.5 \times 10^6$

data represent mean values and standard deviations of samples harvested at 48 h, 72 h and 96 h after seeding
na not applicable
* per cell data not normalized for transfection efficiency, which was routinely 50%-80%

3.4.2 Isolation of active replication complexes from Huh-7 cell harboring subgenomic replicons

We then asked whether the massive surplus of non-structural proteins indeed is directly involved in RNA synthesis or may serve some other function. To distinguish between these two possibilities, I isolated crude replication complexes (CRCs) from replicon cells and further analyzed them *in vitro* for their protein and RNA content. The method for the preparation of CRCs has been described before (chapter 3.1.1) and is again shown schematically in Fig. 45A. To verify for *in vitro* replicase activity, cell lysates were incubated with radiolabeled nucleotides in the presence of Actinomycin D and in the absence of exogenous template RNA. Reaction products were further analyzed by denaturing agarose gel electrophoresis (Fig. 45B). The dominant product of *in vitro* replication was a single band corresponding in size to the full-length replicon RNA (arrowhead). HCV replicase activity was already detectable in the total hypotonic lysate of replicon cells but was enriched in CRCs that were obtained by pelleting the membranous material in supernatant 1 (S1). The resulting supernatant 2 (S2) did not contain any detectable replicase activity. The distribution of the non-structural proteins in different fractions of the CRC preparation is shown in Fig. 45C. Similar proportions of NS3, NS4B, and NS5B were regained in S1 and concentrated in parallel to the replicase activity in the CRC fraction, leaving only minor amounts in S2.

I wanted to exclude that the CRC fraction contained only a minor subpopulation of HCV replication complexes which might not be representative, and therefore followed the fate of viral positive- and negative-strand RNA during CRC preparation (Fig. 45D). I found that 35% of the negative- and 25% of the positive-strand RNA existent in the replicon cells before lysis were recovered in the CRC fraction. The remainder was either associated with the nuclear pellet (40% of negative-strand, 30% of positive-strand RNA), or was destroyed during cell lysis (20% of negative-strand, 30% of positive-strand RNA) or during centrifugation of CRCs (15% of negative-strand and positive-strand RNA, respectively); only traces of RNA were retained in S2. In consequence, about half of the positive-strand RNA and 25% of the negative-strand RNA were degraded most likely by the action of cellular nucleases liberated during cell lysis. This fraction might include damaged replication complexes and positive-strand HCV RNAs that were not integrated into the replication complex but engaged in some other processes such as RNA translation. A variable amount of NS

proteins, HCV RNA and replicase activity always stayed associated with the nuclear pellet and could not be recovered even by vigorous douncing, in all probability on account of the accumulation of replication complexes in the perinuclear region[74] and due to the mild extraction excluding the use of detergents.
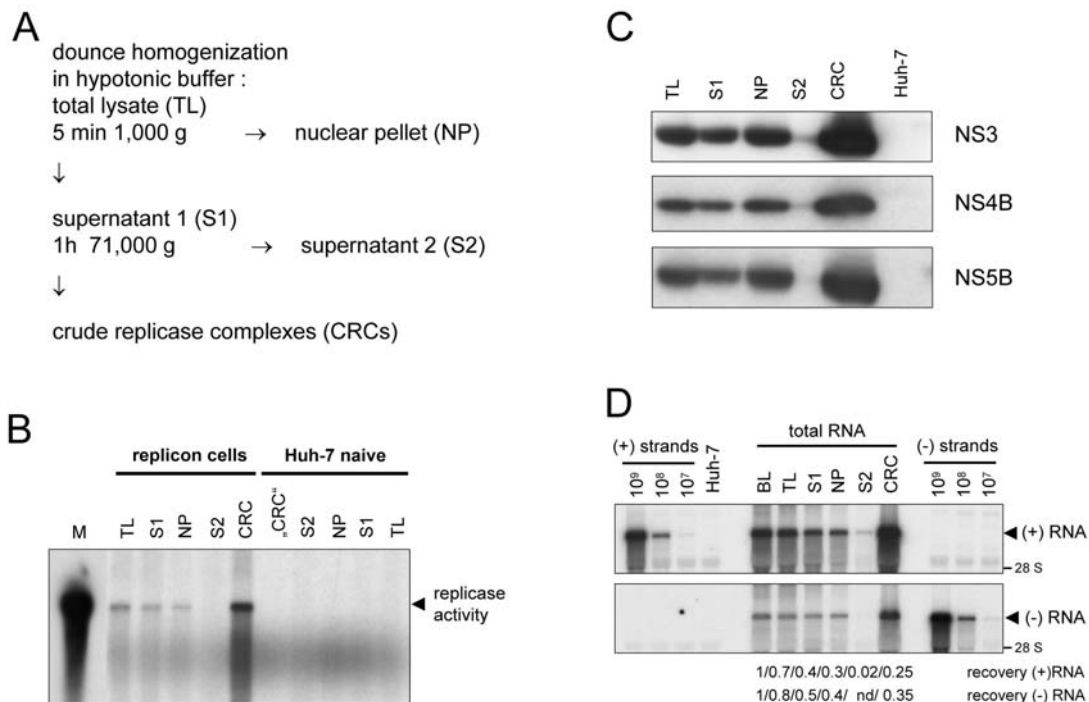
Fig. 45. Preparation and characterization of CRCs from HCV replicon cells. (A) Schematic diagram of the CRC preparation protocol. (B) Analysis of *in vitro* replicase activity in total lysates (TL) and different subcellular fractions of replicon cells (left half) and naïve Huh-7 cells (right half). *In vitro* replicase activity was determined in 4 µl of each fraction, reaction products were analyzed by denaturing glyoxal-gel electrophoresis followed by autoradiography of the dried gel. A radioactively labeled *in vitro* transcript identical in size to the replicon was loaded as a marker (M). The major reaction product of the *in vitro* replicase assay is indicated by an arrowhead. (C) Detection of NS3, NS4B and NS5B in different fractions of the CRC preparation. The volume of the NP fraction was adjusted to the volume of S1 and 10 µl of each fraction were analyzed by immunoblot using a polyclonal antiserum raised against HCV NS3 (upper panel) or NS4B (middle panel) or monoclonal antibodies specific for NS5B (lower panel, [154]) and compared to 10 µl of "CRC"-fraction from naïve Huh-7 cells (Huh-7). (D) Fate of viral positive and negative-strands during hypotonic lysis and CRC-preparation. Total RNA was prepared from 50 µl of a replicon cell suspension before lysis (BL) and from the same volumes of TL, S1, NP (adjusted to the volume of S1), S2 and CRC and subjected to Northern hybridization analysis using the same controls and probes to detect HCV positive (upper panel) and negative-strand RNA (lower panel) as in Fig. 44B. To calculate the recovery rate samples were analyzed by phosphor imaging and correlated with the value obtained before cell lysis (BL). Data of the CRC fraction were corrected for the difference in total volume. For further details refer to the text.

Taken together, CRCs most likely depicted a representative fraction of HCV replication complexes in replicon cell clones and were therefore appropriate to study the stoichiometry of RNA to NS proteins required for RNA replication. I chose the cell

clone 9-13, which harbors a bicistronic replicon, for further experiments, since it was the most efficient source for the preparation of active replication complexes.

3.4.3 *In vitro* replicase activity and viral RNA were fully resistant to nuclease and protease treatment

It has been shown previously that *in vitro* replicase activity is resistant to nuclease and protease treatment[5,8,52,153]. I exploited these results to specify which fraction of viral RNA and proteins is resistant to nuclease and protease, respectively, in order to determine the stoichiometry of the viral components of the HCV replication complex. Therefore, I treated CRCs with high concentrations of proteinase K (0.8 or 8 mg/ml) and/or S7 nuclease (200 or 2000 U/ml), stopped the reaction by adding PMSF or EGTA, respectively, and analyzed an aliquot of the pretreated CRCs for *in vitro* replicase activity. As shown in Fig. 46, *in vitro* replicase activity was neither affected by pretreatment with S7 nuclease (lanes 4 and 5) nor proteinase K (lanes 8 and 9) alone or in combination (lanes 10 and 11). Protease and nuclease resistance was not limited to replicase activity contained in the CRC fraction but was also found for replicase activity in total cell lysate, the nuclear pellet and supernatant 1 (data not shown), indicating that the replication complexes in the CRC fraction were not a selected subpopulation with distinct properties. HCV replicase activity was only abolished by addition of 1% Triton X-100, in the absence (lane 6) or presence (lane 7) of additional nuclease, indicating that the resistance of HCV replicase to proteases and nucleases is mediated by detergent-sensitive structures. The full protease and nuclease resistance of *in vitro* replicase activity enabled me to investigate which portion of viral RNA and proteins were not affected by protease and nuclease and therefore were necessary and sufficient for RNA synthesis. To address this question, I analyzed aliquots of the protease and/or nuclease treated CRCs by Northern hybridization and immunoblot to determine the ratio of HCV RNA and non-structural proteins involved in replication.
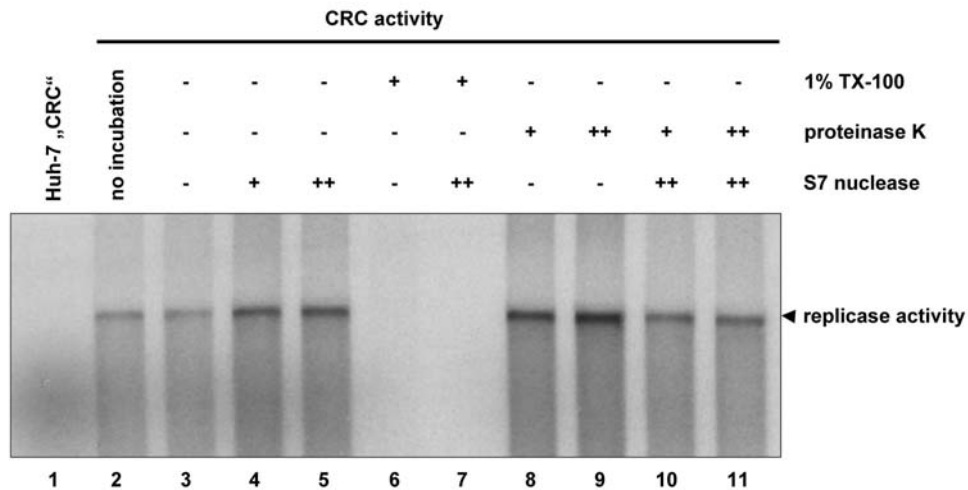
Fig. 46. HCV replicase activity is completely resistant to protease and nuclease treatment. 50 µl of CRCs prepared from replicon cell clone 9-13 were incubated for 60 min at 25°C in the presence of 1% Triton X-100 and/or 0.8 (+) or 8 (++) mg/ml proteinase K and/or 0.2 (+) or 2 (++) U/µl S7-nuclease, respectively as indicated above each lane. After termination of the proteinase K and S7 nuclease digest by the addition of 1.4 mM PMSF and/or 2.75 mM EGTA, respectively, equal amounts of each sample were analyzed for *in vitro* replicase activity. Reaction products were separated by denaturing glyoxal agarose gel electrophoresis and autoradiography. Lane 1 and 2 represent control reactions with CRCs from naïve Huh-7- or replicon cells in the absence of any preincubation. CRCs in lane 3 were mock incubated for 60 min at 25°C prior to the *in vitro* replicase assay.

I first focused upon the effect of S7 nuclease treatment on the fate of viral and cellular RNA (Fig. 47). Viral positive- and negative-strand RNAs were fully resistant to nuclease in CRCs as shown by Northern blot analysis (Fig. 47, top and middle panel, compare lane 3 with lanes 4 and 5). The marked reduction of 28S rRNA in the S7 nuclease treated samples indicated the efficiency of the digest (Fig. 47, top and middle panel, lanes 4, 5, 8 and 9). Protection from nucleases seemed not to be mediated by proteins, since further addition of proteinase K had no effect on RNA stability (lanes 8 and 9). In contrast, addition of Triton X-100 resulted in complete degradation of both viral RNA species, even in the absence of exogenous nuclease (lanes 6 and 7). This signified that membranes rather than proteins protected the RNA and that the loss of replicase activity upon detergent treatment (Fig. 46) was primarily due to the destruction of template RNA by endogenous nucleases and S7 nuclease. In opposition to the viral RNAs, the cellular mRNA, exemplified by β-Actin, was absent in CRCs because it was not attached to membranes or almost completely devastated by the action of endogenous nucleases liberated during CRC-preparation (Fig. 47, lowest panel, lanes 2 and 3) and the remaining traces were fully accessible to S7 nuclease (lanes 4 and 5).

Fig. 47. Quantification of nuclease-resistant HCV positive- and negative-strand RNA and β-Actin mRNA in CRCs. Total RNA equivalent to 5 µl of CRCs treated with 1% Triton X-100, 0.8 (+) or 8 (++) mg/ml proteinase K and/or 0.2 (+) or 2 (++) U/µl S7 nuclease for 60 min at 25°C or from mock treated CRCs, as indicated on top, was subjected to Northern hybridization analysis using a negative-strand riboprobe to detect viral positive-strand RNA (top panel), a positive-strand riboprobe for HCV negative-strand detection (middle panel) and a riboprobe specific for the detection of cellular β-Actin mRNA. The positions of viral positive- and negative-strand RNA and β-Actin are indicated by arrowheads at the right. For quantification, *in vitro* transcribed replicons corresponding to known amounts of viral positive- and negative-strand RNA were mixed with 2 µg of total cellular RNA from naïve Huh-7 cells and loaded as indicated at the bottom of the figure. 4 µg total RNA from naïve Huh-7 cells were used as negative control (Huh-7, lane 1). I quantified the viral RNAs by phosphor imaging and found ca. $3x10^6$ negative-strands and $3x10^7$ positive-strand RNAs per microliter CRC preparation in this particular experiment.

Taken together, my data indicate that the viral positive- and negative-strand RNA in the replication complex is completely protected from nucleases and that this protection is mediated by detergent-sensitive membrane structures rather than by proteins.

3.4.4 Only a minor portion of the HCV NS proteins was resistant to protease treatment

Since *in vitro* replicase activity was completely resistant to protease and nuclease treatment, the ratio of HCV NS proteins to RNA actively involved in RNA synthesis

was determined by the number of nuclease-resistant RNA molecules compared to protease-resistant protein molecules. To measure the fraction of viral NS proteins resistant to protease, aliquots of the differently treated CRC samples were analyzed for the impact of proteinase K incubation by Western blot (Fig. 48B). Even with the lower protease concentrations I found a massive degradation of almost all cellular proteins to nearly undetectable amounts (Fig. 48A, lanes 8-11), whereas detergent and nuclease treatment as expected had no significant effect (lanes 4-7). As an example for a cellular protein I chose Calnexin for a closer analysis by Western blot, using an antiserum directed against its N-terminal part, which is located in the ER lumen and therefore should be protected from proteases in an intact ER structure, whereas the carboxyterminus was expected to be protease-sensitive in a cell lysate[153].
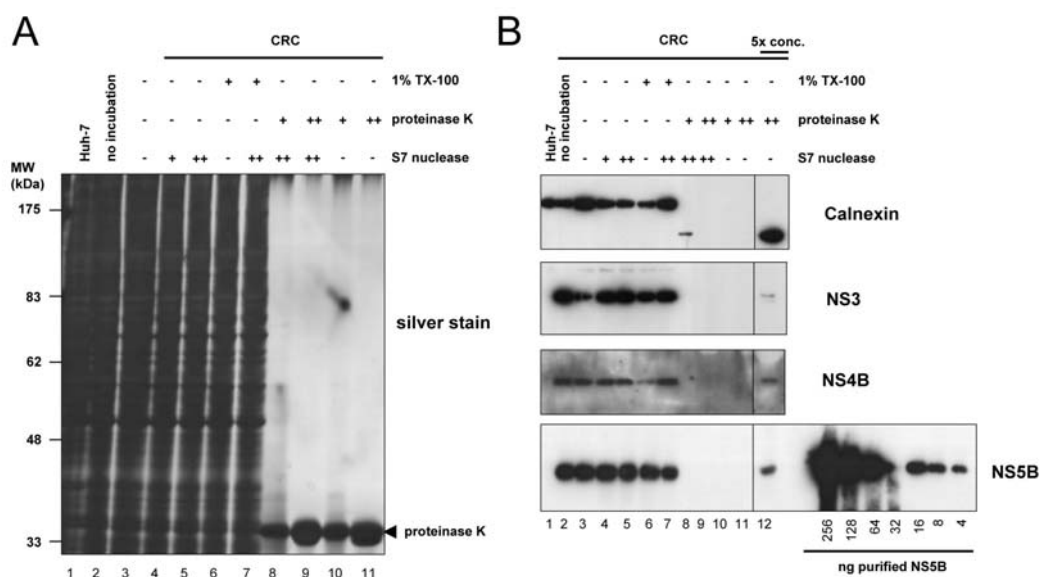
Fig. 48. Effect of proteinase K digest on cellular proteins and quantification of protease-resistant HCV non-structural proteins in CRCs. Equal amounts of CRCs prepared from replicon cell clone 9-13 were incubated for 60 min at 25°C in the presence or absence of 1% Triton X-100 and/or 0.8 (+) or 8 (++) mg/ml proteinase K and/or 0.2 (+) or 2 (++) U/µl S7-nuclease, respectively, as indicated above each lane. The reaction was stopped by addition of 1.4 mM PMSF and 2.75 mM EGTA, boiled in sample buffer and total protein equivalent to 2 µl CRCs was subjected to SDS-10%PAGE. In case of the 5x concentrated samples, proteins were TCA-precipitated and the equivalent of 10 µl CRCs was loaded. Proteins were either visualized by silver staining (A) or subjected to immunoblot analysis (B) using monoclonal antibodies specific for the ER-luminal part of Calnexin (upper panel), a polyclonal antiserum raised against HCV NS3 or NS4B (middle two panels) and monoclonal antibodies specific for HCV NS5B (bottom panel), as indicated at the right. The concentrated fractions (lane 12) are shown from identical expositions of the same blot. A serial dilution of purified NS5B was loaded in parallel for quantification as depicted at the bottom of the figure.

As shown in Figure 48B (top panel), no full-length Calnexin was detectable after protease treatment and only traces of a C-terminally truncated fragment were visible

with the lower amount of protease (lanes 8-11). Only after 5-fold concentration of the sample, I was able to obtain a clear signal (lane 12). The absence of full-length Calnexin even in the concentrated samples indicated that the used amount of proteinase K was sufficient for a complete digest. Since the majority of the ER-luminal N-terminal Calnexin fragments were also accessible to protease (Fig. 48B top panel, signal strength in lanes 1-7 compared with 8-11) it seemed that most of the regular ER-structures were not intact after CRC preparation and protease digest. The HCV replication complex therefore appears to represent a more rigid structure in order to the complete protease and nuclease resistance of *in vitro* replicase activity. However, when I analyzed the viral non-structural proteins 3, 4B and 5B after protease digest (Fig. 48B, second, third and lowest panel, respectively, lanes 8-12), I found detectable amounts again only after 5x concentration of the samples (lane 12). The absence of lower molecular weight products indicated the completeness of digestion. Based on densitometric analysis and including the dilution factor, I calculated that roughly 2.5% of NS5B was resistant to proteinase K digest, but accounted for the full replicase activity (Fig. 46). This result suggested that the majority of viral non-structural proteins was not directly involved in RNA synthesis at a given time point. The portions of protease-resistant NS3 and NS4B were similar, indicating a 1:1 stoichiometry of the NS proteins in the replication complex. A serial dilution of purified NS5B applied on the same Western blot allowed us to quantify the number of NS5B molecules resistant to protease digest (Fig. 48B lowest panel) and we calculated about 5×10^9 molecules NS5B per microliter CRCs in this experiment. Compared to 3×10^6 negative-strands and 3×10^7 positive-strands (Fig. 47), the surprising result was, that although only 2.5 percent of the NS5B molecules were engaged in replicase activity at a given time, I still found a 1,600-fold excess of NS5B compared to negative-strand RNA and a more than 100-fold excess compared to positive-strand RNA in CRCs.

3.4.5 The HCV replication complex contained multiple copies of the non-structural proteins

The data obtained from the experiment shown in Figures 46-48 (experiment 1) and from an additional, independent experiment are summarized in Table 3. Both sets of data displayed very similar results: In preparations of HCV replication complexes,

viral positive- and negative-strand RNA was entirely resistant to nucleases compared to less than 3 percent of NS5B being protease-resistant. The ratio of positive- to negative-strand RNA was varying and might be dependent on the physiological state of the cells at the time of harvest. Negative-strand RNA is the most restricted component in HCV RNA replication and therefore the best indicator for the total number of active replication complexes.

Table 3. Portions and ratios of nuclease-resistant positive-strand, negative-strand and protease-resistant NS5B in CRCs

	Experiment 1	Experiment 2
% protease resistant NS5B	2.5	2.2
% nuclease resistant positive-strand RNA	~ 100	~ 100
% nuclease resistant negative-strand RNA	~ 100	~ 100
ratio positive-strand : negative-strand RNA*	12 +/- 3	6 +/- 2
ratio NS5B : negative-strand RNA*	1,200 +/- 400	700 +/- 400
ratio NS5B : positive-strand RNA*	100 +/- 20	110 +/- 50

* mean and standard deviation of four nuclease treated samples

Based on the data presented in Table 2 and assuming that each active replication complex contains per definition at least one copy of negative-strand RNA, there were on the average less than one hundred active replication complexes per replicon cell but more than a million polymerase molecules. After biochemical preparation of replication complexes and excessive protease digest, I still found more than 1,000 NS5B molecules per negative-strand RNA (Table 3), and similar amounts of NS4B and NS3, indicating that a huge excess of non-structural proteins was required to build up the viral replication complex.

4. Discussion

HCV replication is believed to take place in vesicular membrane structures harboring the viral RNA and non-structural proteins as well as cellular host factors involved in viral RNA amplification. In the present study, we developed a purification strategy for the membrane-associated HCV replication complexes based on their proteinase K (PrK) insensitivity and showed that their *in vitro* activity was different from purified NS5B polymerase activity. Several host factors associated with the purified viral RC were identified by proteomics, and the most reproducible candidate - ANXA2 - was investigated in detail. We found a specific recruitment of ANXA2 by NS5A; however, its functional role in HCV replication remained to be determined. Based on quantitative analysis of nuclease- and protease-resistant RCs, we were able to determine the ratio of viral protein to RNA in enzymatically active RCs and compared it with the ratio in the cell finding in both settings an excess of viral proteins over RNA molecules.

HCV replication occurs at the membranous web, i.e. at vesicular membrane structures harboring the NS proteins and the viral RNA[51,74]. Isolated CRCs are capable of viral RNA amplification, without addition of an exogenous template RNA. These vesicles probably have a connection to the cytoplasm, allowing the constant supply of nucleotides for RNA synthesis. It is still not entirely clear to which extend the isolated CRCs *in vitro* resemble functions of RCs *in vivo*. However, the fact that a non-nucleosidic RdRp inhibitor as well as an inhibitory antibody directed against NS5B[154] did not interfere with *in vitro* replicase activity indicated that not the RdRp activity of NS5B alone is responsible for RNA synthesis in the CRC fraction. Then again it is possible that the NS5B binding sites for both different inhibitors were concealed because NS5B forms a complex with other NS proteins and/or the membrane or that the vesicular structure prevents the access of larger molecules like the inhibitors to the inside.

Miyanari and colleagues found that HCV replicase activity in digitonin-permeabilized cells was resistant to protease[153], and we showed that the *in vitro* activity of isolated HCV replication complexes was not sensitive to proteinase K, too, although the majority of all cellular and viral proteins was degraded. In the present study, I exploited this for the purification of viral replication complexes and their associated cellular factors. However, proteins associated with or localized inside intracellular

membrane compartments, e.g. early and late endosomes, mitochondria, ER, Golgi, etc., are possibly also protected against PrK and thus can still be found in the CRC fraction.

Alternative purification strategies imply the use of detergents since several groups reported that HCV replication occurs on detergent-resistant membranes (DRMs) which are stable to Triton X-100 extraction in the cold[5,193]. Therefore, treating CRCs with TX-100 at 4°C should result in the extraction of all proteins not associated with lipid rafts. Although this approach worked fine in terms of protein purification in my hands, replicase activity was not detectable in the DRM fractions. Most probably the replication complexes were disrupted or dissociated in the presence of the remaining TX-100 when heated up to the incubation temperature of the *in vitro* replicase assay. On the other hand, it was possible that the RNA of the replication complexes was now accessible to cellular nucleases present in these cellular fractions and was therefore degraded. Incubation of CRCs in the presence of other detergents resulted in most cases also in a loss of *in vitro* replicase activity. Since the *in vitro* replicase activity was the most important readout for the integrity of the replication complexes, we refrained from using detergents for the purification of RCs. However, Mannova and coworkers used detergent treatment to isolate lipid rafts and identify protein modifications in these rafts resulting from HCV replication[148].

In the present study, cellular factors associated with the HCV RC were identified by proteomic analyses of PrK-resistant CRC fractions. In the literature, host cell proteins involved in the viral life cycle are identified by diverse methods, e.g. Y2H screens or DNA microarrays showing an upregulation of certain genes. These methods are often useful, although the possible interaction partners are sometimes found under very artificial conditions and not all results can be confirmed *in vivo*. The advantage of the strategy to purify RCs by PrK treatment and sucrose density gradient centrifugation was that the integrity of the complexes seemed to be maintained since the *in vitro* replicase activity was not reduced or inhibited. Thereby, the purified RCs probably resembled closely the RCs found in an *in vivo* situation and reflect their natural composition.

There exist also other possibilities to identify cellular factors putatively involved in viral replication. Harris and coworkers developed a novel RNA affinity capture system in which a biotinylated oligonucleotide was annealed to one end of a run-off transcript corresponding to the positive-strand 3'-NTR of HCV. Subsequent immobilization of

this partial duplex on paramagnetic streptavidin-coated beads and incubation with hepatocyte extracts allowed them to isolate cellular proteins bound to the 3'-NTR RNA[87]. Recently, another interesting strategy was presented: Huang and colleagues inserted a Flag epitope-tagged GFP at the cytosolic C-terminus of NS5A. Membrane-bound NS5A was purified from crude cell lysates by an immuno-isolation technique using magnetic beads coated with anti-Flag[96]. Bound fractions also contained viral NS3, NS4B, and NS5B, as well as viral RNA, but were not tested for *in vitro* replicase activity. Major cellular organelles like Golgi, ER, mitochondria or endosomes did not bind to the beads indicating that a high level of purification was achieved. Interestingly, among the cellular proteins associated with these isolated fractions, they also found ANXA2, but did not further investigate the impact of this protein.

None of the protein spots differentially represented in my comparative 2D gel analyses of PrK treated CRC fractions from replicon-harboring and cured Huh-7 cells was identified as an HCV NS protein. Adessi and colleagues reported that membrane and hydrophobic proteins (like the viral NS proteins) can be poorly represented in the second dimension of a 2D gel analysis, which is probably due to protein/gel interactions during IEF[2]. Some larger proteins may also be lost and it has been suggested that this is due to size exclusion when the proteins are loaded onto the gel. Otherwise, it is possible that the NS protein amount was simply below the detection limit, since the majority of proteins had been digested by PrK. By using fluorescence-based 2D gel analyses like the DIGE system[211,216] which possess a higher sensitivity, it may be possible to identify the protein spots representing the viral NS proteins.

During the present study, I have also analyzed the stoichiometry of HCV RNA and proteins in cells with ongoing HCV replication and found a massive excess of structural and non-structural protein molecules over RNA, indicating that each positive-strand RNA molecule is excessively translated before a replication complex is formed and RNA synthesis is initiated. In agreement with the polyprotein nature of the major HCV ORF, all analyzed cleavage products are found in similar amounts. A ca. 1,000-10,000-fold excess of viral proteins to positive-strand RNA as observed in this study might fit well to the requirements for particle formation, since virions of other enveloped positive-strand RNA viruses like alphaviruses, tick-borne

encephalitis virus or Dengue virus usually contain several hundred copies of structural proteins per particle[60,70,122,164].

I wondered whether a similar excess of non-structural proteins was required for RNA replication and addressed this question by studying crude replication complexes isolated from cells harboring persistent HCV replicons. It has been shown previously that *in vitro* replicase activity is resistant to protease and nuclease treatment in CRCs[5,8,52] and that in digitonin-solubilized replicon cells only a minor portion of the HCV NS proteins is protease-resistant and therefore seems to be involved in replication[153]. My data are in good agreement with these earlier results, however, although I find as well that less than 5 percent of the non-structural proteins in CRCs are protease-resistant and account for full replication activity *in vitro*, this still results in a ca. 1,000 : 1 stoichiometry of NS proteins to active replication complexes, estimated by the number of negative-strand RNA molecules.

Based on my data and on previously published EM-studies[51,74], we propose a tentative model of the HCV replication complex (Fig. 49): Multiple copies of HCV non-structural protein complexes encompassing NS3 to NS5B build up a vesicular membrane structure, which mediates the protection against nucleases and proteases and may hide double strand RNA from detection by the host cells innate immune system. The existence of HCV non-structural protein complexes rather than individual proteins is indicated by similar fractions of NS3, NS4B and NS5B being resistant to protease and seems plausible due to numerous interactions within the non-structural proteins that have been described yet[15,48]. Each vesicle should have a connection to the cytoplasm allowing the constant supply with nucleotides for RNA synthesis, but preventing the access of molecules larger than 16 kDa, e.g. S7 nuclease and proteinase K. A number of these vesicles accumulate at distinct sites in the cytoplasm and form the membranous web, which was shown to be the site of RNA replication[74]. Within every vesicle that contains an active replication complex, I find at least one negative-strand RNA, several positive-strand RNAs and up to one thousand copies of each of the non-structural proteins. The precise stoichiometry of RNA to protein in the replication complex is hard to tell, since a number of replication complexes might await initiation of negative-strand synthesis at a given time and therefore contain only non-structural proteins and positive-strand RNA. If this variant is frequent, ca. 100-200 copies of the non-structural proteins per replication complex would be a more realistic estimate. On the other hand, several replication complexes

might include more than one molecule of negative-strand RNA and therefore the number of non-structural protein molecules per active replication complex could even be higher. Finally, I cannot exclude the existence of vesicles without viral RNA, which still might render the included NS proteins protease resistant, because the induction of membrane alterations is an intrinsic property of NS4B[51] and I do not know whether the presence of RNA is necessary to induce protease resistance of the non-structural proteins.
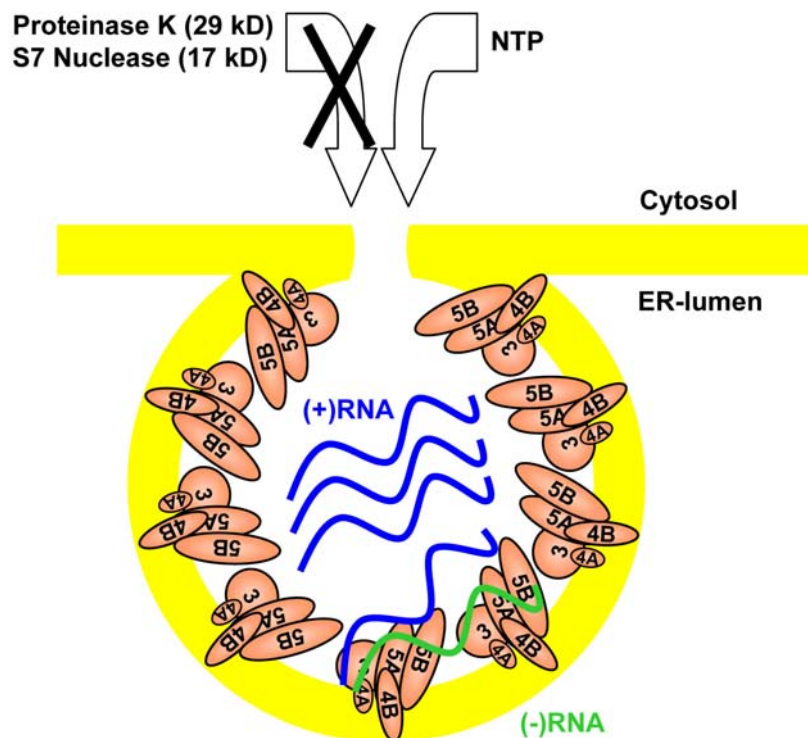
Fig. 49. Schematic model of the HCV replication complex. HCV NS proteins are indicated by orange ellipses; blue and green wavy lines represent viral positive and negative-strand RNA, respectively. Individual NS proteins and RNA are not drawn to scale. For closer explanations refer to the text.

Our picture of the HCV replication complex is very similar to a model suggested by Miyanari et al.[153], however, the data presented in this study provide the first experimental evidence that each HCV replication complex is composed of multiple copies of the viral non-structural proteins. This resembles closely results obtained for brome mosaic virus[190]. It has been shown that 400 copies of protein 1a form a spherular structure connected to the cytoplasm and containing viral RNA together with a few copies of the viral polymerase 2a. Interestingly, a similar virus-induced compartment was lately analyzed by electron microscope tomography. The flock house virus (FHV) replicates in spherules that are outer mitochondrial membrane

invaginations with interiors connected to the cytoplasm by a necked channel of approximately 10-nm diameter[117]. These spherules contain, on average, three RNA replication intermediates and an interior shell of circa 100 membrane-spanning, self-interacting proteins A, which alone is needed for FHV RNA replication. In case of HCV, the majority of protease-resistant non-structural protein complexes might as well be required to build up the vesicular structure, whereas only a few complexes are required for polymerase activity. This calculation is based on the kinetics of RNA and protein synthesis in replicon cells: The intracellular levels of viral RNA and proteins remain relatively constant over years of continuous passaging[166], representing a steady-state situation at any given time point. Since the half-lives of viral NS proteins and viral positive-strand RNA in replicon cells have been shown to be 11-16 h[166,173] the rate of newly synthesized RNA and protein per day should roughly be in the range we find in the steady state situation (Table 2). Based on this and on my data, I estimate that only about 1,000 positive-strand RNA molecules are synthesized per day per cell by ca. 100 replication complexes, but more than 1,000,000 copies of non-structural proteins. In consequence, each newly synthesized positive-strand has to be excessively translated to yield the ascertained surplus of proteins, whereas RNA synthesis is a rather rare event, which most likely is achieved only by a few non-structural protein complexes. Recently, Dahari and coworkers published a mathematical modeling of subgenomic HCV replication[42] that was mainly based on this data. Given my calculation, less than 0.1 % of all NS5B molecules are required to be enzymatically active.

Many positive-strand RNA viruses have evolved strategies to regulate the amounts of active polymerase, either by expression from an independent cistron, like BMV[190], by the expression of a polyprotein containing rarely suppressed stop codons, like alphaviruses[129] or by producing stable precursor intermediates lacking polymerase activity, like poliovirus 3CD[20]. In case of HCV, polymerase activity could be regulated by different conformations of the non-structural protein complex, depending on its function. It has been shown that a carboxyterminal region of NS5B, encompassing amino acids 545-562 inhibits polymerase activity[1] and that only a small fraction of purified NS5B containing this region is enzymatically active[35]. Crystal structure analysis revealed that this carboxyterminal domain protrudes into the RNA binding cavity of NS5B and interferes with template binding[128]. Deletion of this region increases polymerase activity as well as RNA binding of NS5B[128]. Therefore, it is

tempting to speculate that the majority of NS5B is inactive after translation by refolding of the carboxyterminus into the RNA binding cleft, whereas only those few molecules that stay bound to the viral RNA keep the template binding site in an open conformation and retain enzymatic activity. The ability to self-inactivate viral polymerase not required for RNA synthesis might represent an alternate strategy to deal with the stoichiometric constraints of a polyprotein.

In contrast, the majority of non-structural protein complexes not directly involved in RNA synthesis may be required e.g. as a structural component of the membrane vesicle. The viral non-structural protein primarily involved in this process is NS4B, since it is able to induce vesicular structures even in the absence of other HCV proteins[51]. The different roles of non-structural protein complexes might be regulated by the association with individual host cell factors, like hVAP-A, a cellular protein which has been shown to interact with NS5A and NS5B[56,214]. Since this protein is involved in intracellular vesicle trafficking, it seems to be a good candidate for a cofactor of membrane structure rearrangements and has already been suggested to be involved in HCV replication complex formation[5,71]. In addition, other cellular factors might be required for RNA synthesis. A detailed biochemical analysis of the protease-resistant non-structural protein fraction might reveal some of the cellular proteins that are directly involved in the formation of the replication complex and in RNA synthesis.

The functions of the protease-sensitive portion of the non-structural proteins, encompassing more than 95%, remain obscure. Since my analysis presents a snapshot at a given time point and I have no precise data on the dynamics of replication complex assembly and disassembly, parts of these proteins might be in the process of vesicle generation and disintegration. The remainder could simply be a byproduct of structural protein synthesis, which might be required in excess amounts for virus production. Miyanari and coworkers suggested potential roles of the non-structural proteins in virion formation or indirect modulation of viral replication by interaction with host cell proteins[153]. Along the same line, the NS3/4A moiety might be required to block the IRF-3 induced pathway of the host cells' innate immune system, which has been shown to play a critical role in HCV replication[63].

In the present study, I have shown that during the replication cycle of HCV a massive excess of non-structural proteins is produced due to extensive translation. An interesting but yet unanswered question is, how the transition of translation to

replication is regulated. A number of proteins have been shown to bind to the HCV 5'-NTR, which might be involved in this process[6,7,82,111,143]. Alternatively, the switch could rely on concentration-dependent inhibition of translation by an HCV protein. Interestingly, I found no significant differences in the ratio of HCV RNA and protein between an authentic HCV genome, a monocistronic and a bicistronic replicon (Table 2), indicating that the nature of the IRES element directing translation of the non-structural proteins is not important for this stoichiometry. After translation, replication complex formation, and RNA synthesis, the progeny RNA has to get back into the cytoplasm to enter a new round of translation/replication or packaging into particles. We currently do not know if this process includes an active transport, like in the replication cycle of dsRNA reoviruses[181], or if the progeny RNA accumulates in the replication complex and is released by disintegration of the vesicle.

A limitation of my analysis is that no viral particles are produced by the chosen replication systems[172]. Since I do not know how many positive-strand RNA molecules would end up in virions and whether viral genomes undergo translation prior to packaging it is very hard to predict the consequences of simultaneous RNA replication and particle morphogenesis on the ratio of RNA to proteins in infected cells. Shortly after this stoichiometric study, three independent studies demonstrated the production of infectious HCV particles in cell culture using the non-structural proteins of the JFH-1 HCV isolate[133,219,240]. It will be interesting to evaluate my findings in this system covering the whole life cycle of HCV. However, due to the lack of appropriate antibodies, this investigation was not possible within the scope of my PhD thesis.

After the successful establishment of an effective purification strategy for the membrane-bound HCV replication complexes, I had identified cellular proteins associated with the viral RC by proteomic approaches. The most reproducible and therefore promising candidate was Annexin II (ANXA2) which belongs to the Annexins, a large family of structurally similar proteins that bind to negatively charged phospholipids and have versatile functions. They are involved in many membrane-related events, such as the regulated organization of membrane domains and/or membrane-cytoskeleton linkages, certain exocytic and endocytic transport steps and the regulation of ion fluxes across membranes.

Annexins are Ca^{2+}/lipid-binding proteins that differ from most other Ca^{2+}-binding proteins in their Ca^{2+}-binding sites. They have a unique architecture that allows them to dock onto membranes in a peripheral and reversible manner. The conserved Ca^{2+}- and membrane-binding module is the Annexin core domain, which consists of four so-called Annexin repeats, each of which is 70 residues in length. It is highly α-helical and forms a compact, slightly curved disc that has a convex surface harboring the Ca^{2+}- and membrane-binding sites and a concave side that points away from the membrane and is thereby available for other types of interaction/regulation (Fig. 50). The N-terminal region precedes the core domain and is diverse in sequence and length for each single Annexin. It mediates regulatory interactions with protein ligands and regulates the Annexin-membrane association.
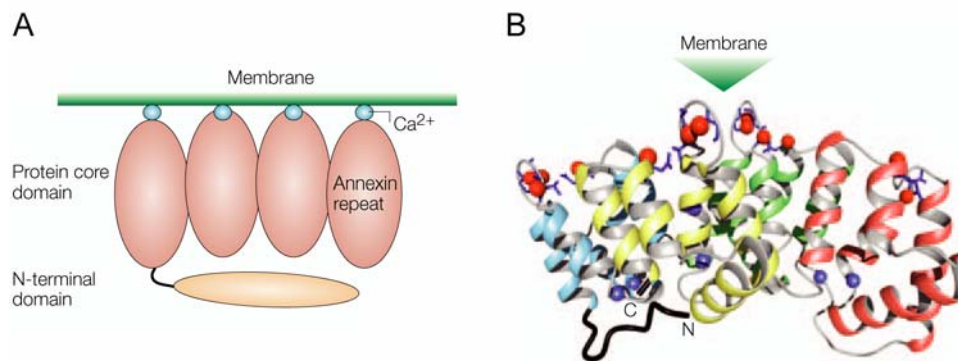

Fig. 50. Annexin structure. (A) Schematic drawing of an Annexin that is peripherally attached to a membrane surface through bound Ca^{2+} ions (blue). (B) Structural model of an Annexin core. Each Annexin repeat (colored differently) contains five α-helices that are connected by short loops or turns. The N and C termini are colored black. Red spheres within stick-representation residues highlight atomic oxygens that are involved in forming the type-II Ca^{2+}-binding sites, whereas blue spheres denote nitrogen atoms of highly conserved basic residues. *Adapted from Gerke et al., Nature Reviews, 2005*[73].

ANXA2 is found intra- and extracellularly serving different functions. In the extracellular compartment, it is involved in fibrinolysis[109]. Intracellularly, ANXA2 serves as membrane scaffold, plays a role in membrane organization and traffic, transport events, endocytosis as well as exocytosis, and exhibits ion channel activity. Annexin II is found in living cells as a monomer, heterodimer and heterotetramer. Monomeric Annexin II is mainly located in the cytosol; however, upon a stimulus like increase in Ca^{2+}-levels or posttranslational modification, it binds to cellular membranes, in particular the cytosolic leaflets of the plasma membrane and various organelle membranes. The heterodimer is composed of two Annexin II monomers and 3-phosphoglycerat-kinase and is located in the nucleus. The most dominant form in most cells is, however, the heterotetrameric complex $(A2\text{-}p11)_2$, composed of two

Annexin II monomers and a dimer of the S100A10 protein (also called p11) which is its major ligand. This heterotetramer is important for numerous functions of ANXA2 and is primarily found at the cytosolic leaflet of the plasma membrane but also extracellularly (reviewed in [73]). In addition, ANXA2 has been reported to bind certain species of RNA[61,218], which indicates a possible role of ANXA2 in RNA transport or export from the nucleus. For HIV, ANXA2 was also shown to be essential for the proper assembly of new virions in monocyte-derived macrophages[183].

In the present study, ANXA2 was associated with the PrK-resistant fraction of CRCs. Its cytoplasmic distribution was rearranged in HCV-harboring cells resulting in a perfect colocalization with the NS protein components of the viral replication complex. This colocalization did not depend on a certain cell type or HCV genotype. Furthermore, it was detected in cells infected or transiently transfected with HCV as well as in cells stably replicating the viral RNA. A colocalization of NS proteins with other Annexins was not observed and neither a colocalization of ANXA2 with other positive-stranded RNA viruses. This indicated a specific interaction of HCV with ANXA2.

It is known that HCV replication takes place in vesicular structures, designated as membranous web, which are probably derived from the Endoplasmic Reticulum (ER)[51,74], although a specific colocalization of the ER marker Calnexin and NS proteins was not visible in this study. ANXA2 interacts with membranes of varying cellular organelles[45,47,55,79], however, a binding of ANXA2 to ER membranes was so far not reported.

Naïve HepG2 cells possess only minor amounts of endogenous ANXA2[175] that were not detectable in our immunofluorescence studies. In contrast, ANXA2 was clearly seen in HepG2 cells stably replicating HCV RNA, indicating an induction, stabilization or simply concentration of this cellular protein by HCV. However, the increased ANXA2 levels in these cells may be attributed to a selection advantage of cells possessing higher endogenous ANXA2 amounts thereby supporting the viral replication more efficiently. Nevertheless, overexpression of ANXA2 in naïve HepG2 cells did not result in an enhanced replication of transiently transfected HCV RNA. On the other hand, silencing of ANXA2 in HepG2 cells persistently harboring subgenomic HCV replicons did also not have any impact on the HCV RNA level suggesting that ANXA2 is not limiting HCV replication in these cells.

Likewise, stable as well as transient silencing of ANXA2 in Huh-7 cells did not influence viral replication levels but indicated a positive correlation of the ANXA2 protein amount and HCV replication. This was corroborated by FACS analyses showing that the HCV levels were slightly decreased in ANXA2-silenced cells compared to control-silenced cells. FACS analyses proved evidence for the increase of ANXA2 levels upon HCV replication, too; however, the mechanism by which HCV induced ANXA2 was not clear. The increased ANXA2 levels in cells transiently transfected with HCV and in presence of siRNA directed against ANXA2 compared to control cells could be explained by either enhanced gene transcription, boosted mRNA translation, decreased mRNA degradation or stabilization of the protein. Our FACS analyses demonstrated a slight but reproducible induction of ANXA2 levels by HCV; however, this could so far not be clearly confirmed by immunoblot assay or RT-PCR.

In addition to the induction of ANXA2 by HCV, it is also possible that the ANXA2 protein is further stabilized by interaction with HCV. It has been reported that downregulation of ANXA2 in HeLa cells by RNA interference (RNAi) efficiently depletes the intracellular ANXA2 pool, however, some ANXA2 remains in the cortex underneath the plasma membrane, presumably because of a significantly longer half-life[243]. In this study of Zobiack et al., the RNAi had no effects on plasma-membrane-related events. In the colocalization studies of my RNAi experiments, I obtained comparable results. It was also observed that the cytosolic ANXA2 was no longer detectable upon ANXA2 silencing, but the colocalization with HCV NS proteins remained. Therefore, it can be assumed that the association of ANXA2 with the HCV replication complex in the membranous web stabilized ANXA2 thereby prolonging its half-life. Strong silencing of ANXA2 only had a moderate impact on HCV replication. A possible explanation was that the functions of ANXA2 were taken over by other Annexins since they possess a high structural similarity or that ANXA2 involved in HCV replication was recruited from stable pools as observed by Zobiack and colleagues. Annexin-knockout models often exhibit no obvious phenotype related to a primary defect in e.g. vesicle docking and/or fusion events[32,88,136]. This indicates that the Annexins targeted in these mice do not serve as essential factors in vesicle docking and/or fusion or that such functions are redundant or taken over by another member of the family during mouse development. Given the sequence and structural homology among the Annexins and their overlapping tissue distributions, such

compensatory mechanisms have to be considered. On the other hand, it was observed that HCV induces ANXA2 which of course might interfere with the ANXA2-silencing. It is not known in which amounts ANXA2 is necessary for HCV replication, and the induction of ANXA2 by HCV is putatively sufficient to counteract the silencing effects.

HCV NS5A was identified as the viral interaction partner of ANXA2 by heterologous expression of the single NS proteins. The expression of NS5A led to the induction and rearrangement of ANXA2 in these cells. NS5A is a versatile protein which has already been shown to interact with many different cellular proteins that influence the viral RNA replication, e.g. Vap-A[214,239], FBL2[221] and amphiphysin II[238]. The precise function of NS5A has not been defined yet, but it has been suggested that it regulates the switch between replication and packaging: cell culture adaptive mutations increasing the RNA replication impede infectivity in chimpanzees[34]. NS5A is a hot spot of cell culture adaptive mutations most of which reduce hyperphosphorylation and seem to interfere with particle production. In addition, hyperphosphorylation of NS5A interferes with efficient RNA replication[56,160] indicating that the transition from replication to virus assembly might be triggered by NS5A phosphorylation. Therefore, the ANXA2-NS5A interaction might play a role in the regulation of replication and packaging.

ANXA2 acts in membrane aggregation by linking two different membranes[126], but does not act as a fusogen. Therefore, a possible function of this protein is the formation of a neck of the vesicle harboring the HCV replication complexes which builds the junction between the vesicle and the cytoplasm (Fig. 51C). In general, the (ANXA2-p11)$_2$ heterotetramer is involved in such membrane aggregations; however, colocalization of p11 with the HCV RC was not observed indicating that it is not involved in HCV replication. Nevertheless, it is possible that either the p11 amounts in the RCs were below detection limit or p11 is replaced by another protein taking over its function. Furthermore, the functions of ANXA2 are controlled by phosphorylation. Membrane aggregation by ANXA2 is strongly inhibited when it is phosphorylated by protein kinase C (PKC)[103]. Interestingly, it was shown that HCV NS3 interferes with the phosphorylation activity of PKC[30] indicating that the inhibition of PKC by HCV NS3 could possibly lead to a stabilization of the membranous web by abrogating phosphorylation of ANXA2. Furthermore, ANXA2 was identified as a substrate of casein kinase I (CKI)[72] which is also responsible for the

hyperphosphorylation of NS5A[178]. It is imaginable that the phosphorylation of ANXA2 by CKI interferes with the membrane aggregation activity of ANXA2, too. Hyperphosphorylation of NS5A by CKI putatively leads to the switch from viral RNA replication to virion assembly. Opening of the membranous vesicles harboring the HCV replication complexes might be necessary to release the viral progeny RNA strands for packaging and could be triggered by CKI-mediated phosphorylation of ANXA2. Furthermore, ANXA2 is a RNA-binding protein like it has been shown for NS5A[61,97] and therefore both proteins could be involved in an interaction with the viral RNA.

Besides the possible neck formation of the RC-harboring vesicle and according to the reported functions of ANXA2, there are other scenarios for its role in the viral RNA replication. Several studies showed that HCV replication occurs on detergent-resistant membranes also referred to as lipid rafts[5,193]. ANXA2 binds to the lipid raft component $PtdIns(4,5)P_2$[89,182] and is involved in cholesteryl-ester transport from caveolae to internal membranes[215] as well as in the organization of cholesterol-rich lipid microdomains[10-12]. By engaging in homophilic lateral interactions, Annexin II could then induce and/or stabilize raft clustering and thereby may provide the platform of viral RNA amplification (Fig 51A). On the one hand, it is plausible that ANXA2 sequesters cholesterol from the plasma membrane to intracellular compartments to form the replication complex. On the other hand, it is possible that ANXA2 is only associated with the replication complex because it simply follows the formation of lipid microdomains through its specific binding to certain head-groups, e.g. $PtdIns(4,5)P_2$. Assuming that ANXA2 is not only a bystander, the recruitment of the HCV RCs to lipid rafts by ANXA2 could occur by its interaction with NS5A or, since ANXA2 has also a RNA-binding activity[61,218], with the viral RNA. This could then lead to the binding of the other RC components and assembly of the RC (Fig. 51A and B).

Although the precise role of ANXA2 in the viral replication remains to be determined, it is likely that this protein is involved in the assembly of the HCV RC. Further studies should be performed to confirm that NS5A is the viral interaction partner and to precisely map the interaction sites. In addition, the mechanism of the ANXA2 induction by HCV has to be analyzed. Despite these open questions, this study greatly helped in understanding the biogenesis and composition of the HCV replication complex.
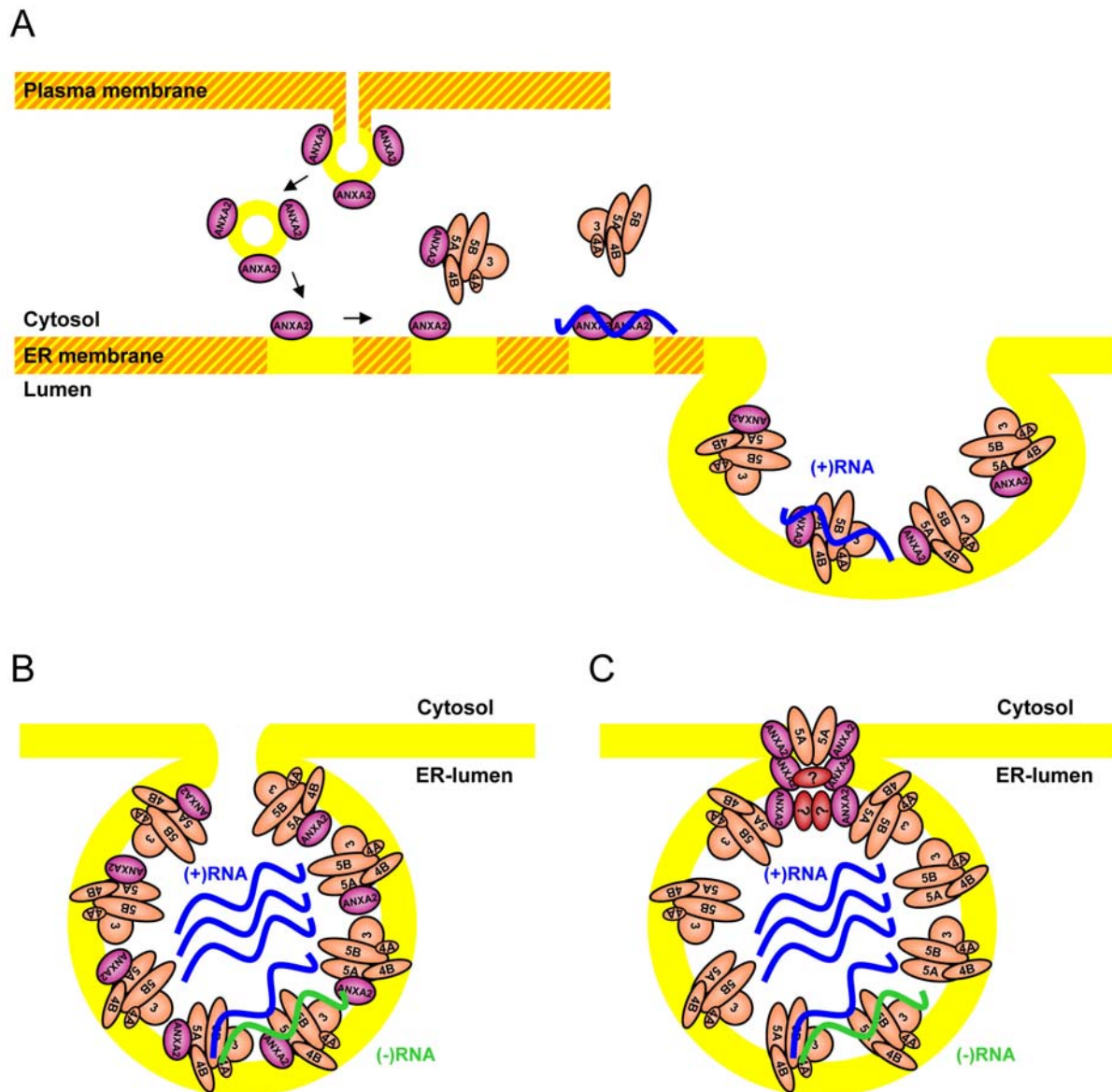
Fig. 51. Hypothetical functions of ANXA2 in HCV replication. (A) Recruitment of lipid microdomains components from the plasma membrane and transport to internal membranes by ANXA2 to provide a platform for HCV RC assembly. ANXA2 sequesters cholesterol or other lipid raft components from the plasma membrane to intracellular compartments. Upon interaction of ANXA2 with HCV NS5A or the viral RNA the missing RC components are recruited to the lipid microdomains and form the RC. Vesicle formation is then induced by NS4B. (B) ANXA2 helps maintaining the vesicular structure by interaction with lipid microdomains and the RC. (C) ANXA2 is involved in formation of a neck of the vesicle which builds the junction between the vesicle and the cytoplasm. It is possible that other factors are involved in this process. Detergent-sensitive membranes are represented by yellow-orange striped structures, lipid rafts by yellow structures. HCV NS proteins are indicated by orange ellipses; blue and green wavy lines represent viral positive and negative-strand RNA, respectively. Violet ellipses indicate ANXA2, red ellipses unknown proteins potentially playing a role in viral replication. Individual proteins and RNA are not drawn to scale.

5. Reference List

1. ADACHI, T., H. AGO, N. HABUKA, K. OKUDA, M. KOMATSU, S. IKEDA, AND K. YATSUNAMI. 2002. THE ESSENTIAL ROLE OF C-TERMINAL RESIDUES IN REGULATING THE ACTIVITY OF HEPATITIS C VIRUS RNA-DEPENDENT RNA POLYMERASE. BIOCHIM. BIOPHYS. ACTA **1601**:38-48.

2. ADESSI, C., C. MIEGE, C. ALBRIEUX, AND T. RABILLOUD. 1997. TWO-DIMENSIONAL ELECTROPHORESIS OF MEMBRANE PROTEINS: A CURRENT CHALLENGE FOR IMMOBILIZED PH GRADIENTS. ELECTROPHORESIS **18**:127-135.

3. AGNELLO, V., G. ABEL, M. ELFAHAL, G. B. KNIGHT, AND Q. X. ZHANG. 1999. HEPATITIS C VIRUS AND OTHER FLAVIVIRIDAE VIRUSES ENTER CELLS VIA LOW DENSITY LIPOPROTEIN RECEPTOR. PROC. NATL. ACAD. SCI. U. S. A **96**:12766-12771.

4. AHOLA, T., A. LAMPIO, P. AUVINEN, AND L. KAARIAINEN. 1999. SEMLIKI FOREST VIRUS MRNA CAPPING ENZYME REQUIRES ASSOCIATION WITH ANIONIC MEMBRANE PHOSPHOLIPIDS FOR ACTIVITY. EMBO J. **18**:3164-3172.

5. AIZAKI, H., K. J. LEE, V. M. SUNG, H. ISHIKO, AND M. M. LAI. 2004. CHARACTERIZATION OF THE HEPATITIS C VIRUS RNA REPLICATION COMPLEX ASSOCIATED WITH LIPID RAFTS. VIROLOGY **324**:450-461.

6. ALI, N. AND A. SIDDIQUI. 1995. INTERACTION OF POLYPYRIMIDINE TRACT-BINDING PROTEIN WITH THE 5' NONCODING REGION OF THE HEPATITIS C VIRUS RNA GENOME AND ITS FUNCTIONAL REQUIREMENT IN INTERNAL INITIATION OF TRANSLATION. J. VIROL. **69**:6367-6375.

7. ALI, N. AND A. SIDDIQUI. 1997. THE LA ANTIGEN BINDS 5' NONCODING REGION OF THE HEPATITIS C VIRUS RNA IN THE CONTEXT OF THE INITIATOR AUG CODON AND STIMULATES INTERNAL RIBOSOME ENTRY SITE-MEDIATED TRANSLATION. PROC. NATL. ACAD. SCI. U. S. A **94**:2249-2254.

8. ALI, N., K. D. TARDIF, AND A. SIDDIQUI. 2002. CELL-FREE REPLICATION OF THE HEPATITIS C VIRUS SUBGENOMIC REPLICON. J. VIROL. **76**:12001-12007.

9. ASABE, S. I., Y. TANJI, S. SATOH, T. KANEKO, K. KIMURA, AND K. SHIMOTOHNO. 1997. THE N-TERMINAL REGION OF HEPATITIS C VIRUS-ENCODED NS5A IS IMPORTANT FOR NS4A-DEPENDENT PHOSPHORYLATION. J. VIROL. **71**:790-796.

10. AYALA-SANMARTIN, J. 2001. CHOLESTEROL ENHANCES PHOSPHOLIPID BINDING AND AGGREGATION OF ANNEXINS BY THEIR CORE DOMAIN. BIOCHEM. BIOPHYS. RES. COMMUN. **283**:72-79.

11. AYALA-SANMARTIN, J., J. P. HENRY, AND L. A. PRADEL. 2001. CHOLESTEROL REGULATES MEMBRANE BINDING AND AGGREGATION BY ANNEXIN 2 AT SUBMICROMOLAR CA(2+) CONCENTRATION. BIOCHIM. BIOPHYS. ACTA **1510**:18-28.

12. BABIYCHUK, E. B. AND A. DRAEGER. 2000. ANNEXINS IN CELL MEMBRANE DYNAMICS. CA(2+)-REGULATED ASSOCIATION OF LIPID MICRODOMAINS. J. CELL BIOL. **150**:1113-1124.

13. BARTENSCHLAGER, R. 2002. HEPATITIS C VIRUS REPLICONS: POTENTIAL ROLE FOR DRUG DEVELOPMENT. NAT. REV. DRUG DISCOV. **1**:911-916.

14. BARTENSCHLAGER, R., L. AHLBORN-LAAKE, J. MOUS, AND H. JACOBSEN. 1994. KINETIC AND STRUCTURAL ANALYSES OF HEPATITIS C VIRUS POLYPROTEIN PROCESSING. J. VIROL. **68**:5045-5055.

15. BARTENSCHLAGER, R., M. FRESE, AND T. PIETSCHMANN. 2004. NOVEL INSIGHTS INTO HEPATITIS C VIRUS REPLICATION AND PERSISTENCE. ADV. VIRUS RES. **63**:71-180.

16. BARTENSCHLAGER, R. AND V. LOHMANN. 2001. NOVEL CELL CULTURE SYSTEMS FOR THE HEPATITIS C VIRUS. ANTIVIRAL RES. **52**:1-17.

17. BARTOSCH, B., J. DUBUISSON, AND F. L. COSSET. 2003. INFECTIOUS HEPATITIS C VIRUS PSEUDO-PARTICLES CONTAINING FUNCTIONAL E1-E2 ENVELOPE PROTEIN COMPLEXES. J. EXP. MED. **197**:633-642.

18. BEAULIEU, P. L., M. BOS, Y. BOUSQUET, P. DEROY, G. FAZAL, J. GAUTHIER, J. GILLARD, S. GOULET, G. MCKERCHER, M. A. POUPART, S. VALOIS, AND G. KUKOLJ. 2004. NON-NUCLEOSIDE INHIBITORS OF THE HEPATITIS C VIRUS NS5B POLYMERASE: DISCOVERY OF BENZIMIDAZOLE 5-CARBOXYLIC AMIDE DERIVATIVES WITH LOW-NANOMOLAR POTENCY. BIOORG. MED. CHEM. LETT. **14**:967-971.

19. BECKER, T., K. WEBER, AND N. JOHNSSON. 1990. PROTEIN-PROTEIN RECOGNITION VIA SHORT AMPHIPHILIC HELICES; A MUTATIONAL ANALYSIS OF THE BINDING SITE OF ANNEXIN II FOR P11. EMBO J. **9**:4207-4213.

20. BEDARD, K. M. AND B. L. SEMLER. 2004. REGULATION OF PICORNAVIRUS GENE EXPRESSION. MICROBES. INFECT. **6**:702-713.

21. BIENZ, K., D. EGGER, T. PFISTER, AND M. TROXLER. 1992. STRUCTURAL AND FUNCTIONAL CHARACTERIZATION OF THE POLIOVIRUS REPLICATION COMPLEX. J. VIROL. **66**:2740-2747.

22. BIGGER, C. B., K. M. BRASKY, AND R. E. LANFORD. 2001. DNA MICROARRAY ANALYSIS OF CHIMPANZEE LIVER DURING ACUTE RESOLVING HEPATITIS C VIRUS INFECTION. J. VIROL. **75**:7059-7066.

23. BIGGER, C. B., B. GUERRA, K. M. BRASKY, G. HUBBARD, M. R. BEARD, B. A. LUXON, S. M. LEMON, AND R. E. LANFORD. 2004. INTRAHEPATIC GENE EXPRESSION DURING CHRONIC HEPATITIS C VIRUS INFECTION IN CHIMPANZEES. J. VIROL. **78**:13779-13792.

24. BINDER, M., D. QUINKERT, O. BOCHKAROVA, R. KLEIN, N. KEZMIC, R. BARTENSCHLAGER, AND V. LOHMANN. 2007. IDENTIFICATION OF DETERMINANTS INVOLVED IN INITIATION OF HEPATITIS C VIRUS RNA SYNTHESIS BY USING INTERGENOTYPIC REPLICASE CHIMERAS. J. VIROL. **81**:5270-5283.

25. BLIGHT, K. J., A. A. KOLYKHALOV, AND C. M. RICE. 2000. EFFICIENT INITIATION OF HCV RNA REPLICATION IN CELL CULTURE. SCIENCE **290**:1972-1974.

26. BLIGHT, K. J., J. A. MCKEATING, J. MARCOTRIGIANO, AND C. M. RICE. 2003. EFFICIENT REPLICATION OF HEPATITIS C VIRUS GENOTYPE 1A RNAS IN CELL CULTURE. J. VIROL. **77**:3181-3190.

27. BLIGHT, K. J., J. A. MCKEATING, AND C. M. RICE. 2002. HIGHLY PERMISSIVE CELL LINES FOR SUBGENOMIC AND GENOMIC HEPATITIS C VIRUS RNA REPLICATION. J. VIROL. **76**:13001-13014.

28. BLIGHT, K. J. AND C. M. RICE. 1997. SECONDARY STRUCTURE DETERMINATION OF THE CONSERVED 98-BASE SEQUENCE AT THE 3' TERMINUS OF HEPATITIS C VIRUS GENOME RNA. J. VIROL. **71**:7345-7352.

29. BORGESE, N., S. COLOMBO, AND E. PEDRAZZINI. 2003. THE TALE OF TAIL-ANCHORED PROTEINS: COMING FROM THE CYTOSOL AND LOOKING FOR A MEMBRANE. J. CELL BIOL. **161**:1013-1019.

30. BOROWSKI, P., W. J. SCHULZE ZUR, K. RESCH, H. FEUCHT, R. LAUFS, AND H. SCHMITZ. 1999. PROTEIN KINASE C RECOGNIZES THE PROTEIN KINASE A-BINDING MOTIF OF NONSTRUCTURAL PROTEIN 3 OF HEPATITIS C VIRUS. J. BIOL. CHEM. **274**:30722-30728.

31. BOULANT, S., M. BECCHI, F. PENIN, AND J. P. LAVERGNE. 2003. UNUSUAL MULTIPLE RECODING EVENTS LEADING TO ALTERNATIVE FORMS OF HEPATITIS C VIRUS CORE PROTEIN FROM GENOTYPE 1B. J. BIOL. CHEM. **278**:45785-45792.

32. BRACHVOGEL, B., J. DIKSCHAS, H. MOCH, H. WELZEL, M. K. VON DER, C. HOFMANN, AND E. POSCHL. 2003. ANNEXIN A5 IS NOT ESSENTIAL FOR SKELETAL DEVELOPMENT. MOL. CELL BIOL. **23**:2907-2913.

33. BRASS, V., E. BIECK, R. MONTSERRET, B. WOLK, J. A. HELLINGS, H. E. BLUM, F. PENIN, AND D. MORADPOUR. 2002. AN AMINO-TERMINAL AMPHIPATHIC ALPHA-HELIX MEDIATES MEMBRANE ASSOCIATION OF THE HEPATITIS C VIRUS NONSTRUCTURAL PROTEIN 5A. J. BIOL. CHEM. **277**:8130-8139.

34. BUKH, J., T. PIETSCHMANN, V. LOHMANN, N. KRIEGER, K. FAULK, R. E. ENGLE, S. GOVINDARAJAN, M. SHAPIRO, M. ST CLAIRE, AND R. BARTENSCHLAGER. 2002. MUTATIONS THAT PERMIT EFFICIENT REPLICATION OF HEPATITIS C VIRUS RNA IN HUH-7 CELLS PREVENT PRODUCTIVE REPLICATION IN CHIMPANZEES. PROC. NATL. ACAD. SCI. U. S. A **99**:14416-14421.

35. CARROLL, S. S., V. SARDANA, Z. YANG, A. R. JACOBS, C. MIZENKO, D. HALL, L. HILL, J. ZUGAY-MURPHY, AND L. C. KUO. 2000. ONLY A SMALL FRACTION OF PURIFIED HEPATITIS C RNA-DEPENDENT RNA POLYMERASE IS CATALYTICALLY COMPETENT: IMPLICATIONS FOR VIRAL REPLICATION AND IN VITRO ASSAYS. BIOCHEMISTRY **39**:8243-8249.

36. CARROLL, S. S., J. E. TOMASSINI, M. BOSSERMAN, K. GETTY, M. W. STAHLHUT, A. B. ELDRUP, B. BHAT, D. HALL, A. L. SIMCOE, R. LAFEMINA, C. A. RUTKOWSKI, B. WOLANSKI, Z. YANG, G. MIGLIACCIO, R. DE FRANCESCO, L. C. KUO, M. MACCOSS, AND D. B. OLSEN. 2003. INHIBITION OF HEPATITIS C VIRUS RNA REPLICATION BY 2'-MODIFIED NUCLEOSIDE ANALOGS. J. BIOL. CHEM. **278**:11979-11984.

37. CHAN, L., S. K. DAS, T. J. REDDY, C. POISSON, M. PROULX, O. PEREIRA, M. COURCHESNE, C. ROY, W. WANG, A. SIDDIQUI, C. G. YANNOPOULOS, N. NGUYEN-BA, D. LABRECQUE, R. BETHELL, M. HAMEL, P. COURTEMANCHE-ASSELIN, L. L'HEUREUX, M. DAVID, O. NICOLAS, S. BRUNETTE, D. BILIMORIA, AND J. BEDARD. 2004. DISCOVERY OF THIOPHENE-2-CARBOXYLIC ACIDS AS POTENT INHIBITORS OF HCV NS5B POLYMERASE AND HCV SUBGENOMIC RNA REPLICATION. PART 1: SULFONAMIDES. BIOORG. MED. CHEM. LETT. **14**:793-796.

38. CHAN, L., O. PEREIRA, T. J. REDDY, S. K. DAS, C. POISSON, M. COURCHESNE, M. PROULX, A. SIDDIQUI, C. G. YANNOPOULOS, N. NGUYEN-BA, C. ROY, D. NASTURICA, C. MOINET, R. BETHELL, M. HAMEL, L. L'HEUREUX, M. DAVID, O. NICOLAS, P. COURTEMANCHE-ASSELIN, S. BRUNETTE, D. BILIMORIA, AND J. BEDARD. 2004. DISCOVERY OF THIOPHENE-2-CARBOXYLIC ACIDS AS POTENT INHIBITORS OF HCV NS5B POLYMERASE AND HCV SUBGENOMIC RNA REPLICATION. PART 2: TERTIARY AMIDES. BIOORG. MED. CHEM. LETT. **14**:797-800.

39. CHASSEROT-GOLAZ, S., N. VITALE, E. UMBRECHT-JENCK, D. KNIGHT, V. GERKE, AND M. F. BADER. 2005. ANNEXIN 2 PROMOTES THE FORMATION OF LIPID MICRODOMAINS REQUIRED FOR CALCIUM-REGULATED EXOCYTOSIS OF DENSE-CORE VESICLES. MOL. BIOL. CELL **16**:1108-1119.

40. CHOMCZYNSKI, P. AND N. SACCHI. 1987. SINGLE-STEP METHOD OF RNA ISOLATION BY ACID GUANIDINIUM THIOCYANATE-PHENOL-CHLOROFORM EXTRACTION. ANAL. BIOCHEM. **162**:156-159.

41. CHOO, Q. L., G. KUO, A. J. WEINER, L. R. OVERBY, D. W. BRADLEY, AND M. HOUGHTON. 1989. ISOLATION OF A CDNA CLONE DERIVED FROM A BLOOD-BORNE NON-A, NON-B VIRAL HEPATITIS GENOME. SCIENCE **244**:359-362.

42. DAHARI, H., R. M. RIBEIRO, C. M. RICE, AND A. S. PERELSON. 2007. MATHEMATICAL MODELING OF SUBGENOMIC HEPATITIS C VIRUS REPLICATION IN HUH-7 CELLS. J. VIROL. **81**:750-760.

43. DATE, T., T. KATO, M. MIYAMOTO, Z. ZHAO, K. YASUI, M. MIZOKAMI, AND T. WAKITA. 2004. GENOTYPE 2A HEPATITIS C VIRUS SUBGENOMIC REPLICON CAN REPLICATE IN HEPG2 AND IMY-N9 CELLS. J. BIOL. CHEM. **279**:22371-22376.

44. DEFORGES, S., A. EVLASHEV, M. PERRET, M. SODOYER, S. POUZOL, J. Y. SCOAZEC, B. BONNAUD, O. DIAZ, G. PARANHOS-BACCALA, V. LOTTEAU, AND P. ANDRE. 2004. EXPRESSION OF HEPATITIS C VIRUS PROTEINS IN EPITHELIAL INTESTINAL CELLS IN VIVO. J. GEN. VIROL. **85**:2515-2523.

45. DEORA, A. B., G. KREITZER, A. T. JACOVINA, AND K. A. HAJJAR. 2004. AN ANNEXIN 2 PHOSPHORYLATION SWITCH MEDIATES P11-DEPENDENT TRANSLOCATION OF ANNEXIN 2 TO THE CELL SURFACE. J. BIOL. CHEM. **279**:43411-43418.

46. DHANAK, D., K. J. DUFFY, V. K. JOHNSTON, J. LIN-GOERKE, M. DARCY, A. N. SHAW, B. GU, C. SILVERMAN, A. T. GATES, M. R. NONNEMACHER, D. L. EARNSHAW, D. J. CASPER, A. KAURA, A. BAKER, C. GREENWOOD, L. L. GUTSHALL, D. MALEY, A. DELVECCHIO, R. MACARRON, G. A. HOFMANN, Z. ALNOAH, H. Y. CHENG, G. CHAN, S. KHANDEKAR, R. M. KEENAN, AND R. T. SARISKY. 2002. IDENTIFICATION AND BIOLOGICAL CHARACTERIZATION OF HETEROCYCLIC INHIBITORS OF THE HEPATITIS C VIRUS RNA-DEPENDENT RNA POLYMERASE. J. BIOL. CHEM. **277**:38322-38327.

47. DIAKONOVA, M., V. GERKE, J. ERNST, J. P. LIAUTARD, D. VAN, V, AND G. GRIFFITHS. 1997. LOCALIZATION OF FIVE ANNEXINS IN J774 MACROPHAGES AND ON ISOLATED PHAGOSOMES. J. CELL SCI. **110 (PT 10)**:1199-1213.

48. DIMITROVA, M., I. IMBERT, M. P. KIENY, AND C. SCHUSTER. 2003. PROTEIN-PROTEIN INTERACTIONS BETWEEN HEPATITIS C VIRUS NONSTRUCTURAL PROTEINS. J. VIROL. **77**:5401-5414.

49. DOMITROVICH, A. M., K. W. DIEBEL, N. ALI, S. SARKER, AND A. SIDDIQUI. 2005. ROLE OF LA AUTOANTIGEN AND POLYPYRIMIDINE TRACT-BINDING PROTEIN IN HCV REPLICATION. VIROLOGY **335**:72-86.

50. DUBUISSON, J., F. PENIN, AND D. MORADPOUR. 2002. INTERACTION OF HEPATITIS C VIRUS PROTEINS WITH HOST CELL MEMBRANES AND LIPIDS. TRENDS CELL BIOL. **12**:517-523.

51. EGGER, D., B. WOLK, R. GOSERT, L. BIANCHI, H. E. BLUM, D. MORADPOUR, AND K. BIENZ. 2002. EXPRESSION OF HEPATITIS C VIRUS PROTEINS INDUCES DISTINCT MEMBRANE ALTERATIONS INCLUDING A CANDIDATE VIRAL REPLICATION COMPLEX. J. VIROL. **76**:5974-5984.

52. EL HAGE, N. AND G. LUO. 2003. REPLICATION OF HEPATITIS C VIRUS RNA OCCURS IN A MEMBRANE-BOUND REPLICATION COMPLEX CONTAINING NONSTRUCTURAL VIRAL PROTEINS AND RNA. J. GEN. VIROL. **84**:2761-2769.

53. ELAZAR, M., K. H. CHEONG, P. LIU, H. B. GREENBERG, C. M. RICE, AND J. S. GLENN. 2003. AMPHIPATHIC HELIX-DEPENDENT LOCALIZATION OF NS5A MEDIATES HEPATITIS C VIRUS RNA REPLICATION. J. VIROL. **77**:6055-6061.

54. ELAZAR, M., P. LIU, C. M. RICE, AND J. S. GLENN. 2004. AN N-TERMINAL AMPHIPATHIC HELIX IN HEPATITIS C VIRUS (HCV) NS4B MEDIATES MEMBRANE ASSOCIATION, CORRECT LOCALIZATION OF REPLICATION COMPLEX PROTEINS, AND HCV RNA REPLICATION. J. VIROL. **78**:11393-11400.

55. EMANS, N., J. P. GORVEL, C. WALTER, V. GERKE, R. KELLNER, G. GRIFFITHS, AND J. GRUENBERG. 1993. ANNEXIN II IS A MAJOR COMPONENT OF FUSOGENIC ENDOSOMAL VESICLES. J. CELL BIOL. **120**:1357-1369.

56. EVANS, M. J., C. M. RICE, AND S. P. GOFF. 2004. PHOSPHORYLATION OF HEPATITIS C VIRUS NONSTRUCTURAL PROTEIN 5A MODULATES ITS PROTEIN INTERACTIONS AND VIRAL RNA REPLICATION. PROC. NATL. ACAD. SCI. U. S. A **101**:13038-13043.

57. EVANS, M. J., T. VON HAHN, D. M. TSCHERNE, A. J. SYDER, M. PANIS, B. WOLK, T. HATZIIOANNOU, J. A. MCKEATING, P. D. BIENIASZ, AND C. M. RICE. 2007. CLAUDIN-1 IS A HEPATITIS C VIRUS CO-RECEPTOR REQUIRED FOR A LATE STEP IN ENTRY. NATURE **446**:801-805.

58. FAILLA, C., L. TOMEI, AND R. DE FRANCESCO. 1994. BOTH NS3 AND NS4A ARE REQUIRED FOR PROTEOLYTIC PROCESSING OF HEPATITIS C VIRUS NONSTRUCTURAL PROTEINS. J. VIROL. **68**:3753-3760.

59. FEINSTONE, S. M., A. Z. KAPIKIAN, R. H. PURCELL, H. J. ALTER, AND P. V. HOLLAND. 2001. TRANSFUSION-ASSOCIATED HEPATITIS NOT DUE TO VIRAL HEPATITIS TYPE A OR B. 1975. REV. MED. VIROL. **11**:3-8.

60. FERLENGHI, I., M. CLARKE, T. RUTTAN, S. L. ALLISON, J. SCHALICH, F. X. HEINZ, S. C. HARRISON, F. A. REY, AND S. D. FULLER. 2001. MOLECULAR ORGANIZATION OF A RECOMBINANT SUBVIRAL PARTICLE FROM TICK-BORNE ENCEPHALITIS VIRUS. MOL. CELL **7**:593-602.

61. FILIPENKO, N. R., T. J. MACLEOD, C. S. YOON, AND D. M. WAISMAN. 2004. ANNEXIN A2 IS A NOVEL RNA-BINDING PROTEIN. J. BIOL. CHEM. **279**:8723-8731.

62. FORTON, D. M., P. KARAYIANNIS, N. MAHMUD, S. D. TAYLOR-ROBINSON, AND H. C. THOMAS. 2004. IDENTIFICATION OF UNIQUE HEPATITIS C VIRUS QUASISPECIES IN THE CENTRAL NERVOUS SYSTEM AND COMPARATIVE ANALYSIS OF INTERNAL TRANSLATIONAL EFFICIENCY OF BRAIN, LIVER, AND SERUM VARIANTS. J. VIROL. **78**:5170-5183.

63. FOY, E., K. LI, C. WANG, R. SUMPTER, JR., M. IKEDA, S. M. LEMON, AND M. GALE, JR. 2003. REGULATION OF INTERFERON REGULATORY FACTOR-3 BY THE HEPATITIS C VIRUS SERINE PROTEASE. SCIENCE **300**:1145-1148.

64. FREEMAN, A. J., G. J. DORE, M. G. LAW, M. THORPE, J. VON OVERBECK, A. R. LLOYD, G. MARINOS, AND J. M. KALDOR. 2001. ESTIMATING PROGRESSION TO CIRRHOSIS IN CHRONIC HEPATITIS C VIRUS INFECTION. HEPATOLOGY **34**:809-816.

65. FRESE, M., K. BARTH, A. KAUL, V. LOHMANN, V. SCHWARZLE, AND R. BARTENSCHLAGER. 2003. HEPATITIS C VIRUS RNA REPLICATION IS RESISTANT TO TUMOUR NECROSIS FACTOR-ALPHA. J. GEN. VIROL. **84**:1253-1259.

66. FRESE, M., V. SCHWARZLE, K. BARTH, N. KRIEGER, V. LOHMANN, S. MIHM, O. HALLER, AND R. BARTENSCHLAGER. 2002. INTERFERON-GAMMA INHIBITS REPLICATION OF SUBGENOMIC AND GENOMIC HEPATITIS C VIRUS RNAS. HEPATOLOGY **35**:694-703.

67. FRIEBE, P. AND R. BARTENSCHLAGER. 2002. GENETIC ANALYSIS OF SEQUENCES IN THE 3' NONTRANSLATED REGION OF HEPATITIS C VIRUS THAT ARE IMPORTANT FOR RNA REPLICATION. J. VIROL. **76**:5326-5338.

68. FRIEBE, P., J. BOUDET, J. P. SIMORRE, AND R. BARTENSCHLAGER. 2005. KISSING-LOOP INTERACTION IN THE 3' END OF THE HEPATITIS C VIRUS GENOME ESSENTIAL FOR RNA REPLICATION. J. VIROL. **79**:380-392.

69. FRIEBE, P., V. LOHMANN, N. KRIEGER, AND R. BARTENSCHLAGER. 2001. SEQUENCES IN THE 5' NONTRANSLATED REGION OF HEPATITIS C VIRUS REQUIRED FOR RNA REPLICATION. J. VIROL. **75**:12047-12057.

70. FULLER, S. D. 1987. THE T=4 ENVELOPE OF SINDBIS VIRUS IS ORGANIZED BY INTERACTIONS WITH A COMPLEMENTARY T=3 CAPSID. CELL **48**:923-934.

71. GAO, L., H. AIZAKI, J. W. HE, AND M. M. LAI. 2004. INTERACTIONS BETWEEN VIRAL NONSTRUCTURAL PROTEINS AND HOST PROTEIN hVAP-33 MEDIATE THE FORMATION OF HEPATITIS C VIRUS RNA REPLICATION COMPLEX ON LIPID RAFT. J. VIROL. **78**:3480-3488.

72. GAO, Z. H., J. METHERALL, AND D. M. VIRSHUP. 2000. IDENTIFICATION OF CASEIN KINASE I SUBSTRATES BY IN VITRO EXPRESSION CLONING SCREENING. BIOCHEM. BIOPHYS. RES. COMMUN. **268**:562-566.

73. GERKE, V., C. E. CREUTZ, AND S. E. MOSS. 2005. ANNEXINS: LINKING Ca^{2+} SIGNALLING TO MEMBRANE DYNAMICS. NAT. REV. MOL. CELL BIOL. **6**:449-461.

74. GOSERT, R., D. EGGER, V. LOHMANN, R. BARTENSCHLAGER, H. E. BLUM, K. BIENZ, AND D. MORADPOUR. 2003. IDENTIFICATION OF THE HEPATITIS C VIRUS RNA REPLICATION COMPLEX IN HUH-7 CELLS HARBORING SUBGENOMIC REPLICONS. J. VIROL. **77**:5487-5492.

75. GOSERT, R., A. KANJANAHALUETHAI, D. EGGER, K. BIENZ, AND S. C. BAKER. 2002. RNA REPLICATION OF MOUSE HEPATITIS VIRUS TAKES PLACE AT DOUBLE-MEMBRANE VESICLES. J. VIROL. **76**:3697-3708.

76. GRAKOUI, A., D. W. McCOURT, C. WYCHOWSKI, S. M. FEINSTONE, AND C. M. RICE. 1993. A SECOND HEPATITIS C VIRUS-ENCODED PROTEINASE. PROC. NATL. ACAD. SCI. U. S. A **90**:10583-10587.

77. GRAKOUI, A., C. WYCHOWSKI, C. LIN, S. M. FEINSTONE, AND C. M. RICE. 1993. EXPRESSION AND IDENTIFICATION OF HEPATITIS C VIRUS POLYPROTEIN CLEAVAGE PRODUCTS. J. VIROL. **67**:1385-1395.

78. GRIFFIN, S. D., L. P. BEALES, D. S. CLARKE, O. WORSFOLD, S. D. EVANS, J. JAEGER, M. P. HARRIS, AND D. J. ROWLANDS. 2003. THE P7 PROTEIN OF HEPATITIS C VIRUS FORMS AN ION CHANNEL THAT IS BLOCKED BY THE ANTIVIRAL DRUG, AMANTADINE. FEBS LETT. **535**:34-38.

79. GRUENBERG, J. AND H. STENMARK. 2004. THE BIOGENESIS OF MULTIVESICULAR ENDOSOMES. NAT. REV. MOL. CELL BIOL. **5**:317-323.

80. GUNJI, T., N. KATO, M. HIJIKATA, K. HAYASHI, S. SAITOH, AND K. SHIMOTOHNO. 1994. SPECIFIC DETECTION OF POSITIVE AND NEGATIVE STRANDED HEPATITIS C VIRAL RNA USING CHEMICAL RNA MODIFICATION. ARCH. VIROL. **134**:293-302.

81. GUO, J. T., V. V. BICHKO, AND C. SEEGER. 2001. EFFECT OF ALPHA INTERFERON ON THE HEPATITIS C VIRUS REPLICON. J. VIROL. **75**:8516-8523.

82. HAHM, B., Y. K. KIM, J. H. KIM, T. Y. KIM, AND S. K. JANG. 1998. HETEROGENEOUS NUCLEAR RIBONUCLEOPROTEIN L INTERACTS WITH THE 3' BORDER OF THE INTERNAL RIBOSOMAL ENTRY SITE OF HEPATITIS C VIRUS. J. VIROL. **72**:8782-8788.

83. HAMAMOTO, I., Y. NISHIMURA, T. OKAMOTO, H. AIZAKI, M. LIU, Y. MORI, T. ABE, T. SUZUKI, M. M. LAI, T. MIYAMURA, K. MORIISHI, AND Y. MATSUURA. 2005. HUMAN VAP-B IS INVOLVED IN HEPATITIS C VIRUS REPLICATION THROUGH INTERACTION WITH NS5A AND NS5B. J. VIROL. **79**:13473-13482.

84. HAN, D. S., B. HAHM, H. M. RHO, AND S. K. JANG. 1995. IDENTIFICATION OF THE PROTEASE DOMAIN IN NS3 OF HEPATITIS C VIRUS. J. GEN. VIROL. **76 (PT 4)**:985-993.

85. HARDER, T. AND V. GERKE. 1993. THE SUBCELLULAR DISTRIBUTION OF EARLY ENDOSOMES IS AFFECTED BY THE ANNEXIN II2P11(2) COMPLEX. J. CELL BIOL. **123**:1119-1132.

86. HARDY, R. W., J. MARCOTRIGIANO, K. J. BLIGHT, J. E. MAJORS, AND C. M. RICE. 2003. HEPATITIS C VIRUS RNA SYNTHESIS IN A CELL-FREE SYSTEM ISOLATED FROM REPLICON-CONTAINING HEPATOMA CELLS. J. VIROL. **77**:2029-2037.

87. HARRIS, D., Z. ZHANG, B. CHAUBEY, AND V. N. PANDEY. 2006. IDENTIFICATION OF CELLULAR FACTORS ASSOCIATED WITH THE 3'-NONTRANSLATED REGION OF THE HEPATITIS C VIRUS GENOME. MOL. CELL PROTEOMICS. **5**:1006-1018.

88. HAWKINS, T. E., J. ROES, D. REES, J. MONKHOUSE, AND S. E. MOSS. 1999. IMMUNOLOGICAL DEVELOPMENT AND CARDIOVASCULAR FUNCTION ARE NORMAL IN ANNEXIN VI NULL MUTANT MICE. MOL. CELL BIOL. **19**:8028-8032.

89. HAYES, M. J., C. J. MERRIFIELD, D. SHAO, J. AYALA-SANMARTIN, C. D. SCHOREY, T. P. LEVINE, J. PROUST, J. CURRAN, M. BAILLY, AND S. E. MOSS. 2004. ANNEXIN 2 BINDING TO PHOSPHATIDYLINOSITOL 4,5-BISPHOSPHATE ON ENDOCYTIC VESICLES IS REGULATED BY THE STRESS RESPONSE PATHWAY. J. BIOL. CHEM. **279**:14157-14164.

90. HIJIKATA, M., H. MIZUSHIMA, T. AKAGI, S. MORI, N. KAKIUCHI, N. KATO, T. TANAKA, K. KIMURA, AND K. SHIMOTOHNO. 1993. TWO DISTINCT PROTEINASE ACTIVITIES REQUIRED FOR THE PROCESSING OF A PUTATIVE NONSTRUCTURAL PRECURSOR PROTEIN OF HEPATITIS C VIRUS. J. VIROL. **67**:4665-4675.

91. HIJIKATA, M., H. MIZUSHIMA, Y. TANJI, Y. KOMODA, Y. HIROWATARI, T. AKAGI, N. KATO, K. KIMURA, AND K. SHIMOTOHNO. 1993. PROTEOLYTIC PROCESSING AND MEMBRANE ASSOCIATION OF PUTATIVE NONSTRUCTURAL PROTEINS OF HEPATITIS C VIRUS. PROC. NATL. ACAD. SCI. U. S. A **90**:10773-10777.

92. HO, S. N., H. D. HUNT, R. M. HORTON, J. K. PULLEN, AND L. R. PEASE. 1989. SITE-DIRECTED MUTAGENESIS BY OVERLAP EXTENSION USING THE POLYMERASE CHAIN REACTION. GENE **77**:51-59.

93. HOOFNAGLE, J. H. 2002. COURSE AND OUTCOME OF HEPATITIS C. HEPATOLOGY **36**:S21-S29.

94. HOUSHMAND, H. AND A. BERGQVIST. 2003. INTERACTION OF HEPATITIS C VIRUS NS5A WITH LA PROTEIN REVEALED BY T7 PHAGE DISPLAY. BIOCHEM. BIOPHYS. RES. COMMUN. **309**:695-701.

95. HSU, M., J. ZHANG, M. FLINT, C. LOGVINOFF, C. CHENG-MAYER, C. M. RICE, AND J. A. MCKEATING. 2003. HEPATITIS C VIRUS GLYCOPROTEINS MEDIATE PH-DEPENDENT CELL ENTRY OF PSEUDOTYPED RETROVIRAL PARTICLES. PROC. NATL. ACAD. SCI. U. S. A **100**:7271-7276.

96. HUANG, H., F. SUN, D. M. OWEN, W. LI, Y. CHEN, M. GALE, JR., AND J. YE. 2007. HEPATITIS C VIRUS PRODUCTION BY HUMAN HEPATOCYTES DEPENDENT ON ASSEMBLY AND SECRETION OF VERY LOW-DENSITY LIPOPROTEINS. PROC. NATL. ACAD. SCI. U. S. A **104**:5848-5853.

97. HUANG, L., J. HWANG, S. D. SHARMA, M. R. HARGITTAI, Y. CHEN, J. J. ARNOLD, K. D. RANEY, AND C. E. CAMERON. 2005. HEPATITIS C VIRUS NONSTRUCTURAL PROTEIN 5A (NS5A) IS AN RNA-BINDING PROTEIN. J. BIOL. CHEM. **280**:36417-36428.

98. HUGLE, T., F. FEHRMANN, E. BIECK, M. KOHARA, H. G. KRAUSSLICH, C. M. RICE, H. E. BLUM, AND D. MORADPOUR. 2001. THE HEPATITIS C VIRUS NONSTRUCTURAL PROTEIN 4B IS AN INTEGRAL ENDOPLASMIC RETICULUM MEMBRANE PROTEIN. VIROLOGY **284**:70-81.

99. IKEDA, M., M. YI, K. LI, AND S. M. LEMON. 2002. SELECTABLE SUBGENOMIC AND GENOME-LENGTH DICISTRONIC RNAS DERIVED FROM AN INFECTIOUS MOLECULAR CLONE OF THE HCV-N STRAIN OF HEPATITIS C VIRUS REPLICATE EFFICIENTLY IN CULTURED HUH7 CELLS. J. VIROL. **76**:2997-3006.

100. ISHIDO, S., T. FUJITA, AND H. HOTTA. 1998. COMPLEX FORMATION OF NS5B WITH NS3 AND NS4A PROTEINS OF HEPATITIS C VIRUS. BIOCHEM. BIOPHYS. RES. COMMUN. **244**:35-40.

101. IVASHKINA, N., B. WOLK, V. LOHMANN, R. BARTENSCHLAGER, H. E. BLUM, F. PENIN, AND D. MORADPOUR. 2002. THE HEPATITIS C VIRUS RNA-DEPENDENT RNA POLYMERASE MEMBRANE INSERTION SEQUENCE IS A TRANSMEMBRANE SEGMENT. J. VIROL. **76**:13088-13093.

102. JOHNSSON, N., G. MARRIOTT, AND K. WEBER. 1988. P36, THE MAJOR CYTOPLASMIC SUBSTRATE OF SRC TYROSINE PROTEIN KINASE, BINDS TO ITS P11 REGULATORY SUBUNIT VIA A SHORT AMINO-TERMINAL AMPHIPHATIC HELIX. EMBO J. **7**:2435-2442.

103. JOHNSTONE, S. A., I. HUBAISHY, AND D. M. WAISMAN. 1992. PHOSPHORYLATION OF ANNEXIN II TETRAMER BY PROTEIN KINASE C INHIBITS AGGREGATION OF LIPID VESICLES BY THE PROTEIN. J. BIOL. CHEM. **267**:25976-25981.

104. JONES, C. T., C. L. MURRAY, D. K. EASTMAN, J. TASSELLO, AND C. M. RICE. 2007. HEPATITIS C VIRUS P7 AND NS2 PROTEINS ARE ESSENTIAL FOR INFECTIOUS VIRUS PRODUCTION. J. VIROL.

105. KALAJZIC, I., M. L. STOVER, P. LIU, Z. KALAJZIC, D. W. ROWE, AND A. C. LICHTLER. 2001. USE OF VSV-G PSEUDOTYPED RETROVIRAL VECTORS TO TARGET MURINE OSTEOPROGENITOR CELLS. VIROLOGY **284**:37-45.

106. KANEKO, T., Y. TANJI, S. SATOH, M. HIJIKATA, S. ASABE, K. KIMURA, AND K. SHIMOTOHNO. 1994. PRODUCTION OF TWO PHOSPHOPROTEINS FROM THE NS5A REGION OF THE HEPATITIS C VIRAL GENOME. BIOCHEM. BIOPHYS. RES. COMMUN. **205**:320-326.

107. KATO, T., T. DATE, M. MIYAMOTO, A. FURUSAKA, K. TOKUSHIGE, M. MIZOKAMI, AND T. WAKITA. 2003. EFFICIENT REPLICATION OF THE GENOTYPE 2A HEPATITIS C VIRUS SUBGENOMIC REPLICON. GASTROENTEROLOGY **125**:1808-1817.

108. KIM, D. W., Y. GWACK, J. H. HAN, AND J. CHOE. 1995. C-TERMINAL DOMAIN OF THE HEPATITIS C VIRUS NS3 PROTEIN CONTAINS AN RNA HELICASE ACTIVITY. BIOCHEM. BIOPHYS. RES. COMMUN. **215**:160-166.

109. KIM, J. AND K. A. HAJJAR. 2002. ANNEXIN II: A PLASMINOGEN-PLASMINOGEN ACTIVATOR CO-RECEPTOR. FRONT BIOSCI. **7**:D341-D348.

110. KIM, J. E., W. K. SONG, K. M. CHUNG, S. H. BACK, AND S. K. JANG. 1999. SUBCELLULAR LOCALIZATION OF HEPATITIS C VIRAL PROTEINS IN MAMMALIAN CELLS. ARCH. VIROL. **144**:329-343.

111. KIM, J. H., K. Y. PAEK, S. H. HA, S. CHO, K. CHOI, C. S. KIM, S. H. RYU, AND S. K. JANG. 2004. A CELLULAR RNA-BINDING PROTEIN ENHANCES INTERNAL RIBOSOMAL ENTRY SITE-DEPENDENT TRANSLATION THROUGH AN INTERACTION DOWNSTREAM OF THE HEPATITIS C VIRUS POLYPROTEIN INITIATION CODON. MOL. CELL BIOL. **24**:7878-7890.

112. KIM, Y. K., C. S. KIM, S. H. LEE, AND S. K. JANG. 2002. DOMAINS I AND II IN THE 5' NONTRANSLATED REGION OF THE HCV GENOME ARE REQUIRED FOR RNA REPLICATION. BIOCHEM. BIOPHYS. RES. COMMUN. **290**:105-112.

113. KOCH, J. O. AND R. BARTENSCHLAGER. 1999. MODULATION OF HEPATITIS C VIRUS NS5A HYPERPHOSPHORYLATION BY NONSTRUCTURAL PROTEINS NS3, NS4A, AND NS4B. J. VIROL. **73**:7138-7146.

114. KOLYKHALOV, A. A., E. V. AGAPOV, AND C. M. RICE. 1994. SPECIFICITY OF THE HEPATITIS C VIRUS NS3 SERINE PROTEASE: EFFECTS OF SUBSTITUTIONS AT THE 3/4A, 4A/4B, 4B/5A, AND 5A/5B CLEAVAGE SITES ON POLYPROTEIN PROCESSING. J. VIROL. **68**:7525-7533.

115. KOLYKHALOV, A. A., S. M. FEINSTONE, AND C. M. RICE. 1996. IDENTIFICATION OF A HIGHLY CONSERVED SEQUENCE ELEMENT AT THE 3' TERMINUS OF HEPATITIS C VIRUS GENOME RNA. J. VIROL. **70**:3363-3371.

116. KOLYKHALOV, A. A., K. MIHALIK, S. M. FEINSTONE, AND C. M. RICE. 2000. HEPATITIS C VIRUS-ENCODED ENZYMATIC ACTIVITIES AND CONSERVED RNA ELEMENTS IN THE 3' NONTRANSLATED REGION ARE ESSENTIAL FOR VIRUS REPLICATION IN VIVO. J. VIROL. **74**:2046-2051.

117. KOPEK, B. G., G. PERKINS, D. J. MILLER, M. H. ELLISMAN, AND P. AHLQUIST. 2007. THREE-DIMENSIONAL ANALYSIS OF A VIRAL RNA REPLICATION COMPLEX REVEALS A VIRUS-INDUCED MINI-ORGANELLE. PLOS. BIOL. **5**:E220.

118. KOUTSOUDAKIS, G., E. HERRMANN, S. KALLIS, R. BARTENSCHLAGER, AND T. PIETSCHMANN. 2007. THE LEVEL OF CD81 CELL SURFACE EXPRESSION IS A KEY DETERMINANT FOR PRODUCTIVE ENTRY OF HEPATITIS C VIRUS INTO HOST CELLS. J. VIROL. **81**:588-598.

119. KOUTSOUDAKIS, G., A. KAUL, E. STEINMANN, S. KALLIS, V. LOHMANN, T. PIETSCHMANN, AND R. BARTENSCHLAGER. 2006. CHARACTERIZATION OF THE EARLY STEPS OF HEPATITIS C VIRUS INFECTION BY USING LUCIFERASE REPORTER VIRUSES. J. VIROL. **80**:5308-5320.

120. KRIEGER, N., V. LOHMANN, AND R. BARTENSCHLAGER. 2001. ENHANCEMENT OF HEPATITIS C VIRUS RNA REPLICATION BY CELL CULTURE-ADAPTIVE MUTATIONS. J. VIROL. **75**:4614-4624.

121. KRONKE, J., R. KITTLER, F. BUCHHOLZ, M. P. WINDISCH, T. PIETSCHMANN, R. BARTENSCHLAGER, AND M. FRESE. 2004. ALTERNATIVE APPROACHES FOR EFFICIENT INHIBITION OF HEPATITIS C VIRUS RNA REPLICATION BY SMALL INTERFERING RNAS. J. VIROL. **78**:3436-3446.

122. KUHN, R. J., W. ZHANG, M. G. ROSSMANN, S. V. PLETNEV, J. CORVER, E. LENCHES, C. T. JONES, S. MUKHOPADHYAY, P. R. CHIPMAN, E. G. STRAUSS, T. S. BAKER, AND J. H. STRAUSS. 2002. STRUCTURE OF DENGUE VIRUS: IMPLICATIONS FOR FLAVIVIRUS ORGANIZATION, MATURATION, AND FUSION. CELL **108**:717-725.

123. KUJALA, P., A. IKAHEIMONEN, N. EHSANI, H. VIHINEN, P. AUVINEN, AND L. KAARIAINEN. 2001. BIOGENESIS OF THE SEMLIKI FOREST VIRUS RNA REPLICATION COMPLEX. J. VIROL. **75**:3873-3884.

124. KWONG, A. D., J. L. KIM, AND C. LIN. 2000. STRUCTURE AND FUNCTION OF HEPATITIS C VIRUS NS3 HELICASE. CURR. TOP. MICROBIOL. IMMUNOL. **242**:171-196.

125. LAI, V. C., S. DEMPSEY, J. Y. LAU, Z. HONG, AND W. ZHONG. 2003. IN VITRO RNA REPLICATION DIRECTED BY REPLICASE COMPLEXES ISOLATED FROM THE SUBGENOMIC REPLICON CELLS OF HEPATITIS C VIRUS. J. VIROL. **77**:2295-2300.

126. LAMBERT, O., V. GERKE, M. F. BADER, F. PORTE, AND A. BRISSON. 1997. STRUCTURAL ANALYSIS OF JUNCTIONS FORMED BETWEEN LIPID MEMBRANES AND SEVERAL ANNEXINS BY CRYO-ELECTRON MICROSCOPY. J. MOL. BIOL. **272**:42-55.

127. LANFORD, R. E., C. SUREAU, J. R. JACOB, R. WHITE, AND T. R. FUERST. 1994. DEMONSTRATION OF IN VITRO INFECTION OF CHIMPANZEE HEPATOCYTES WITH HEPATITIS C VIRUS USING STRAND-SPECIFIC RT/PCR. VIROLOGY **202**:606-614.

128. LEVEQUE, V. J., R. B. JOHNSON, S. PARSONS, J. REN, C. XIE, F. ZHANG, AND Q. M. WANG. 2003. IDENTIFICATION OF A C-TERMINAL REGULATORY MOTIF IN HEPATITIS C VIRUS RNA-DEPENDENT RNA POLYMERASE: STRUCTURAL AND BIOCHEMICAL ANALYSIS. J. VIROL. **77**:9020-9028.

129. LI, G. P. AND C. M. RICE. 1989. MUTAGENESIS OF THE IN-FRAME OPAL TERMINATION CODON PRECEDING NSP4 OF SINDBIS VIRUS: STUDIES OF TRANSLATIONAL READTHROUGH AND ITS EFFECT ON VIRUS REPLICATION. J. VIROL. **63**:1326-1337.

130. LIN, C., B. D. LINDENBACH, B. M. PRAGAI, D. W. MCCOURT, AND C. M. RICE. 1994. PROCESSING IN THE HEPATITIS C VIRUS E2-NS2 REGION: IDENTIFICATION OF P7 AND TWO DISTINCT E2-SPECIFIC PRODUCTS WITH DIFFERENT C TERMINI. J. VIROL. **68**:5063-5073.

131. LIN, C., B. M. PRAGAI, A. GRAKOUI, J. XU, AND C. M. RICE. 1994. HEPATITIS C VIRUS NS3 SERINE PROTEINASE: TRANS-CLEAVAGE REQUIREMENTS AND PROCESSING KINETICS. J. VIROL. **68**:8147-8157.

132. LIN, C., J. W. WU, K. HSIAO, AND M. S. SU. 1997. THE HEPATITIS C VIRUS NS4A PROTEIN: INTERACTIONS WITH THE NS4B AND NS5A PROTEINS. J. VIROL. **71**:6465-6471.

133. LINDENBACH, B. D., M. J. EVANS, A. J. SYDER, B. WOLK, T. L. TELLINGHUISEN, C. C. LIU, T. MARUYAMA, R. O. HYNES, D. R. BURTON, J. A. MCKEATING, AND C. M. RICE. 2005. COMPLETE REPLICATION OF HEPATITIS C VIRUS IN CELL CULTURE. SCIENCE **309**:623-626.

134. LINDENBACH, B. D., P. MEULEMAN, A. PLOSS, T. VANWOLLEGHEM, A. J. SYDER, J. A. MCKEATING, R. E. LANFORD, S. M. FEINSTONE, M. E. MAJOR, G. LEROUX-ROELS, AND C. M. RICE. 2006. CELL CULTURE-GROWN HEPATITIS C VIRUS IS INFECTIOUS IN VIVO AND CAN BE RECULTURED IN VITRO. PROC. NATL. ACAD. SCI. U. S. A **103**:3805-3809.

135. LINDENBACH, B. D. AND C. M. RICE. 2005. UNRAVELLING HEPATITIS C VIRUS REPLICATION FROM GENOME TO FUNCTION. NATURE **436**:933-938.

136. LING, Q., A. T. JACOVINA, A. DEORA, M. FEBBRAIO, R. SIMANTOV, R. L. SILVERSTEIN, B. HEMPSTEAD, W. H. MARK, AND K. A. HAJJAR. 2004. ANNEXIN II REGULATES FIBRIN HOMEOSTASIS AND NEOANGIOGENESIS IN VIVO. J. CLIN. INVEST **113**:38-48.

137. LO, S. Y., M. J. SELBY, AND J. H. OU. 1996. INTERACTION BETWEEN HEPATITIS C VIRUS CORE PROTEIN AND E1 ENVELOPE PROTEIN. J. VIROL. **70**:5177-5182.

138. LOHMANN, V., S. HOFFMANN, U. HERIAN, F. PENIN, AND R. BARTENSCHLAGER. 2003. VIRAL AND CELLULAR DETERMINANTS OF HEPATITIS C VIRUS RNA REPLICATION IN CELL CULTURE. J. VIROL. **77**:3007-3019.

139. LOHMANN, V., F. KORNER, A. DOBIERZEWSKA, AND R. BARTENSCHLAGER. 2001. MUTATIONS IN HEPATITIS C VIRUS RNAS CONFERRING CELL CULTURE ADAPTATION. J. VIROL. **75**:1437-1449.

140. LOHMANN, V., F. KORNER, J. KOCH, U. HERIAN, L. THEILMANN, AND R. BARTENSCHLAGER. 1999. REPLICATION OF SUBGENOMIC HEPATITIS C VIRUS RNAS IN A HEPATOMA CELL LINE. SCIENCE **285**:110-113.

141. LOHMANN, V., A. ROOS, F. KORNER, J. O. KOCH, AND R. BARTENSCHLAGER. 1998. BIOCHEMICAL AND KINETIC ANALYSES OF NS5B RNA-DEPENDENT RNA POLYMERASE OF THE HEPATITIS C VIRUS. VIROLOGY **249**:108-118.

142. LORENZ, I. C., J. MARCOTRIGIANO, T. G. DENTZER, AND C. M. RICE. 2006. STRUCTURE OF THE CATALYTIC DOMAIN OF THE HEPATITIS C VIRUS NS2-3 PROTEASE. NATURE **442**:831-835.

143. LU, H., W. LI, W. S. NOBLE, D. PAYAN, AND D. C. ANDERSON. 2004. RIBOPROTEOMICS OF THE HEPATITIS C VIRUS INTERNAL RIBOSOMAL ENTRY SITE. J. PROTEOME. RES. **3**:949-957.

144. LUNDIN, M., M. MONNE, A. WIDELL, G. VON HEIJNE, AND M. A. PERSSON. 2003. TOPOLOGY OF THE MEMBRANE-ASSOCIATED HEPATITIS C VIRUS PROTEIN NS4B. J. VIROL. **77**:5428-5438.

145. LUO, G., R. K. HAMATAKE, D. M. MATHIS, J. RACELA, K. L. RIGAT, J. LEMM, AND R. J. COLONNO. 2000. DE NOVO INITIATION OF RNA SYNTHESIS BY THE RNA-DEPENDENT RNA POLYMERASE (NS5B) OF HEPATITIS C VIRUS. J. VIROL. **74**:851-863.

146. LYLE, J. M., E. BULLITT, K. BIENZ, AND K. KIRKEGAARD. 2002. VISUALIZATION AND FUNCTIONAL ANALYSIS OF RNA-DEPENDENT RNA POLYMERASE LATTICES. SCIENCE **296**:2218-2222.

147. MA, H. C., C. H. KE, T. Y. HSIEH, AND S. Y. LO. 2002. THE FIRST HYDROPHOBIC DOMAIN OF THE HEPATITIS C VIRUS E1 PROTEIN IS IMPORTANT FOR INTERACTION WITH THE CAPSID PROTEIN. J. GEN. VIROL. **83**:3085-3092.

148. MANNOVA, P., R. FANG, H. WANG, B. DENG, M. W. MCINTOSH, S. M. HANASH, AND L. BERETTA. 2006. MODIFICATION OF HOST LIPID RAFT PROTEOME UPON HEPATITIS C VIRUS REPLICATION. MOL. CELL PROTEOMICS. **5**:2319-2325.

149. MASUMI, A., H. AIZAKI, T. SUZUKI, J. B. DUHADAWAY, G. C. PRENDERGAST, K. KOMURO, AND H. FUKAZAWA. 2005. REDUCTION OF HEPATITIS C VIRUS NS5A PHOSPHORYLATION THROUGH ITS INTERACTION WITH AMPHIPHYSIN II. BIOCHEM. BIOPHYS. RES. COMMUN. **336**:572-578.

150. MCKERCHER, G., P. L. BEAULIEU, D. LAMARRE, S. LAPLANTE, S. LEFEBVRE, C. PELLERIN, L. THAUVETTE, AND G. KUKOLJ. 2004. SPECIFIC INHIBITORS OF HCV POLYMERASE IDENTIFIED USING AN NS5B WITH LOWER AFFINITY FOR TEMPLATE/PRIMER SUBSTRATE. NUCLEIC ACIDS RES. **32**:422-431.

151. MCLAUCHLAN, J. 2000. PROPERTIES OF THE HEPATITIS C VIRUS CORE PROTEIN: A STRUCTURAL PROTEIN THAT MODULATES CELLULAR PROCESSES. J. VIRAL HEPAT. **7**:2-14.

152. MIGLIACCIO, G., J. E. TOMASSINI, S. S. CARROLL, L. TOMEI, S. ALTAMURA, B. BHAT, L. BARTHOLOMEW, M. R. BOSSERMAN, A. CECCACCI, L. F. COLWELL, R. CORTESE, R. DE FRANCESCO, A. B. ELDRUP, K. L. GETTY, X. S. HOU, R. L. LAFEMINA, S. W. LUDMERER, M. MACCOSS, D. R. MCMASTERS, M. W. STAHLHUT, D. B. OLSEN, D. J. HAZUDA, AND O. A. FLORES. 2003. CHARACTERIZATION OF RESISTANCE TO NON-OBLIGATE CHAIN-TERMINATING RIBONUCLEOSIDE ANALOGS THAT INHIBIT HEPATITIS C VIRUS REPLICATION IN VITRO. J. BIOL. CHEM. **278**:49164-49170.

153. MIYANARI, Y., M. HIJIKATA, M. YAMAJI, M. HOSAKA, H. TAKAHASHI, AND K. SHIMOTOHNO. 2003. HEPATITIS C VIRUS NON-STRUCTURAL PROTEINS IN THE PROBABLE MEMBRANOUS COMPARTMENT FUNCTION IN VIRAL GENOME REPLICATION. J. BIOL. CHEM. **278**:50301-50308.

154. MORADPOUR, D., E. BIECK, T. HUGLE, W. WELS, J. Z. WU, Z. HONG, H. E. BLUM, AND R. BARTENSCHLAGER. 2002. FUNCTIONAL PROPERTIES OF A MONOCLONAL ANTIBODY INHIBITING THE HEPATITIS C VIRUS RNA-DEPENDENT RNA POLYMERASE. J. BIOL. CHEM. **277**:593-601.

155. MORADPOUR, D., V. BRASS, E. BIECK, P. FRIEBE, R. GOSERT, H. E. BLUM, R. BARTENSCHLAGER, F. PENIN, AND V. LOHMANN. 2004. MEMBRANE ASSOCIATION OF THE RNA-DEPENDENT RNA POLYMERASE IS ESSENTIAL FOR HEPATITIS C VIRUS RNA REPLICATION. J. VIROL. **78**:13278-13284.

156. MORADPOUR, D., M. J. EVANS, R. GOSERT, Z. YUAN, H. E. BLUM, S. P. GOFF, B. D. LINDENBACH, AND C. M. RICE. 2004. INSERTION OF GREEN FLUORESCENT PROTEIN INTO NONSTRUCTURAL PROTEIN 5A ALLOWS DIRECT VISUALIZATION OF FUNCTIONAL HEPATITIS C VIRUS REPLICATION COMPLEXES. J. VIROL. **78**:7400-7409.

157. MORADPOUR, D., T. WAKITA, K. TOKUSHIGE, R. I. CARLSON, K. KRAWCZYNSKI, AND J. R. WANDS. 1996. CHARACTERIZATION OF THREE NOVEL MONOCLONAL ANTIBODIES AGAINST HEPATITIS C VIRUS CORE PROTEIN. J. MED. VIROL. **48**:234-241.

158. NAKABAYASHI, H., K. TAKETA, K. MIYANO, T. YAMANE, AND J. SATO. 1982. GROWTH OF HUMAN HEPATOMA CELLS LINES WITH DIFFERENTIATED FUNCTIONS IN CHEMICALLY DEFINED MEDIUM. CANCER RES. **42**:3858-3863.

159. NEDDERMANN, P., A. CLEMENTI, AND R. DE FRANCESCO. 1999. HYPERPHOSPHORYLATION OF THE HEPATITIS C VIRUS NS5A PROTEIN REQUIRES AN ACTIVE NS3 PROTEASE, NS4A, NS4B, AND NS5A ENCODED ON THE SAME POLYPROTEIN. J. VIROL. **73**:9984-9991.

160. NEDDERMANN, P., M. QUINTAVALLE, C. DI PIETRO, A. CLEMENTI, M. CERRETANI, S. ALTAMURA, L. BARTHOLOMEW, AND R. DE FRANCESCO. 2004. REDUCTION OF HEPATITIS C VIRUS NS5A HYPERPHOSPHORYLATION BY SELECTIVE INHIBITION OF CELLULAR KINASES ACTIVATES VIRAL RNA REPLICATION IN CELL CULTURE. J. VIROL. **78**:13306-13314.

161. NEUMANN, A. U., N. P. LAM, H. DAHARI, D. R. GRETCH, T. E. WILEY, T. J. LAYDEN, AND A. S. PERELSON. 1998. HEPATITIS C VIRAL DYNAMICS IN VIVO AND THE ANTIVIRAL EFFICACY OF INTERFERON-ALPHA THERAPY. SCIENCE **282**:103-107.

162. OH, J. W., T. ITO, AND M. M. LAI. 1999. A RECOMBINANT HEPATITIS C VIRUS RNA-DEPENDENT RNA POLYMERASE CAPABLE OF COPYING THE FULL-LENGTH VIRAL RNA. J. VIROL. **73**:7694-7702.

163. PALLAORO, M., A. LAHM, G. BIASIOL, M. BRUNETTI, C. NARDELLA, L. ORSATTI, F. BONELLI, S. ORRU, F. NARJES, AND C. STEINKUHLER. 2001. CHARACTERIZATION OF THE HEPATITIS C VIRUS NS2/3 PROCESSING REACTION BY USING A PURIFIED PRECURSOR PROTEIN. J. VIROL. **75**:9939-9946.

164. PAREDES, A. M., D. T. BROWN, R. ROTHNAGEL, W. CHIU, R. J. SCHOEPP, R. E. JOHNSTON, AND B. V. PRASAD. 1993. THREE-DIMENSIONAL STRUCTURE OF A MEMBRANE-CONTAINING VIRUS. PROC. NATL. ACAD. SCI. U. S. A **90**:9095-9099.

165. PATEL, K., A. J. MUIR, AND J. G. MCHUTCHISON. 2006. DIAGNOSIS AND TREATMENT OF CHRONIC HEPATITIS C INFECTION. BMJ **332**:1013-1017.

166. PAUSE, A., G. KUKOLJ, M. BAILEY, M. BRAULT, F. DO, T. HALMOS, L. LAGACE, R. MAURICE, M. MARQUIS, G. MCKERCHER, C. PELLERIN, L. PILOTE, D. THIBEAULT, AND D. LAMARRE. 2003. AN NS3 SERINE PROTEASE INHIBITOR ABROGATES REPLICATION OF SUBGENOMIC HEPATITIS C VIRUS RNA. J. BIOL. CHEM. **278**:20374-20380.

167. PAVLOVIC, D., D. C. NEVILLE, O. ARGAUD, B. BLUMBERG, R. A. DWEK, W. B. FISCHER, AND N. ZITZMANN. 2003. THE HEPATITIS C VIRUS P7 PROTEIN FORMS AN ION CHANNEL THAT IS INHIBITED BY LONG-ALKYL-CHAIN IMINOSUGAR DERIVATIVES. PROC. NATL. ACAD. SCI. U. S. A **100**:6104-6108.

168. PEDERSEN, K. W., M. Y. VAN DER, N. ROOS, AND E. J. SNIJDER. 1999. OPEN READING FRAME 1A-ENCODED SUBUNITS OF THE ARTERIVIRUS REPLICASE INDUCE ENDOPLASMIC RETICULUM-DERIVED DOUBLE-MEMBRANE VESICLES WHICH CARRY THE VIRAL REPLICATION COMPLEX. J. VIROL. **73**:2016-2026.

169. PENIN, F., V. BRASS, N. APPEL, S. RAMBOARINA, R. MONTSERRET, D. FICHEUX, H. E. BLUM, R. BARTENSCHLAGER, AND D. MORADPOUR. 2004. STRUCTURE AND FUNCTION OF THE MEMBRANE ANCHOR DOMAIN OF HEPATITIS C VIRUS NONSTRUCTURAL PROTEIN 5A. J. BIOL. CHEM. **279**:40835-40843.

170. PENIN, F., J. DUBUISSON, F. A. REY, D. MORADPOUR, AND J. M. PAWLOTSKY. 2004. STRUCTURAL BIOLOGY OF HEPATITIS C VIRUS. HEPATOLOGY **39**:5-19.

171. PIETSCHMANN, T., A. KAUL, G. KOUTSOUDAKIS, A. SHAVINSKAYA, S. KALLIS, E. STEINMANN, K. ABID, F. NEGRO, M. DREUX, F. L. COSSET, AND R. BARTENSCHLAGER. 2006. CONSTRUCTION AND CHARACTERIZATION OF INFECTIOUS INTRAGENOTYPIC AND INTERGENOTYPIC HEPATITIS C VIRUS CHIMERAS. PROC. NATL. ACAD. SCI. U. S. A **103**:7408-7413.

172. PIETSCHMANN, T., V. LOHMANN, A. KAUL, N. KRIEGER, G. RINCK, G. RUTTER, D. STRAND, AND R. BARTENSCHLAGER. 2002. PERSISTENT AND TRANSIENT REPLICATION OF FULL-LENGTH HEPATITIS C VIRUS GENOMES IN CELL CULTURE. J. VIROL. **76**:4008-4021.

173. PIETSCHMANN, T., V. LOHMANN, G. RUTTER, K. KURPANEK, AND R. BARTENSCHLAGER. 2001. CHARACTERIZATION OF CELL LINES CARRYING SELF-REPLICATING HEPATITIS C VIRUS RNAS. J. VIROL. **75**:1252-1264.

174. PILERI, P., Y. UEMATSU, S. CAMPAGNOLI, G. GALLI, F. FALUGI, R. PETRACCA, A. J. WEINER, M. HOUGHTON, D. ROSA, G. GRANDI, AND S. ABRIGNANI. 1998. BINDING OF HEPATITIS C VIRUS TO CD81. SCIENCE **282**:938-941.

175. PUISIEUX, A., J. JI, AND M. OZTURK. 1996. ANNEXIN II UP-REGULATES CELLULAR LEVELS OF P11 PROTEIN BY A POST-TRANSLATIONAL MECHANISMS. BIOCHEM. J. **313 (PT 1)**:51-55.

176.   QIN, W., T. YAMASHITA, Y. SHIROTA, Y. LIN, W. WEI, AND S. MURAKAMI. 2001. MUTATIONAL ANALYSIS OF THE STRUCTURE AND FUNCTIONS OF HEPATITIS C VIRUS RNA-DEPENDENT RNA POLYMERASE. HEPATOLOGY **33**:728-737.

177.   QUINKERT, D., R. BARTENSCHLAGER, AND V. LOHMANN. 2005. QUANTITATIVE ANALYSIS OF THE HEPATITIS C VIRUS REPLICATION COMPLEX. J. VIROL. **79**:13594-13605.

178.   QUINTAVALLE, M., S. SAMBUCINI, C. DI PIETRO, R. DE FRANCESCO, AND P. NEDDERMANN. 2006. THE ALPHA ISOFORM OF PROTEIN KINASE CKI IS RESPONSIBLE FOR HEPATITIS C VIRUS NS5A HYPERPHOSPHORYLATION. J. VIROL. **80**:11305-11312.

179.   QUINTAVALLE, M., S. SAMBUCINI, V. SUMMA, L. ORSATTI, F. TALAMO, R. DE FRANCESCO, AND P. NEDDERMANN. 2007. HEPATITIS C VIRUS NS5A IS A DIRECT SUBSTRATE OF CASEIN KINASE I-ALPHA, A CELLULAR KINASE IDENTIFIED BY INHIBITOR AFFINITY CHROMATOGRAPHY USING SPECIFIC NS5A HYPERPHOSPHORYLATION INHIBITORS. J. BIOL. CHEM. **282**:5536-5544.

180.   RALSTON, R., K. THUDIUM, K. BERGER, C. KUO, B. GERVASE, J. HALL, M. SELBY, G. KUO, M. HOUGHTON, AND Q. L. CHOO. 1993. CHARACTERIZATION OF HEPATITIS C VIRUS ENVELOPE GLYCOPROTEIN COMPLEXES EXPRESSED BY RECOMBINANT VACCINIA VIRUSES. J. VIROL. **67**:6753-6761.

181.   REINISCH, K. M., M. L. NIBERT, AND S. C. HARRISON. 2000. STRUCTURE OF THE REOVIRUS CORE AT 3.6 A RESOLUTION. NATURE **404**:960-967.

182.   RESCHER, U., D. RUHE, C. LUDWIG, N. ZOBIACK, AND V. GERKE. 2004. ANNEXIN 2 IS A PHOSPHATIDYLINOSITOL (4,5)-BISPHOSPHATE BINDING PROTEIN RECRUITED TO ACTIN ASSEMBLY SITES AT CELLULAR MEMBRANES. J. CELL SCI. **117**:3473-3480.

183.   RYZHOVA, E. V., R. M. VOS, A. V. ALBRIGHT, A. V. HARRIST, T. HARVEY, AND F. GONZALEZ-SCARANO. 2006. ANNEXIN 2: A NOVEL HUMAN IMMUNODEFICIENCY VIRUS TYPE 1 GAG BINDING PROTEIN INVOLVED IN REPLICATION IN MONOCYTE-DERIVED MACROPHAGES. J. VIROL. **80**:2694-2704.

184.   SANTOLINI, E., L. PACINI, C. FIPALDINI, G. MIGLIACCIO, AND N. MONICA. 1995. THE NS2 PROTEIN OF HEPATITIS C VIRUS IS A TRANSMEMBRANE POLYPEPTIDE. J. VIROL. **69**:7461-7471.

185.   SCARSELLI, E., H. ANSUINI, R. CERINO, R. M. ROCCASECCA, S. ACALI, G. FILOCAMO, C. TRABONI, A. NICOSIA, R. CORTESE, AND A. VITELLI. 2002. THE HUMAN SCAVENGER RECEPTOR CLASS B TYPE I IS A NOVEL CANDIDATE RECEPTOR FOR THE HEPATITIS C VIRUS. EMBO J. **21**:5017-5025.

186.   SCHAAD, M. C., P. E. JENSEN, AND J. C. CARRINGTON. 1997. FORMATION OF PLANT RNA VIRUS REPLICATION COMPLEXES ON MEMBRANES: ROLE OF AN ENDOPLASMIC RETICULUM-TARGETED VIRAL PROTEIN. EMBO J. **16**:4049-4059.

187.   SCHALLER, T., N. APPEL, G. KOUTSOUDAKIS, S. KALLIS, V. LOHMANN, T. PIETSCHMANN, AND R. BARTENSCHLAGER. 2007. ANALYSIS OF HEPATITIS C VIRUS SUPERINFECTION EXCLUSION BY USING NOVEL FLUOROCHROME GENE-TAGGED VIRAL GENOMES. J. VIROL. **81**:4591-4603.

188.   SCHMIDT-MENDE, J., E. BIECK, T. HUGLE, F. PENIN, C. M. RICE, H. E. BLUM, AND D. MORADPOUR. 2001. DETERMINANTS FOR MEMBRANE ASSOCIATION OF THE HEPATITIS C VIRUS RNA-DEPENDENT RNA POLYMERASE. J. BIOL. CHEM. **276**:44052-44063.

189.   SCHUSTER, C., C. ISEL, I. IMBERT, C. EHRESMANN, R. MARQUET, AND M. P. KIENY. 2002. SECONDARY STRUCTURE OF THE 3' TERMINUS OF HEPATITIS C VIRUS MINUS-STRAND RNA. J. VIROL. **76**:8058-8068.

190.   SCHWARTZ, M., J. CHEN, M. JANDA, M. SULLIVAN, J. DEN BOON, AND P. AHLQUIST. 2002. A POSITIVE-STRAND RNA VIRUS REPLICATION COMPLEX PARALLELS FORM AND FUNCTION OF RETROVIRUS CAPSIDS. MOL. CELL **9**:505-514.

191.   SEEFF, L. B. 1997. THE NATURAL HISTORY OF CHRONIC HEPATITIS C VIRUS INFECTION. CLIN. LIVER DIS. **1**:587-602.

192.   SELBY, M. J., E. GLAZER, F. MASIARZ, AND M. HOUGHTON. 1994. COMPLEX PROCESSING AND PROTEIN:PROTEIN INTERACTIONS IN THE E2:NS2 REGION OF HCV. VIROLOGY **204**:114-122.

193.   SHI, S. T., K. J. LEE, H. AIZAKI, S. B. HWANG, AND M. M. LAI. 2003. HEPATITIS C VIRUS RNA REPLICATION OCCURS ON A DETERGENT-RESISTANT MEMBRANE THAT COFRACTIONATES WITH CAVEOLIN-2. J. VIROL. **77**:4160-4168.

194. SHIM, J., G. LARSON, V. LAI, S. NAIM, AND J. Z. WU. 2003. CANONICAL 3'-DEOXYRIBONUCLEOTIDES AS A CHAIN TERMINATOR FOR HCV NS5B RNA-DEPENDENT RNA POLYMERASE. ANTIVIRAL RES. **58**:243-251.

195. SHIMAKAMI, T., M. HIJIKATA, H. LUO, Y. Y. MA, S. KANEKO, K. SHIMOTOHNO, AND S. MURAKAMI. 2004. EFFECT OF INTERACTION BETWEEN HEPATITIS C VIRUS NS5A AND NS5B ON HEPATITIS C VIRUS RNA REPLICATION WITH THE HEPATITIS C VIRUS REPLICON. J. VIROL. **78**:2738-2748.

196. SHIROTA, Y., H. LUO, W. QIN, S. KANEKO, T. YAMASHITA, K. KOBAYASHI, AND S. MURAKAMI. 2002. HEPATITIS C VIRUS (HCV) NS5A BINDS RNA-DEPENDENT RNA POLYMERASE (RDRP) NS5B AND MODULATES RNA-DEPENDENT RNA POLYMERASE ACTIVITY. J. BIOL. CHEM. **277**:11149-11155.

197. SIMMONDS, P. 2004. GENETIC DIVERSITY AND EVOLUTION OF HEPATITIS C VIRUS--15 YEARS ON. J. GEN. VIROL. **85**:3173-3188.

198. SIMMONDS, P., J. BUKH, C. COMBET, G. DELEAGE, N. ENOMOTO, S. FEINSTONE, P. HALFON, G. INCHAUSPE, C. KUIKEN, G. MAERTENS, M. MIZOKAMI, D. G. MURPHY, H. OKAMOTO, J. M. PAWLOTSKY, F. PENIN, E. SABLON, I. SHIN, L. J. STUYVER, H. J. THIEL, S. VIAZOV, A. J. WEINER, AND A. WIDELL. 2005. CONSENSUS PROPOSALS FOR A UNIFIED SYSTEM OF NOMENCLATURE OF HEPATITIS C VIRUS GENOTYPES. HEPATOLOGY **42**:962-973.

199. SMITH, R. M., C. M. WALTON, C. H. WU, AND G. Y. WU. 2002. SECONDARY STRUCTURE AND HYBRIDIZATION ACCESSIBILITY OF HEPATITIS C VIRUS 3'-TERMINAL SEQUENCES. J. VIROL. **76**:9563-9574.

200. SONEOKA, Y., P. M. CANNON, E. E. RAMSDALE, J. C. GRIFFITHS, G. ROMANO, S. M. KINGSMAN, AND A. J. KINGSMAN. 1995. A TRANSIENT THREE-PLASMID EXPRESSION SYSTEM FOR THE PRODUCTION OF HIGH TITER RETROVIRAL VECTORS. NUCLEIC ACIDS RES. **23**:628-633.

201. STEINKUHLER, C., A. URBANI, L. TOMEI, G. BIASIOL, M. SARDANA, E. BIANCHI, A. PESSI, AND R. DE FRANCESCO. 1996. ACTIVITY OF PURIFIED HEPATITIS C VIRUS PROTEASE NS3 ON PEPTIDE SUBSTRATES. J. VIROL. **70**:6694-6700.

202. STEINMANN, E., F. PENIN, S. KALLIS, A. H. PATEL, R. BARTENSCHLAGER, AND T. PIETSCHMANN. 2007. HEPATITIS C VIRUS p7 PROTEIN IS CRUCIAL FOR ASSEMBLY AND RELEASE OF INFECTIOUS VIRIONS. PLoS. PATHOG. **3**:E103.

203. SU, A. I., J. P. PEZACKI, L. WODICKA, A. D. BRIDEAU, L. SUPEKOVA, R. THIMME, S. WIELAND, J. BUKH, R. H. PURCELL, P. G. SCHULTZ, AND F. V. CHISARI. 2002. GENOMIC ANALYSIS OF THE HOST RESPONSE TO HEPATITIS C VIRUS INFECTION. PROC. NATL. ACAD. SCI. U. S. A **99**:15669-15674.

204. SUZICH, J. A., J. K. TAMURA, F. PALMER-HILL, P. WARRENER, A. GRAKOUI, C. M. RICE, S. M. FEINSTONE, AND M. S. COLLETT. 1993. HEPATITIS C VIRUS NS3 PROTEIN POLYNUCLEOTIDE-STIMULATED NUCLEOSIDE TRIPHOSPHATASE AND COMPARISON WITH THE RELATED PESTIVIRUS AND FLAVIVIRUS ENZYMES. J. VIROL. **67**:6152-6158.

205. TAKYAR, S. T., D. LI, Y. WANG, R. TROWBRIDGE, AND E. J. GOWANS. 2000. SPECIFIC DETECTION OF MINUS-STRAND HEPATITIS C VIRUS RNA BY REVERSE-TRANSCRIPTION POLYMERASE CHAIN REACTION ON POLYA(+)-PURIFIED RNA. HEPATOLOGY **32**:382-387.

206. TANAKA, T., N. KATO, M. J. CHO, AND K. SHIMOTOHNO. 1995. A NOVEL SEQUENCE FOUND AT THE 3' TERMINUS OF HEPATITIS C VIRUS GENOME. BIOCHEM. BIOPHYS. RES. COMMUN. **215**:744-749.

207. TANJI, Y., M. HIJIKATA, Y. HIROWATARI, AND K. SHIMOTOHNO. 1994. IDENTIFICATION OF THE DOMAIN REQUIRED FOR TRANS-CLEAVAGE ACTIVITY OF HEPATITIS C VIRAL SERINE PROTEINASE. GENE **145**:215-219.

208. TANJI, Y., M. HIJIKATA, S. SATOH, T. KANEKO, AND K. SHIMOTOHNO. 1995. HEPATITIS C VIRUS-ENCODED NONSTRUCTURAL PROTEIN NS4A HAS VERSATILE FUNCTIONS IN VIRAL PROTEIN PROCESSING. J. VIROL. **69**:1575-1581.

209. THIMME, R., J. BUKH, H. C. SPANGENBERG, S. WIELAND, J. PEMBERTON, C. STEIGER, S. GOVINDARAJAN, R. H. PURCELL, AND F. V. CHISARI. 2002. VIRAL AND IMMUNOLOGICAL DETERMINANTS OF HEPATITIS C VIRUS CLEARANCE, PERSISTENCE, AND DISEASE. PROC. NATL. ACAD. SCI. U. S. A **99**:15661-15668.

210. TOMASSINI, J. E., E. BOOTS, L. GAN, P. GRAHAM, V. MUNSHI, B. WOLANSKI, J. F. FAY, K. GETTY, AND R. LAFEMINA. 2003. AN IN VITRO FLAVIVIRIDAE REPLICASE SYSTEM CAPABLE OF AUTHENTIC RNA REPLICATION. VIROLOGY **313**:274-285.

211. **TONGE, R., J. SHAW, B. MIDDLETON, R. ROWLINSON, S. RAYNER, J. YOUNG, F. POGNAN, E. HAWKINS, I. CURRIE, AND M. DAVISON**. 2001. VALIDATION AND DEVELOPMENT OF FLUORESCENCE TWO-DIMENSIONAL DIFFERENTIAL GEL ELECTROPHORESIS PROTEOMICS TECHNOLOGY. PROTEOMICS. **1**:377-396.

212. **TSCHERNE, D. M., C. T. JONES, M. J. EVANS, B. D. LINDENBACH, J. A. MCKEATING, AND C. M. RICE**. 2006. TIME- AND TEMPERATURE-DEPENDENT ACTIVATION OF HEPATITIS C VIRUS FOR LOW-PH-TRIGGERED ENTRY. J. VIROL. **80**:1734-1741.

213. **TSUKIYAMA-KOHARA, K., N. IIZUKA, M. KOHARA, AND A. NOMOTO**. 1992. INTERNAL RIBOSOME ENTRY SITE WITHIN HEPATITIS C VIRUS RNA. J. VIROL. **66**:1476-1483.

214. **TU, H., L. GAO, S. T. SHI, D. R. TAYLOR, T. YANG, A. K. MIRCHEFF, Y. WEN, A. E. GORBALENYA, S. B. HWANG, AND M. M. LAI**. 1999. HEPATITIS C VIRUS RNA POLYMERASE AND NS5A COMPLEX WITH A SNARE-LIKE PROTEIN. VIROLOGY **263**:30-41.

215. **UITTENBOGAARD, A., W. V. EVERSON, S. V. MATVEEV, AND E. J. SMART**. 2002. CHOLESTERYL ESTER IS TRANSPORTED FROM CAVEOLAE TO INTERNAL MEMBRANES AS PART OF A CAVEOLIN-ANNEXIN II LIPID-PROTEIN COMPLEX. J. BIOL. CHEM. **277**:4925-4931.

216. **UNLU, M., M. E. MORGAN, AND J. S. MINDEN**. 1997. DIFFERENCE GEL ELECTROPHORESIS: A SINGLE GEL METHOD FOR DETECTING CHANGES IN PROTEIN EXTRACTS. ELECTROPHORESIS **18**:2071-2077.

217. **VARAKLIOTI, A., N. VASSILAKI, U. GEORGOPOULOU, AND P. MAVROMARA**. 2002. ALTERNATE TRANSLATION OCCURS WITHIN THE CORE CODING REGION OF THE HEPATITIS C VIRAL GENOME. J. BIOL. CHEM. **277**:17713-17721.

218. **VEDELER, A. AND H. HOLLAS**. 2000. ANNEXIN II IS ASSOCIATED WITH MRNAS WHICH MAY CONSTITUTE A DISTINCT SUBPOPULATION. BIOCHEM. J. **348 PT 3**:565-572.

219. **WAKITA, T., T. PIETSCHMANN, T. KATO, T. DATE, M. MIYAMOTO, Z. ZHAO, K. MURTHY, A. HABERMANN, H. G. KRAUSSLICH, M. MIZOKAMI, R. BARTENSCHLAGER, AND T. J. LIANG**. 2005. PRODUCTION OF INFECTIOUS HEPATITIS C VIRUS IN TISSUE CULTURE FROM A CLONED VIRAL GENOME. NAT. MED. **11**:791-796.

220. **WALEWSKI, J. L., T. R. KELLER, D. D. STUMP, AND A. D. BRANCH**. 2001. EVIDENCE FOR A NEW HEPATITIS C VIRUS ANTIGEN ENCODED IN AN OVERLAPPING READING FRAME. RNA. **7**:710-721.

221. **WANG, C., M. GALE, JR., B. C. KELLER, H. HUANG, M. S. BROWN, J. L. GOLDSTEIN, AND J. YE**. 2005. IDENTIFICATION OF FBL2 AS A GERANYLGERANYLATED CELLULAR PROTEIN REQUIRED FOR HEPATITIS C VIRUS RNA REPLICATION. MOL. CELL **18**:425-434.

222. **WANG, C., S. Y. LE, N. ALI, AND A. SIDDIQUI**. 1995. AN RNA PSEUDOKNOT IS AN ESSENTIAL STRUCTURAL ELEMENT OF THE INTERNAL RIBOSOME ENTRY SITE LOCATED WITHIN THE HEPATITIS C VIRUS 5' NONCODING REGION. RNA. **1**:526-537.

223. **WANG, C., P. SARNOW, AND A. SIDDIQUI**. 1993. TRANSLATION OF HUMAN HEPATITIS C VIRUS RNA IN CULTURED CELLS IS MEDIATED BY AN INTERNAL RIBOSOME-BINDING MECHANISM. J. VIROL. **67**:3338-3344.

224. **WATASHI, K., N. ISHII, M. HIJIKATA, D. INOUE, T. MURATA, Y. MIYANARI, AND K. SHIMOTOHNO**. 2005. CYCLOPHILIN B IS A FUNCTIONAL REGULATOR OF HEPATITIS C VIRUS RNA POLYMERASE. MOL. CELL **19**:111-122.

225. **WATTENBERG, B. AND T. LITHGOW**. 2001. TARGETING OF C-TERMINAL (TAIL)-ANCHORED PROTEINS: UNDERSTANDING HOW CYTOPLASMIC ACTIVITIES ARE ANCHORED TO INTRACELLULAR MEMBRANES. TRAFFIC. **2**:66-71.

226. **WELBOURN, S., R. GREEN, I. GAMACHE, S. DANDACHE, V. LOHMANN, R. BARTENSCHLAGER, K. MEEROVITCH, AND A. PAUSE**. 2005. HEPATITIS C VIRUS NS2/3 PROCESSING IS REQUIRED FOR NS3 STABILITY AND VIRAL RNA REPLICATION. J. BIOL. CHEM. **280**:29604-29611.

227. **WESTAWAY, E. G., A. A. KHROMYKH, AND J. M. MACKENZIE**. 1999. NASCENT FLAVIVIRUS RNA COLOCALIZED IN SITU WITH DOUBLE-STRANDED RNA IN STABLE REPLICATION COMPLEXES. VIROLOGY **258**:108-117.

228. **WINDISCH, M. P., M. FRESE, A. KAUL, M. TRIPPLER, V. LOHMANN, AND R. BARTENSCHLAGER**. 2005. DISSECTING THE INTERFERON-INDUCED INHIBITION OF HEPATITIS C VIRUS REPLICATION BY USING A NOVEL HOST CELL LINE. J. VIROL. **79**:13778-13793.

229. WU, S. X., P. AHLQUIST, AND P. KAESBERG. 1992. ACTIVE COMPLETE IN VITRO REPLICATION OF NODAVIRUS RNA REQUIRES GLYCEROPHOSPHOLIPID. PROC. NATL. ACAD. SCI. U. S. A **89**:11136-11140.

230. XU, Z., J. CHOI, T. S. YEN, W. LU, A. STROHECKER, S. GOVINDARAJAN, D. CHIEN, M. J. SELBY, AND J. OU. 2001. SYNTHESIS OF A NOVEL HEPATITIS C VIRUS PROTEIN BY RIBOSOMAL FRAMESHIFT. EMBO J. **20**:3840-3848.

231. YANAGI, M., R. H. PURCELL, S. U. EMERSON, AND J. BUKH. 1999. HEPATITIS C VIRUS: AN INFECTIOUS MOLECULAR CLONE OF A SECOND MAJOR GENOTYPE (2A) AND LACK OF VIABILITY OF INTERTYPIC 1A AND 2A CHIMERAS. VIROLOGY **262**:250-263.

232. YANAGI, M., M. ST CLAIRE, S. U. EMERSON, R. H. PURCELL, AND J. BUKH. 1999. IN VIVO ANALYSIS OF THE 3' UNTRANSLATED REGION OF THE HEPATITIS C VIRUS AFTER IN VITRO MUTAGENESIS OF AN INFECTIOUS CDNA CLONE. PROC. NATL. ACAD. SCI. U. S. A **96**:2291-2295.

233. YEN, T., E. B. KEEFFE, AND A. AHMED. 2003. THE EPIDEMIOLOGY OF HEPATITIS C VIRUS INFECTION. J. CLIN. GASTROENTEROL. **36**:47-53.

234. YI, M. AND S. M. LEMON. 2003. 3' NONTRANSLATED RNA SIGNALS REQUIRED FOR REPLICATION OF HEPATITIS C VIRUS RNA. J. VIROL. **77**:3557-3568.

235. YI, M., Y. MA, J. YATES, AND S. M. LEMON. 2007. COMPENSATORY MUTATIONS IN E1, P7, NS2, AND NS3 ENHANCE YIELDS OF CELL CULTURE-INFECTIOUS INTERGENOTYPIC CHIMERIC HEPATITIS C VIRUS. J. VIROL. **81**:629-638.

236. YI, M., R. A. VILLANUEVA, D. L. THOMAS, T. WAKITA, AND S. M. LEMON. 2006. PRODUCTION OF INFECTIOUS GENOTYPE 1A HEPATITIS C VIRUS (HUTCHINSON STRAIN) IN CULTURED HUMAN HEPATOMA CELLS. PROC. NATL. ACAD. SCI. U. S. A **103**:2310-2315.

237. YOU, S., D. D. STUMP, A. D. BRANCH, AND C. M. RICE. 2004. A CIS-ACTING REPLICATION ELEMENT IN THE SEQUENCE ENCODING THE NS5B RNA-DEPENDENT RNA POLYMERASE IS REQUIRED FOR HEPATITIS C VIRUS RNA REPLICATION. J. VIROL. **78**:1352-1366.

238. ZECH, B., A. KURTENBACH, N. KRIEGER, D. STRAND, S. BLENCKE, M. MORBITZER, K. SALASSIDIS, M. COTTEN, J. WISSING, S. OBERT, R. BARTENSCHLAGER, T. HERGET, AND H. DAUB. 2003. IDENTIFICATION AND CHARACTERIZATION OF AMPHIPHYSIN II AS A NOVEL CELLULAR INTERACTION PARTNER OF THE HEPATITIS C VIRUS NS5A PROTEIN. J. GEN. VIROL. **84**:555-560.

239. ZHANG, J., O. YAMADA, T. SAKAMOTO, H. YOSHIDA, T. IWAI, Y. MATSUSHITA, H. SHIMAMURA, H. ARAKI, AND K. SHIMOTOHNO. 2004. DOWN-REGULATION OF VIRAL REPLICATION BY ADENOVIRAL-MEDIATED EXPRESSION OF SIRNA AGAINST CELLULAR COFACTORS FOR HEPATITIS C VIRUS. VIROLOGY **320**:135-143.

240. ZHONG, J., P. GASTAMINZA, G. CHENG, S. KAPADIA, T. KATO, D. R. BURTON, S. F. WIELAND, S. L. UPRICHARD, T. WAKITA, AND F. V. CHISARI. 2005. ROBUST HEPATITIS C VIRUS INFECTION IN VITRO. PROC. NATL. ACAD. SCI. U. S. A **102**:9294-9299.

241. ZHONG, W., A. S. USS, E. FERRARI, J. Y. LAU, AND Z. HONG. 2000. DE NOVO INITIATION OF RNA SYNTHESIS BY HEPATITIS C VIRUS NONSTRUCTURAL PROTEIN 5B POLYMERASE. J. VIROL. **74**:2017-2022.

242. ZOBIACK, N., V. GERKE, AND U. RESCHER. 2001. COMPLEX FORMATION AND SUBMEMBRANOUS LOCALIZATION OF ANNEXIN 2 AND S100A10 IN LIVE HEPG2 CELLS. FEBS LETT. **500**:137-140.

243. ZOBIACK, N., U. RESCHER, C. LUDWIG, D. ZEUSCHNER, AND V. GERKE. 2003. THE ANNEXIN 2/S100A10 COMPLEX CONTROLS THE DISTRIBUTION OF TRANSFERRIN RECEPTOR-CONTAINING RECYCLING ENDOSOMES. MOL. BIOL. CELL **14**:4896-4908.

244. ZUFFEREY, R., D. NAGY, R. J. MANDEL, L. NALDINI, AND D. TRONO. 1997. MULTIPLY ATTENUATED LENTIVIRAL VECTOR ACHIEVES EFFICIENT GENE DELIVERY IN VIVO. NAT. BIOTECHNOL. **15**:871-875.

6. Publications and presentations

This thesis describes work carried out from October 2003 to August 2007 in the Department of Molecular Virology at the Ruperto-Carola University of Heidelberg. The work was performed in the group of Dr. Volker Lohmann who was also responsible for the supervision.

6.1 Publications

Binder M.[1], <u>Quinkert D.</u>[1], Bochkarova O., Klein R., Kezmic N., Bartenschlager R., Lohmann V. (2007)
Identification of determinants involved in initiation of hepatitis C virus RNA synthesis by using intergenotypic replicase chimeras. *J Virol.* 81(10):5270-83.

<u>Quinkert D.</u>, Bartenschlager R., Lohmann V. (2005)
Quantitative analysis of the hepatitis C virus replication complex. *J Virol.* 79(21):13594-605.

[1] with equal contribution

6.2 Presentations

8th International Symposium on Positive-strand RNA Viruses
May 26-30, 2007, Renaissance Hotel Mayflower, Washington, D.C., USA
Poster: "Identification of determinants involved in initiation of hepatitis C virus RNA synthesis by using intergenotypic replicase chimeras"

Annual meeting of the German Society of Virology
Mar 16-19, 2005, University of Hannover, Hannover, Germany
Talk: "Quantitative analysis of the Hepatitis C Virus"

11th International Symposium on Hepatitis C Virus and Related Viruses
Oct 3-7, 2004, University of Heidelberg, Heidelberg, Germany
Talk: "Quantitative analysis of the Hepatitis C Virus"

Annual meeting of the German Society of Virology
Mar 26-29, 2003, Neue Charité, Berlin, Germany
Short talk and poster: "Preparation and Analysis of Hepatitis C Virus Replication Complexes"

Additional conferences

Annual meeting of the German Society of Virology
Mar 15-18, 2006, Technical University of Munich, Munich, Germany

SFB Spring Meeting, SFB 638 "Dynamics of macromolecular complexes in biosynthetic transport"
Apr 16-17, 2005, Hotel Wiesengrund, Lindenfels-Winkel, Germany
Talk: "Quantitative analysis of the Hepatitis C Virus"

7. Abbreviations

2D: two-dimensional

aa: amino acid

ab: antibody

ANXA2: Annexin II

ARF: alternative reading frame

ATP: adenosine triphosphate

bp: base pairs

BrdU: 5-bromo-2-deoxyuridine

CFP: cyan fluorescent protein

CMC: critical micellar concentration

Con: consensus

CRC: crude replicase complex

CyPB: Cyclophilin B

DM: dodecyl maltoside

DMEM: Dulbecco's Modified Eagle Medium

DMSO: dimethyl sulfoxide

DNA: desoxyribonucleic acid

dNTP: desoxynucleotide triphosphate

DOC: (sodium) desoxycholate

DRM: detergent-resistant membrane

dsRNA: double strand RNA

DTT: dithiothreitol

DV: Dengue virus

EGTA: ethylene glycol tetraacetic acid

EI: Encephalomyocarditis virus IRES

EMCV: Encephalomyocarditis virus

emGFP: emerald green fluorescent protein

ER: Endoplasmic Reticulum

FACS: fluorescence activated cell sorting

FBL2: F-box and leucine rich protein 2

FCS: fetal calf serum

Fig.: figure

GFP: green fluorescent protein

HCV: Hepatitis C Virus

HCVpp: HCV pseudoparticles

IEF: isoelectric focusing

IF(A): immunofluorescence (assay)

IFN: Interferon

Ig: immunoglobulin

IP: immunoprecipitation

IRES: internal ribosome entry site

JFH: Japanese fulminant hepatitis

kb: kilobases

kDa: kilo-Dalton

LDL: low density lipoprotein

luc: luciferase

MALDI-TOF MS: matrix-assisted laser desorption/ionization -time-of-flight-mass spectrometry

MW: molecular weight

NaAc: sodium acetate

NB: Northern blot

neo: neomycin phosphotransferase

NP: nuclear pellet

NP40: Nonidet P40

NS: non-structural

nts: nucleotides

NTP: nucleotide triphosphate

NTR: non-translated region

OG: octyl glucoside

ORF: open reading frame

p.i.: post infection

p.tr.: post transfection

PBS: phosphate buffered saline

PCR: polymerase chain reaction

PFA: paraformaldehyde

pI: isoelectric point

PI: Poliovirus IRES

PMSF: phenyl methyl sulfonyl fluoride

PrK: proteinase K

PTB: polypyrimidine tract binding

RC: replication complex

RdRp: RNA-dependent RNA polymerase

RFP: red fluorescent protein

RNA: ribonucleic acid

RNAi: RNA interference

rpm: rounds per minute

RT-PCR: reverse transcriptase PCR

S1: supernatant 1

SDS: sodium dodecyl sulphate

SDS-PAGE: SDS polyacrylamide gel electrophoresis

SFV: Semliki Forest virus

shRNA: short hairpin RNA

siRNA: small interfering RNA

SL: stem loop

SRBI: scavenger receptor class B type I

ssRNA: single stranded RNA

TCA: trichloroacetic acid

TL: total lysate

tSNARE: target membrane-associated soluble N-ethylmaleimide-sensitive factor-attachment protein receptor

TX-100: Triton X-100

U: units

Vap-A: vesicle-associated-membrane-protein associated protein A

vol: volume/volumina

WB: Western blot

wt: wild type

Y2H: yeast two-hybrid

α: anti (antibodies) or alpha

β-ME: β-mercapto-ethanol